Flashback Studies with Premixed Swirl Combustion

A Thesis Submitted to Cardiff University
for the Degree of Doctor of Philosophy
in Mechanical Engineering

By

Nasser Shelil

B. Sc. & M. Sc., Mechanical Power Engineering

Institute of Energy

Cardiff School of Engineering

Cardiff University

Cardiff / UK

2009

ProQuest LLC
789 East Eisenhower Parkway
P.O. Box 1346
Ann Arbor, MI 48106-1346

Declaration

This work has not previously been accepted in substance for any degree and is not concurrently submitted in candidature for any other higher degree.

Signed:.....N. Shelil.....(Candidate) Date:...15/12/2009.....

Statement 1

This thesis is being submitted in partial fulfilment of the requirements for the degree of ....PhD.....(insert as appropriate PhD, MPhil, EngD)

Signed:...N. Shelil.....(Candidate) Date:....15/12/2009....

Statement 2

This thesis is the result of my own independent work/investigation, except where otherwise stated. Other sources are acknowledged by explicit references.

Signed:.....N. Shelil.....(Candidate) Date:...15/12/2009.....

Statement 3

I hereby give consent for my thesis, if accepted, to be available for photocopying, inter-library loan and for the title and summary to be made available to outside organisations.

Signed:.....N. Shelil.....(Candidate) Date:...15/12/2009.....

ABSTRACT

Lean premixed combustion is promoted as one of the new technologies which can be applied to gas turbines to enable the reduction of pollutant emissions, especially of NOx. Some of the main advantages of lean premixed operation are lower overall combustion temperatures, shorter flame lengths and better fuel burnout. The swirl lean premixed combustion provides the initial stability and flexibility for the system. However, there are still problems that can occur during the combustion process including those related to flashback especially for high burning velocity fuels such as hydrogen enriched fuels.

CFD modelling is used to simulate the combustion of premixed swirl burner that uses different types of fuels. A three dimensional – finite volume model is used to study the flashback phenomenon. It was realized that two different types of flashback can take place, partial flashback and full flashback. The partial flashback exists due to the extension of a Central Recirculation Zone (CRZ) back into the burner exit and that allows the hot gases to return to the burner and cause flashback. The other type of flashback is caused by the low velocity of the raw gases that may drop below the local burning velocity and thus causes full flashback. The results show the possibility of reducing or virtually eliminating partial flashback by using passive constrictions at the burner exit which can manipulate the CRZ and hence avoid partial flashback. The passive constrictions are not able to prevent full flashback but there are other methods that are introduced to improve the stability limits of the flame and reduce the system flashback tendency. The results are generally confirmed for methane by experiments using a model burner operated at atmospheric pressure, although there are regions around the fuel nozzle where CFD cannot pick out the finer detail of the flames found.

Full flashback can be reduced by lowering the turbulent intensity, adding carbon dioxide to the fuel and/or operating at equivalence ratios less than about 0.65. CFD Modelling for premixed swirl combustion is initially performed to simulate the combustion of Methane-Air with carbon dioxide dilution. The impact of CO_2 addition to the premixed air fuel mixture is studied, this being representative of various future gas turbine fuels. The results show that the stability limits of CH_4 combustion can be improved by CO_2 addition to the flame as the flame velocity decreases with the increase of CO_2 addition. This is confirmed experimentally although the CFD code overestimates the conditions at which flashback will occur, except at very weak and rich conditions

Flashback simulations studies were also performed for a wide range of hydrogen/methane (H_2/CH_4) blends using the same swirl burner under premixed conditions. The laminar flame speed was calculated for H_2/CH_4 blends from pure methane up to pure hydrogen at various pressures, temperatures and equivalence ratios. This was done by using CHEMKIN-PRO software package with PREMIX code and an algebraic expression derived by asymptotic methods incorporated with Le Chatelier's Rule-like correlation. The feasibility of using a new approximation for laminar flame speed of H_2/CH_4 blends based on the gravimetric mixture ratio was checked and compared with the previous calculations. The new approximation gave a good prediction at various conditions. The numerical values for laminar flame speed calculated by CHEMKIN are then fed to a FLUENT CFD model to create a PDF table for turbulent premixed

combustion calculations and flashback studies. Flashback limits were defined and determined for H_2/CH_4 blends ranging from 0% (pure methane) up to 100% (pure hydrogen) based on the volumetric composition at atmospheric pressure and 300K for various equivalence ratios. The results show that the use of up to 50% blends of methane and hydrogen causes fewer problems with flame stability and flashback compared with the use of pure hydrogen. Also, the flashback limits depend on the values for both laminar and turbulent flame speed. What emerges is the need for more theoretical and experimental research work to obtain more accurate values for flame speeds.

CFD simulations using FLUENT were carried on for the definition of turbulent parameters and confirmation of the accuracy between empirical and numerical results, as well as extrapolating the results to high pressure and air preheat. The experimental validations allowed the numerical analysis of cases with hydrogen enriched blends, plus the use of diluting components such as CO_2, augmenting the understanding of flashback using these types of passive methods of suppression and their efficiency in the avoidance of the flashback phenomenon.

The important conclusion was reached that when combusting H_2/CH_4 fuel mixes flashback behaviour approaches that of pure methane for equivalence ratios less than about 0.65, all pressures investigated up to 7 bara and air inlet temperatures of 300 and 473K. Significant deleterious changes in flashback behaviour for H_2/CH_4 fuel mixes occurred for air inlet temperatures of 673K, although operation at weak equivalence ratios less than 0.65 was still beneficial.

ACKNOWLEDGEMENTS

*First and foremost, I would like to thank **ALLAH** for helping me to complete this thesis.*

I wish to express my deep gratitude for my supervisors, Prof. Nick Syred and Prof. Anthony Griffiths for their continuous guidance, useful discussions and valuable suggestions through this research work.

I would like also to thank the staff of Gas Turbine Research Centre (GTRC) and the staff of mechanical engineering work shop.

I would like to extend my thanks for the Egyptian Government for sponsoring my research study, and many thanks for the staff of the Egyptian cultural and educational bureau in London for their help during my stay in the UK.

My greatest thanks and appreciations for all of my family, brothers, sisters and special thanks for my wife and my lovely kids, Sama, Mohamed and Ahmed. This work would not have been completed without their love and continuous support.

TABLE OF CONTENTS

LIST OF FIGURES

Chapter 5

LIST OF TABLES

NOMENCLATURE

A	=	Model constant (-)
AFR	=	Air to Fuel Ratio (-)
c	=	Mean reaction progress variable (-)
f	=	Mixture fraction (-)
g		The mass fraction (-)
H_{comb}	=	Heat of combustion for burning 1 kg of fuel (J/kg)
$\dot{m}$	=	Mass flow rate (kg/s)
$\dot{m}_{oFB}$	=	Mass flow rate at which flashback occurs for stoichiometric methane/air mixture at the standard ambient conditions (1 atm and 25°C) (kg/s)
m_r	=	Relative mass flow rate (-)
n	=	Number of products (-)
P	=	The static pressure (Pa)
Q_{EAS}	=	The Equiangle Skew
Q_{EVS}	=	The Equivolume Skew
R^{ϕ}	=	The residual
S	=	Swirl number (-)
S_c	=	Reaction progress source term (s^{-1})
Sc_t	=	Turbulent Schmidt number (-)
$S_{h,chem}$	=	Heat gains due to chemical reaction ($j/s.m^3$)
$S_{h,rad}$	=	Heat losses due to radiation ($j/s.m^3$)
S_L	=	Laminar flame speed (m/s)
S_{Mi}	=	The body force in i-direction (N/m^3)
S_T	=	Turbulent flame speed (m/s)
t	=	Time (s)
u'	=	Root-mean-square (RMS) velocity (m/s)
U	=	Velocity vector (m/s)
U	=	average axial velocity at the burner exit (m/s)
u, v, w	=	Velocity components in x, y, and z respectively
$U_{o\,FB}$	=	Average axial velocity at the burner exit at which flashback occurs for stoichiometric methane/air mixture at the standard ambient conditions (1 atm and 25°C) (m/s)
U_r	=	Relative velocity (-)
Y_{fuel}	=	Fuel mass fraction of unburnt mixture (-)
Y_i	=	Mass fraction of product species i (-)
$Y_{i,eq}$	=	Equilibrium mass fraction of product species i (-)

Greek Letters

α = Molecular heat transfer coefficient of unburnt mixture (thermal diffusivity) (m^2/s)

β = The mole fraction of CO_2 in CO_2/CH_4 mixture (-)

ℓ_t = Turbulence length scale (m)

τ_c = Chemical time scale (s)

τ_t = Turbulence time scale (s)

γ = The mole fraction of H_2 in H_2/CH_4 mixture (-)

ϕ = Equivalence ratio (-)

ρ = Fluid density (kg/m^3)

τ = Viscous stress (N/m^2)

τ_{ij} = Viscous stress component acts in the j-direction on a surface normal to i-direction (N/m^2)

ρ_u = Density of burnt mixture (kg/m^3)

ε = Turbulence dissipation rate (m^2/s^3)

ω = Specific dissipation rate (1/s)

ABBREVIATIONS

CFD	Computational Fluid Dynamics
CIVB	Combustion Induced Vortex Breakdown
CRZ	Central Recirculation Zone
CTRZ	Central Toroidal Recirculation Zone
DES	Detached Eddy Simulation
DNS	Direct Numerical Solution
EGR	Exhaust Gas Recirculation
FGR	Flue Gas Recirculation
GHG	Green House Gas
GT	Gas Turbine
GTRC	Gas Turbine Research Centre
GUI	Graphical User Interface
HiTAC	High-Temperature Air Combustion
HPOC	High Pressure Optical Combustor
ICE	Internal Combustion Engines
IEA	International Energy Agency
IGCC	Integrated Gasification Combined Cycle
IPCC	Intergovernmental Panel on Climate Change
IRZ	Inner Recirculation Zone
LES	Large Eddy Simulation
LNG	Liquefied Natural Gas
LPM	Lean-Premixed
LPMC	Lean Premixed Combustion
Mtoe	Million ton oil equivalent (Mtoe = 10^{10} kcal = 11630 GWh)
NTP	Normal Temperature and Pressure
OECD	Organisation for Economic Co-operation and Development
PDF	Probability Density Function
PVC	Precessing Vortex Core
RFZ	Reverse Flow Zone
RNG	Renormalization-Group
RSM	Reynolds Stress Model
SI	spark ignition
SST	Shear-Stress Transport
STP	Standard Temperature and Pressure

Chapter 1

INTRODUCTION

1.1 World Energy and Environmental Aspects

Energy plays an important role in the economics of all countries. It is the driving engine to development and one of the basic factors to improve the quality of life and economic viability. The policies of the electricity and energy sector aim to optimum utilization of primary energy sources.

In 2008, the worldwide energy consumption of the human race was estimated at 11294.9 million ton oil equivalent (Mtoe) with 88.2% from burning fossil fuels; coal, oil and natural gas. Figure 1.1 represents the trend of world energy consumption from 1983 until 2008. World primary energy consumption grew by 1.4% in 2008, this is the weakest growth since 2001. Oil remains the world's dominant fuel, though it has steadily lost market share to coal and natural gas in recent years. However it is still counted as the primary energy source with 34.8% of the total energy supply falling from 38.7% over the past decade. Oil consumption and nuclear power generation declined last year, while natural gas and coal consumption, as well as hydroelectric generation, increased [1]. In this review, primary energy comprises commercially traded fuels only. Therefore, fuels such as wood, peat and animal waste that, though important in many countries, are excluded. This is because they are unreliably documented in terms of consumption statistics. Also wind, geothermal and solar power generation are excluded. Other statistics of International Energy Agency (IEA) [2] and Organisation for Economic Co-operation and Development (OECD) [3] that consider the energy produced from combustible renewables and waste count it as 10.1% of the total primary energy consumption in 2006 and the energy produced from wind, geothermal and solar power generation are 0.6%. A complete survey of the world energy resources is in [4].

Regarding the electricity generation, Figure 1.2 represents the fuel shares in electricity generation in 2006. It is realized that the main energy contribution in the electrical power generation field is the fossil fuel (coal, oil, and gas) with a total percentage about 66.9%. While the nuclear energy contributes 14.8% and hydro power contributes 16% from the total electricity generation of 18,930 TWh [2].

From the previous statistics, it can be concluded that thermal energy is still the main energy source all over the world and deserves appropriate research.

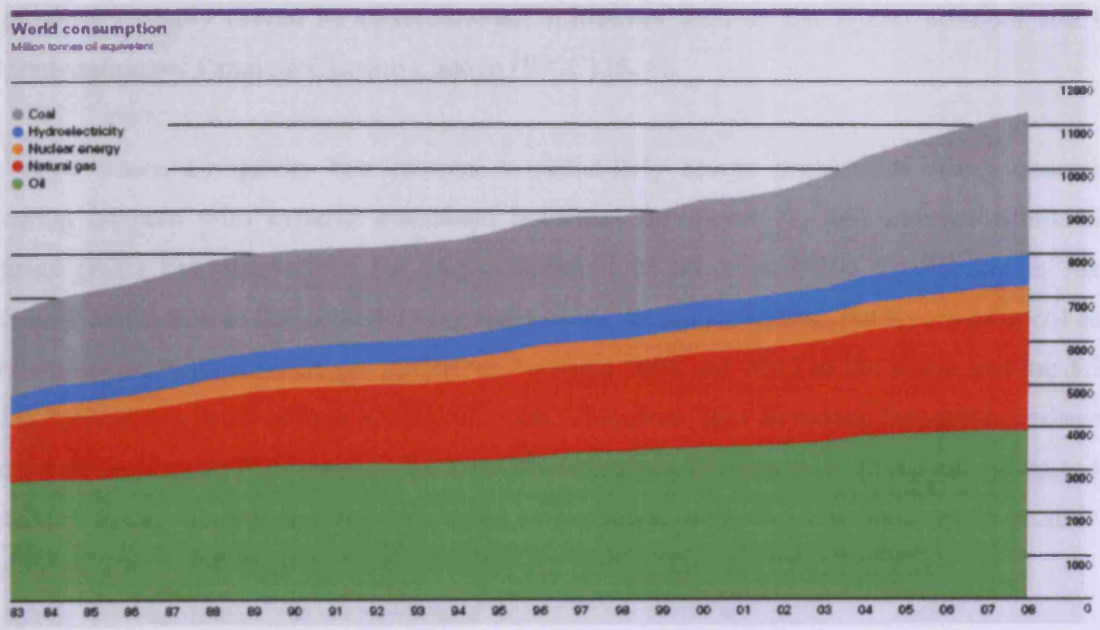

Figure 1.1: The trend of world energy consumption from 1983 until 2008 [1]

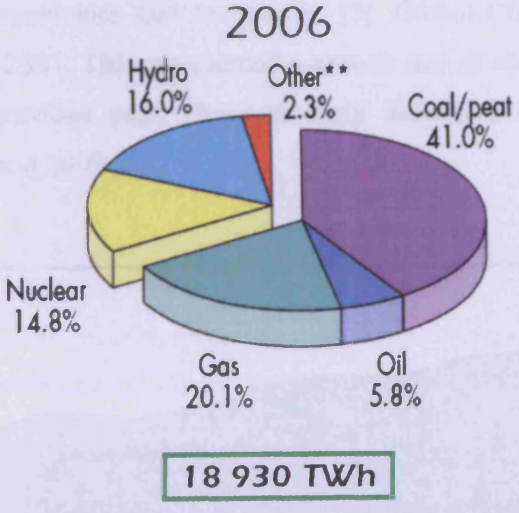

Figure 1.2: The fuel shares in electricity generation [2]

The environmental impact of the use of fossil fuels and potential scarcity of supply are the major driving forces behind current energy policies. The environmental problems associated with fossil fuel consumption are the major problems that most research tackles.

Energy production from fossil fuel combustion results in the emission of greenhouse gases, the dominant contributor being CO_2. Public awareness and legislation have led to a policy of reduction of greenhouse gas emissions in most economically well-developed countries, with the regulations partially driven by (international) initiatives such as the Kyoto protocol and the Intergovernmental Panel on Climate Change (IPCC) [5, 6].

In recent years, air quality has become a particularly severe problem in many countries. Growing concern with exhaust emissions from gas turbines (GT) and internal combustion engines (ICE) has resulted in the implementation of strict emission regulations in many industrial areas such as the United States and Europe. In the meantime, the Kyoto protocol calls for a reduction in greenhouse gas emissions between 2008 and 2012 to the levels that are 5.2% below 1990 levels in 38 industrialized countries. Therefore, how to reduce hazardous emissions and greenhouse gases from engines has now become a research focus. If driven according to the certifying cycle, modern engines with three way catalyst emit very low amounts of hazardous emissions, along with large amounts of water and carbon dioxide (CO_2) emissions.

According to IEA statistics, the world CO_2 emissions doubled from 1971 till 2006 as shown in Figure 1.3. Emissions were 28100 Mt in 2006. This amount were calculated using IEA energy databases and the default methods and emissions factors from the Revised 1996 IPCC Guidelines for National Greenhouse Gas Inventories [2]. Global CO_2 emissions increased by 900 Mt between 2006 and 2007. This represented a growth rate of about 3% in CO_2 emissions, identical to that of the previous year. However early indicators suggested that growth in emissions slowed in 2008 and 2009 [7].

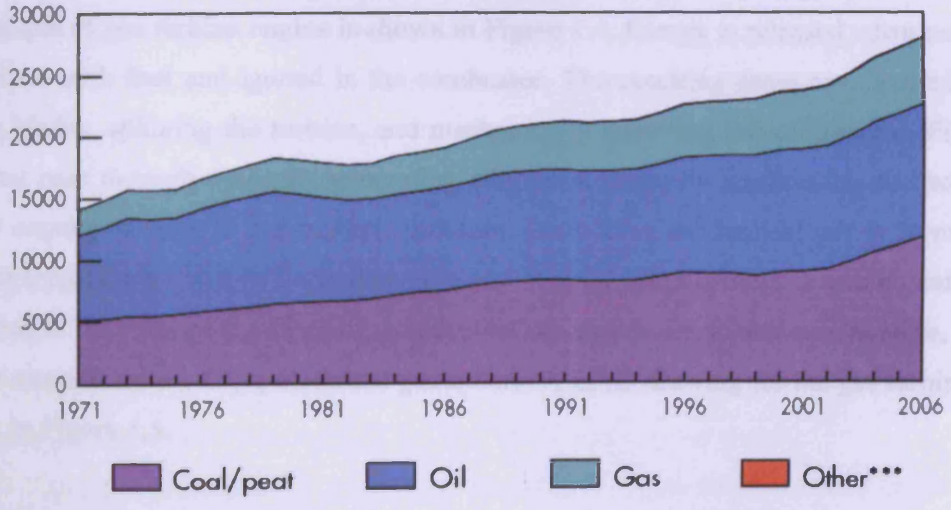

Figure 1.3: World CO_2 emissions evolution from 1971 to 2006 by fuel (Mt of CO_2) [2]

CO_2 is a greenhouse gas in the exhaust gases of combustion from GTs and ICEs. CO_2 emissions from engines can be reduced by improving fuel economy, using a fuel with higher hydrogen to carbon ratio (H/C) or using a renewable fuel. The fuel economy of GT and ICE can be improved by operating the engine with diluted mixtures through extra air or exhaust gas recirculation (EGR) due to low temperature combustion, low heat transfer losses and low pumping losses at part loads. Direct injection SI engines have reduced pumping losses and heat transfer losses and, hence, have low fuel consumption. Homogenous charge compression ignition (HCCI) gasoline engines using diluted mixtures can also improve their fuel economy [8].

CO_2 is not the only harmful pollutant resulting form fossil fuel combustion but many other pollutants are produced. Combustion of standard fossil fuels in commercial and industrial combustors results in the following nine emissions; carbon dioxide, nitrogen, oxygen, water, carbon monoxide, nitrogen oxide, sulphur oxides, volatile organic compounds, and particulate matter. The latter five products of combustion are considered pollutants and are known to, either directly or indirectly, cause harmful affects on humans and the environment [9].

1.2 Gas Turbines

1.2.1 Overview

A gas turbine extracts energy from a flow of hot gas produced by combustion of gas or fuel oil in a stream of compressed air. It has an upstream air compressor (radial or axial flow) mechanically coupled to a downstream turbine and a combustion chamber in between. "Gas turbine" may also refer to just the turbine element.

The principle of gas turbine engine is shown in Figure 1.4. Energy is released when compressed air is mixed with fuel and ignited in the combustor. The resulting gases are directed over the turbine's blades, spinning the turbine, and mechanically powering the compressor. Finally, the gases may pass through a nozzle, generating additional thrust by accelerating the hot exhaust gases by expansion back to atmospheric pressure. Generating mechanical power from a power turbine or thrust from a nozzle depends on the commercial usage of the gas turbine unit. Energy is extracted in the form of shaft power, compressed air and thrust, in any combination, and used to power aircraft, trains, ships, electrical generators. A CAD drawing for the gas turbine engine is shown in Figure 1.5.

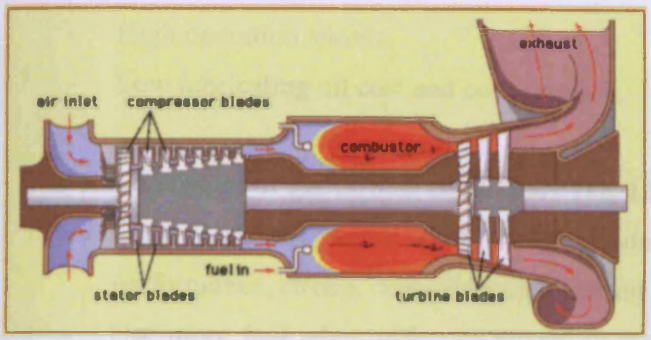

Figure 1.4: Gas turbine cycle principle [10]

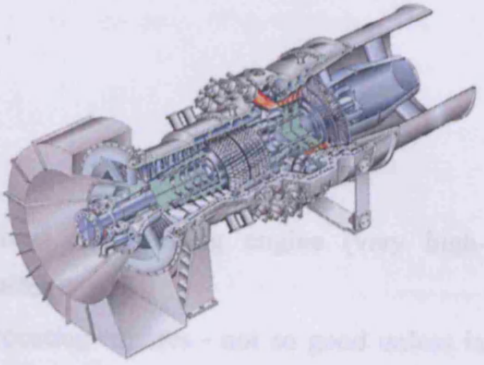

Figure 1.5: Gas turbine engine [11]

The use of gas turbine technology has substantially grown during the last century. It has wide applications in both stationary power generation and aircraft sectors. Furthermore gas turbine technology has steadily advanced since its inception in the early 1900s and continues to evolve specially after the second world war. The manufacture of gas turbines is now a major industry in most of highly industrialized nations of the world. Research has been active in design, production and development of gas turbines. In recent years, the research has refocussed to studying the visibility of using a new alternative fuels whilst recognizing the emissions and environmental aspects. The use of computers in analysis and design, specifically CFD software, allows a wide diversity in studying and comparing different choices of design and fuel varieties.

Gas turbine technology has steadily advanced since its inception and continues to evolve; research is active in producing ever smaller gas turbines. Computer design, specifically CFD and finite element analysis along with material advances, has allowed higher compression ratios and temperatures, more efficient combustion, better cooling of engine parts and reduced emissions. On the emissions side, one challenge in technology is actually getting a catalytic combustor running properly in order to achieve single digit NOx emissions to cope with the latest regulations, although other methods also prove promising. Additionally, compliant foil bearings were commercially introduced to gas turbines in the 1990s. They can withstand over a hundred thousand start/stop cycles and eliminated the need for an oil system [12].

The advantages of gas turbine engines can be summarized as follows [12, 13]:

- Very high power-to-weight ratio, compared to reciprocating engines (i.e. most road vehicle engines);
- Smaller than most reciprocating engines of the same power rating;
- Rotates in one direction only, with far less vibration than a reciprocating engine, so very reliable;
- Simpler design.

- Low operating pressures.
- High operation speeds.
- Low lubricating oil cost and consumption.

The disadvantages of gas turbine engines are [12, 13]:

- Cost is much greater than for a similar-sized reciprocating engine (very high-performance, strong, heat-resistant materials needed);
- Use more fuel when idling compared to reciprocating engines - not so good unless in continual operation.

These disadvantages explain why road vehicles, which are smaller, cheaper and follow a less regular pattern of use than tanks, helicopters, large boats and so on, do not use gas turbine engines, regardless of the size and power advantages imminently available.

1.2.2 Combustion in Gas Turbine

Gas turbine engines for power generation and propulsion applications have traditionally used diffusion-flame combustors because of their reliable performance and reasonable stability characteristics. Unfortunately, this type of combustor usually produces unacceptably high levels of thermal NOx. The increasingly strict regulation for pollutant emissions has recently led engine manufacturers to develop combustors that meet various regulatory requirements [14, 15]. New concepts for combustion technology have been introduced to the gas turbine industry, including lean-premixed (LPM) combustion (or lean-premixed prevaporized (LPP) combustion when liquid fuels are employed), rich-burn quick-quench lean-burn (RQL) combustion, and catalytic combustion [16, 17]. Among these three methods, RQL techniques are hampered by soot formation and incomplete mixing between fuel-rich combustion products and air. Catalytic combustion suffers from challenges associated with cost, durability and safety. Lean-premixed (prevaporized) combustion appears to be the most promising technology for practical systems at the present time (note that for aero-engine gas turbines using liquid fuels, lean direct injection (LDI) combustion is often adopted for pollution control because of its superior stability behavior). In LPM combustion, the fuel and air are premixed upstream of the combustor to avoid the formation of stoichiometric regions. The combustion zone is operated with excess air to reduce the flame temperature; consequently, thermal NOx is virtually eliminated [18].

Lean premixed combustion is often chosen as the principle strategy to reduce pollutants produced in such devices (mainly NOx,, CO and UHC), but with ever more stringent emissions regulations a more thorough understanding of combustor design becomes increasingly

necessary. An intrinsic feature of all premixed combustion systems is a tendency toward flashback.

The basic principle involved in flame stabilization is quite simple. If combustion is initiated in a flowing stream, and if the gas velocity is higher than the flame speed, the flame moves downstream, while if the flame speed is higher than the gas velocity, the flame moves upstream [19, 20].

Flashback constitutes an obstacle for lean premixed technology for fuels have high burning velocity such as hydrogen rich fuels, which makes it one of the gas turbine industry priority issues that needs attention. Flashback can cause a system failure as shown in Figure 1.6. A new burner assembly is shown in the same figure for comparison.

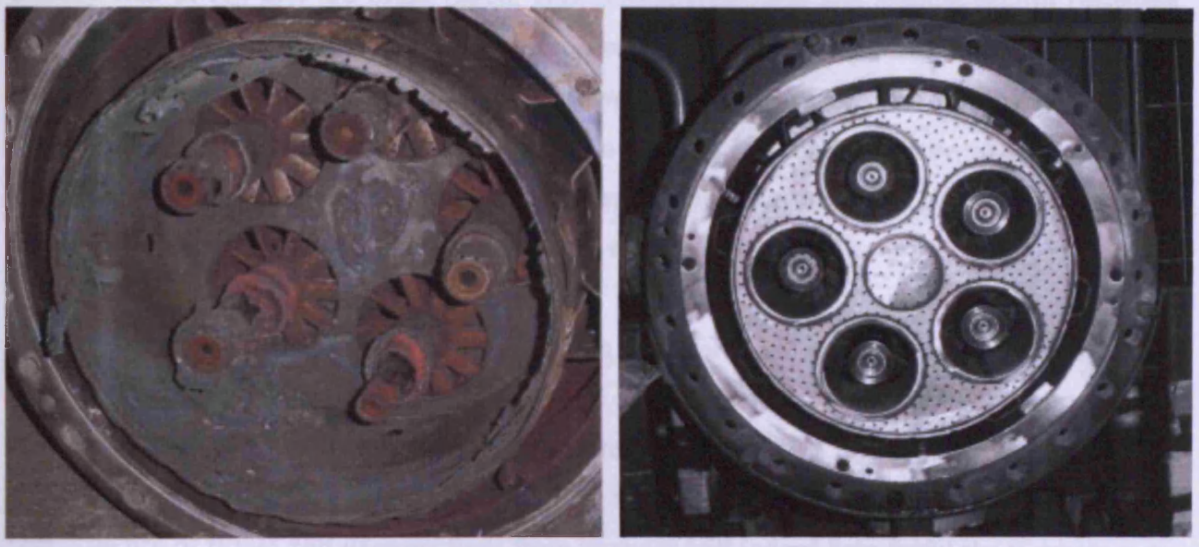

Fig. 1.6: Burner assembly (left) damaged by combustion instability and new burner assembly (right) [21].

1.2.3 Gas Turbines Fuels

The most dominant fuel issues of today are those of cost and availability. After 1973, the price of crude oil rapidly increased three to four times. This major price change had a market impact on the economy of the industrial nations. It is now generally accepted that the availability of previously abundant high grade crudes is decreasing and will probably fail to meet the demand sometimes in the future. So, the diminishing of world fossil fuel reserve and the pollution problems resulted from its use, specially its effect on the global warming, opens the way to extend the using of alternative clean fuels and energies.

The increased use of gas turbines for power generation is accompanied by the need to use some more cost-effective alternative fuels with a wide range of heating value. In the past kerosene was the main fuel of gas turbines but recently natural gas replaced kerosene in most stationary gas turbines. Although natural gas is the primary fuel for most stationary gas turbine engines nowadays, there is growing interest, due to ever-increasing natural gas prices, in burning alternative fuels. These alternative fuels, including coal-derived syngas (synthetic fuel gas), biomass and landfill gases, and liquefied natural gas (LNG). They are usually significantly different from natural gas in terms of physical and chemical properties. For example, syngas obtained from gasification of coal is typically a mixture of methane (CH_4), hydrogen (H_2), and carbon monoxide (CO), with smaller amounts of CO_2 and N_2. Advanced power systems based on the integrated gasification combined cycle (IGCC) technology have been developed utilizing syngas as the primary fuel. The composition of syngas, however, can vary widely depending on the source and processing technique. Refineries and chemical plants produce by-product gases, usually rich in H_2, that are often flared. Biomass-derived fuels and sewage/landfill off-gases represent another economical energy source. For the longer term, methane and hydrogen are among the candidate fuels now being considered. Methane combustion is of great interest, because its low molar ratio of carbon to hydrogen signifies that it can generate power with fewer greenhouse gas emissions. Lean turbulent methane combustion has great potential for reduced NOx emissions in spark ignition engines and gas turbines [18, 22, 23].

The ability to effectively burn these fuels in gas turbines will provide substantial cost advantages, while minimizing adverse effects on the environment. The economical end environmental benefits are an immediate motivator to develop fuel flexible gas turbine systems capable of using many different fuels containing various blends of hydrogen and hydrocarbons [22]. The use of liquid and gaseous fuels from biomass will indeed help fulfill the Kyoto targets concerning GHG emissions. In addition, to make industrial processes more environmentally friendly, waste gases could be used as a potential gas turbine fuel [24]. The change in fuel type and composition usually leads to significant changes in the characteristic time scale of chemical reactions in the combustion system, which consequently has a major impact on combustion operability, including flashback, auto-ignition, lean blowout, and combustion dynamics [18]. Developing fuel-flexible combustion systems capable of burning a variety of fuels without significantly altering combustor operability and performance is a motivation for extensive research work.

1.3 Modelling of Combustion

During the last three decades, computational fluid dynamics (CFD) has emerged as an important element in professional engineering practice, cutting across several branches of engineering disciplines. That was due to the growth in the processing speed with which arithmetic operations can be performed on a computer.

Computational fluid dynamics (CFD) is concerned with numerical solution of differential equations governing transport of mass, momentum, and energy in moving fluids. CFD activity emerged and gained prominence with availability of computers in the early 1960s. Today, CFD finds extensive usage in basic and applied research, in design of engineering equipment, and in calculation of environmental and geophysical phenomena. Since the early 1970s, commercial software packages (or computer codes) became available, making CFD an important component of engineering practise in industrial, defence, and environmental organizations [25].

For a long time, design (as it relates to sizing, economic operation, and safety) of engineering equipment such as heat exchangers, furnaces, cooling towers, internal combustion engines, gas turbine engines, hydraulic pumps and turbines, aircraft bodies, sea-going vessels, and rockets depended on painstakingly generated empirical information. The same was the case with numerous industrial processes such as casting, welding, alloying, mixing, drying, air-conditioning, spraying, environmental discharging of pollutants, and so on. The empirical information is typically displayed in the form of correlations or tables and figures among the main influencing variables.

The main difficulty with empirical information is that it is applicable only to the limited range of scales of fluid velocity, temperature, time, or length for which it is generated. Thus, to take advantage of economies of scale, for example, when engineers were called upon to design a higher capacity power plant, boiler furnaces, condensers, and turbines of ever larger dimensions had to be designed for which new empirical information had to be generated all over again. The generation of this new information was by no means an easy task. This was because the information applicable to bigger scales had to be, after all, generated via laboratory-scale models. This required establishment of scaling laws to ensure geometric, kinematic, and dynamic similarities between models and the full-scale equipment. This activity required considerable experience as well as ingenuity, for it is not an easy matter to simultaneously maintain the three aforementioned similarities. The activity had to, therefore, be supported by flow-visualization studies and by simple (typically, one-dimensional) analytical solutions to equations governing the phenomenon under consideration. Ultimately, experience permitted

judicious compromises. Being very expensive to generate, such information is often of a proprietary kind. In more recent times, of course, scaling difficulties are encountered in the opposite direction. This is because electronic equipment is considerably miniaturised and, in materials processing, for example, the more relevant phenomena occur at microscales (even molecular or atomic scales where the continuum assumption breaks down). Similarly, small-scale processes occur in biocells [25].

Combustion problems are among the most complex that CFD codes are used to solve because they usually involve complicated geometries and fluid dynamics, heat transfer, and chemical reactions. As the complexity of the problem increases, so do the number of iterations required to get a converged solution. The large number of grid-points and complicated physics often equate to long computational times [26].

It is desired to use CFD to design new combustion equipment because it is often much cheaper and faster than building prototypes that are usually tested first under controlled laboratory conditions before trying them out in the actual field installations. Furthermore, it is also desired to use CFD to guarantee the performance of combustion equipment because it may difficult to test the equipment in every conceivable type of application. CFD can be used to dramatically reduce the cycle times for developing new products. It can be also used to simulate the processes under hazardous conditions.

The quantitatively correct numerical simulation of turbulent reacting gas flows is currently one of the most challenging problems, particularly in the context of low emission combustion. Advances in computing has led to significantly improved combustion models, but a key difficulty still remains in the elaboration of physical and chemical models.

1.4 Aims of the Thesis

One of the most important technologies used in gas turbine combustors is the swirl lean premixed combustion. It provides the initial stability and flexibility for the system. Lean premixed combustion enables techniques that can be used to minimize the impact and production of NOx. Combustion instability in lean-premixed combustion systems remains a substantial challenge for designers. The focus of this research is concentrated on the flashback limits of the flame and how can these limits be improved. CFD combustion simulation is used to determine the stability limits for various fuels and experimental measurements are used to validate the model.

The aims of this work can be introduced as follows:

- To enhance the techniques that can be used for reducing the combustion emissions and pollutants. These techniques such as:
  - Lean premixed combustion which can be used for reducing NOx emissions,
  - CO_2 recirculation or using syngas (the gas resulted from biomass gasification and contains CO_2, CO, and H_2) that can be used for reducing CO_2 emissions, and
  - Using H_2 as a new clean fuel and can be used for reducing both NOx and CO_2 emissions.
- To study the main problem of premixed combustion that is recognized as flame flashback.
- To reduce the existence of flashback in practical swirl burner by using burner nozzle modifications.
- To define the stability limits for flames. These limits are recognized by defining the normal combustion and flashback zones with respect to mixture mass flow rates at various equivalence ratios.
- To study the effect of operating pressure and air preheat temperature on the stability limits.
- Trying to improve the stability limits of methane by adding CO_2 to the fuel.
- Introducing H_2 as a promising clean fuel and improving its stability by using hybrid mixture with CH_4, the main component of natural gas. This hybrid fuel can be considered as an environment friendly fuel.
- To implement CFD simulation as a guide to the experimental work to gain the advantages of modelling regarding cost, time, ... etc.

1.5 Structure of the Thesis

In this thesis, CFD analysis is used to highlight the flashback problem which occurs by using premixed combustion in gas turbines. Methods are suggested to improve the stability limits of premixed flames.

The thesis consists of eight chapters. These chapters are organized as follows:

Chapter1 outlines the current world energy consumptions and future trends and needs. The environmental requirements and restrictions are shown. The principles of gas turbine are introduced. The general aspects of combustion in gas turbine and the fuels used are mentioned.

The importance of modeling combustion is clarified. The aims of the research work are stated and the thesis structure is outlined.

Chapter 2 describes the combustion technology in gas turbines. The lean premixed combustion is introduced as a promising technique for emissions reduction but it is hindered by stability problems. Swirl combustion is mentioned as flame stabilizing technique. The general aspects of swirl combustion are presented. The stability problem and the flashback definitions are presented in the context of discussing the causes of flashback and instability. CO_2 dilution is introduced as a new technique that can be used for stabilizing fuels of high flame speeds. H_2/CH_4 mixtures are mentioned as a promoted fuel that can be used in existing gas turbine systems and so the effect of the mixing percentage on flame stability is studied in this research.

Chapter 3 identifies the principle of computational fluid dynamics. The advantages of using CFD modeling are highlighted. Laws of fluid motion are presented. Planning the CFD analysis is shown. Turbulence models and combustion models are surveyed. Fluent as a CFD code that is used for the simulation is discussed. Due to the importance of laminar flame speed in combustion modelling, a general review of the methods used for calculating the laminar flame speed of methane and hydrogen and their blends are presented.

Chapter 4 describes the design of combustion system used in this research. The model development, model quality, calculation parameters and the numerical description of the original combustion system are described. The CFD analyses for the original system are performed based on experimental data produced by the working team in the research centre. The effect of turbulence on flashback is illustrated.

Chapter 5 presents the swirl burner. Both partial and full flashbacks are defined. Two modifications for the swirl burner are suggested with different nozzle geometries. The modifications are aimed to eliminate the partial flashback. Both modifications are simulated and compared with the original swirl model with different operating conditions. The effect of combustion operating conditions (pressure, mixture temperature, equivalence ratio and, mixture mass flow rate) on flashback are studied and stability limits of flames are determined. Also, the size and shape of the recirculation zone associated region of high turbulence are studied as they are critical to flame stability, combustion intensity and performance.

In ***Chapter 6***, the stability limits of CH_4 flames are determined at various operating conditions. The modified swirl burner model is used to determine the stability limits for methane flames. The feasibility of improving the stability limits of methane flame by diluting an amount of CO_2

in the fuel is studied for premixed flames. The flashback limits are modelled for pure CH_4 and with addition of CO_2 up to 30%. Experimental measurements are performed to determine the stability limits of CH_4 at the atmospheric conditions. The measurements are compared with the CFD simulation findings. Also the effect of CO_2 addition to CH_4 combustion is studied experimentally at the atmospheric conditions. The stability limits of CH_4 with the addition of CO_2 of 15 and 30% by volume are measured and compared with the model results. Also the effect of using turbulence plates upstream is examined.

In ***Chapter 7*** two main topics are considered; the first is the determination of laminar flame speed for H_2/CH_4 blends and the second is the determination of stability limits of such blends. The laminar flame speed was calculated for H_2/CH_4 blends from pure methane up to pure hydrogen at various pressures, temperatures and equivalence ratios by using two methods in the literature. A new approximation for laminar flame speed of H_2/CH_4 blends based on the gravimetric mixture ratio was suggested and compared with the previous calculations. The Flashback limits are determined for H_2/CH_4 blends ranging from 0% (pure methane) up to 100% (pure hydrogen) based on the volumetric composition at atmospheric pressure and 300 K. Three combustion regimes for H_2/CH_4 blends are defined. The stability limits of methane-dominated combustion (up to 50% blends of methane and hydrogen) has been extensively studied at different pressures and temperatures to show the effect of the combustion conditions on H_2/CH_4 blends flame stability. Experimental measurements are performed at the atmospheric conditions to determine the stability limits for H_2/CH_4 flames. Two blends are used with H_2 contents of 0.15 and 0.30 in the fuel. The measurements are used to validate the CFD simulation findings. Also, the effect of mixing H_2 and CH_4 on the stability limits is recognized.

Chapter 8 concludes the findings of this work and recommends future research topics in this research field.

Chapter 2

COMBUSTION TECHNOLOGY IN GAS TURBINES

2.1 Introduction

The gas turbine combustor is a complex combustion device within which there exists a wide range of coupled, interacting physical and chemical phenomena. The combustion performance and emissions are mainly influenced by the combustion technique and fuel type. In the design of gas turbine combustors, effort must be made to ensure that combustion is virtually 100% efficient whilst emissions are minimal. Also it must be ensured that combustion can be sustained over the entire range of engine operating conditions, including the transient states of rapid acceleration and deceleration. Efficient combustion must be maintained in a highly turbulent air stream flowing at velocities that greatly exceed the normal burning velocity of the fuel. Furthermore, the flame must stay alight during the various abnormal conditions that sometimes are encountered during combustion.

Lean premixed combustion (LPMC) is currently considered one of the most promising concepts methods to reduce pollutant emissions, particularly NOx emissions. Lean premixed (LPM) gas turbine combustion has considerable advantages in terms of allowing lower overall flame temperatures, whilst smearing the flame and combustion processes over larger volumes.

Combustion instability remains a critical issue limiting the development of low-emission, lean-premixed gas turbine combustion systems. Most gas turbines and other combustion systems use swirl as a method of flame stabilization. Swirling flows can in themselves generate several different types of flow and flame stability. Strong efforts are currently undertaken for the numerical simulation of swirl-stabilized flames with the intentional use for the design of improved gas turbine combustors.

In this chapter, the concept of using lean premixed combustion to reduce the emissions in gas turbines is discussed and it is shown that LPMC is encountered by instability problems. The stability problem and the flashback definitions are presented in the context of discussing the causes of flashback and instability, whilst discussing methods of alleviation. Swirl flows and combustion are discussed with a review of the research work in the area.

As a new technique that can be used for stabilizing hydrogen rich fuel mixes, CO_2 dilution is introduced. Previous researchers observed that the laminar flame speed decreases when the CO_2 dilution rate increases with methane combustion and thus these studies are continued for a variety of fuel mixes in this thesis in the context of practical swirl burners.

Hydrogen fuel mixes can give substantial advantages in terms of emission reduction and thus are being extensively studied at the moment as they allow existing equipment to be used with alternative fuels with minimal redesign and modification. The main problem with hydrogen is its high flame speed and its high tendency to flashback. H_2/CH_4 mixtures are being widely promoted for use in existing gas turbine systems so here the effect of the mixing percentage on flame stability is studied.

2.2 Premixed Combustion and gas turbines

Satisfactory combustion is attained when the exhaust flow products are clean and non toxic, and contain the appropriate level of excess air (up to 100%) to give the required inlet temperature to the turbine section of the gas turbine (typically up to 1400°C for the latest generation of power systems). Furthermore, the combustion system shouldn't make an excessive noise. The quality of combustion is controlled by the proportioning of fuel and air, mixing and combustion in the burner head, dilution air, and available space in which combustion can be completed [9].

There are different methods of distributing the fuel and oxidizer required for combustion to a flame; diffusion flame and premixed flame. In diffusion flames, oxygen and fuel diffuse into each other; where they meet the flame occurs. Candle flames are diffusive in nature and operate through melting and evaporation of the candle wax which rises in a laminar flow of hot gas which then mixes with surrounding oxygen and combusts. In premixed flames, the oxygen and fuel are premixed beforehand, which results in a different type of flame. The best example of this type of flame is the common Bunsen flame, in which the premixed gases flow up a burner tube at a rate which exceeds the normal burning velocity of the mixture, a steady flame being maintained above the burner top [27].

In the early 1970's, when emission controls were first introduced, the pollutant of primary concern to regulators shifted to NOx. For the relatively low levels of NOx reduction initially required, the injection of water or steam into the combustion zone produced the required reduction in NOx emissions with minimal performance impact. In addition, the emissions of other pollutants (CO, VOC) did not increase significantly. To comply with the greater NOx reduction requirements imposed during the 1980's, further attempts were made to utilize

increased quantities of water/steam injection to ensure compliance. These attempts proved detrimental to cycle performance and part lives, and the emission rates for other pollutants also began to rise significantly. Other control methodologies needed to be developed, which led to the introduction of the LPM combustor [28].

Premixed combustion has been extensively researched in the last decade. At the same time, gas turbines have been promoted to the fore front of power generation. There has been a strong interest in achieving lean premixed combustion in many practical applications for power generation such as stationary and other gas turbines. The Gas Turbine Association defines Lean Premix Stationary Combustion Turbine as "Lean premixed stationary combustion turbine means any stationary combustion turbine designed to operate at base load with the air and fuel thoroughly mixed to form a lean mixture before delivery to the combustor". Mixing may occur before or in the combustion chamber. A lean premixed turbine may operate in diffusion flame mode during operating conditions such as startup and shutdown, low or transient loads and cold ambient conditions. The advantages of operating at lean mixture conditions are high thermal efficiency and preventing local "hot spots" within the combustor volume that can lead to significant NOx formation which means low emissions of NOx due to lower flame temperatures [28, 29].

Combustion instabilities are commonly encountered in the development of LPM gas-turbine engines. Most LPM gas-turbine engines utilize swirling flows to stabilize the flame for efficient and clean combustion. One of the most important flow features produced by a swirl injector is a central toroidal recirculation zone (CTRZ), which serves as a flame stabilization mechanism. Flows in this region are, in general, associated with high shear rates and strong turbulence intensities resulting from vortex breakdown. Although this type of flow has been extensively studied, there remain many unresolved issues, such as swirl generation, vortex breakdown, axisymmetry breaking, and azimuthal instability. In particular, the effect of flow swirl on combustion dynamics has not been well studied, at least in a quantitative sense [20, 30].

2.3 Combustion Stability and Flashback Problem

An intrinsic feature of all premixed combustion systems is a tendency toward flashback. For practical combustors flashback is defined as fast chemical reaction, accompanied by significant heat release, in the premixed section of the combustor, owing to upstream propagation of a flame from the main combustion zone [19].

Flashback is also a concern as the central recirculation zone can extend back around the fuel injector to the burner backplate, thus increasing the risk of flashback [20, 31-33]. If the Central Recirculation Zone (CRZ) does extend back to the injector, this can leave thick layers of carbonaceous deposit on the injector surfaces, reducing the efficiency and increasing maintenance requirements. Flashback is an important issue in lean premixed combustion systems that use hydrogen as an additive fuel due to the widely varying flame speeds of the mixtures considered. As such, the effect of fuel composition variation upon flashback depends upon the corresponding change in local flame speed, both laminar and turbulent [34].

Flashback occurs when the gas velocity becomes smaller than the burning velocity and the flame propagates upstream into the premixer passages. Since these passages cannot withstand high temperatures, hence hardware damage occurs [35-37]. In swirling flows, in particular, several potential modes of flashback can occur [38, 39]. The first mode is that of flashback in the boundary layer due to the low velocities. The second mode refers to flashback in the core flow. The two modes take place when local burning velocity exceeds the flow velocity, allowing the flame to propagate upstream into the premixer passages. In some cases, flashback can occur even though the local flame velocity is less than the flow velocity. The flame can cause the vortex upstream to breakdown and this creates a negative flow region to form ahead of it (due to adverse pressure gradients) which causes it to advance further upstream. This phenomenon is referred to "combustion induced vortex breakdown" and is caused by the temperature ratio across the flame [38, 40]. Lieuwen et al. concluded further that "combustion induced vortex breakdown" is not influenced by the chemical kinetic characteristics of the mixture [41]. Furthermore, Noble and coworkers related this phenomenon to the pressure rise upstream of the flame due to the divergence of the upstream flow caused by the inclined flame front [42]. In general, flashback is greatly influenced by the variations in fuel composition that affect the combustion properties of the mixture, notably, the local burning velocity [43].

2.3.1 Types of Flashback

Two main types of flashback have been identified: the first type is the flashback occurring in the free stream and the second type is the flashback occurring through the low velocity flow in the boundary layer along the surfaces of the flame holder, any support struts, and walls of the premixing section.

The most obvious free stream mechanism would involve flashback due to a flow reversal in the bulk flow through the combustor. This flow reversal could be a result of compressor surge, a large disturbance due to foreign object passing through the engine, or combustion instability.

Flashback can also occur in the absence of flow reversal if the turbulent flame speed through the gas in the premixing section is greater than the local bulk velocity. Lean combustion tends to reduce flame speeds, but other factors associated with the engine cycle, such as high temperatures, pressures, and turbulence levels, and preignition reactions in the gas due to appreciable residence times at high temperature levels, cause increase flame speed. Therefore, flame speed may be sufficiently high to necessitate increasing minimum allowable velocity in premix section to unacceptable levels so as to avoid anticipated disturbances of the combustion process [19].

The boundary layer mechanism involves flashback through retarded flow in a boundary layer. Important relevant parameters include the wall temperature and temperature distribution and boundary layer structure, turbulence, and thickness.

Generally, flashback can be initiated by the four following causes, [39, 44-46]:

- Flame propagation in the boundary layer,
- Turbulent flame propagation in the core flow,
- Violent combustion instabilities, and
- Combustion induced vortex breakdown (CIVB).

i. Flashback in the Boundary Layer

This type of flashback is often predominant in non-swirling low-turbulence flows due to low flow velocities in the boundary layer which promote the upstream flame propagation whereas the heat loss to the wall can cause flame quenching [44]. For laminar flows, Lewis and von Elbe [47] balance the velocity gradient g_v at the wall with the laminar flame speed S_L divided by the quenching distance d_q, that is defined as the critical size that the inflamed volume must attain to propagate unaided, as the flashback criterion.

$$g_v = \left.\frac{\partial u}{\partial r}\right|_R = \frac{S_L}{d_q} \qquad 2.4.1$$

According to equation (2.4.1) a critical velocity gradient $g_v < (S_L/d_q)$ leads to upstream flame propagation near the wall. In order to generalize the experimental results, a dimensionless relation was proposed as a flashback criterion [48]. In this framework, the balance of the downstream convective transport and the upstream flame propagation with heat loss to the wall is expressed in terms of Peclet numbers. The velocity gradient is replaced by an average velocity and a characteristic length scale. Although the theories can also be formally applied to turbulent boundary layers, it is known that the same criteria do not apply in the turbulent case.

The critical velocity gradient is much higher than the laminar one, since the axial turbulent diffusion above the laminar sub-layer increases the flame speed [37].

ii. Turbulent Flame Propagation in the Core Flow

If the turbulent burning velocity exceeds the local flow velocity in the core flow, flashback is the consequence. The turbulent burning velocity depends on the chemical kinetics and the turbulence structure, i.e., the length scales and the local velocity fluctuations. Many studies on the correlation of the turbulent burning velocity with the turbulent velocity fluctuations in the flow have been published. However, the results obtained from different correlations scatter widely and the proper determination of turbulent flame velocities remains a challenging task because of the complex interaction of turbulence and chemistry [44].

Swirling flames have a highly wrinkled and corrugated structure, which increases the flame surface considerably above the surface of a laminar flame. Mainly this effect is responsible for the increase of the turbulent flame speed above the laminar value. Whether distributed reaction zones or even well stirred local zones are of strong significance under gas turbine conditions could not be demonstrated yet. If these effects exist, they have an additional effect on the turbulent flame propagation. Turbulent burning velocities show a correlation with the laminar flame speed. This implies that, while burning fuels with high laminar burning velocities, burners with a low turbulence level are more appropriate than high swirl designs in order to give a sufficient margin against flashback [49].

For stable fuels like natural gas at moderate mixture temperatures, flashback in the core flow is less critical even in highly turbulent flows due to the low laminar flame speed. A simple design rule for the optimum safety against flame propagation in the main flow is to avoid local zones of low axial flow velocity and wake regions in the mixing zone [48].

iii. Flashback due to Combustion Instabilities

Combustion instabilities can be responsible for the upstream flame propagation, both in the boundary layer and in the core flow. The driving force for noise and pulsations in gas turbine combustion systems is the fluctuating heat release of the reacting mixture in the primary zone. Four different mechanisms can contribute to the noise spectrum peaks. First of all, the turbulent noise produces a background noise level. This broad-band excitation can be considerably amplified at the eigenfrequencies of the combustion system so that they produce distinct pulsation. Swirling flows particularly tend to form natural coherent flow structures like precessing vortex cores [50] or vortices generated near the transition from the mixing section

into the combustion chamber. This second physical phenomenon can result in flow oscillations at specific Strouhal numbers even in the isothermal flow and leads to an amplification of the combustion noise if the excitation meets an eigenfrequency of the system. The third driving mechanism are forced coherent flow structures. They are observed if the flow instabilities respond to the triggering by velocity perturbations with subsequent phase-locking. The classical mode of unstable self-excitation is the fourth potential cause of pulsations.

High amplitudes of periodic flow velocity fluctuations at the burner exit, as a result of the mentioned instability mechanisms, lead to a periodic displacement of the reaction zone. The consequence is a periodic variation of the burner pressure loss, which again incites the oscillations. This feedback loop finally leads to periodic flashbacks. Pulsation initiated flashback requires a high pulsation level to occur, which is far beyond the acceptable noise levels of combustion systems. This kind of flashback can be interpreted as the final terminating step of a highly unstable combustion process after sufficient amplification [44].

iv. Combustion-Induced Vortex Breakdown (CIVB)

Many gas turbine burner designs follow the basic philosophy to stabilize the flame in the combustion chamber and to avoid reaction within the burner. Burners with a centerbody or fuel lance provide a recirculation zone on the axis even without swirl. However, imposing swirl on the main flow leads to a strong amplification of the backflow of hot gases and a better flame stabilization. An advantage of designs with centerbody is that the swirl level can be selected over a wide window, which is primarily limited by the propagation of the vortex breakdown upstream and the formation of a recirculation zone around the centerbody [44].

Experimental flashback studies with CIVB are focused on burners without fuel lances in the center of the mixing zone. The design of swirlers without centerbody requires a thorough tailoring of the swirling flow, since the flame holding capability depends entirely on the vortex breakdown without the aid of a bluff body. It can be shown that in tubular flows axial profiles with a jet on the axis are required for a stable transition of the vortex flow into its annular form in the combustion chamber. It is well known that a reduction of the swirl around the vortex core by friction or an abrupt change in the cross section leads to a pressure rise on the axis. The positive pressure gradient reduces the axial velocity in the vortex core, which at the same time effects radial transport of angular momentum. Therefore the vortex core grows and again supports the positive pressure gradient. These effects govern the transition of the vortex from its closed into its annular form [44].

The formation of the vortex breakdown strongly depends on the geometry and the distribution of the axial and circumferential velocity. When the inlet swirl-number increases, the central recirculation zone due to the vortex breakdown moves upstream and eventually overrides the wake recirculation zone. A higher swirl number tends to increase the turbulence intensity and the flame speed, and consequently shorten the flame length. However, excessive swirl can cause the central recirculating flow to enter into the inlet annulus and leads to the occurrence of flame flashback [30]. If the swirl number exceeds a critical value, the recirculation zone is able to extend itself throughout the entire mixing section. It is shown subsequently for the first time that even if the swirl number is well adapted to prevent this effect in the isothermal flow, the chemical reaction can nevertheless lead to a breakdown of the flow, combined with an upstream flame propagation. This effect could be observed in the present work as a characteristic flashback mechanism in swirling flows and henceforth will be called combustion-induced vortex breakdown.

2.3.2 Methods of Flame Stabilization

Flame stabilization is one of the important subjects in combustion research, and many efforts have been made on this problem. As illustrated in Figure 2.1, conventional ways to stabilize flame in a high-speed stream are to insert a bluff body and to use its rear stagnation region with recirculation of hot burned gas or to use an opposing jet to stabilize combustion in its stagnation region of low-velocity. The pressure loss in the main stream, however, is significantly large because the drag force is proportional to the square of its velocity. To avoid this difficulty, one can use a recess wall or a step and a pilot flame. The flame, however, is prone to blow-off because the flow in the wall recess or the pilot flame is disturbed directly by the main stream; the hot recirculating gas in the wall recess or the pilot flame is strongly perturbed by strong velocity fluctuations of the main stream [51].

Another well known method for flame stabilization is by using swirl burners. Swirling flows may affect flame dynamics in two aspects. First, large scale unsteady motions arising from shear-layer instability and vortex breakdown, as well as precession of vortex core (PVC), may couple resonantly with acoustic waves in the combustor, and subsequently cause combustion instabilities. Second, flow swirl may alter the flame structure and combustion intensity, and as a consequence influence the heat-release behavior in a combustion chamber. The ensuing effects on the stability characteristics could be substantial. Several attempts have been conducted to investigate the effect of swirl on the flow and flame dynamics in combustion systems [30]. The recirculation zone created by swirl effect is shown in Figure 2.2. The recirculation bubble plays an important role in flame stabilization by providing a hot flow of recirculated combustion

products and a reduced velocity region where the flame speed and floe velocity can be matched. The size and shape of the recirculation zone and associated region of high turbulence are critical for flame stability, combustion intensity and performance. More details about swirl flows are discussed in the following section.

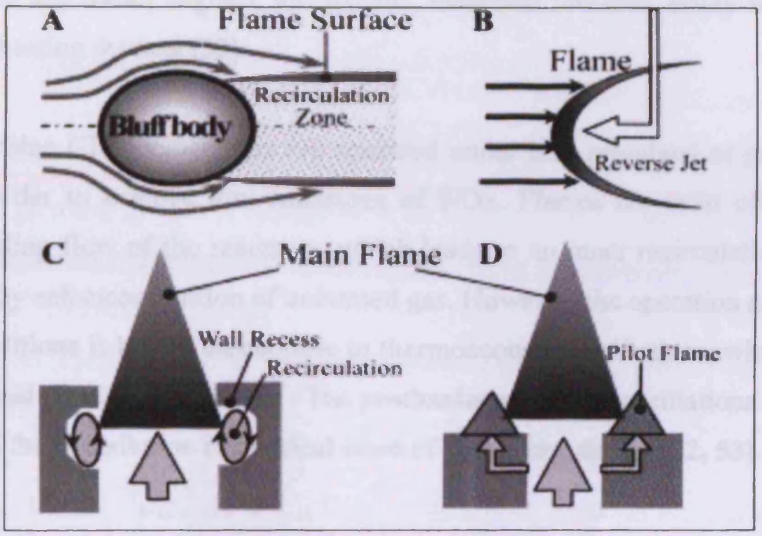

Figure 2.1: Methods of flame stabilization, (A) bluff body, (B) opposing jet, (C) recess wall, and (D) pilot flame.

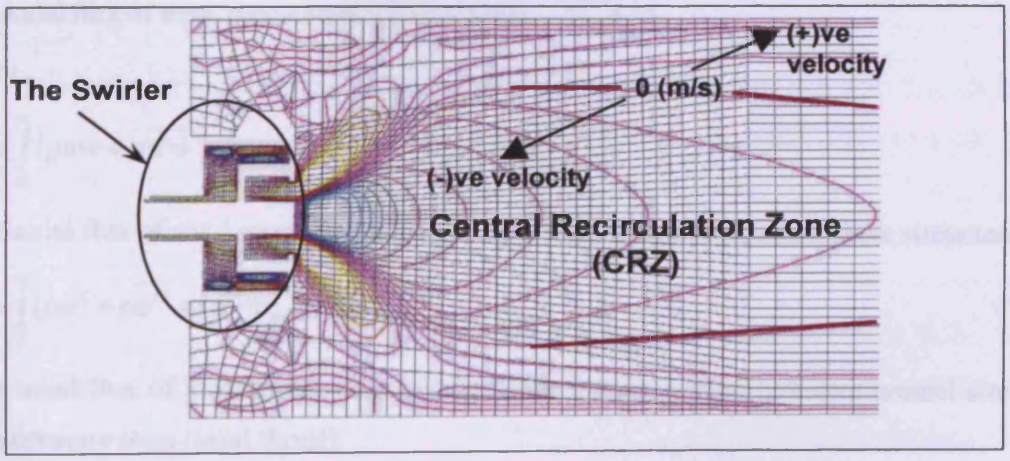

Figure 2.2: Axial velocity profile for swirl flow

2.4 Swirl Flow

2.4.1 Overview

Swirl Flows are important. They are found in nature and are utilized in a very wide range of reacting and non reacting applications. In combustion systems, the strong favourable effect of applying swirl to injected air and fuel are extensively used as an aid to stabilization of the high intensity combustion process and efficient clean combustion in a variety of practical situations such as gasoline and diesel engines, gas turbine, industrial furnaces, utility boilers, and many other practical heating devices [20].

Modern gas turbine (GT) combustors are operated under lean premixed or partially premixed conditions in order to achieve low emissions of NOx. Flames are most often stabilized by inducing a swirling flow of the reactants, which leads to an inner recirculation of hot burned gases and thereby enhances ignition of unburned gas. However, the operation of GT combustors under such conditions is highly susceptible to thermoacoustic oscillations, which may strongly affect lifetime and reliability of the GT. The mechanisms of these oscillations are still not well understood, and their prediction is a critical issue of combustor design [52, 53].

Swirl combustors and burners are usually characterized by the degree of swirl which is introduced by the swirl number (S). It is a non-dimensional number representing axial flux of swirl momentum divided by axial flux of axial momentum, times the equivalence nozzle radius [20, 54]. That is:

$$S = \frac{\text{Axial flux of angular momentum}}{\text{Axial flux of axial momentum} \times \text{Exit Radius}} = \frac{G_\theta}{G_x.d/2} \qquad 2.4.1$$

where

$$G_\theta = \int_0^\infty (\rho uw + \rho\overline{u'w'})\, r^2 dr \qquad 2.4.2$$

is the axial flux of swirl momentum, including the x-θ direction turbulent shear stress term.

$$G_x = \int_0^\infty (\rho u^2 + \rho\overline{u'^2} + (p - p_\infty))\, r\, dr \qquad 2.4.3$$

is the axial flux of axial momentum and includes the x direction turbulent normal stress term and a pressure term (axial thrust)

d/2 = nozzle radius

u, v, w = velocity components in (x, r, θ) cylindrical polar coordinate directions.

2.4.2 Generation and Effect of Swirling Flows

The three main principles of generating swirl flows are [20]:

1. Tangential entry swirl generator.
2. Guided vanes.
3. Direct Rotation.

The swirl generation method determines the size and behaviour of the Reverse Flow Zone (RFZ) and other vortex breakdown characteristics which very considerably depending on the method used [55] and hence the efficiency of the device.

The efficiency of the swirl generation is defined as the ratio of the angular kinetic energy at the burner throat to pressure drop between the air inlet and the throat. Axial vane swirlers have low efficiencies at high swirl, although this can be improved by profiling the vanes. Tangential entry and radial swirler have efficiencies about 70 to 80% [56]. A compilation of efficiencies is given by Syred and Beer [54]. In general strong evidence of high swirl phenomena is unusual with axial vane type swirlers.

As the degree of swirl is increased the effects of inlet flow swirl on the subsequent flow field produced are increasingly dramatic. The effects of introducing swirl on turbulent jets are to cause an increase in width, rate of entrainment and rate of decay of the jet. These effects increase with increasing degree of swirl. The degree of swirl can be classified as follows [20]:

- Very weak swirl ($S \leq 0.2$)
- Weak Swirl ($S \leq 0.4$)
- Strong swirl ($S \geq 0.6$)

For very weak swirl ($S \leq 0.2$), swirl velocities decay rapidly with downstream distance and axial sub-pressure, sub atmospheric pressure may occur. Hence a small adverse axial pressure gradient may occur on the axis and the weakly swirling boundary layer jet flows retain their main characteristics. This adverse pressure gradient is not enough to cause axial recirculation.

For weak swirl ($S \leq 0.4$), the axial velocity distribution remains Gaussian in form, with the maximum velocity on the axis of the jet. Although there may be significant lateral (or radial) pressure gradient given at any axial station from the pressure distribution resulting from the swirl motion, they do not give rise to more than a slight longitudinal (or axial) pressure gradient. Jet growth, entrainment and decay are enhanced progressively as the degree of swirl is increased.

For strong swirl ($S \geq 0.6$), strong radial and axial pressure gradients are set up near the nozzle exit, resulting in axial recirculation in the form of a Central Toroidal Recirculation Zone (CTRZ). The CTRZ, when it occurs, is in addition to any CRZ that may be provoked by the sudden expansion in cross sectional area. The precise effect is found to depend on many factors as well as the swirl number, e.g. nozzle geometry and size of the enclosure.

The effect of strong swirl in particular can be extensively used as an aid to efficient clean combustion in a variety of practical situations, e.g. gasoline engines, diesel engines, gas turbines, industrial furnaces. Highly advantageous features of strong swirling vortex region that help to meet many combustor performance requirements are:

- Reduction of combustion length because of high rates of entrainment of ambient fluid, fast mixing close to the nozzle and near recirculation zone boundaries.
- Improved flame stability because of the presence of a CTRZ, which recirculates hot, chemically active, combustion products.
- Minimized maintenance and extended life of equipment, since the blockage is aerodynamic and flame impingement on the solid surfaces is minimized, for example, compared with bluff body method.

2.4.3 Previous Work in Swirl Combustion

Swirl burners have been used for the combustion of various fuels over 200 years ago. They have been used to burn coal efficiently from around 1920 where suspension firing of pulverized coal became the preferred method of combustion in utility boilers. Pulverized coal is premixed with small quantities of primary and secondary air and staging applied to increase the recirculation zone near the burner exit to improve the overall combustion efficiency and reduce the NOx emissions.

The effect of swirl does allow the flow to be aerodynamically staged. This may produce an area of fuel rich combustion at high temperature at the centre near the exit of the swirl generator. Here, most of the NOx formed is reduced back to N_2 by reducing radicals present. Outside this zone there is an area of fuel lean combustion in which the final burnout occurs. The burner thus causes less pollution and higher combustion efficiencies.

Higher degrees of swirl result in high stability limits for combustion and may allow the combustion of very low calorific value fuels without the aid of additional fuels. These fuels may have previously been released into atmosphere causing pollution or, more recently, burned in combination with costly higher calorific value fuels in which case further emissions are produced. In both cases valuable energy is wasted.

Early work on the swirl phenomenon has been reported by Alexander [57] and Iinoya [58], they did their research on cyclones and introduced some description for the cyclone characteristics and pressure drop. Vonnegut [59] described the vortex whistle. He revealed that an unconfined swirling jet emitted a characteristic note varied with flow rate. Chanaud [60] followed them and tried to explain the vortex whilstle. The formation of the inner recirculation zone (IRZ) results from vortex breakdown of the swirling flow was described in [20, 61, 62]. An important aspect of this phenomenon is the occurrence of large-scale coherent structures such as the Precessing Vortex Core (PVC). The PVC is an unsteady vortex located in the shear layer of the IRZ that precesses around the central axis. Syred and Beer [63] first defined the term (PVC) and carried out intensive studies on the phenomenon. The vortex core is represented by the point of zero velocity in the tangential flow. It does not remain close to the central axis as experimental work as revealed. Syred et al. found a PVC under reacting conditions and discussed its effect of increased mixing [64]. Fick [65] studied the characterization and the effects of the PVC in swirl burner/furnaces systems for both combusting and isothermal flows. He used PIV and LDA measurements and defined a correlation between the input flow rate and the frequency of precession. Vanoverberghe [33] investigates the interaction between flow structure, turbulence characteristics and combustion phenomena of partially premixed natural gas flames that issued from an annular swirl burner.

The occurrence and role of PVCs under combustion conditions is a complex issue and strongly depends on mode of fuel entry, equivalence ratio and combustor geometry [66]. Only few experimental studies have addressed the interaction of flame and PVC, and the mechanisms are largely unclear. Schildmacher and Koch reported the presence of a PVC under isothermal conditions which disappeared for the reacting case with same flow conditions [67]. Li et al. proposed that a PVC is the main factor driving the combustion instability in a swirl-dump combustor [68]. Stöhr [52] found that the averaged flow field with inner and outer recirculation zones is typical of swirl-stabilized flames, and the instantaneous measurements show the presence of a helical vortex (PVC) located in the inner shear layer. The PVC, which usually rotates with a different frequency than any thermoacoustic oscillation, leads to an enhanced mixing of burned and unburned gas and thus to stabilization of the flame.

The efficient combustion of low calorific value gas and poor quality fuels using swirl combustion was studied by Syred et al. [54, 69, 70]. A major problem arising when dealing with low calorific value fuels is the flame stabilization. Gupta et al. [71] used a multi-annular swirl burner which had a wider stability limits, turn down ratio, volumetric heat release rate etc. compared to the conventional single annular tangential entry (or vane type) swirl flame

stabilizer. Grinstein et al. [72] simulated the flow dynamics in a swirl combustor with either a single or triple swirlers. Emphasis was placed on the effect of inlet conditions (including swirl number, inlet length, and characteristic velocity) on the unsteady flow dynamics in the combustors.

Tangirala et al. [73] studied the influence of swirl and heat release on the flow structures and flame properties in a non-premixed swirl burner. Their results showed that mixing and flame stability can be improved by increasing the swirl number up to approximately unity, further increases in swirl actually reduced the turbulence levels and flame stability. Excessive swirl also had the disadvantage of forcing the flame to move upstream to a position closer to the burner walls, resulting in excessive wall heating.

Broda et al. [74] and Seo [75] performed an experimental study of combustion dynamics in a lean-premixed swirl-stabilized combustor. The dominant acoustic motion corresponds to the first longitudinal mode of the chamber. An increase in swirl number tends to decrease the instability amplitude. Stone and Menon [76, 77] investigated a swirl-stabilized combustor flow and studied the impact of varying swirl and equivalence ratio on flame dynamics.

Huang et al. [30, 78-81] investigated stable flame evolution, the flame bifurcation phenomenon, and unstable flame dynamics for a fixed inlet swirl number but with different inlet flow conditions. They numerically investigated the effect of inlet swirl on the flow development and combustion dynamics in a lean-premixed swirl-stabilized combustor using a large-eddy-simulation (LES) technique along with a level-set flamelet library approach. They studied the effect of swirl on flow development, acoustic properties, and flame evolution; and investigated the interactions between turbulent flame dynamics and flow oscillations. Their results indicate that when the inlet swirl number exceeds a critical value, a vortex-breakdown-induced central toroidal recirculation zone is established in the downstream region. In their system as the swirl number increases further, the recirculation zone moves upstream and merges with the wake recirculation zone behind the centerbody. Excessive swirl may cause the central recirculating flow to penetrate into the inlet annulus and lead to the occurrence of flame flashback. A higher swirl number tends to increase the turbulence intensity, and consequently the flame speed. As a result, the flame surface area is reduced. The net heat release, however, remains almost unchanged because of the enhanced flame speed. Transverse acoustic oscillations often prevail under the effects of strong swirling flows, whereas longitudinal modes dominate the wave motions in cases with weak swirl. The ensuing effect on the flow/flame interactions in the chamber is substantial.

2.5 CO_2 Addition to Methane Flames

2.5.1 Advantages of Adding CO_2 to Methane Combustion

Recently, the addition of significant amounts of CO_2 into the fresh gases of premixed combustion in stationary gas turbine has become an important research topic. There are several reasons that urge adding CO_2 to gaseous fuels such as methane. The first reason is related to fuel flexibility issues. In order to diversify fuel resources and to move away from fossil fuels, gas turbines can be fed by gaseous fuels containing CO_2. Such fuels may have several origins such as biogas generated from the anaerobic digestion of biomass organic waste or industrial waste gases containing hydrogen and CO_2 [24]. The second reason for popularizing CO_2 addition studies in turbulent premixed combustion is the reduction of NO_x emissions by using flue gas recirculation (FGR) technique. The external recirculation of the hot product gases enables the reduction of flame temperature and therefore NOx emissions [82]. When exhaust gas recirculation (EGR) is used in IC engines, a flame is formed under conditions of not only low oxygen concentration but also under conditions of high pressure and high temperature because the mixture is compressed before combustion. It is therefore supposed that EGR of IC engines has features similar to those of so-called high-temperature air combustion (HiTAC). Turbulent flames under HiTAC conditions with reduced oxygen concentration are characterized by a time-averaged heat release region. It is therefore expected that if turbulent flame characteristics under HiTAC conditions are realized at high pressure, the stable operation of premixed-type gas-turbine combustors will be possible [83]. It is also expected that by reducing the heat release rate in the combustion chamber, the stable flame regime can be extended to mixtures with lower equivalence ratios. This turbulent combustion regime is therefore close to the so called extended or distributed combustion zone regime [84]. Another reason which prompted the investigation of CO_2 addition studies is related to carbon capture and sequestration technologies in large thermal plants. The present carbon capture technologies are best applicable when the CO_2 concentration in the fuel gases is above a threshold of the order of 15% by volume. Therefore, internal or external recirculation of CO_2 in gas turbines is envisaged in order to increase the CO_2 concentration and ease the application of carbon capture technologies at reduced cost [6, 84]. For all these reasons it is necessary to properly understand the effects of CO_2 addition in premixed combustion.

2.5.2 Previous Work on CO_2 Addition to Flames

Some studies have been made recently to study the effect of CO_2 dilution in methane combustion. Most of these studies are concerned with the effect of CO_2 addition on burning

velocity. One of the first studies in this area was conducted by Gelfand et al. [85] with lean H_2–CO_2–air premixed flames. They used a spherical bomb experimental setup, which enabled them to collect flame velocity data at a maximum pressure of 0.5 MPa and turbulence intensity up to 10 m/s. Their results show that turbulent premixed flames in the mixtures diluted with CO_2 exhibit turbulent quenching The flame speed increases initially with turbulence up to a point where this speed decreases just prior to quenching of the flame The extinction limits in turbulent flames of hydrogen-air-carbon dioxide mixtures were at concentrations of hydrogen and carbon dioxide close to the limiting concentrations obtained in the experiments with laminar flames. The variation of initial pressure from 0.1 to 0.5 MPa did not affect the turbulent combustion rate.

A recent comprehensive work on this topic is that of Kobayashi et al. [83, 86] with CH_4–CO_2–air flames. The mixture was preheated up to 573 K and the maximum pressure is 1 MPa. The main results from this work are that the turbulent burning velocity, S_T, normalized using laminar burning velocity, S_L, became smaller when the mixture was diluted with CO_2. They also realized that the combustion intensity S_T/S_L and the mean fuel consumption rate decrease with the CO_2 dilution ratio. The results imply that exhaust gas recirculation for high-pressure, high-temperature turbulent premixed flames is effective for restraining combustion oscillation of premixed-type gas-turbine combustors.

Other works on CO_2 diluted flames [82, 87-89] concern mainly counterflow diffusion flames. These studies have shown that CO_2 dilution implies a decrease of the flame temperature, and consequently that of the thermal NO formation. Finally all studies observed that the laminar flame speed decreases when the CO_2 dilution rate increases. The methodology developed in this study is to keep parameters under control by changing one parameter at a time and work under conditions close to gas turbine operation modes and parameters.

Cohe′ et al. aimed in their work [84, 90] to contribute to the characterization of fuel lean CH_4–CO_2–air premixed laminar and turbulent flames at different pressures and CO_2 addition rates by studying laminar and turbulent flame propagation velocities, the flame surface density and the instantaneous flame front wrinkling parameters. They studied the pressure effects on the flame structure. They derived an experimental data set for CO_2 added to laminar CH_4/air flames using an axisymmetric Bunsen type burner. Their analysis shows that although the height of the turbulent flame increases with the CO_2 addition rate, the flame instantaneous structure is quite similar for all CO_2 addition rates. This implies that the flame wrinkling parameters and flame surface density are indifferent to the CO_2 addition. However, the pressure increase has a drastic effect on both parameters. This is also confirmed by a fractal analysis of instantaneous images.

It is also observed that the combustion intensity S_T/S_L increases both with pressure and the CO_2 addition rate. Finally, the mean fuel consumption rate decreases with the CO_2 addition rate but increases with the pressure.

In this thesis, the focus of the research is concentrated on the factors that affect flashback limits of the flame. The effect of mixture mass flow rate, equivalence ratio, pressure and temperature are studied. Also the effect of adding CO_2 to CH_4 flame flashback is studied.

2.5.3 Combustion Equation with CO_2 Addition

The stoichiometric combustion of hydrocarbon in air is described by the following equation:

$$C_xH_y+\left(x+\frac{y}{4}\right)(O_2+3.76N_2)\rightarrow xCO_2+\left(\frac{y}{2}\right)H_2O+3.76\left(x+\frac{y}{4}\right)N_2 \qquad 2.5.1$$

For CO_2 added to hydrocarbon/air flames, the stoichiometric burning equation of hydrocarbon with diluted CO_2 is:

$$(1-\beta)C_xH_y+\beta CO_2+(1-\beta)\left(x+\frac{y}{4}\right)(O_2+3.76N_2)\rightarrow xCO_2+(1-\beta)\left(\frac{y}{2}\right)H_2O+3.76(1-\beta)\left(x+\frac{y}{4}\right)N_2 \qquad 2.5.2$$

where β is the CO_2 mole fraction in the fuel diluted with CO_2 i.e., β is defined as:

$$\beta=\frac{n_{(CO_2)}}{n_{(C_xH_y)}+n_{(CO_2)}} \qquad 2.5.3$$

For excess air combustion with α excess air parameter, the global combustion reaction is:

$$(1-\beta)C_xH_y+\beta CO_2+(1-\beta)\left(x+\frac{y}{4}+\alpha\right)(O_2+3.76N_2)\rightarrow xCO_2+(1-\beta)\left(\frac{y}{2}\right)H_2O+3.76(1-\beta)\left(x+\frac{y}{4}\right)N_2+(1-\beta)\left(x+\frac{y}{4}+\alpha\right)(O_2+3.76N_2) \qquad 2.5.4$$

The air to fuel ratio (AFR) for the combustion with excess air for hydrocarbon with diluted CO_2 can be calculated in mass base as:

$$AFR=\frac{(1-\beta)\left(x+\frac{y}{4}+\alpha\right)(32+3.76\times 28)}{(1-\beta)\times(12x+y)+\beta\times 44} \qquad 2.5.5$$

For CO_2 added to CH_4/air flames, the combustion equation becomes:

$$(1-\beta)CH_4 + \beta CO_2 + (1-\beta)(2+\alpha)(O_2 + 3.76N_2) \rightarrow CO_2 + (1-\beta)(2)H_2O + 3.76(1-\beta)(2)N_2 + (1-\beta)(2+\alpha)(O_2 + 3.76N_2) \quad 2.5.6$$

AFR for stoichiometric combustion (α=0) for CH_4 with diluted CO_2 can be calculated on a mass basis as:

$$AFR_{st} = \frac{(1-\beta)(2)(32+3.76\times 28)}{(1-\beta)\times(16)+\beta\times 44}$$

$$AFR_{st} = \frac{274.56(1-\beta)}{16(1-\beta)+44\beta} \quad 2.5.7$$

For example,

- for pure CH_4 combustion: ($\beta = 0$) , $AFR_{st} = 17.16$
- for (85% CH_4 + 15% CO_2): ($\beta = 0.15$) , $AFR_{st} = 11.55$
- for (70% CH_4 + 30% CO_2): ($\beta = 0.30$) , $AFR_{st} = 7.88$

2.6 Hydrogen Combustion

2.6.1 Introduction

Hydrogen shows considerable promise as a primary energy carrier for the future. First it can be produced directly from all primary energy resources, enabling energy feedstock diversity for the transportation sector. These alternative energy resources include wind, solar power, and biomass (plant material), which are all renewable fuel sources. H_2 can be produced directly through electrolysis of water or thermo-chemical cycles [22, 91]. While this process is not economically attractive at current cost, if the electricity required to convert H_2O to H_2 is provided by wind or solar power, then the H_2 is produced without creating CO_2. Given the intermittent nature of wind and solar power sources, surplus energy produced during very windy or bright sunny days could be used to produce H_2 that is stored for later use. Under these conditions the stored H_2 becomes an energy carrier that can be used later to produce power where it is needed, either in conjunction with a fuel cell to produce electricity or in the combustor to produce power by gas turbines or internal combustion engines.

Alternatively, H_2 can be produced through coal gasification, or by steam reforming of natural gas, both of which are non-renewable fossil fuels but are abundantly available throughout the world. Combining the latter technologies with carbon capture and storage would provide a significant increase in sources of clean burning H_2 while at the same time eliminating green gas emissions [22].

2.6.2 H_2/CH_4 Combustion

Methane combustion is of great interest, because of its low molar ratio of carbon to hydrogen signifies that it can generate power with fewer greenhouse gases emissions. But there are two problems in using lean methane combustion: a large increase in misfires and a substantial decrease of laminar burning velocities (S_L). Several attempts have been made to lessen these two problems, such as using higher ignition energy or stratified combustion. Though these attempts can certainly improve lean premixed combustion performance to some extent, to burn even leaner mixtures at higher burning velocities requires other methods. This motivates the hydrogen addition, because H_2 has a very low lean flammability limit with high burning velocities [92].

Hydrogen–methane blends are receiving attention as alternative fuels for power generation applications for two main reasons. The first reason is related to the opportunity of adding hydrogen to methane in order to improve performance, to extend operability ranges and to reduce pollutant emissions of lean combustion in both stationary and mobile systems [93]. The second reason is due to concerns about global warming and the prospect of using hydrogen in both fuel cells and combustion devices [94-97]. However, stringent problems of safety and storage strongly complicate the use of pure hydrogen. To bypass these difficulties, substitution of hydrogen with methane or other hydrocarbons has been proposed as an interim solution towards a fully developed hydrogen economy [98].

Karim et al. [99] and Nagalingam et al. [100] found that the performance of a spark ignition engine fuelled with methane can be improved significantly through mixing some hydrogen with the methane. The output power and engine indicated efficiency increase with the increase of hydrogen percentage in the mixture, while the exhaust gas concentrations of CO, CO_2 are decreased. However they found an increase in NOx emissions due to high temperatures in the engine, not unexpectedly.

2.6.3 Technical Challenge for H_2 Combustion in Gas Turbine

The higher flame speeds found with H_2 as a fuel could require some design modifications for optimum gas turbine combustor performance. Since flames typically stabilize, or anchor, in regions where the local flow velocity is near the local flame speed, the higher flame velocities may have to be taken into account in both combustor geometry and the manner in which the premixed reactants are introduced.

The laminar flame speed for pure hydrogen is very high compared with the laminar flame speed of methane at the same conditions. For example, at the standard temperature and pressure (STP) and an equivalence ratio of 0.6, the laminar flame speed of H_2 is about 1 m/s while for methane is about 0.1 m/s. So, the use of H_2 may require combustor modifications since the flame stabilization location is largely determined by flow mechanics (i.e., where low velocity, recirculation regions are established). The higher flame speed of H_2 may tend to flashback which could lead to significant overheating and damage to the premixer and other engine hardware.

2.6.4 H_2 Combustion Research Work

The laminar burning velocity of hydrogen and hydrogen–methane/air premixed flames may be considered as the most important parameter to be studied in hydrogen combustion. It has been experimentally measured at different values of equivalence ratio and fuel composition. In 1959, Scholte and Vaags [101] carried out the first measurements by means of the tube burner method. Together with the more recent work by Liu et al. [102], this is the most extensive experimental study since it investigates a wide range of equivalence ratios at hybrid fuel compositions varying from pure methane to pure hydrogen. All the other experimental papers may be classified into two categories: the first deals with the study of the effect of hydrogen addition to methane [102-106] and the second with the effect of substitution of hydrogen by methane [98, 107].

Chiesa et al. [91] studied the possibility to burn hydrogen in a large size, heavy-duty gas turbine designed to run on natural gas as a possible short-term measure to reduce greenhouse emissions of the power industry. They applied some strategies and recommended the usage of H_2 in gas turbine with little modifications in the system.

Schefer et al. [108-110] and Wicksall et al. [111] studied the combustion characteristics of a premixed, swirl-stabilized flame to determine the effects of enriching methane with hydrogen under fuel-lean conditions. The results show that the addition of a moderate amount of hydrogen to the methane/air mixture increased the peak OH concentration. Hydrogen addition resulted in a significant change in the flame structure, indicated by a shorter and more robust appearing flame. Also, hydrogen addition significantly improves flame stability and allows stable burner operation at the lean fuel/air ratios needed for reduced NOx emissions.

Jackson et al. [112] studied experimentally and numerically the influence of H_2 on the response of lean premixed CH_4 flames. Furthermore, Kido et al. [113] used a small amount of hydrogen

as an additive to improve turbulent combustion performance of lean hydrocarbon mixtures. They correlated turbulent burning velocities, S_T, with pressure–time measurements in an explosion-type burner, similar to the explosion bomb used by Bradley and co-workers at Leeds University [114]. Though the aforementioned studies have shown the advantages of hydrogen addition for lean premixed methane turbulent combustion, such as the increase of burning velocities, the extension of lean flammability limit of methane combustion, and the reduction of unburned hydrocarbons, several unresolved problems still remain.

Many studies are concerned on the measurement of flame velocities, laminar and turbulent, experimentally or analytically. The results of this work are discussed in the next chapter. Other studies are performed on many other aspects such as the effect of hydrogen addition on methane combustion characteristics and ignition temperature [115-117], non-premixed hydrogen flames [118].

2.6.5 Combustion Equation for Hybrid H_2/CH_4 Fuel

If H_2 is combusted in air the stoichiometric combustion equation for H_2 become:

$$H_2 + \left(\frac{1}{2}\right)(O_2 + 3.76N_2) \rightarrow H_2O + \frac{3.76}{2}N_2 \qquad 2.6.1$$

The stoichiometric combustion equation for CH_4 is:

$$CH_4 + (2)(O_2 + 3.76N_2) \rightarrow CO_2 + (2)H_2O + 3.76(2)N_2 \qquad 2.6.2$$

For hybrid H_2/CH_4 fuel, the stoichiometric burning equation is:

$$(1-\gamma)C_xH_y + \gamma H_2 + [(1-\gamma)\left(x+\frac{y}{4}\right)+\frac{1}{2}\gamma](O_2 + 3.76N_2) \rightarrow (1-\gamma)xCO_2 + [(1-\gamma)\left(\frac{y}{2}\right)+\gamma]H_2O + 3.76[(1-\gamma)\left(x+\frac{y}{4}\right)+\frac{1}{2}\gamma]N_2 \qquad 2.6.3$$

where γ is the H_2 mole fraction in the hybrid fuel consists of H_2 and CH_4 i.e., γ is defined as:

$$\gamma = \frac{n_{(H_2)}}{n_{(C_xH_y)} + n_{(H_2)}} \qquad 2.6.4$$

AFR for stoichiometric H_2/CH_4 combustion can be calculated on a mass basis as:

$$AFR_{st} = \frac{[(1-\gamma)(2)+\frac{1}{2}\gamma](32+3.76\times 28)}{(1-\gamma)\times(16)+\gamma\times 2}$$

$$AFR_{st} = \frac{274.56(1-0.75\gamma)}{16-14\gamma} \qquad 2.6.5$$

For example,

- for pure H_2 combustion: ($\gamma = 1$) , $AFR_{st} = 34.32$
- for (15% H_2 + 85% CH_4): ($\gamma = 0.15$) , $AFR_{st} = 17.53$
- for (30% H_2 + 70% CH_4): ($\gamma = 0.30$) , $AFR_{st} = 18.03$

2.7 Summary

In this chapter, a literature survey has been carried out for some important topics related to combustion in gas turbines and associated flame stability. The following can be concluded:

- Lean premixed combustion is considered as one of the most promising concept for substantial reduction of gas turbine emissions, especially NOx, while maintaining high efficiency.
- The main problem for all premixed combustion systems is the instability problem and the tendency of the combustible mixture toward flashback.
- Most of gas turbines use swirl burners to reduce but not eliminate such problems.
- CO_2 dilution in methane combustion is a new research topic. It can be used for NOx emission reduction as a result of reducing the flame temperature. The effect of CO_2 dilution in methane combustion on flashback limits is studied here.
- Hydrogen combustion has attracted much attention recently because of the need for clean alternative energy source. H_2 is a carbon-free energy carrier, so it plays an important role in serving the constraints on greenhouse gas emissions.
- The challenge on using H_2 is its high burning velocity that results in its high tendency to flashback or locating the flame in regions of relative high velocity where methane flames will not stabilize.
- H_2/CH_4 hybrid fuel may have advantages over certain ranges of equivalence ratios.

Chapter 3

COMBUSTION MODELLING BY CFD

3.1 Introduction

The use of computational fluid dynamics (CFD) to predict internal and external flows has risen dramatically in the past decade. The widespread availability of engineering workstations together with the efficient solution of algorithms and sophisticated pre- and post- processing facilities enable the use of commercial CFD codes by graduate engineers for research, development and design task in industry. Increasingly CFD is becoming a vital component in the design of industrial products and processes. Also the rapid progress in generating high-powered super-fast computers helps in creating more efficient CFD software that have higher accuracy and more efficient prediction with lower cost [119].

CFD packages are generally comprised of two programmes, one for geometry drawing, mesh creation and boundaries and zones assignment and the other program for defining the operating conditions, parameters, and materials. Also it contains the solver, fluid mechanic, heat transfer, chemical reactions and combustion calculations and etc. In this investigation the CFD code, FLUENT 6.3.26, was utilised and is the most recent addition to the Fluent series of solvers. The geometry and mesh creation tool used in this study was GAMBIT 2.3.16. Gambit allows physical geometries to be modelled and can mesh them into smaller elements to allow interior flows and heat transfer to be modelled by a finite difference method, as used by Fluent. Geometries are created by constructing a series of major shapes and editing them using the programmes tools and functions to create a single volume. Once a volume has been created it needs to be meshed into smaller elements. Complex geometries such as swirlers can be meshed by dividing its volume to smaller volumes that are connected together. The new small volumes are meshed with the required type and with the suitable number of elements. The more elements contained in the geometry, the more accurate the results will be. However, this will also be more computationally expensive in terms of time and memory.

For this study, there are two models that were needed to be meshed. The first model was for the original combustion system. This model was initially meshed using 800,000 elements. The second model was for swirl burner. The first trial to mesh this model was by using 700,000 elements which consumes about one week for the solution to reach the convergence in the Fluent solver. After many trials and refinements both models were used but now with about

130,000 elements. But for some special cases, for partial flashback, the swirl model is found producing better results with 440,000 elements.

In this chapter, CFD description, how CFD works, and how to plan the simulation work are discussed and the basic CFD governing equations are presented. As there is no single turbulence model that can resolve the physics at all flow conditions, the turbulence models are reviewed. Also the combustion models that are offered by Fluent are surveyed.

The utilization of CFD code "FLUENT" is initially discussed, starting with model preparation (drawing and meshing) by Gambit software, followed by running the solver and settling the boundary conditions, and finally checking the model convergence and stability.

The laminar flame speed is considered as an important modelling variable in combustion. It is required as an input in turbulent combustion modelling. Thus, at the end of this chapter, a general review of the methods used for calculating the laminar flame speed of methane and hydrogen and their blends are presented.

3.2 CFD Definition and Advantages

Computational Fluid Dynamics (CFD) is the analysis of systems involving fluid flow, heat transfer and associated phenomena such as chemical reactions by means of computer based simulation. The technique is very powerful and spans a wide range in industrial and non-industrial application areas such as aerodynamics of aircrafts, hydrodynamics of ships, environmental engineering and combustion in internal combustion engines and gas turbines [119].

The ultimate aim of developments in the CFD field is to provide a capability comparable to the other Computer-Aided Engineering (CAD) tools such as stress analysis codes. The main reason why CFD has lagged behind is the tremendous complexity of the underlying behaviour; at the moment this precludes a complete description of fluid flows and assumptions of time averaged flows is commonly made to give representative solutions that are at the same time economical and sufficiently complete. The availability of affordable high performance computing hardware and the introduction of user friendly interfaces have led to recent upsurge of the interest in CFD for use in many different research and industrial communities.

There are several advantages of CFD over experiment-based approaches to fluid systems design [119]:

- Substantial reduction of lead times and costs of new designs.
- Ability to study systems where controlled experiments are difficult or impossible to perform (e.g. very large systems)
- Ability to study systems under hazardous conditions at and beyond their normal performance limits (e.g. safety studies and accident scenarios)
- Practically unlimited level of detail of results.

The other reasons behind the introduction and increased importance of CFD are [120]:

1. Insight: There are many devices and systems that are very difficult to prototype. Often, CFD analysis shows you parts of the system or phenomena happening within the system that would not otherwise be visible through any other means. CFD gives you a means of visualising and enhanced understanding of your designs.

2. Foresight: Because CFD is a tool for predicting what will happen under a given set of circumstances, it can answer many 'what if?' questions very quickly. You give it variables. It gives you outcomes. In a short time, you can predict how your design will perform, and test many variations until you arrive at an optimal result. All of this is done before physical prototyping and testing. The foresight you gain from CFD helps you to design better and faster.

3. Efficiency: Better and faster design or analysis leads to shorter design cycles. Time and money are saved. Products get to market faster. Equipment improvements are built and installed with minimal downtime. CFD is a tool for compressing the design and development cycle.

4. Cost: Cost of Experimentation- experimentation, the only alternative to simulation is very costly.

5. Practicality: Impossibility of experiments - in some instances, experiments are impossible to conduct. For example, atmospheric nuclear explosions and biomedical situations that would endanger patient life.

6. Computer speed and memory: In 1965, Intel cofounder Gordon Moore made a memorable observation. When he started to graph data about the growth in memory chip performance, he realized there was a striking trend. Each new chip contained roughly twice as much capacity as its predecessor, and each chip was released within 18-24 months of the previous chip. In subsequent years, the pace slowed down a bit, but data density has doubled approximately every 18 months. At the same time, algorithm development continues to improve the accuracy and performance of models.

3.3 How does a CFD code work?

CFD codes are structured around the numerical algorithms that can tackle fluid flow problems. In order to provide easy access to their solving power all commercial CFD packages include sophisticated user interfaces to input problem parameters and to examine the results. Hence all codes contain three main elements: a pre-processor, a solver and, a post-processor.

i. The pre-processor:

Pre-processing consists of the input of a flow problem to a CFD program by means of an operator-friendly interface and the subsequent transformation of this input into a form suitable for use by the solver. The user activities at the pre-processing stage involve [119]:

- Definition of the geometry of the region of interest.
- Grid generation: This means the subdivision of the region (the computational domain) into a number of smaller, non overlapping sub-domains. This process generates a grid (or mesh) of cells (or control volumes or elements)
- Selection of the physical and chemical phenomena that need to be modelled.
- Definition of fluid properties.
- Specification of appropriate boundary conditions at cells which coincide with or touch the domain boundary.

ii. The solver:

There are three distinct streams of numerical solution techniques: finite difference, finite element and spectral methods. In outline the numerical methods that form the basis of the solver perform the following steps [119, 121]:

- Approximation of the unknown flow variables by means of simple functions.
- Discretization by substitution of the approximations into the governing flow equations and subsequent mathematical manipulations.
- Solution of the algebraic equations.

The main differences between the three separate streams are associated with the way in which the flow variables are approximated and with the discretization process.

Finite Difference Method:

Finite difference methods (FDM) describe the unknown ϕ of the flow problem by means of point samples at the node points of a grid of co-ordinate lines. Truncated Taylor series

expansions are often used to generate finite difference approximations of derivatives of ϕ in terms of point samples of ϕ at each grid point and its immediate neighbours. Those derivatives appearing in the governing equations are replaced by finite differences yielding an algebraic equation for the value of ϕ at each grid point.

Finite Element Method:

Finite element methods (FEM) use simple piecewise functions (e.g. linear or quadratic) valid on elements to describe the local variations of unknown flow variables ϕ. The governing equation is precisely satisfied by the exact solution ϕ. If the piecewise approximating functions for ϕ are substituted into the equation it will not hold exactly and a residual is defined to measure the errors. Next the residuals (and hence the errors) are minimised in some sense by multiplying them by a set of weighting functions and integrating. As a result a set of algebraic equations for the unknown coefficients is obtained.

Finite Volume Method:

The Finite Volume Method (FVM) was originally developed as a special finite difference formulation. It is one of the most versatile discretization techniques used in CFD. Based on the control volume formulation of analytical fluid dynamics, the first step in the FVM is to divide the domain into a number of control volumes (aka cells, elements) where the variable of interest is located at the centroid of the control volume. The next step is to integrate the differential form of the governing equations (very similar to the control volume approach) over each control volume. Interpolation profiles are then assumed in order to describe the variation of the concerned variable between cell centroids. The resulting equation is called the discretized or discretization equation. In this manner, the discretization equation expresses the conservation principle for the variable inside the control volume [122].

The most compelling feature of the FVM is that the resulting solution satisfies the conservation of quantities such as mass, momentum, energy, and species. This is exactly satisfied for any control volume as well as for the whole computational domain and for any number of control volumes. Even a coarse grid solution exhibits exact integral balances.

Spectral Method:

Spectral methods approximate the unknown by means of truncated Fourier series or series of Chebyshev polynomials. Unlike the finite difference or finite element approach the approximations are not local but valid throughout the entire computational domain. Again the unknowns are replaced in the governing equation by truncated series. The constraint that leads

to the algebraic equations for the coefficients of the Fourier or Chebyshev series is provided by a weighted residuals concept similar to the finite element method or by making the approximate function coincide with the exact solution at a number of grid points.

iii. The post-processor:

CFD packages are equipped with versatile data visualisation tools. These include:

- Domain geometry and grid display
- Vector plots
- Line and shaded contour plots
- 2D and 3D surface plots
- Particle tracking
- View manipulation (translation, rotation, scaling, etc.)
- Colour postscript output.

3.4 Planning CFD Analysis

When using CFD to look at fluid dynamic problems, it is important to give consideration to the following steps [123]:

1. Definition of the modelling goals – What specific results are required from the CFD model and how will they be used? What degree of accuracy is required form the model?

2. Choice of the computational model - What are the boundary conditions? Can a Two Dimensional model be used or are Three Dimensions required? What type of grid topology is best suited to the model?

3. Choice of physical model - Is the flow inviscid, laminar, or turbulent in nature? Is the flow steady or unsteady? Is heat transfer important?

4. Determination of the solution procedure - How long will the problem take to converge on your computer? Can convergence be accelerated with a different solution procedure?

Consideration of these steps will reduce computer-processing time and contribute to the success of the modelling.

3.5 Conservation Laws of Fluid Motion

The governing equations of fluid flow represent mathematical statements of the conservation laws of physics [25, 26, 119]:

- The mass of fluid is conserved.
- The rate of change of momentum equals the sum of the forces on a fluid particle (Newton's second law).
- The rate of change of energy is equal to the sum of the rate of heat addition and the rate of work done on a fluid particle (first law of thermodynamics).

3.5.1. Mass conservation in three dimensions

The mass balance for a fluid element or the continuity equation states that the rate of increase of mass in fluid element equals to the net rate of flow of mass into fluid element. This can be expressed mathematically by:

$$\frac{\partial \rho}{\partial t} + \frac{\partial(\rho u)}{\partial x} + \frac{\partial(\rho v)}{\partial y} + \frac{\partial(\rho w)}{\partial z} = 0 \qquad 3.5.1$$

Or in more compact vector notation

$$\frac{\partial \rho}{\partial t} + \mathrm{div}(\rho U) = 0 \qquad 3.5.2$$

where

ρ	=	Fluid density
t	=	Time
u, v, w	=	Velocity components in x, y, and z respectively
U	=	Velocity vector

Equation (3.5.2) is the unsteady, three-dimensional mass conservation or continuity equation at appoint in a compressible fluid. The first term on the left hand side is the rate of change in time of the density (mass per unit volume). The second term describes the net flow of mass out of the element across its boundaries and called the convective term.

3.5.2. Momentum Equation

Newton's second law states that the rate of change of momentum of a fluid particle equals the sum of the forces acting on the particle. Applying this to a fluid passing through an infinitesimal, fixed control volume, yields the following equations:

(The x-component of the momentum equation):

$$\rho\frac{Du}{Dt}=\frac{\partial(-p+\tau_{xx})}{\partial x}+\frac{\partial\tau_{yx}}{\partial y}+\frac{\partial\tau_{zx}}{\partial z}+S_{Mx} \qquad 3.5.3.a$$

(The y-component of the momentum equation):

$$\rho\frac{Dv}{Dt}=\frac{\partial\tau_{xy}}{\partial x}+\frac{\partial(-p+\tau_{yy})}{\partial y}+\frac{\partial\tau_{zy}}{\partial z}+S_{My} \qquad 3.5.3.b$$

(The z-component of the momentum equation):

$$\rho\frac{Dw}{Dt}=\frac{\partial\tau_{xz}}{\partial x}+\frac{\partial\tau_{yz}}{\partial y}+\frac{\partial(-p+\tau_{zz})}{\partial z}+S_{Mz} \qquad 3.5.3.c$$

where

P = The static pressure

τ = Viscous stress

τ_{ij} = Viscous stress component acts in the j-direction on a surface normal to i-direction.

S_{Mi} = The body force in i-direction

In a Newtonian fluid the viscous stresses are proportional to the rates of deformation. The three dimensional form of Newton's law of viscosity for compressible flow involves two constants of proportionality: the dynamic viscosity, μ, to relate stresses to linear deformations, and the viscosity, λ, to relate stresses to the volumetric deformation. The viscous stress components are related to μ and λ. By substituting the values of viscous stress in the momentum equations yields the s-called Navier-Stokes equations:

$$\rho\frac{Du}{Dt}=-\frac{\partial p}{\partial x}+\text{div}(\mu\,\text{grad}\,u)+S_{Mx}$$

$$\rho\frac{Dv}{Dt}=-\frac{\partial p}{\partial y}+\text{div}(\mu\,\text{grad}\,v)+S_{My} \qquad 3.5.4$$

$$\rho\frac{Dw}{Dt}=-\frac{\partial p}{\partial z}+\text{div}(\mu\,\text{grad}\,w)+S_{Mz}$$

3.5.3. Energy Equation

The energy equation is derived from the first law of thermo dynamics which states that the rate of change of energy of a fluid particle is equal to the rate of heat addition to the fluid particle plus the rate of work done on the particle.

The rate of increase of energy of a fluid particle per unit volume is given by $\rho\frac{DE}{Dt}$. While the total rate of work done on a fluid particle by a surface force can be expressed as

$$[-\text{div}(\rho U)]+\left[\frac{\partial(u\tau_{xx})}{\partial x}+\frac{\partial(u\tau_{yx})}{\partial y}+\frac{\partial(u\tau_{zx})}{\partial z}\right.$$
$$\left.+\frac{\partial(v\tau_{xy})}{\partial x}+\frac{\partial(v\tau_{yy})}{\partial y}+\frac{\partial(v\tau_{zy})}{\partial z}+\frac{\partial(w\tau_{xz})}{\partial x}+\frac{\partial(w\tau_{yz})}{\partial y}+\frac{\partial(w\tau_{zz})}{\partial z}\right] \quad 3.5.5$$

And the net rate of heat transfer to the fluid particle due to heat conduction across element boundaries: can be written as

$$-\text{div } q = \text{div (k grad T)} \quad 3.5.6$$

If there any source of energy exists with energy S_E per unit volume per unit time, the energy equation will be:

$$\rho\frac{DE}{Dt}=-\text{div}(\rho U)+\left[\frac{\partial(u\tau_{xx})}{\partial x}+\frac{\partial(u\tau_{yx})}{\partial y}+\frac{\partial(u\tau_{zx})}{\partial z}\right.$$
$$\left.+\frac{\partial(v\tau_{xy})}{\partial x}+\frac{\partial(v\tau_{yy})}{\partial y}+\frac{\partial(v\tau_{zy})}{\partial z}+\frac{\partial(w\tau_{xz})}{\partial x}+\frac{\partial(w\tau_{yz})}{\partial y}+\frac{\partial(w\tau_{zz})}{\partial z}\right] \quad 3.5.7$$
$$+\text{div (k grad T)}+S_E$$

3.5.4. General Transport Equation

It is clear that there are significant commonalities between the various equations. If a general variable ϕ is introduced, the conservative form of all fluid flow equations can usefully be written in the following form:

$$\frac{\partial(\rho\phi)}{\partial t}+\text{div}(\rho\phi U)=\text{div}(\Gamma\,\text{grad}\,\phi)+S_\phi \quad 3.5.8$$

In words

Rate of increase of ϕ of fluid element	+	*Net rate of flow of ϕ out of fluid element*	=	*Rate of increase of ϕ due to diffusion*	+	*Rate of increase of ϕ due to sources*

The equation (3.5.8) is the so-called transport equation of property ϕ. It is clearly highlights the various transport processes: the rate of change term and the convective term in the left hand side and the diffusive term (Γ : diffusion coefficient) and the source term respectively on the right hand side.

3.6 Turbulence Modelling

3.6.1 The Nature of Turbulence

When laminar conditions exist, flows can be entirely described by Navier-Stokes equations and a suitable method of closure. With steady flows, the flow will not vary with time and will characterise real flows with Reynolds number below the critical which is specific to each particular case, and which must be determined experimentally.

The study of turbulence is an interdisciplinary activity, which has a very large range of applications. Although most flows occurring in nature and engineering applications are turbulent it is difficult to give a precise definition of turbulence. Turbulent flows are irregular, contain vorticity, three-dimensional and unsteady. According to Hinze [124], "*Turbulent fluid motion is an irregular condition of flow in which the various quantities show a random variation with time and space co-ordinates so that the statistically distinct average values can be discerned*". The characteristics of turbulence depend on its environment. Because of this, turbulence theory does not attempt to deal with all kinds and types of flows in a general way. Instead theoreticians concentrate on families of flows with fairly simple boundary conditions, like boundary layer, jets and wakes.

The first aim of the turbulence theory is the prediction of turbulent flow and properties in various applications. Turbulent flows have been investigated for more than a century, but no general approach to the solution of the problems in turbulence exists. Therefore the theory of turbulence is quite far away from a solution, through the transport equations of fluid mechanics, which are part of the classical fundamental physical laws. One problem is the solution of the non-linear equations, which describe three-dimensional flows without simplification e.g. linearization. The theory of turbulence includes methods of mathematical statistics and probability theory may well relate to the small turbulent scales, which have the best prospect of being universal or quasi-universal.

Turbulent flows are characterised by velocity fields of a fluctuating nature. These fluctuations mix transported quantities such as momentum, energy and species concentration and cause those quantities to fluctuate as well. However, these fluctuations can be of small scale and high frequency and are too computationally expensive to simulate directly. Instead, the exact instantaneous governing equations can be averaged in a number of ways in order to remove the small scales resulting in a set of equations that are less resource consuming to solve. However, these new equations contain a set of unknown variables and turbulence models are needed to determine these new variables in terms of the known quantities [125].

The majority of flows of interest to engineers are turbulent. The minimum scale of this turbulence will generally below the scale of the fluid elements used with CFD modelling, for reasons of economy, as computing power is still a finite resource. Given sufficient resources and time it is possible for a model to be constructed of the most simple of engineering problems with sufficiently small elements and time steps for turbulent flow to be completely described. This method is referred to as Direct Numerical Solution (DNS), and though it could be considered the ideal use of the Navier-Stokes equations. But this method is primarily of academic interest at the moment and not relevant to commercial engineering CFD modelling. To successfully model turbulent flows, a method enabling consideration of the effect of viscous turbulence on the mean flow is necessary.

3.6.2 Turbulence Models

The general questions of turbulent flow are "*what are the characteristics of turbulence motion in turbulent flows?*" and "*Can these characteristics be predicted from equations governing fluid motion?*". Many publications have been produced to answer these questions [124, 126-133]. The conclusion that may be summarized is that we can use some models that can describe the highly approximated behaviour of turbulence motion but there is no general model that is able to solve all the turbulent flow problems. A model which can be described as a very good fit in solving a certain case may fail to solve another case. Many different techniques have been used to address different questions concerning turbulent flows.

A turbulent model is a computational procedure to close the system with mean flow equations so that a more or less wide variety of flow problem can be calculated [119]. For most engineering purposes it is unnecessary to resolve the details of the turbulent fluctuations. Only the effects of the turbulence on the mean flow are usually sought. For a turbulence model to be useful in a general purpose CFD code it must have wide applicability, be accurate, simple and economical to run. The choice of turbulence model will depend on considerations such as the physics encompassed in the flow, the established practice for a specific class of problem, the level of accuracy required, the available computational resources, and the amount of time available for the simulation. To make the most appropriate choice of model for a specific application, it is needed to understand the capabilities and limitations of the various options [123].

The most common turbulence models are [119, 123, 127, 132, 133]:

i. Classical Models: Those are based on (time-average) Reynolds equation:

1. Zero-equation model – mixing length model
2. One-equation model – Spalart-Allmaras model
3. Two-equation model – k-ε model and k-ω model
4. Reynolds stress equation model
5. Algebraic stress model

ii. Large Eddy Simulation (LDS): That is based on space-filtered equations.

The classical models use the Reynolds equations and from the basis of turbulence calculations in currently available commercial CFD codes. These models have a comparatively reduced computational time and are widely adopted for practical engineering applications.

Large Eddy Simulations (LES) are turbulence models where the time dependant flow equations are solved for the mean flow and the largest eddies and where the affects of the smaller eddies are modelled. It was argued earlier that the largest eddies interact strongly with the mean flow and contains most of the energy so this approach results in a good model of the main effects of turbulence. LES are at present at the research stage and the calculations are too costly to merit consideration in general purpose computing at present, although anticipated improvements in computer hardware may change this perspective in the future.

3.6.3 Modelling Turbulent Flows in Fluent

Fluent provides a wide variety of models to suit the demands of individual classes of problems. The choice of the turbulence model depends on the required level of accuracy, available computational resources, and the required turnaround time. The turbulent models available in Fluent 6.3.26 are [123]:

- Spalart-Allmaras model
- k-ε models
  - Standard k-ε model
  - Renormalization-group (RNG) k-ε model
  - Realizable k-ε model
- k-ω models
  - Standard k-ω model
  - Shear-stress transport (SST) k-ω model
- υ^2-f model

- Reynolds stress model (RSM)
- Detached eddy simulation (DES) model
- Large eddy simulation (LES) model

Key features of the commonly used turbulence models available in Fluent are described in the following table [123, 134].

Model	Features	
Spalart-Allmaras model	One-equation model	Designed specially for aerospace applications, involving wall-bounded high speed flows.
Standard k-ε model	Simplest of two-equation models	Robust. Suitable for initial iterations.
(RNG) k-ε model	– Variant of standard k-ε – Has an additional term in ε equation.	Accurate for rapidly strained and swirling flows.
Realizable k-ε model	– Variant of Standard k-ε model – New formulation for turbulent viscosity – New transport equation for ε	Accurate for spreading of both planar and rounded jets. Recommended for flows with boundary layers under strong adverse ∇p, separation and recirculation.
Standard k-ω model	Solves for k-ω ω = Specific dissipation rate (ε/k)	Recommended for low-Re flows, wall bounded boundary layer, and for transitional flows.
(SST) k-ω model	– Variant of Standard k-ω model – Behaves like k-ω in near wall region – Behaves like standard k -ε in the free stream	More accurate and reliable for a wider class of flows, like adverse ∇p in airfoils, transonic shock waves, etc.
Reynolds stress model	– Five-equation model – Avoids isotropic formulation of turbulent viscosity	Suitable for complex 3D flows with strong swirl/rotation. Run time and memory intensive.

3.6.4 Shear-Stress Transport (SST) k-ω model

The most suitable turbulent model for the research in this thesis is the RSM. It is suitable for complex 3D flows with strong swirl. The main problem with this model is the run time to reach convergence. It closes the Reynolds-average Navier-Stokes equations by solving transport equations for the Reynolds stress together with an equation for the dissipation rate. This means that five additional transport equations are required in 2D flows and seven additional transport equations must be solved in 3D. So, for the primary runs here, the RSM is used and the other models are compared with its results. It is found that the closest results to RSM are produced

when using the shear-stress transport (SST) k-ω model. Thus due to the huge number of runs needed, the SST k-ω model is chosen to continue the modelling in the rest of the thesis.

The shear-stress transport (SST) k-ω model was developed by Menter [135]. It is so named because the definition of the turbulent viscosity is modified to account for the transport of the principal turbulent shear stress. It has feature that gives the SST k-ω model an advantage in terms of performance over both the standard k-ω model and the standard k-ε model. Other modifications include the addition of a cross-diffusion term in the ω equation and a blending function to ensure that the model equations behave appropriately in both the near-wall and far-field zones [123].

The SST k-ω model has a similar form to the standard k-ω model. The turbulence kinetic energy, k, and the specific dissipation rate, ω, are obtained from the following transport equations:

$$\frac{\partial}{\partial t}(\rho k)+\frac{\partial}{\partial x_i}(\rho k u_i)=\frac{\partial}{\partial x_j}(\Gamma_k \frac{\partial k}{\partial x_j})+\tilde{G}_k-Y_k+S_k \qquad 3.6.1$$

and

$$\frac{\partial}{\partial t}(\rho \omega)+\frac{\partial}{\partial x_i}(\rho \omega u_i)=\frac{\partial}{\partial x_j}(\Gamma_\omega \frac{\partial \omega}{\partial x_j})+G_\omega-Y_\omega+D_\omega+S_\omega \qquad 3.6.2$$

where

G_k represents the generation of turbulence kinetic energy due to mean velocity gradients. G_ω represents the generation of ω. Γ_k and Γ_ω represent the effective diffusivity of k and ω, respectively. Y_k and Y_ω represent the dissipation of k and ω due to turbulence. D_ω represents the cross-diffusion term. S_k and S_ω are user-defined source terms. Calculations for all previous terms have been fully described in [123].

3.7 Combustion Modelling

During combustion a fuel (e.g. a mixture of hydrocarbons) reacts with an oxidant stream (e.g. air) to form products of combustion. The products are not usually formed in a single chemical reaction; the fuel components and the oxidant undergo a series of reactions. For example, over 40 elementary reactions are involved in the combustion of methane (CH_4), the simplest hydrocarbon fuel. In addition to all flow equations, the transport equations for the mass fraction m_i of each species i must be solved. The species equation can be written down by using the general transport equation [119]:

$$\frac{\partial(\rho m_i)}{\partial t} + \text{div}\,(\rho m_i U) = \text{div}\,(\Gamma\ \text{grad}\ m_i) + S_i \qquad 3.7.1$$

The volumetric rate of generation (or destruction) of a species due to chemical reactions appears as the source (or sink) term S_i in each of their transport equations.

In simple chemical reaction system, infinitely fast chemical reactions are assumed and the intermediate reactions are ignored. The transport equations for the fuel and oxygen mass fraction may be written as:

$$\frac{\partial(\rho m_f)}{\partial t} + \text{div}\,(\rho m_f U) = \text{div}\,(\Gamma_f\ \text{grad}\ m_f) + S_f \qquad 3.7.2$$

$$\frac{\partial(\rho m_o)}{\partial t} + \text{div}\,(\rho m_o U) = \text{div}\,(\Gamma_o\ \text{grad}\ m_o) + S_o \qquad 3.7.3$$

where the subscript "f " refers to fuel and "o" refers to oxidizer.

Under the assumption of equal diffusivities $\Gamma_f = \Gamma_o = \Gamma$, the species equations can be reduced to a single equation for the mixture fraction, f

$$f = \frac{Z_i - Z_{i,ox}}{Z_{i,fuel} - Z_{i,ox}} \qquad 3.7.4$$

where Z_i is the elemental mass fraction for element, i. The subscript "ox" denotes the value at the oxidizer stream inlet and the subscript fuel denotes the value at the fuel stream inlet.
The reaction source terms in the species equations is cancelled, and thus f is a conserved quantity. While the assumption of equal diffusivities is problematic for laminar flows, it is generally acceptable for turbulent flows where turbulent convection overwhelms molecular diffusion.

3.7.1 Combustion Models in FLUENT

FLUENT 6.3.26 provides several models for chemical species transport and chemical reactions. It can model species transport with or without chemical reactions.
FLUENT provides five approaches to modelling gas phase reacting flows [123]:

- Generalized finite-rate model
- Non-premixed combustion model
- Premixed combustion model
- Partially premixed combustion model
- Composition PDF Transport model

i. Generalized Finite-Rate Model

This approach is based on the solution of transport equations for species mass fractions. The reaction rates that appear as source terms in the species transport equations are computed from Arrhenius rate expressions. Chemical kinetic mechanisms can be used from the FLUENT database, can be created, or imported a mechanism in Chemkin format. For turbulent flows, turbulence-chemistry interaction can be ignored using the Laminar Finite-Rate model, or modelled with the Eddy Dissipation [136] or EDC models [137]. The Generalized Finite-Rate Model is suitable for a wide range of applications including premixed, partially premixed, non-premixed turbulent combustion, and ignition delay in diesel engines.

This model is suitable to be used for cases involving the mixing, transport, or reaction of chemical species, or reactions on the surface of a wall or particle (e.g., chemical vapour deposition).

ii. Non-Premixed Combustion Model

In this approach individual species transport equations are not solved. Instead, transport equations for one or two conserved scalars (the mixture fractions) are solved and individual component concentrations are derived from the predicted mixture fraction distribution. This approach has been specifically developed for the simulation of turbulent diffusion flames and offers many benefits over the finite-rate formulation. In the Non-Premixed Combustion Model, turbulence effects are accounted for with the help of an assumed shape Probability Density Function (PDF). Reaction mechanisms are not required; species and temperature can be modelled as in chemical equilibrium. Alternatively, the steady Laminar Flamelet model can include local finite-rate kinetic effects due to straining by the turbulence.

This model is suitable to be used for reacting systems involving turbulent diffusion flames that are near chemical equilibrium where the fuel and oxidizer enter the domain in two or three distinct streams

iii. Premixed Combustion Model

This model can be applied to turbulent combustion systems that are of the purely premixed type. In these problems perfectly mixed reactants and burned products are separated by a flame front. The "reaction progress variable" is solved to predict the position of this front. The influence of

turbulence is accounted for by means of a turbulent flame speed. This model is suitable to be used for cases with a single, perfectly premixed reactant stream.

iv. Partially Premixed Combustion Model

The partially premixed combustion model has been developed for turbulent reacting flows that have a combination of non-premixed and premixed combustion. The mixture fraction equations and the reaction progress variable are solved to determine the species concentrations and position of the flame front, respectively. This model is suitable to be used for cases involving premixed flames with varying equivalence ratio in the domain.

v. Composition PDF Transport Combustion Model

The composition PDF transport model simulates realistic finite-rate kinetic effects in turbulent flames. Arbitrary chemical mechanisms can be imported into FLUENT, and kinetic effects such as non-equilibrium species and ignition/extinction can be captured. This model is suitable for use in turbulent flames where finite-rate chemistry is important. It is applicable to premixed, non-premixed, and partially premixed flames. It is, however, computationally expensive.

3.7.2 Non-Premixed Combustion Modelling

In non-premixed combustion, fuel and oxidizer enter the reaction zone in distinct streams. This is in contrast to premixed systems, in which reactants are mixed at the molecular level before burning. Examples of non-premixed combustion include pulverized coal furnaces, diesel internal-combustion engines and pool fires.

Under certain assumptions, the thermochemistry can be reduced to a single parameter: the mixture fraction. The mixture fraction, denoted by f, is the mass fraction that originated from the fuel stream. In other words, it is the local mass fraction of burnt and unburnt fuel stream elements (C, H, etc.) in all the species (CO_2, H_2O, O_2, etc.). The approach is elegant because atomic elements are conserved in chemical reactions. In turn, the mixture fraction is a conserved scalar quantity, and therefore its governing transport equation does not have a source term. Combustion is simplified to a mixing problem, and the difficulties associated with closing non-linear mean reaction rates are avoided. Once mixed, the chemistry can be modelled as in chemical equilibrium, or near chemical equilibrium with the laminar flamelet model.

The non-premixed modelling approach has been specifically developed for the simulation of turbulent diffusion flames with fast chemistry. For such systems, the method offers many benefits over the eddy-dissipation formulation. The non-premixed model allows intermediate

(radical) species prediction, dissociation effects, and rigorous turbulence-chemistry coupling. The method is computationally efficient in that it does not require the solution of a large number of species transport equations. When the underlying assumptions are valid, the non-premixed approach is preferred over the eddy-dissipation formulation.

Restrictions on the Mixture Fraction Approach

- The chemical system must be of the diffusion type with discrete fuel and oxidizer inlets (spray combustion and pulverized fuel flames may also fall into this category).
- The Lewis number must be unity. (This implies that the diffusion coefficients for all species and enthalpy are equal, a good approximation in turbulent flow).
- When a single mixture fraction is used, the following conditions must be met:
  - Only one type of fuel is involved.
  - Only one type of oxidizer is involved.
- When two mixture fractions are used, three streams can be involved in the system. Valid systems are as follows:
  - Two fuel streams with different compositions and one oxidizer stream.
  - Mixed fuel systems including gas-liquid, gas-coal, or liquid-coal fuel mixtures with a single oxidizer. In systems with a gas-coal or liquid-coal fuel mixture, the coal volatiles and char are treated as a single composite fuel stream.
  - Coal combustion in which volatile and char off-gases are tracked separately.
  - Two oxidizer streams with different compositions and one fuel stream.
  - A fuel stream, an oxidizer stream, and a non-reacting secondary stream.
- The flow must be turbulent.

3.7.3 Premixed Combustion Modelling

In premixed combustion, fuel and oxidizer are mixed at the molecular level prior to ignition. Combustion occurs as a flame front propagating into the unburnt reactants. Examples of premixed combustion include aspirated internal combustion engines, lean premixed gas turbine combustors, and gas-leak explosions.

Premixed combustion is much more difficult to model than non-premixed combustion. The reason for this is that premixed combustion usually occurs as a thin, propagating flame that is stretched and contorted by turbulence. For subsonic flows, the overall rate of propagation of the flame is determined by both the laminar flame speed and the turbulent eddies. The laminar flame speed is determined by the rate that species and heat diffuse upstream into the reactants

and burn. To capture the laminar flame speed, the internal flame structure would need to be resolved, as well as the detailed chemical kinetics and molecular diffusion processes. Since practical laminar flame thicknesses are of the order of millimetres or smaller, resolution requirements are usually unaffordable. The effect of turbulence is to wrinkle and stretch the propagating laminar flame sheet, increasing the sheet area and, in turn, the effective flame speed. The large turbulent eddies tend to wrinkle and corrugate the flame sheet, while the small turbulent eddies, if they are smaller than the laminar flame thickness, may penetrate the flame sheet and modify the laminar flame structure.

Limitations of Using the Premixed Model

The following limitations apply to the premixed combustion model:

- The segregated solver must be used. The premixed combustion model is not available with either of the coupled solvers.
- The premixed combustion model is valid only for turbulent, subsonic flows. These types of flames are called deagrations. Explosions, also called detonations, where the combustible mixture is ignited by the heat behind a shock wave, can be modelled with the finite-rate model using the coupled solver.
- The premixed combustion model cannot be used in conjunction with the pollutant (i.e., soot and NOx) models. However, a perfectly premixed system can be modelled with the partially premixed model which can be used with the pollutant models.
- It cannot be used to simulate reacting discrete-phase particles, since these would result in a partially premixed system. Only inert particles can be used with the premixed combustion model.

Premixed Combustion Theory

Premixed combustion is much more difficult to model than non-premixed combustion. As discussed above the reason for this is that premixed combustion usually occurs as a thin, propagating flame that is stretched and contorted by turbulence. For subsonic flows, the overall rate of propagation of the flame is determined by both the laminar flame speed and the turbulent eddies. The laminar flame speed is determined by the rate that species and heat diffuse upstream into the reactants and burn.

The turbulent premixed combustion model, based on work by Zimont et al. [138-141], involves the solution of a transport equation for the reaction progress variable. The closure of this equation is based on the definition of the turbulent flame speed.

The flame front propagation is modelled by solving a transport equation for the density-weighted mean reaction progress variable, denoted by c [139]:

$$\frac{\partial}{\partial t}(\rho c) + \nabla \cdot (\rho \vec{v} c) = \nabla \cdot (\frac{\mu_t}{Sc_t} \nabla c) + \rho S_c \qquad 3.7.5$$

where

c = mean reaction progress variable

Sc_t = turbulent Schmidt number

S_c = reaction progress source term (s^{-1})

The progress variable is defined as a normalized sum of the product species,

$$c = \sum_{i=1}^{n} Y_i / \sum_{i=1}^{n} Y_{i,eq} \qquad 3.7.6$$

where

n = number of products

Y_i = mass fraction of product species i

$Y_{i,eq}$ = equilibrium mass fraction of product species i

Based on this definition, c = 0 where the mixture is unburnt and c = 1 where the mixture is burnt. The value of c is defined as a boundary condition at all flow inlets. It is usually specified as either 0 (unburnt) or 1 (burnt).

The mean reaction rate in equation (3.7.5) is modelled as

$$\rho S_c = \rho_u S_T |\nabla c| \qquad 3.7.7$$

where

ρ_u = density of burnt mixture

S_T = turbulent flame speed.

The turbulent flame speed is computed using a model of wrinkled and thickened flame fronts:

$$S_T = A(u')^{3/4} S_L^{1/2} \alpha^{-1/4} \ell_t^{1/4} = Au' \left(\frac{\tau_t}{\tau_c}\right)^{1/4} \qquad 3.7.8$$

where

A =	model constant
u′ =	root-mean-square (RMS) velocity (m/s)
S_L =	laminar flame speed (m/s)
$\alpha = \kappa / \rho c_p$ =	molecular heat transfer coefficient of unburnt mixture (thermal diffusivity) (m^2/s)
ℓ_t =	turbulence length scale (m)
$\tau_t = \ell_t / u'$ =	turbulence time scale (s)
$\tau_c = \alpha / S_L^2$ =	chemical time scale (s)

The turbulence length scale ℓ_t is computed from

$$\ell_t = C_D \frac{(u')^3}{\varepsilon} \qquad 3.7.9$$

where ε is the turbulence dissipation rate.

The model is based on the assumption of equilibrium small-scale turbulence inside the laminar flame, resulting in a turbulent flame speed expression that is purely in terms of the large-scale turbulent parameters. The default values of 0.52 for A, 0.37 for C_D are recommended by Zimont et al. [139], and are suitable for most premixed flames.

Non-adiabatic premixed combustion model is considered. The energy transport equation is solved in order to account for any heat losses or gains within the system. These losses/gains may include heat sources due to chemical reaction or radiation heat losses.

The energy equation in terms of sensible enthalpy, h, for the fully premixed fuel is as follows:

$$\frac{\partial}{\partial t}(\rho h) + \nabla \cdot (\rho \vec{v} h) = \nabla \cdot \left(\frac{k + k_t}{c_p} \nabla h \right) + S_{h,chem} + S_{h,rad} \qquad 3.7.10$$

$S_{h,rad}$ represents the heat losses due to radiation and $S_{h,chem}$ represents the heat gains due to chemical reaction:

$$S_{h,chem} = \rho S_c H_{comb} Y_{fuel} \qquad 3.7.11$$

where

S_c = normalized average rate of product formation (s^{-1})

H_{comb} = heat of combustion for burning 1 kg of fuel (J/kg)

Y_{fuel} = fuel mass fraction of unburnt mixture

3.7.4 Partially Premixed Combustion Modelling

Partially premixed combustion systems are premixed flames with non-uniform fuel-oxidizer mixtures (equivalence ratios). Such flames include premixed jets discharging into a quiescent atmosphere, lean premixed combustors with diffusion pilot flames and/or cooling air jets, and imperfectly mixed inlets.

The partially premixed model in FLUENT is a simple combination of the non-premixed model and the premixed model. The premixed reaction-progress variable, c, determines the position of the flame front. Behind the flame front (c = 1), the mixture is burnt and the equilibrium or laminar flamelet mixture fraction solution is used. Ahead of the flame front (c = 0), the species mass fractions, temperature, and density are calculated from the mixed but unburnt mixture

fraction. Within the flame ($0 < c < 1$), a linear combination of the unburnt and burnt mixtures is used.

Limitations of Using Partially Premixed Model

The underlying theory, assumptions, and limitations of the non-premixed and premixed models apply directly to the partially premixed model. In particular, the single-mixture fraction approach is limited to two inlet streams, which may be pure fuel, pure oxidizer, or a mixture of fuel and oxidizer. The two-mixture-fraction model extends the number of inlet streams to three, but incurs a major computational overhead.

Both nonpremixed and premixed systems are considered in this research. For the nonpremixed systems, the nonpremixed model is used for simulation. In the case of premixed systems, even it is suitable to use the premixed model for the simulation but it is preferred to use the partially premixed model to simulate the premixed combustion as it is possible to extend the analysis to perform pollutant analysis. The pollutant analysis is restricted with the premixed models but it can be performed with the partially premixed model.

3.8 CFD Code

In the following subsections the question, "*How is the CFD simulation performed in this research study?* ", will be answered. But before answering the question, let us first define the aims and objectives of the modelling in our case and how can they be achieved.

The modelling goals are:

- to built a reliable model grid that is able to be applicable for different solver applications as some grids fall to achieve the simulation for some models or do not give a converged solution.
- to study the isothermal behaviour of the model.
- to simulate three dimensional swirl burner which is turbulent in nature.
- to use different types of combustion modelling.
- to simulate the combustion of different gases with different compositions and characteristics.
- to simulate the combustion at different operating conditions (pressures, temperatures, and equivalence ratios)
- to have a balanced fast and accurate model.

In this research, FLUENT 6.3.26 software is used to achieve the modelling and simulation. The pre-processor used to construct the model grid is GAMBIT 2.3.16.

Fluent is a programme that uses the mesh created in its pre-processor Gambit, and applies the governing equations of fluid dynamics. Fluid dynamics is concerned with the dynamics of liquids and gases. The analysis of the behaviour of fluids is based upon the fundamental laws of applied mechanics, which relate to the conservation of mass-energy and the force momentum equations, Douglas et al [142]. Obviously, these equations vary depending on the properties of the flow in question and additional equations are solved for flows such as this one involving heat transfer and species transport. In addition, transport equations are also solved if the flow is turbulent. These equations are then replaced by equivalent numerical descriptions that are solved by a finite volume method, to give solutions for the flow at discrete locations within the flow field [123].

3.8.1 Mesh Construction

GAMBIT software was used for establishing the pre-processing phase of modelling i.e. drawing the model, constructing the grid and defining the boundaries and zones. GAMBIT was designed to help in analyzing and designing of mesh building models for computational fluid dynamics (CFD) and other scientific applications. GAMBIT receives user input primarily by means of its graphical user interface (GUI).

3.8.1.1 The Finite Volume Grid

One of the first steps in computing a numerical solution to the equations that describe a physical process is the construction of a grid (which is essentially a sub-division of the computational domain). Gambit is one of the pre-processing programs compatible with the Fluent solver. Here the geometry shape is created, the boundaries are identified and the shape is meshed. The computation domain is created using standard tools building blocks and by the use of Boolean operations (subtract, unite, etc...).

The mesh is critical to the modelling process. Without it, the finite volume method used in solving the governing equations could not be utilized as the mesh dictates where the equations are to be applied. For 2D applications, quadrilateral and triangular cells are accepted, and in 3D, hexahedral, tetrahedral, pyramid, and wedge cells can be used. Figure 3.1 depicts each of these cell types. Both single-block and multi-block structured meshes are acceptable, as well as hybrid meshes containing quadrilateral and triangular cells or hexahedral, tetrahedral, pyramid, and wedge cells [123].

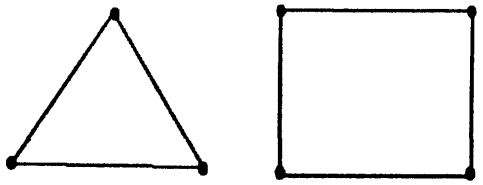

Triangle **Quadrilateral**

(a) 2D Cell types

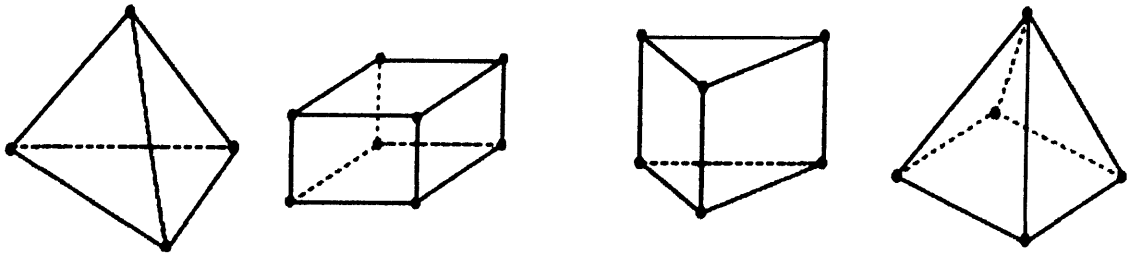

Tetrahedron **Hexahedron** **Prism/Wedge** **Pyramid**

(b) 3D Cell types

Figure 3.1: Cell types

After meshing is complete, the final stage is to specify appropriate conditions at cells, which coincide with or touch the domain boundary. The accuracy of a CFD solution is governed by the number of cells in the grid.

In general, the larger the number of cells the better the solution accuracy. Both the accuracy of a solution and its cost in terms of necessary computer hardware and calculation time are dependant on the fineness of the grid [123, 125].

3.8.1.2 Mesh (Grid) Quality

The quality of the mesh plays a major role in the stability and accuracy of the numerical computation. Mesh quality is where the CFD analyst has the largest impact on solution quality - after all, the numerical algorithms and physical models are dictated by choice of the solver. A high quality mesh increases the accuracy of the CFD solution and improves convergence relative to a poor quality mesh. Therefore, it's important for a mesher to provide tools for obtaining and improving a mesh. Some meshing software uses hundreds of unnecessary blocks as a crutch to obtain a decent mesh [143].

The features associated with mesh quality are node point distribution, smoothness and skewness which can be discussed as follow:

Node Point Distribution: The degree to which the salient features of the flow are resolved depends on the density and distribution of nodes in the mesh. Poor resolution in critical regions can dramatically alter the flow characteristics. For example, the resolution of the boundary layer (i.e., mesh spacing near walls) plays a significant role in the accuracy of the computed wall shear stress and heat transfer coefficient. Proper resolution of the mesh for turbulent flows is also very important. Due to the strong interaction of the mean flow and turbulence, the numerical results for turbulent flows tend to be more susceptible to grid dependency than those for laminar flows.

Smoothness: Rapid changes in cell volume between adjacent cells translate into larger truncation errors. Truncation error is the difference between the partial derivatives in the governing equations and their discrete approximations.

Skewness: The shape of the cell (including its skewness and aspect ratio) has a significant impact on the accuracy of the numerical solution. Skewness can be defined as the difference between the cell's shape and the shape of an equilateral cell of equivalent volume. Highly skewed cells can decrease accuracy and destabilize the solution. For example, optimal quadrilateral meshes will have vertex angles close to 90 degrees, while triangular meshes should preferably have angles of close to 60 degrees and have all angles less than 90 degrees. The aspect ratio is a measure of the stretching of the cell. For highly anisotropic flows, extreme aspect ratios may yield accurate results with fewer cells. However, a general rule of thumb is to avoid aspect ratios in excess of 5:1.

Grid quality can generally be monitored by the definition of two characteristics describing the mesh. These are Equiangle Skew and Equivolume Skew [125].

The Equiangle Skew (Q_{EAS})

It is a normalized measure of skewness that is defined as follows:

$$Q_{EAS} = \max\left\{\frac{\theta_{max} - \theta_{eq}}{180 - \theta_{eq}}\right\}, \left\{\frac{\theta_{eq} - \theta_{min}}{\theta_{eq}}\right\} \qquad 3.8.1$$

where θ_{max} and θ_{min} are the maximum and minimum angles (in degrees) between the edges of the element, and θeq is the characteristic angle corresponding to an equilateral cell of similar

form. For triangular and tetrahedral elements, θeq= 60. For quadrilateral and hexahedral elements, θeq= 90.

The Equivolume Skew (Q_{EVS})

It is a measure of skewness that is defined as:

$$Q_{EVS} = \frac{(V_{eq} - V)}{V_{eq}} \qquad 3.8.2$$

where V is volume of the mesh element, and V_{eq} is the maximum volume of an equilateral cell the circumscribing radius of which is identical to that of the mesh element.

By definition,

$$0 \leq Q_{EAS} / Q_{EVS} \leq 1 \qquad 3.8.3$$

where Q_{EAS} or Q_{EVS} = 0 describes an equilateral element, and Q_{EAS} or Q_{EVS} = 1 describes a completely degenerate (poo rly shaped) element.

Table 3.1 outlines the overall relationship between skew and element quality.

Table 3.1: Skew vs. Mesh Quality

Skew	Quality
Skew = 0	Perfect (Equilateral)
0 < Skew ≤ 0.25	Excellent
0.25 < Skew ≤ 0.5	Good
0.5 < Skew ≤ 0.75	Fair
0.75 < Skew ≤ 0.9	Poor
0.9 < Skew < 1	Very Poor
Skew = 1	Degenerate

In general, high-quality meshes contain elements that possess average Q_{EAS} or Q_{EVS} values of 0.1 for (2-D) and 0.4 for (3-D) [123].

3.8.2 CFD Code (Fluent) Solver

Fluent uses a well-developed technique known as a finite volume method (or control volume) method, which replaces the continuous computational domain with a set of nodes or grid points. It is these non-overlapping control volumes, or cells in which formal integration of the governing equations of fluid flow occur to construct algebraic equations for the discrete dependent variables ("unknowns") such as velocities, pressures, temperature, and conserved

scalars. Following this the discrete, non-linear governing equations are linearized to produce a system of equations for the dependant variables in every computational cell. The resultant linear system is then solved to yield an updated flow-field solution.

The governing equations are linearized using an implicit form with respect to the dependant variable of interest. In other words, for a given variable, the unknown value in each cell is computed using a relation that includes both existing and unknown values from neighbouring cells. Therefore each unknown will appear in more than one equation in the system, and these equations must be solved simultaneously to give the unknown quantities.

Two numerical methods are allowed in Fluent; segregated solver and coupled solver. The segregated solver is the solution algorithm in which the governing equations are solved sequentially (i.e., segregated from one another). Because the governing equations are non-linear (and coupled), numerous iterations of the solution loop must be performed before a converged solution is obtained. Each iteration consists of the steps illustrated in Figure 3.2.

The coupled solver solves the governing equations of continuity, momentum, and (where appropriate) energy and species transport simultaneously (i.e., coupled together). Governing equations for additional scalars will be solved sequentially (i.e., segregated from one another and from the coupled set). Because the governing equations are non-linear (and coupled), several iterations of the solution loop must be performed before a converged solution is obtained. Each iteration consists of the steps illustrated in Figure 3.3.

In both the segregated and coupled solution methods the discrete, non-linear governing equations are linearized to produce a system of equations for the dependent variables in every computational cell. The resultant linear system is then solved to yield an updated flow-field solution.

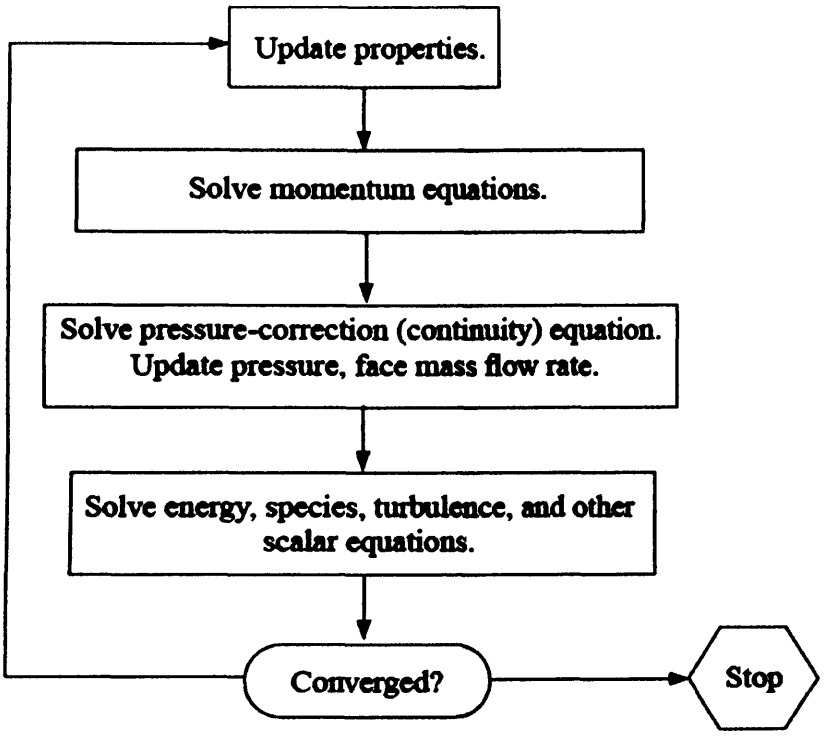

Figure 3.2: Overview of the Segregated Solution Method [123]

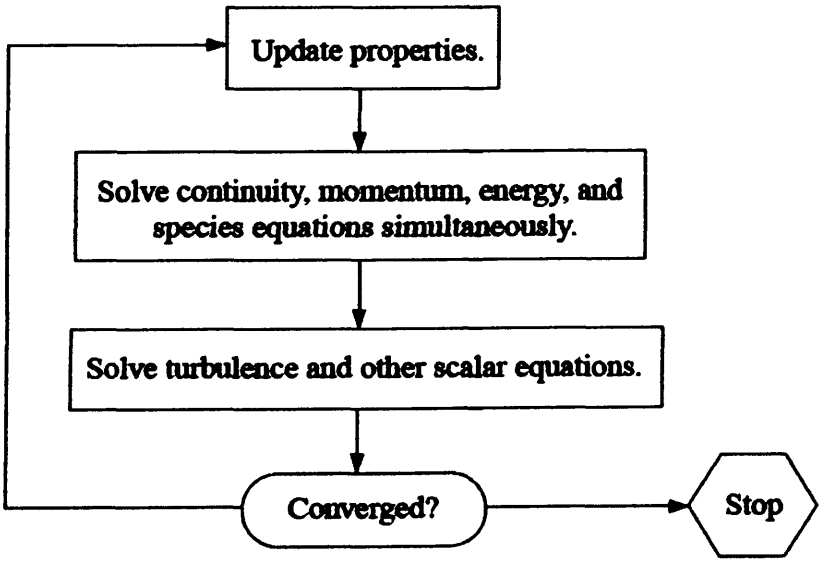

Figure 3.3: Overview of the Coupled Solution Method [123]

3.8.3 Convergence and Stability

The accuracy and numerical stability of the solution will obviously depend on the density and distribution of the grid, as well as on the interpolation or differencing schemes and their ability to resolve the variation between the cells. Convergence can be hindered by a number of factors. Large numbers of computational cells, overly conservative under-relaxation factors, and complex flow physics are often the main causes. Sometimes it is difficult to know whether you have a converged solution.

There are no universal metrics for judging convergence. Residual definitions that are useful for one class of problem are sometimes misleading for other classes of problems. Therefore it is a good idea to judge convergence not only by examining residual levels, but also by monitoring relevant integrated quantities such as drag or heat transfer coefficient.

The Residual

At the end of each solver iteration, the residual sum for each of the conserved variables is computed and stored, thus recording the convergence history. After discretization, the conservation equation for a general variable ϕ at a cell P can be written as [123]:

$$a_p\phi_p = \sum_{nb} a_{nb}\phi_{nb} + b \qquad 3.8.4$$

where a_p is the center coefficient, a_{nb} are the influence coefficients for the neighboring cells, and b is the contribution of the constant part of the source term.

The residual R^{ϕ} computed by Fluent's segregated solver is the imbalance in Equation 3.8.4 summed over all computational cells P. This is referred to as the "unscaled" residual and is given by:

$$R^{\phi} = \sum_{\text{cells } p} \left| \sum_{nb} a_{nb}\phi_{nb} + b - a_p\phi_p \right| \qquad 3.8.5$$

In general, it is difficult to judge convergence by examining the residuals defined by Equation 3.8.5 since no scaling is employed; therefore, Fluent scales the residual using a scaling factor representative of the flow rate of ϕ through the domain. This "scaled" residual is defined as:

$$R^{\phi} = \frac{\sum_{\text{cells } p} \left| \sum_{nb} a_{nb}\phi_{nb} + b - a_p\phi_p \right|}{\sum_{\text{cells } p} \left| a_p\phi_p \right|} \qquad 3.8.6$$

For the momentum equations the denominator term $a_p\phi_p$ is replaced by $a_p\upsilon_p$, where υ_p is the magnitude of the velocity at cell *P*. For the continuity equation, the unscaled residual is defined as:

$$R^c = \sum_{\text{cells } p} |\text{Rate of mass creation in cell P}| \qquad 3.8.7$$

And the segregated solver's scaled residual for the continuity equation is defined as:

$$\frac{R^c_{\text{iteration N}}}{R^c_{\text{iteration 5}}} \qquad 3.8.8$$

The denominator is the largest absolute value of the continuity residual in the first five iterations.

The scaled residuals described above are useful indicators of solution convergence. It is sometimes useful to determine how much a residual has decreased during calculations as an additional measure of convergence. For this purpose Fluent allows the residual to be normalized (either scaled or un-scaled) by dividing the maximum residual value after 5 iterations (the denominator in Equation 3.8.8).

For most problems, the default convergence criterion in Fluent is sufficient. This criterion requires that the scaled residuals defined by Equation 3.8.6 decrease to 10^{-3} for all equations except the energy and P-1 equations, for which the criterion is 10^{-6}. Unfortunately, this convergence criterion often failed in this research application. Convergence of a problem can be affected by a number of factors. Large numbers of computational cells, overly conservative under-relaxation factors, and complex flow physics are often the main causes.

Under Relaxation

In the iterative solution of the algebraic equations or in the overall iterative scheme employed for handling non-linearity, it is often desirable to slow down the changes, from iteration to iteration, in the values of the dependent variable. This process is called under-relaxation. In a simple form, the new value of the variable ϕ within a cell depends upon the old value, ϕ_{old}, the computed change in ϕ, $\Delta\phi$, and the under-relaxation factor, α, as follows [123]:

$$\phi = \phi_{old} + \alpha\,\Delta\phi \qquad 3.8.9$$

When the relaxation factor α in Equation 3.8.9 is between 0 and 1, its effect is under relaxation and when greater than 1, over-relaxation is produced. The optimum value of a depends on a number of factors, such as the nature of the problem, the number of grid points, the grid

spacing, and the iterative procedure used. Usually, a suitable value of a can be found by experience and from exploratory computations for the given problem.

3.9 Laminar Flame Speed

Laminar flame velocity (S_L) of a premixed flame is defined as the propagation velocity of a plane, undisturbed flame without heat loss and buoyancy effect. Although such flame may be difficult to produce experimentally, the definition is very suitable for numerical calculations using detailed kinetic reaction schemes. Laminar burning velocity is a constant under conditions of specific pressure and temperature and can provide reliable data on global flame propagation.

The laminar burning velocity is an important property for several reasons. The knowledge of S_L becomes important in the trade off between combustion stability and pollutants emissions. For example at very fuel lean conditions the laminar burning velocity decreases sharply and the flame is becoming less stable due to the partial or complete quenching (blow-out) of flames. This affects the emissions of carbon-monoxide and unburnt hydrocarbons. Hence, in lean premixed combustion a choice has to be made, in determining how lean one should operate. There is a trade-off between low pollutant emissions by operating at very lean conditions and a higher power output at slightly richer conditions. A higher power output gives more carbon monoxide and unburnt hydrocarbon emissions by avoiding flame quenching. Also related to the stability of flames is the so-called flash back phenomenon. In combustion systems flashback is a dangerous aspect which can for example occur when operating a system in a modulated manner, e.g. by changing the equivalence ratio, altering fuel composition or preheating of the fuel [144].

The laminar burning velocity is also an important parameter in turbulent combustion modelling. Often turbulence models assume that combustion takes place in the so-called flamelet regime [145]. Such flames can be considered as a front which is locally propagating as a stretched laminar flame. This flame stretching due to turbulence increases the flame surface which results in an increase of the (turbulent) burning velocity. For very low turbulent velocities the ratio between turbulent and laminar burning velocities S_T/S_L increases almost linearly with the ratio u'/S_L . For stronger turbulence and thus higher u′ the turbulent burning velocity St increases less fast with u′ or can even decrease [146].

This can be explained by increased flame quenching of the flame due to locally highly stretched flames. Here, the production of flame surface is competing with local flame quenching. This different behavior at various turbulence intensities demands different modeling approaches, although Lipatnikov and Chomiak [147] showed in a comprehensive evaluation of turbulent

premixed combustion models that the laminar burning velocity is commonly considered as an essential parameter characterizing the turbulent burning velocity.

Fuels such as methane and hydrogen very often serve as alternative fuels for combustion studies in gas turbines Therefore, there is a need for reliable data of burning velocities for these fuels at high pressure and preheat temperatures and at various equivalence ratios. Many studies are concerned on the measurement of flame velocities, laminar and turbulent, experimentally or analytically [93, 103, 116, 148-156].

3.9.1 Calculation of Laminar Flame Speed in Fluent

Both premix and partially premix models require the laminar flame speed as a material property. Laminar flame speed depends strongly on the composition, temperature, and pressure of the unburnt mixture. For perfectly premixed systems, the reactant stream has one composition, and the laminar flame speed is approximately constant throughout the domain. However, in partially premixed systems, the laminar flame speed will change as the reactant composition (equivalence ratio) changes, and this must be taken into account.

Accurate laminar flame speeds are difficult to determine analytically, and are usually measured from experiments or computed from 1D simulations. FLUENT uses fitted curves obtained from numerical simulations of the laminar flame speed [153, 157]. These curves were determined for hydrogen (H_2), methane (CH_4), acetylene (C_2H_2), ethylene (C_2H_4), ethane (C_2H_6), and propane (C_3H_8) fuels. They are valid for inlet compositions ranging from the lean limit through unity equivalence ratio (stoichiometric), for unburnt temperatures from 298 K to 800 K, and for pressures from 1 bar to 40 bars.

FLUENT fits these curves to a piecewise-linear polynomial. These flame speed fits are accurate for air mixtures with pure fuels of H_2, CH_4, C_2H_2, C_2H_4, C_2H_6, and C_3H_8. If an oxidizer other than air or a different fuel is used, if the mixture is rich, or if the unburnt temperature or pressure is outside the range of validity, then the curve fits will be incorrect. So, it is not possible to run with the values of laminar flame speed that are calculated by default for other fuels that are not mentioned before, mixtures leaner than the lean limit or richer than the rich limits, and/or mixtures that have conditions outside the specified pressure and temperature limits.

The laminar flame speed must be specified by using another source such as experimental measurements or chemical kinetics software with detailed 1D simulations. The required inputs

are values for the mean mixture fraction (f) at 10 laminar flame speeds. The minimum and maximum mixture fraction limits for the laminar flame speed are the first and last values of f that are input.

3.9.2 Methane and Hydrogen Laminar Flame Speed

Laminar flame velocity of a premixed flame is defined as the propagation velocity of a plane, undisturbed flame without heat loss and buoyancy effect. Although such flames may be difficult to produce experimentally, the definition is very suitable for numerical calculations using detailed kinetic reaction schemes. Laminar burning velocity is a constant; under specific pressure and temperature, that provides reliable data on global flame propagation.

Fuels such as methane and hydrogen very often serve as fuels for combustion studies in gas turbines. Therefore, there is a need for reliable data of burning velocities for these fuels at high pressure and preheat temperatures and at various equivalence ratios.

Peters et al. [150] considered methane, ethylene, ethane, acetylene, and propane flames, numerically generated burning velocities were approximated using an algebraic expression that had been derived for methane-air flames by asymptotic methods [158]. The approximation uses the inner layer temperature as an auxiliary variable and thereby provides a means of calculating effective Zel'dovich numbers as a function of equivalence ratio, pressure, and preheat temperature. Their work is extended to include n-heptane, iso-octane, and methanol in [153, 157]. They also report predictions of the response of laminar premixed flames to stretch, characterized by Markstein numbers, for methane, ethylene, ethane, propane, and iso-octane/air flames. The Markstein number predictions are compared with measurements reported by others. A technique is described by Kwon et al. [159] to eliminate this difficulty of comparison between the results in [153, 157] and those of other authors.

By this method of approximation, the burning velocities of lean methane-air mixtures can be calculated in the range of preheat temperatures between 298 K and 800 K and pressures between 1 bar and 40 bar. The equation that can be used for the burning velocity S_L of stoichiometric methane-air flames has the general form

$$S_L = A(T^0) Y_{F,u}^m \frac{T_u}{T^0} \left(\frac{T_b - T^0}{T_b - T_u} \right)^n \qquad 3.9.1$$

where, T^0 is the inner layer temperature, representing the crossover temperature between chain-branching and chain-breaking reactions. Within the temperature profile of a premixed flame it

marks the transition from the inert preheat zone to the reaction zone, and it is therefore the point where the second derivative vanishes and the slope is maximum. The function $A(T^0)$ only depends on thermodynamic and kinetic properties and $Y_{F,u}$ is the mass fraction of the fuel in the unburnt gas. The temperatures T_u , and T_b are those in the unburnt and the burnt gas, respectively. m and n are constants for the fuel.

The relation between the inner layer temperature and the pressure and the function $A(T^0)$ are approximated as

$$p = B\,exp\left(-\frac{E}{T^0}\right) \qquad 3.9.2$$

or simply

$$T^0 = \frac{E}{ln\frac{B}{p}} \qquad 3.9.3$$

and,

$$A(T^0) = F\,exp\left(-\frac{G}{T^0}\right) \qquad 3.9.4$$

And the adiabatic flame temperature can be calculated for lean flames as:

$$T_b = aT_u + b + c\phi + d\phi^2 + e\phi^3, \qquad \phi \leq 1 \qquad 3.9.5$$

The parameters for methane and hydrogen:

	a	b [K]	c [K]	d [K]	e [K]
CH_4	0.627	1270.15	-2449	6776	-3556
H_2	0.522	673.8	807.9	2515.6	-1765.9

	B [bar]	E [K]	m	F [cm/s]	G [K]	N
CH_4	$3.1557*10^8$	23873	0.565	22.176	-6444.27	2.516
H_2	30044.1	10200.9	1.08721	1292880	2057.56	3.535

3.9.3 Hydrogen/Methane Laminar Flame Speed

If H_2/CH_4 blend is considered as a fuel with hydrogen and methane mole fractions n_{H_2} and n_{CH_4} respectively then the hydrogen volumetric fraction γ is defined as:

$$\gamma = \frac{n_{H_2}}{n_{H_2} + n_{CH_4}} \qquad 3.9.6$$

Sarli and Benedetto [105] calculated the laminar burning velocities of hydrogen–methane/air mixtures at NTP conditions using the CHEMKIN PREMIX code with the GRI kinetic mechanism. Their results show that the values of the blends laminar burning velocities are always smaller than those obtained by averaging the laminar burning velocities of the pure fuels according to their molar proportions. The linear combination of the laminar burning velocity of the pure fuels can be calculated as follows:

$$S_{L\_linear}(\phi, \gamma) = \gamma \cdot S_{L\_H2}(\phi) + (1-\gamma) \cdot S_{L\_CH4}(\phi) \qquad 3.9.7$$

where S_{L_H2} and S_{L_CH4} are the laminar burning velocity of hydrogen and methane evaluated at the same equivalence ratio of the hybrid fuel (ϕ).

It appears that the computed values of the mixture laminar burning velocity are always well below those obtained by averaging the flame speeds of the constituent gases in molar proportions This implies the presence of strong non-linear effects in chemical kinetics that emphasize the weight of the more slowly reacting methane in the composite fuel combustion. Moreover, in lean mixtures the hydrogen addition enhances the methane reactivity slightly, while a strong inhibiting effect of the hydrogen substitution by methane is observed at rich conditions.

A correlation for evaluating the laminar burning velocity of hydrogen–methane/air mixtures at NTP conditions as a function of equivalence ratio and fuel composition has been proposed by Yu et al. [106] for hydrogen mole fraction in the fuel up to 0.7. The authors have been able to linearly correlate the laminar burning velocity of the hybrid flames with the burning velocity without hydrogen addition and a single parameter indicating the extent of the hydrogen content. More precisely, hydrogen has been considered to be present only in stoichiometrically small quantities, its combustion requiring four times less oxygen than methane. Consequently, they have assumed that there is enough air to facilitate a complete oxidation of hydrogen, while the remaining air is used to oxidize methane. An effective methane/air equivalence ratio, ϕ_F, has been therefore defined as follows:

$$\phi_F = \frac{C_F / [C_A - C_H / (C_H / C_A)_{st}]}{(C_F / C_A)_{st}} \qquad 3.9.8$$

while the relative amount of hydrogen addition, R_H, has been expressed according to

$$R_H = \frac{C_H + C_H / (C_H / C_A)_{st}}{C_F + [C_A - C_H / (C_H / C_A)_{st}]} \qquad 3.9.9$$

where C_A, C_F and C_H are the initial mole fractions of the air, methane and hydrogen, respectively (the subscript 'st' denotes the stoichiometric conditions). In the explored ranges of

ϕ_F (0.51-1.37) and R_H (0-0.5), the laminar burning velocity (S_L) has been then correlated by the following equation:

$$S_L(\phi_F,R_H) = S_L(\phi_F, 0) + 0.8R_H \text{ (m/s)} \qquad 3.9.10$$

More recently, El-Sherif [149] has numerically reproduced the experimental results by Yu et al. [106] at ϕ_F ranging from 0.62 to 1.2 and R_H varying up to 0.4. In this parameter range he has proposed the following correlation:

$$S_L(\phi_F,R_H) = 0.38\phi_F^{-0.35}\ exp[-5.5(\phi_F - 1.1)^2] + 0.84R_H \text{ (m/s)} \qquad 3.9.11$$

with ϕ_F and R_H defined according to (3.9.8) and (3.9.9), respectively.

Equation 3.9.11 is similar to Equation 3.9.10, but it presents the explicit dependence of the laminar burning velocity without hydrogen on the fuel/air equivalence ratio (ϕ_F). Equations 3.9.10 and 3.9.11 are able to take into account the linear trend of the laminar burning velocity with hydrogen addition on the methane rich side. Due to the expressions of the parameters ϕ_F and R_H defining the composition of the hybrid fuel/air mixtures, these equations are intrinsically valid only for low hydrogen contents.

Another correlation for laminar burning velocities of H_2/CH_4 mixture was proposed by Liu et al. [102]. The correlation uses Le Chatelier's Rule-like formula that can be expressed according

$$S_{L\_LC}(\phi,\gamma) = \frac{1}{\frac{\gamma}{S_{L\_H2}(\phi)} + \frac{1-\gamma}{S_{L\_CH4}(\phi)}} \qquad 3.9.12$$

where S_{L_H2} and S_{L_CH4} are the laminar burning velocity of hydrogen and methane evaluated at the same equivalence ratio of the hybrid fuel (ϕ).

Sarli and Benedetto [93] tested the feasibility of a Le Chatelier's Rule-like formula at different values of inlet pressure (1, 5 and 10 atm) and temperature (300, 350 and 400 K), respectively. A good prediction is obtained, except for rich mixtures with high hydrogen contents. With this limitation, the proposed formula is successfully applied also to mixtures at higher than normal values of initial pressure (up to 10 atm) and temperature (up to 400 K). They do think that the Le Chatelier's Rule-like formula 3.9.12 is able to take into account the kinetic interaction between radicals. However, at rich conditions when dealing with high hydrogen (and then H radicals) contents the interaction is too strong to be reproduced by Equation 3.9.12 and a more sophisticated formula is required.

3.9.4 CHEMKIN-PRO software package for calculation of the laminar burning velocity

An unstretched laminar burning velocity of methane methane/carbon dioxide and methane/hydrogen flames has been calculated using CHEMKIN-PRO [160] software package. CHEMKIN-PRO consists of a set of different application models, which are used to solve various chemical kinetic problems. "Flame Speed Calculator" reactor model has been used to determine the laminar speed of one-dimensional freely propagating flame. PREMIX [161] code, which has been developed by Sandia National Laboratories, has been used to run this model.

"Flame Speed Calculator" model with "Parameter Study Facility" option has been utilised to perform the numerical burning velocity calculations. The model simulates a freely propagating flame in which the point of reference is a fixed position on the flame, thus the flame speed is defined as the velocity of unburned gas moving towards the flame [160]. This model uses mixture averaged transport properties with correction velocity formulation. Equivalence ratio has been chosen as variable parameter. A number of runs have been performed for different temperature and pressure conditions. The domain length of 10 cm has been specified and the grid of 200 points has been selected, which has facilitated faster convergence. Adaptive grid control parameter based on gradient GRAD = 0.1 and adaptive grid control parameter based curvature CURV = 0.1 have bee selected. An Initial grid based on temperature profile estimate has been specified. Mixture averaged transport, correction velocity formalism with automatic estimation of temperature profile options have been used.

Different kinetic models should be used for different gas mixtures as no one mechanism can be considered as universal model for all possible gas mixtures. GRI-Mech [162] mechanism is often used in the research of methane and methane based gases combustion. It considers 53 species and 325 elementary reactions. This mechanism has been developed to investigate methane and natural gas flames and has been validated extensively at various pressure and temperature conditions. The researchers have reported that this mechanism could also be suitable to some extent for biomass gasification-derived producer gas [163], methane hydrogen mixtures [164, 165] and for hydrogen air mixtures [166, 167] at atmospheric conditions. However there have been larger discrepancies observed between experimental data and numerical calculations using GRI-Mech kinetic mechanism for pure and diluted hydrogen at higher pressures [166, 168].

Another well known kinetic mechanism, which has been developed by University of California in San Diego [65], has been used this research. This kinetic mechanism considers 46 species and 235 elementary reactions and is often used for hydrocarbon combustion research.

There are several kinetic mechanisms, developed for hydrogen combustion. The group of researchers from Princeton University [169], O'Conaire et al. [168] and Konnov [170] have developed hydrogen combustion models, which have been validated at different experimental conditions [171]. Konnov reviewed [171] currently existing hydrogen combustion mechanisms and pointed out the remaining uncertainties of these models.

The O'Conaire et al. mechanism has been developed to simulate the combustion of hydrogen and oxygen in a variety of combustion environments and over a wide range of temperatures, pressures and equivalence ratios. The O'Conaire kinetic mechanism comprises 8 species and 19 elementary reactions. The temperature ranges from 298 to 2,700 K, the pressure from 0.05 to 87 atmospheres, and the equivalence ratios from 0.2 to 6. Ströhle and Myhrvold reported [166] that Li et al. [169] and O'Conaire et al. [168] chemical kinetics mechanisms provide much more accurate results in comparison with experimental data at elevated pressures whilst GRI-Mech underpredicts laminar flame speed considerably. They also showed that the San Diego mechanism yields reasonable results for helium diluted high pressure hydrogen flames. Lafay et al. [172] have utilised the GRI-Mech and San Diego mechanisms to calculate flame thickness. They have shown that these mechanisms are in good agreement with the experimental data at atmospheric conditions at equivalence ratios above 0.55. Sarli and Benedetto [93] found that the GRI-Mech kinetic mechanism, used in their simulation, underpredicted laminar burning velocity at high hydrogen content with methane-hydrogen mixtures. They identified three different regimes in flame propagation depending on hydrogen mole fraction in the fuel mixture.

Taking into account the above it has been decided to use different mechanisms for different methane/hydrogen fuel mixtures. The GRI-Mech mechanism has been used for methane/hydrogen with hydrogen content up to 50%, because it is believed that methane combustion kinetics prevail in the combustion process. The San Diego mechanism has been chosen for the investigation of methane – hydrogen mixtures with the hydrogen content above 50%, because it has been shown [166] that this mechanism predicts hydrogen laminar flame speed more accurately at elevated pressures. The O'Conaire at el. mechanism has been utilised for laminar flame speed calculation for pure hydrogen, as its accuracy has been supported by various researchers [166, 168].

3.10 Summary

Computational Fluid Dynamics (CFD) techniques have emerged with the advent of digital computers. Since then, a large number of numerical methods have been developed to solve flow problems using this approach. The main purpose of a flow simulation is to find out how the flow behaves in a given system for a given set of initial and boundary conditions. In many design and analysis applications, it is preferable to use CFD methods as they are cheap (in cost and maintenance), fast (in time) and safe (in hazard design processes) and often give satisfactory results, when suitably calibrated against available experimental data.

In this chapter, CFD is introduced as an important tool in designing combustion systems in gas turbines. Features of CFD modelling, turbulent models and combustion models are surveyed. The following can be concluded:

- CFD is an important tool for analysing systems involving fluid flow, heat transfer and combustion.
- The commercial CFD packages contain three main elements: a pre-processor, a solver and, a post-processor.
- CFD codes are structured around the numerical algorithms that can tackle fluid flow problems. The solution is based on solving the main flow governing equations.
- There is no general turbulent model that is able to perfect for all turbulent flow problems.
- Many Turbulent models are available in Fluent software. One must choose the turbulent model that can perform the modelling requirements with acceptable accuracy and time.
- Fluent provides several models for chemical species transport and chemical reactions. The choice of the suitable combustion model must consider the system physics and the model restrictions.
- The model preparation (mesh construction) plays an important role in the simulation accuracy and the solution convergence.
- Fluent uses segregated solver to solve the combustion models problems.
- Laminar flame velocity is an important parameter in both laminar and turbulent combustion modelling.
- There are many studies concerned about the measurement and analysis of flame velocities, both laminar and turbulent.
- Fluent provides data for laminar flame velocity that can be used for CH_4 and H_2 combustion simulation from lean mixtures up to stoichiometric mixtures.

- For fuel blends, such as H_2/CH_4, laminar flame speed must be calculated by other mean (chemical kinetics software, analytically or experimentally) and then fed to Fluent as an input data to establish a PDF table for turbulent combustion calculations.

Chapter 4

COMBUSTOR MODELLING AND SIMULATION SET-UP

4.1 Introduction

This chapter and the following chapters describe the work achieved in this research study. The combustion system considered in this research is an original burner as fitted to the system, then a generic swirl burner to fit into the high pressure optical combustor (HPOC) rig at the gas turbine research centre of Cardiff University in Port Tabot. This is complemented with a very similar generic swirl burner system for use at atmospheric pressure and temperature in the laboratories at Cardiff University. Differences between the high pressure generic swirl burner for use in the HPOC and laboratory based system at atmospheric pressure arise from safety consideration and the use of premixed air gas mixtures

The HPOC combustion system comprises of a burner and combustion chamber. The HPOC simulation and analysis are performed on two types of burners. The first burner is the original burner installed in the system and is a simple Bunsen type burner which is used to perform primary calculations for the system. The second burner considered is a generic swirl type burner representative of industrial practice. Most of the flashback analyses are performed on this generic swirl burner as it is has the inherent advantages of swirl burners described in Chapter 2 for flame stability and emissions reduction. Finally the third burner was designed for calibration purposes at atmospheric pressure and temperature conditions, fired on natural gas so that matches between predictions and experimental data can be assessed, allowing more confidence to be had in the predictions made for high pressure and temperature.

In this chapter, the combustion system used in this research is described. The initial analysis was performed on the original burner system installed in the HPOC. The model development, model quality, calculation parameters and the numerical description of the original system are described. The CFD analyses for the original system are performed based on experimental data produced by the working team in the research centre.

The flow chart shown in Figure 4.1 summarizes the work carried out, outlining the main topics discussed in the following chapters.

4.2 The High Pressure Optical Combustor (HPOC)

A High Pressure Optical Combustor (HPOC) Test Module has been designed for use on the High Pressure Combustor Rig (HPCR) which is located at the Gas Turbine Research Centre (GTRC) of Cardiff University in Port Talbot, Wales, UK.

The HPOC consists of a single horizontal burner and an axi-symmetric chamber. The burner is firing into an inner combustion chamber, enclosed within an optical pressure casing as shown in Figure 4.2. The pressure casing is a cylindrical geometry with four diametrically opposed quartz windows, affording excellent optical access. The optical combustion section is fitted with a heat exchanger, allowing combustion air to be preheated to required operating temperatures. The inner combustion chamber consists of two jointed parts. The first part is the optical section while the other is the non optical part. Both parts have the same shape and dimensions with square cross sections, to allow good optical access for combustion diagnostics; each (152 x 152 mm) and 208 mm long. All edges are chamfered at 24 mm at each corner. The optical part has four internal quartz windows which align with the outer casing, giving full optical access to the combustion chamber. It is fitted with a heat exchanger, allowing combustion air to be preheated to required operating temperatures.

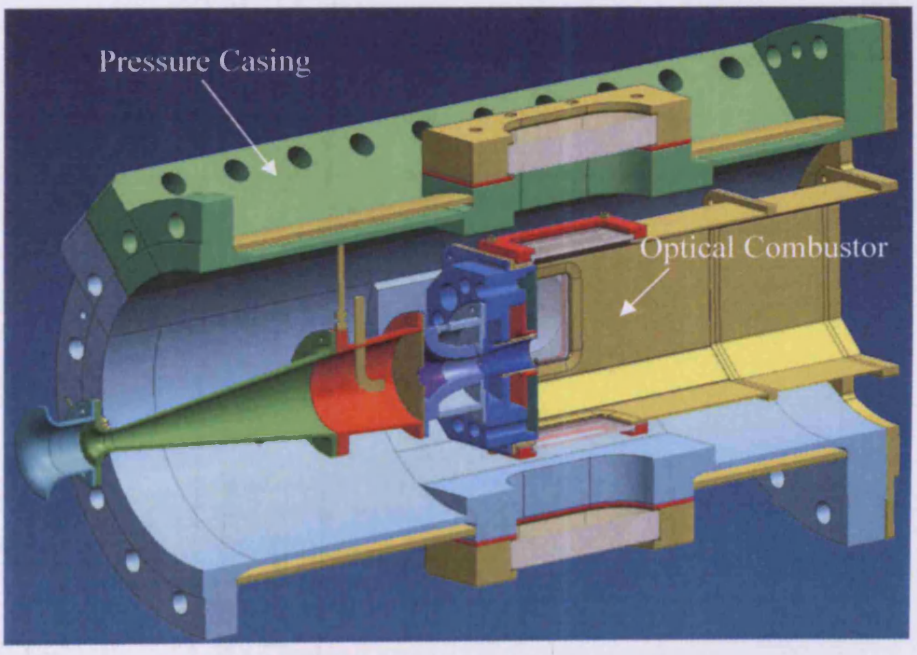

Figure 4.2: High Pressure Optical Combustor

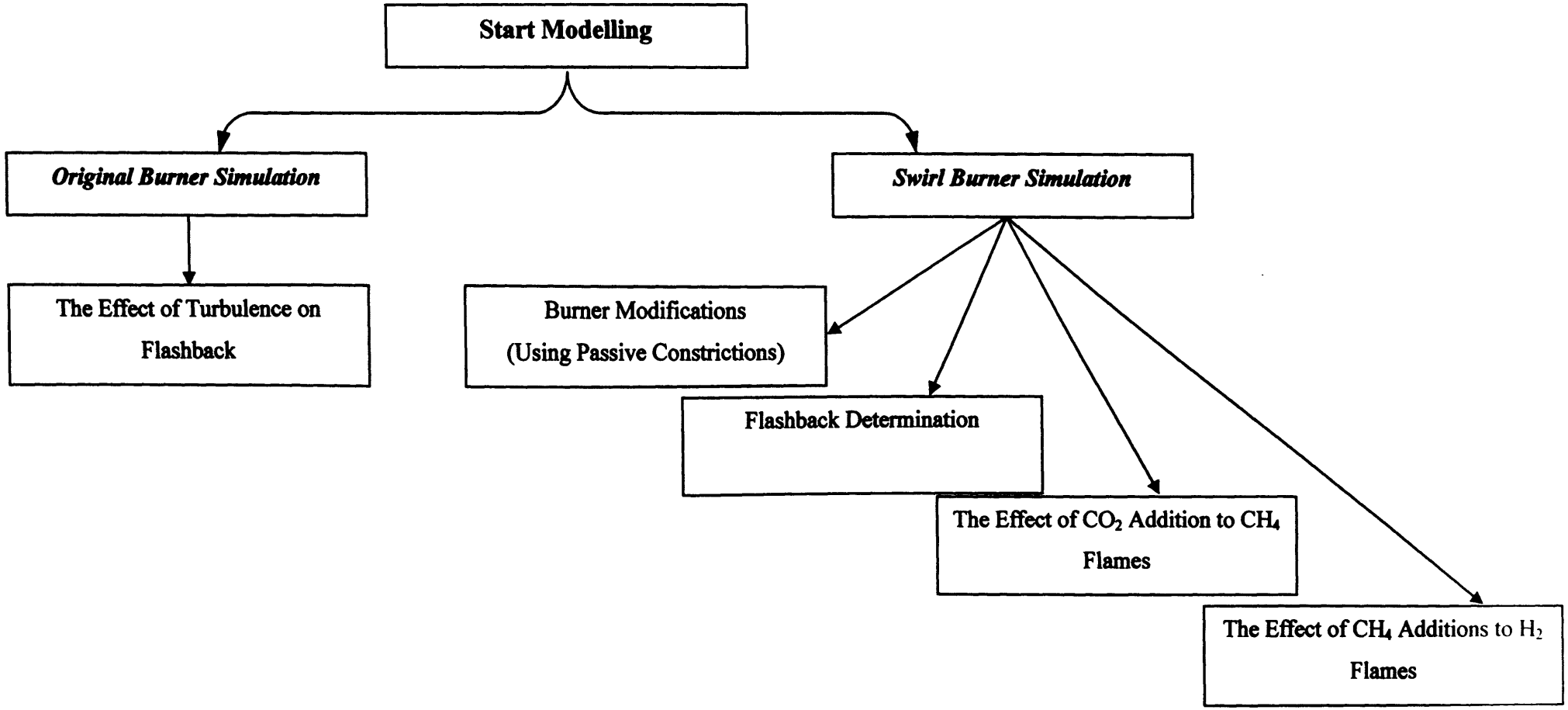

Figure 4.1: Outlines of the research work

The HPOC has the flexibility to be fired with variable quality gaseous and liquid fuels. The original system burner consists of a premixed main with diffuse CH_4 pilot. It is supplied by a range of heavy-duty industrial components and control systems, including a compressor, large-scale heat exchanger, high-specification pipe-work with a dedicated control room. The air supply for both the HPOC and burner is pressurized by the main facility compressor which is capable of delivering 5 kg/s at 16 bar absolute pressure. Seeded air for combustion is delivered by an auxiliary compressor. Fuel gases are supplied from premixed cylinders.

The combustion facility operating range for the optical combustor are:

Air flow rate: < 5 kg/s

Absolute Pressure: < 16 bar

Preheat temperature: < 900 K

The realistic working section operating conditions up to ~2.5kg/s air through combustor head at 15 bar & 875K

The Flexible premixed burners for HPOC are:

10g/s < air flow < 1kg/s, and

0.5g/s < fuel flow < 30g/s

The original gas burner fitted in the HPCR is a simple Bunsen type burner that is fired into the combustion chamber through a 25 mm diameter nozzle. The burner is fed a premix of fuel and air via a turbulence mixing plate, 50 mm diameter, which is fitted inside the mixing chamber shown in Figure 4.3. Two turbulence plates are used for simulation. The first is shown in Figure 4.4 (a) and is used to produce high turbulence via with 82 holes each of 1 mm diameter. The second turbulence plate is shown in Figure 4.4 (b) and is used to produce low turbulence via 53 holes each of 1.5 mm diameter, blockage ratio 95%. This claimed to create a uniform turbulence and aid in the mixing of the reactants. The preheated air and fuel gas supply are connected to a mixing chamber upstream of this plate. The preheated air is delivered radially through the preheater to the top of the mixing chamber of the burner while the fuel is fed axially from the centre. The burner is fitted with an annular pilot which supplies a methane diffusion flame to aid stability while adjusting the operating conditions. This pilot is switched off prior to making measurements. The assembly of the system is shown in Figure 4.5 and a photo for the rig during operation is shown in Figure 4.6.

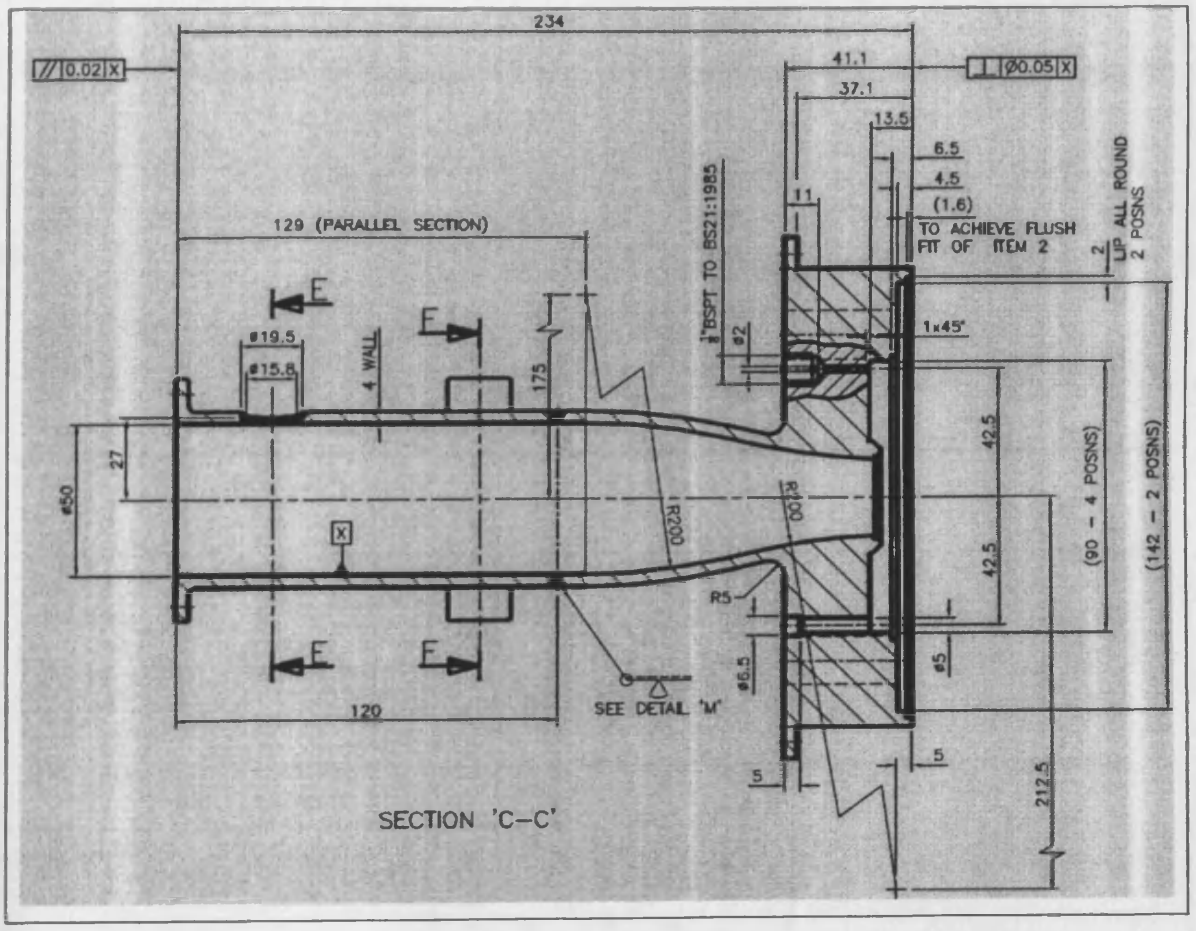

Figure 4.3: The mixing chamber

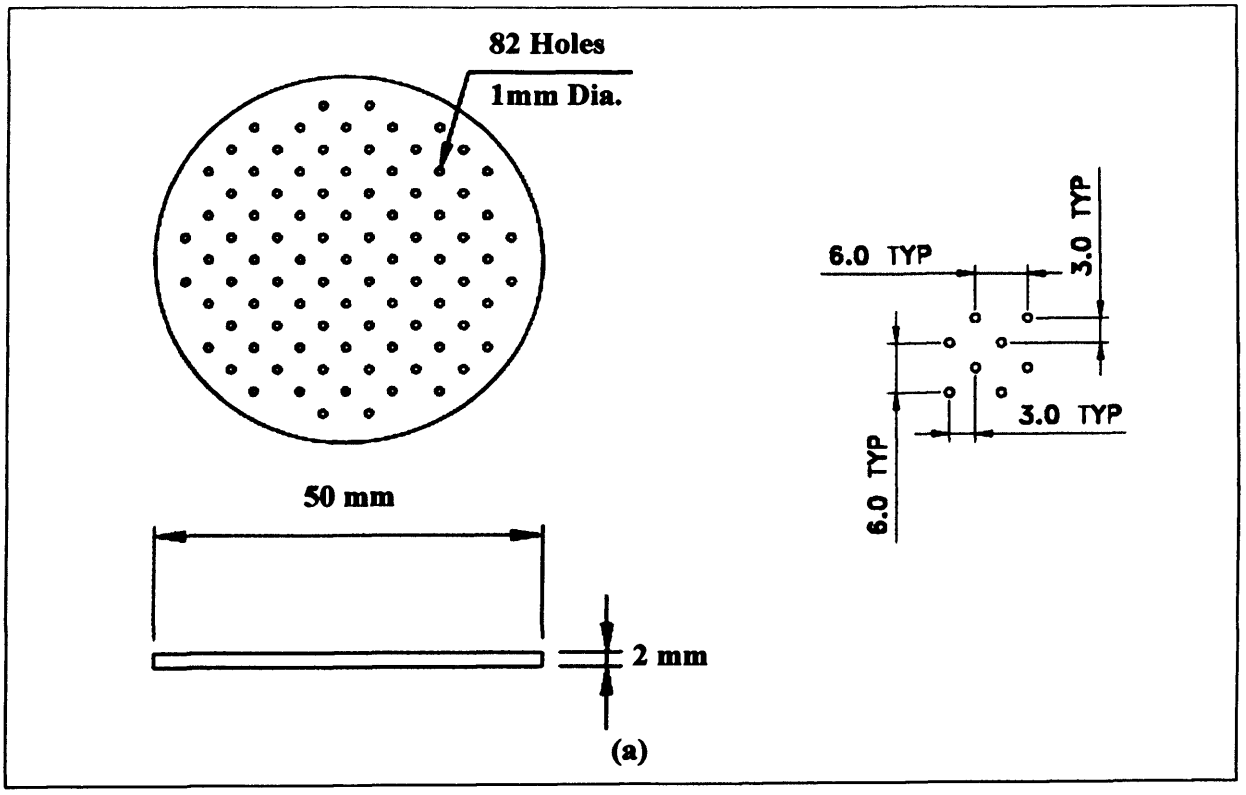

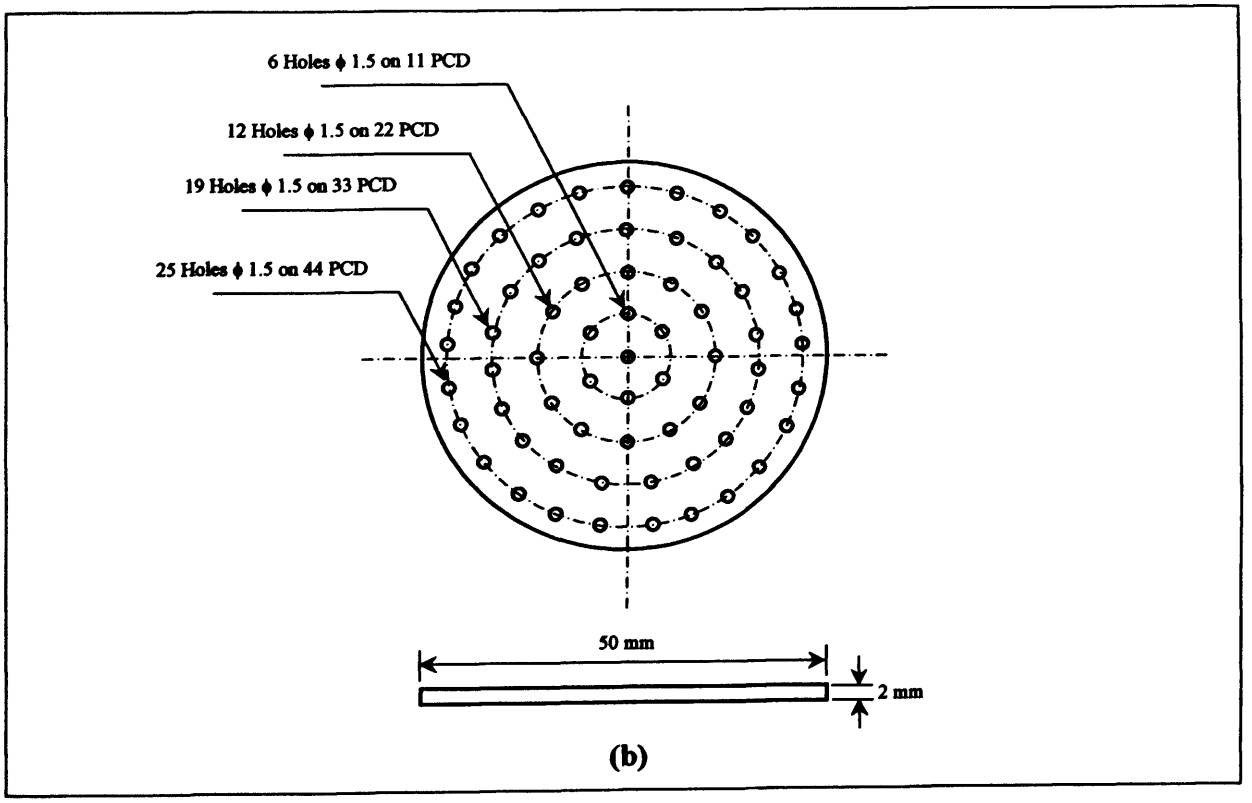

Figure 4.4: The Turbulence Plates

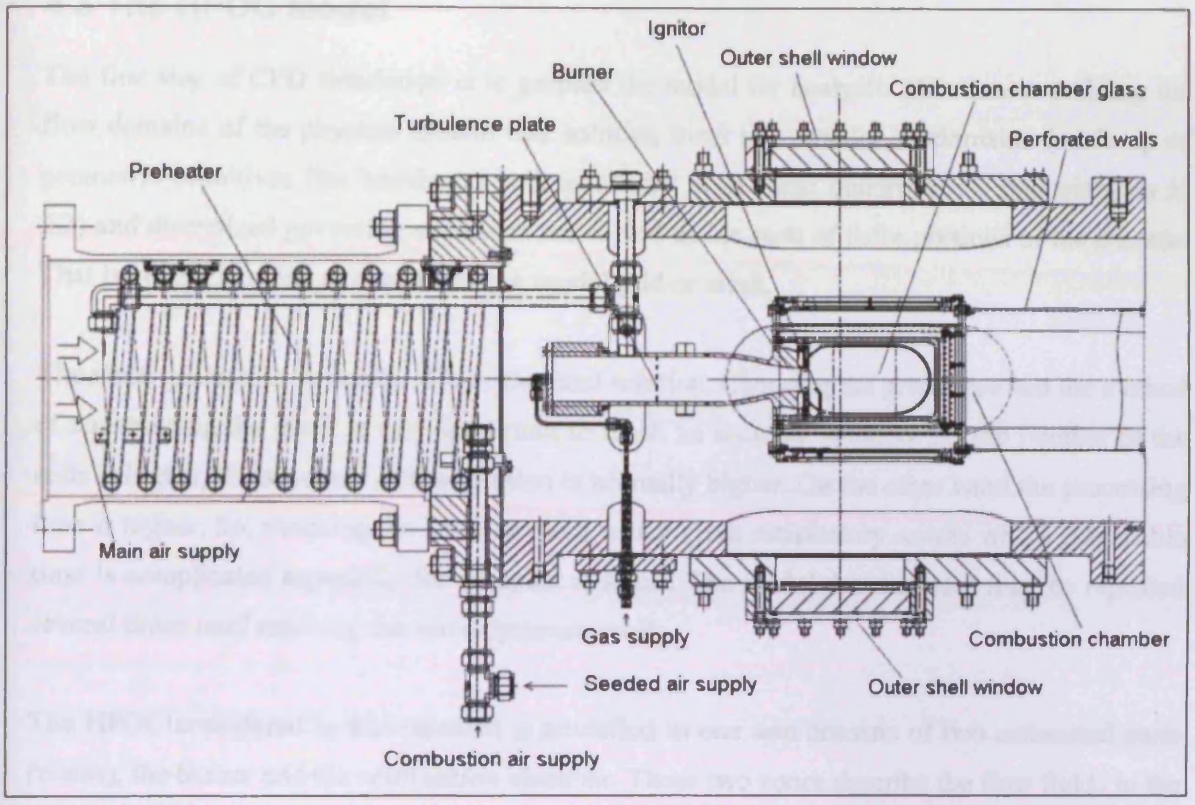

Figure 4.5: The Optical Combustor Assembly

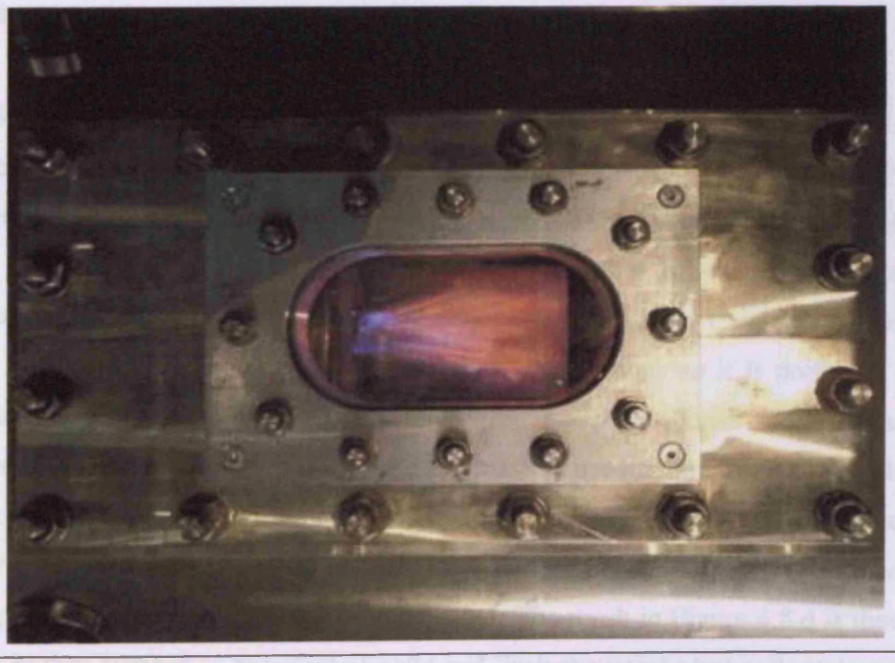

Figure 4.6: Photo for The Optical Combustor during an Experiment

4.3 The HPOC Model

The first step of CFD simulation is to prepare the model for analysis. This means defining the flow domains of the physical system and splitting them into smaller subdomains (made up of geometric primitives like hexahedra and tatrahedra in 3D, and quadrilaterals and triangles in 2D) and discretized governing equations are solved inside each of these portions of the domain. That is generally refers to constructing a model grid or mesh.

The mesh generation normally affects the final solution. Choosing the grids type and the method of constructing the mesh is very important to reach an accurate solution. As the number of the cells is higher, the accuracy of the solution is normally higher. On the other hand the processing time is higher. So, choosing the suitable mesh which gives satisfactory results with a reasonable time is complicated especially for complex systems. The model development may be repeated several times until reaching the semi-optimum mesh.

The HPOC considered in this research is modelled as one unit consists of two connected parts (zones); the burner and the combustion chamber. These two zones describe the flow fields in the system as shown in Figure 4.7. The first zone is the burner or mixing cylinder in which the air and fuel are mixed together and the turbulence is produced by using a turbulence disc. There is no combustion in this zone under the normal combustion conditions, nor is it desired. The other zone is the combustion chamber which includes both optical and non-optical parts. Combustion is achieved within this zone in the normal combustion conditions.

Gambit 2.3.16 is used for constructing the model mesh. A three dimensional model is used for the simulation. Due to the symmetry of the model, it was preferred to simulate only half of the system to reduce the computational time. The complete system can be easily meshed by a tetrahedral unstructured mesh but it leads to higher number of elements generated which translates to longer computational times, whilst the solution is not stable for some viscous models. A hexahedral mesh can give faster and stable solutions so it is preferred to be used more than tetrahedral mesh. The main problem in this model was constructing the mesh for the tiny holes of the turbulence plate. Hence a mixed mesh is used but mainly a hexahedral mesh is used for the combustion zone and a part of the mixing zone as shown in Figures 4.8.a, 4.8.b and 4.8.c. while tetrahedral mesh is used for the other part of the mixing zone which contains the turbulence plate as shown in Figures 4.8.c and 4.8.d. The mesh in Figure 4.8.d is then modified to include a higher number of hexahedral cells and limit the tetrahedral cells to be only around the turbulence plate as shown in Figures 4.8.e. The total number of cells in this model was 1,058,012 cells.

During the CFD simulation of this model the presence of reversed flow was found at the end of the combustion chamber; this affects both the convergence and the accuracy of the solution. To solve this problem it was suggested to add an extension to the combustion chamber as shown in Figures 4.9. The extension was chosen to have the same dimensions of the non-optical part of the combustion chamber (which is similar to the optical part too). This extension increased the total number of the cells by 83,940 cells and then the total number of cells was 1,141,952 cells.

The main problem with this model was the huge number of cells which affects the time for the solution to become converged. Roughly, the consumed time for only one run was about 15 days. Hence the volume of the cells was increased to reduce their number, via the modifications as shown in Figure 4.10. The number of cells was reduced to 775,945 cells which still gave too long a time for a converged solution. Several trials are done until the suitable mesh was constructed as shown in Figure 4.11. The final mesh was satisfactory from both the accuracy and consumed time view points and it contains 178,530 cells which consumed about one day for the solution to be converged.

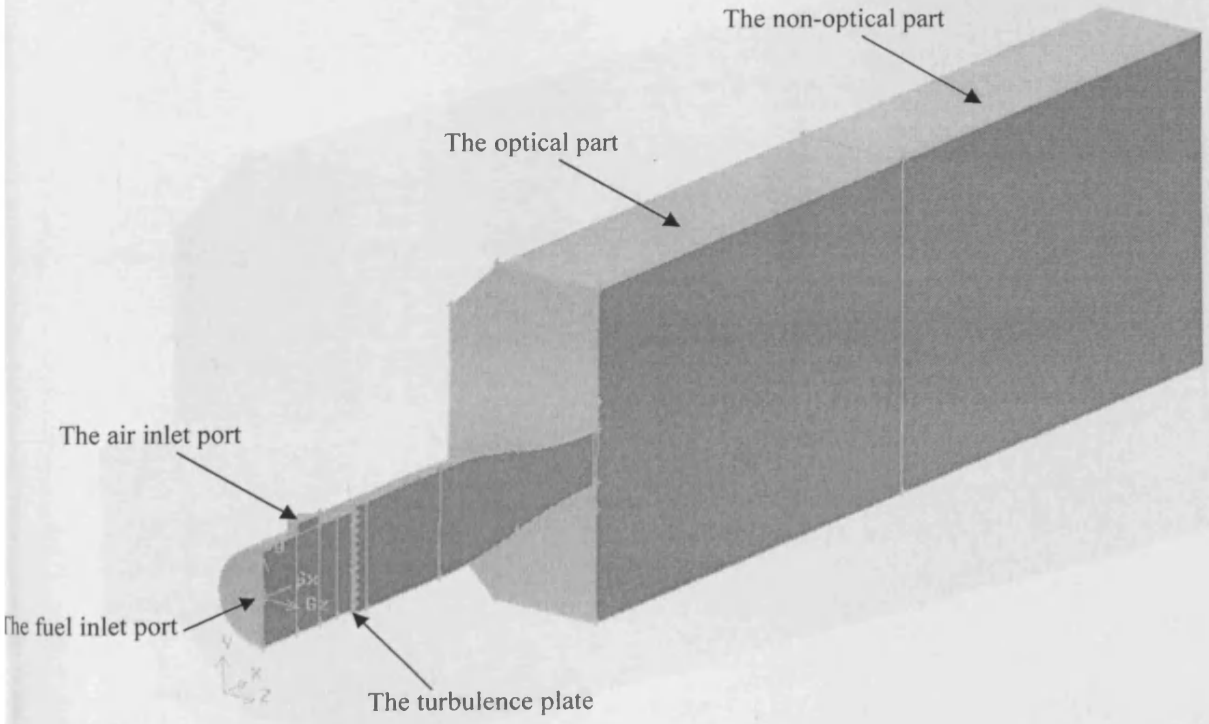

Figure 4.7: The HPOC combustor flow fields

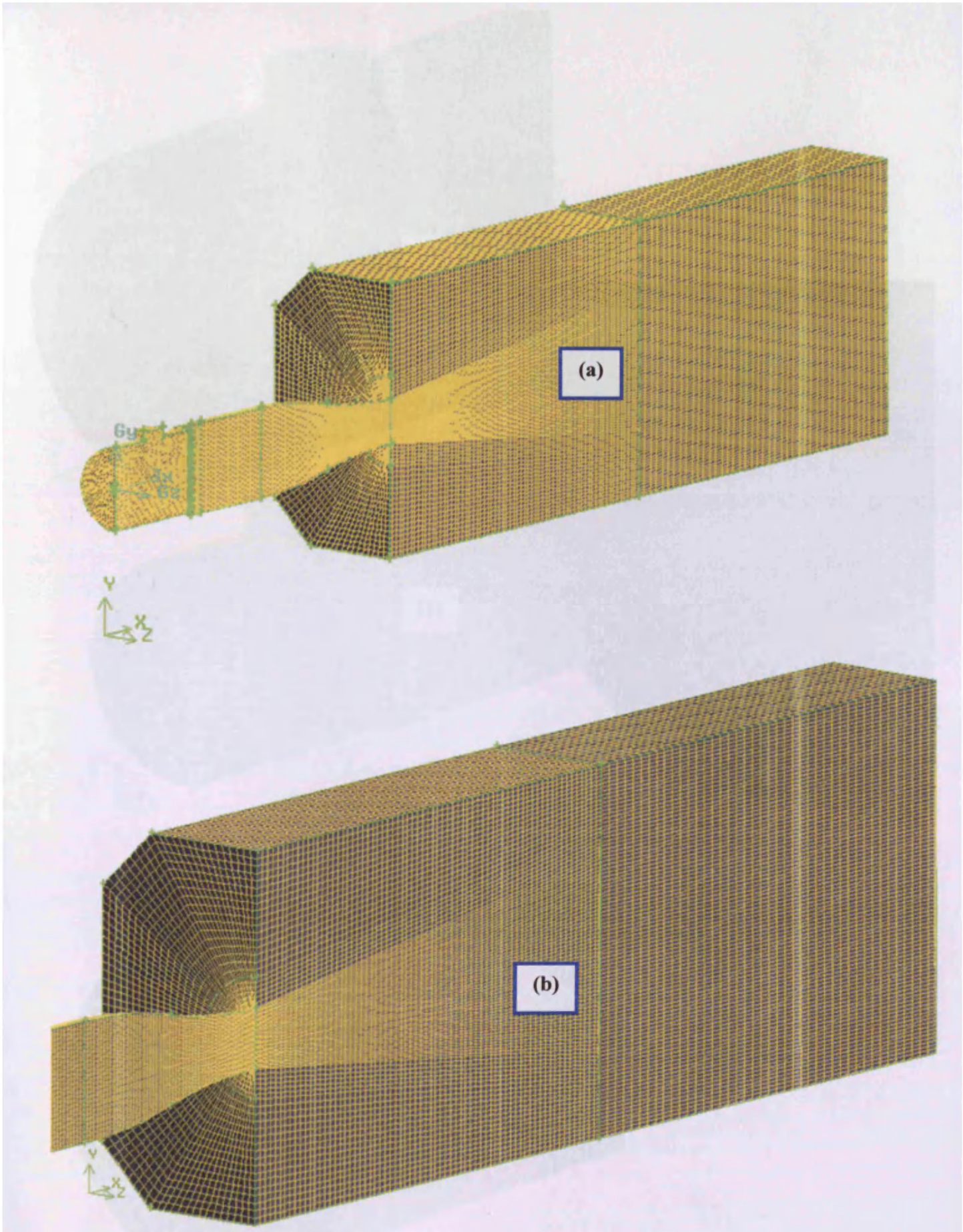

Figure 4.8: The HPOC combustor mesh

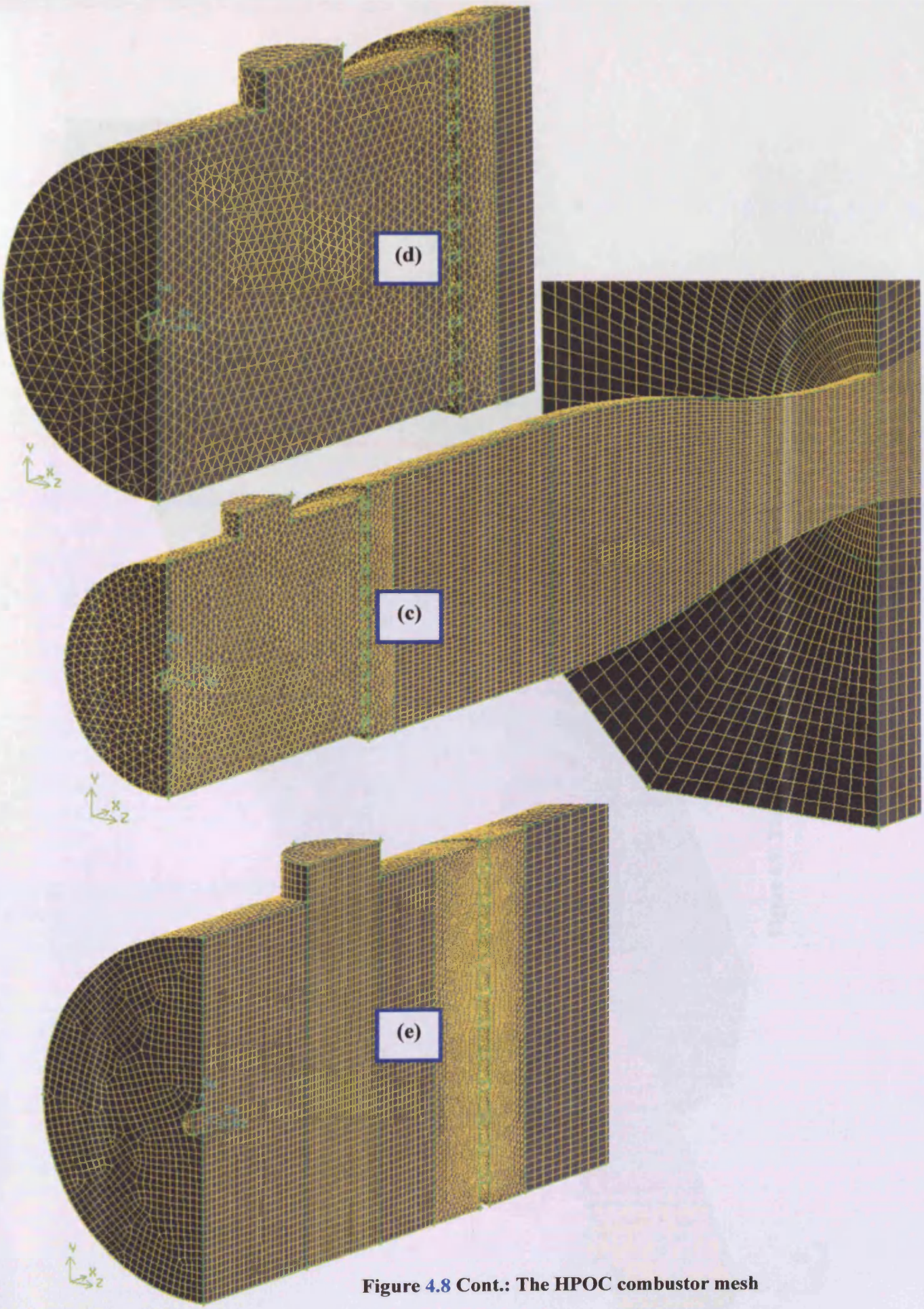

Figure 4.8 Cont.: The HPOC combustor mesh

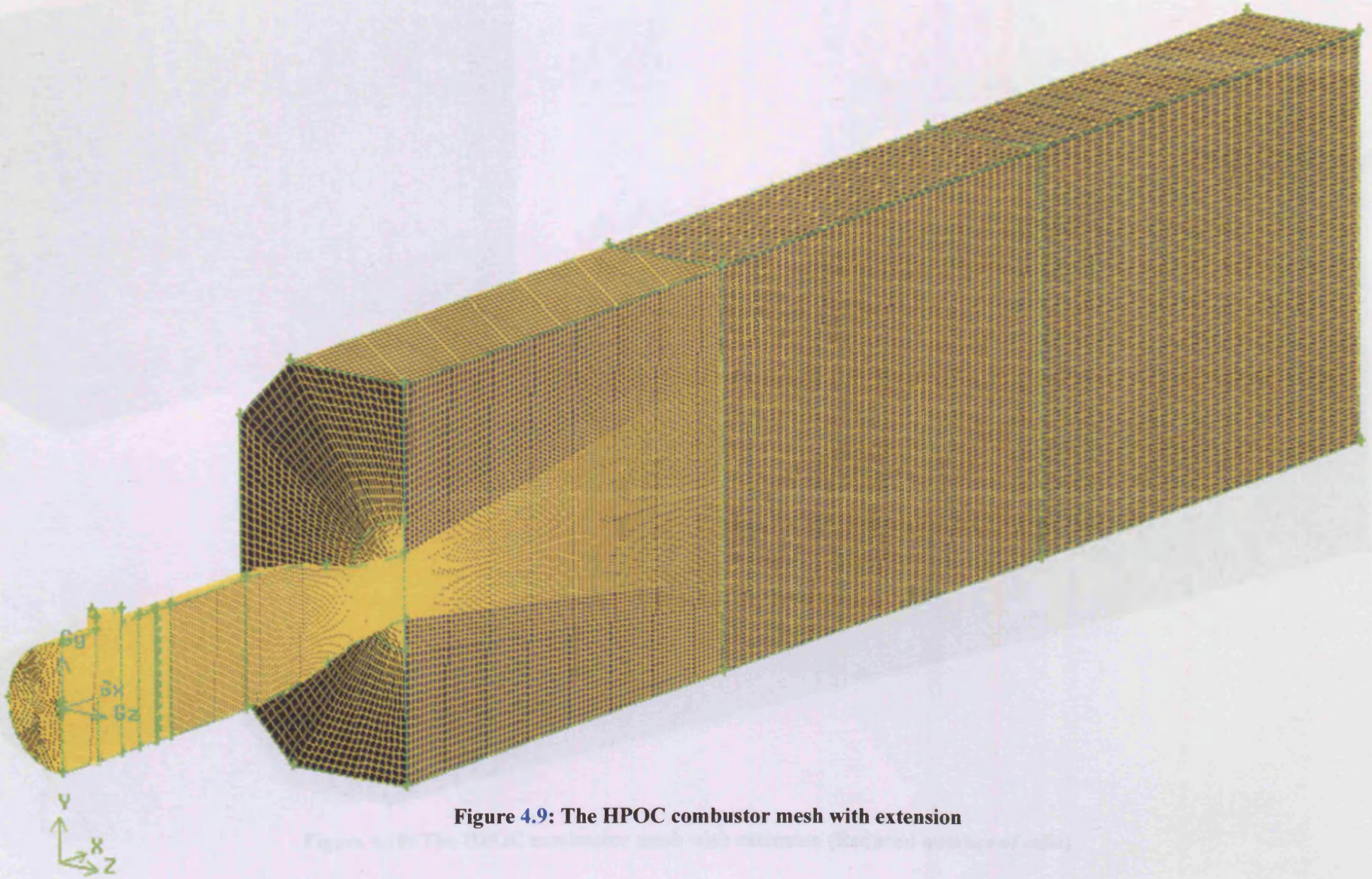

Figure 4.9: The HPOC combustor mesh with extension

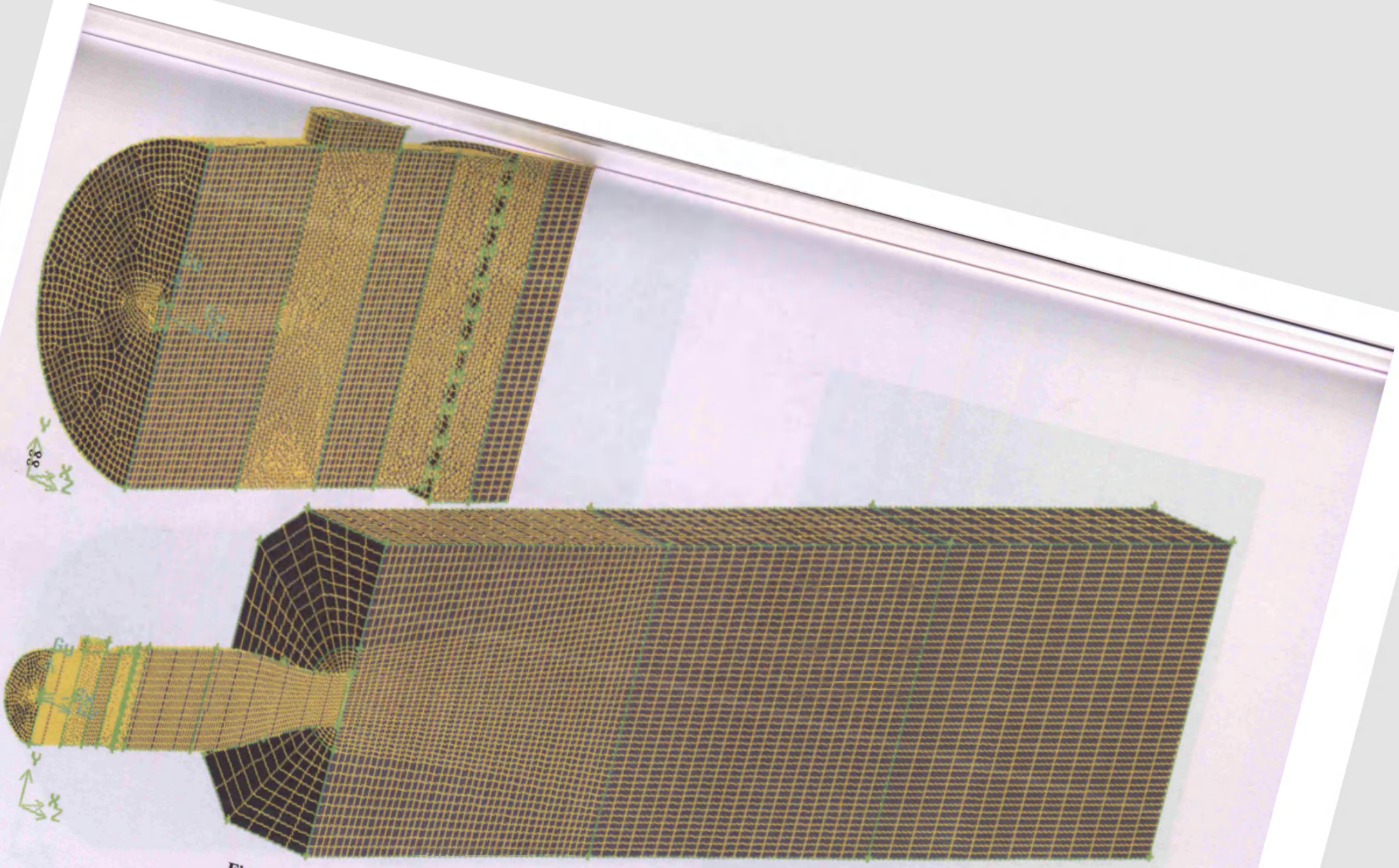

Figure 4.10: The HPOC combustor mesh with extension (Reduced number of cells)

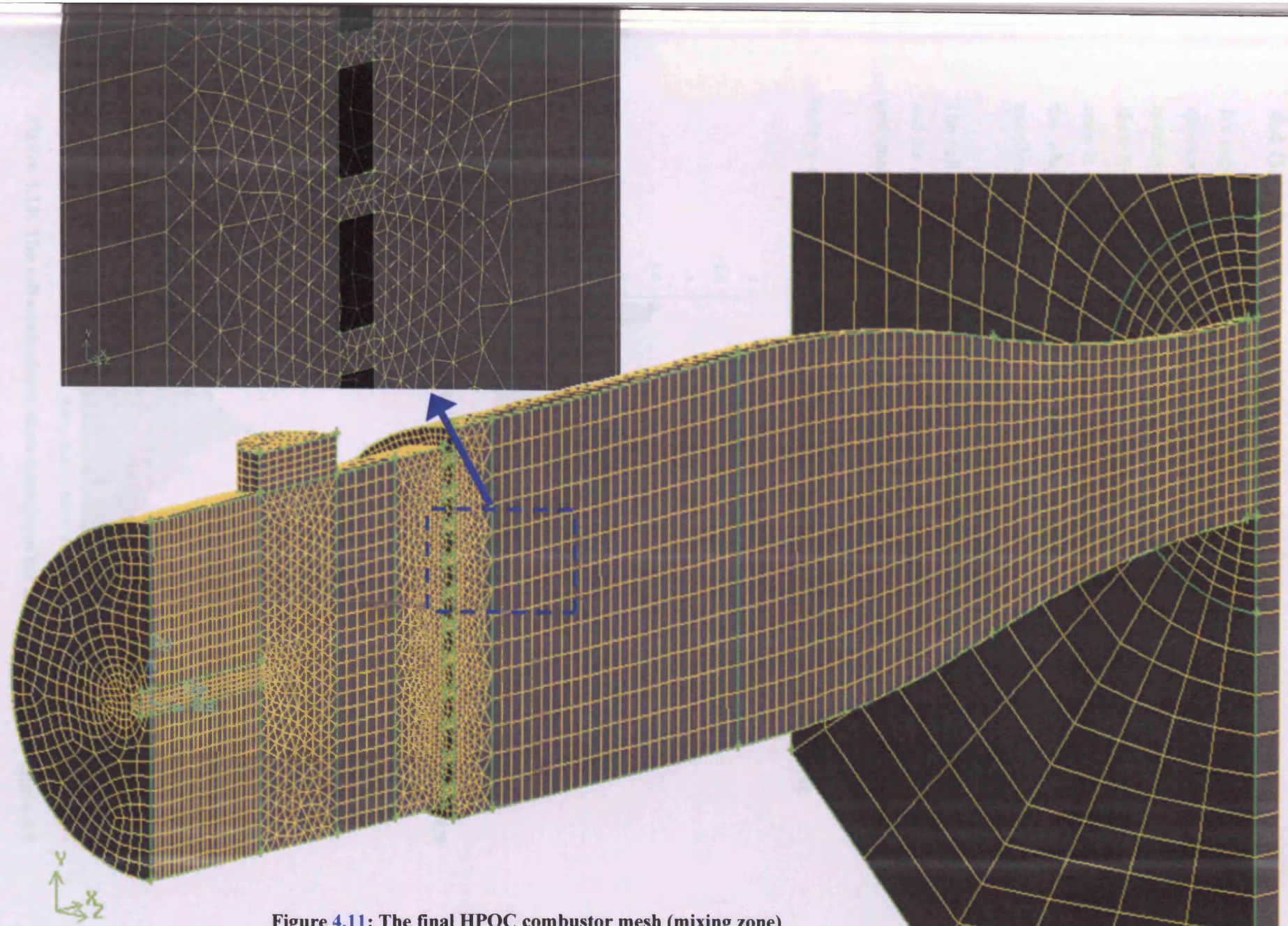

Figure 4.11: The final HPOC combustor mesh (mixing zone)

4.4 Grid Quality

It's important to check the grid quality to ensure good quality results. The grid of Figure 4.9 is checked based on the volume-weighted average method. The cell equiangle skew for the combustion zone is 0.1528 and for the mixing zone is 0.162 and hence the net cell equiangle skew for the whole model is 0.153. Furthermore the cell equivolume skew for the combustion zone is 0.1528 and for the mixing zone is 0.14677 and hence the net cell equivolume skew for the whole model is 0.15269. So, referring to table 3.1, the mesh quality is considered as excellent.

The cell equiangle skew histogram for the model shown in Figure 4.9 is plotted in Figure 4.12 and the cell equivolume skew histogram in Figure 4.13. The data from these plots show that the grid quality is within the range of good and excellent.

Note: y-axis is the percentage of the number of cells to the total number of cells (%).

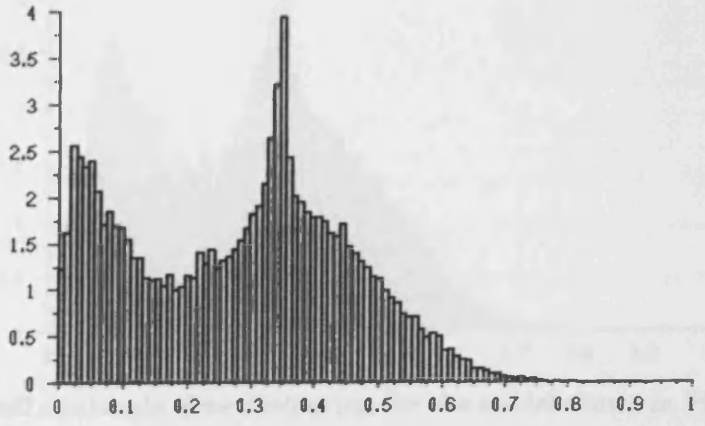

Figure 4.12: The cell equiangle skew histogram for the model shown in figure 4.9

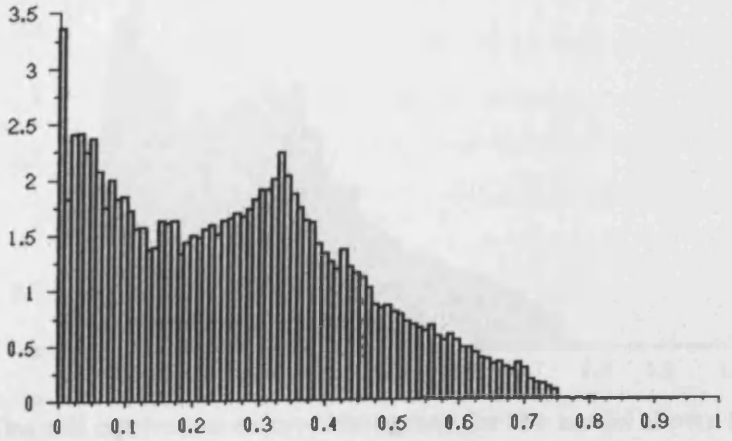

Figure 4.13: The cell equivolume skew histogram for the model shown in figure 4.9

For the final model with reduced number of elements that is shown in Figure 4.11, based on the volume-weighted average method, the cell equiangle skew for the combustion zone is 0.165 and for the mixing zone is 0.1886 and hence the net cell equiangle skew for the whole model is 0.156. Furthermore the cell equivolume skew for the combustion zone is 0.165 and for the mixing zone is 0.181 and hence the net cell equivolume skew for the whole model is 0.1657. So, refereeing to table 3.1, the mesh quality is considered as excellent again.

The cell equiangle skew histogram for the model shown in Figure 4.11 is plotted in Figure 4.14 and the cell equivolume skew histogram is plotted in Figure 4.15. The data from these plots show that the grid quality is within the range of good and excellent. So, the model with reduced number of cells has the same mesh quality as the original model shown in Figure 4.9.

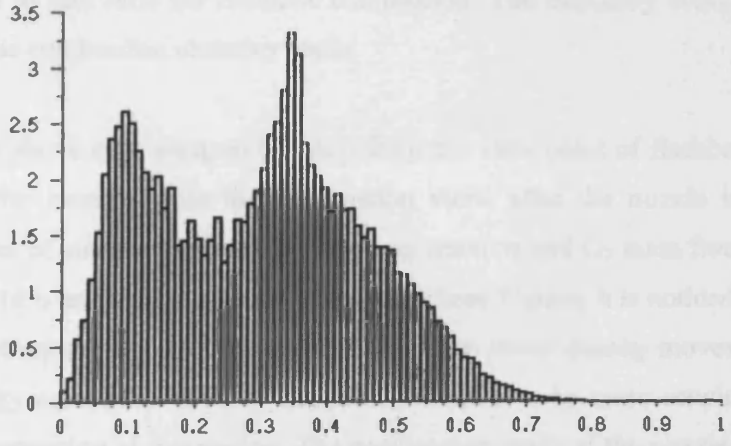

Figure 4.14: The cell equiangle skew histogram for the model shown in Figure 4.11

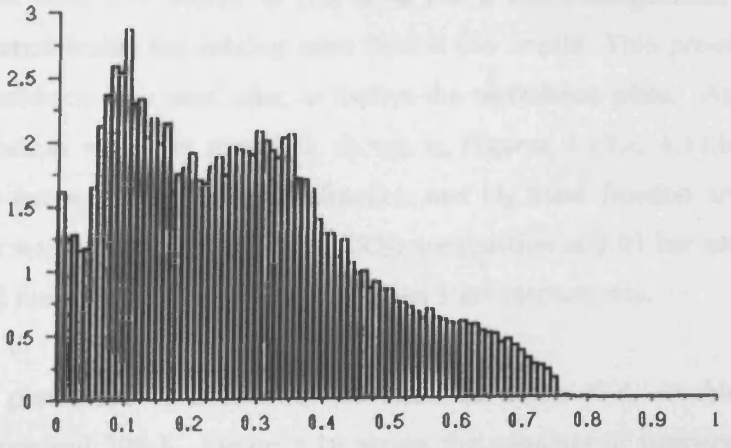

Figure 4.15: The cell equivolume skew histogram for the model shown in Figure 4.11

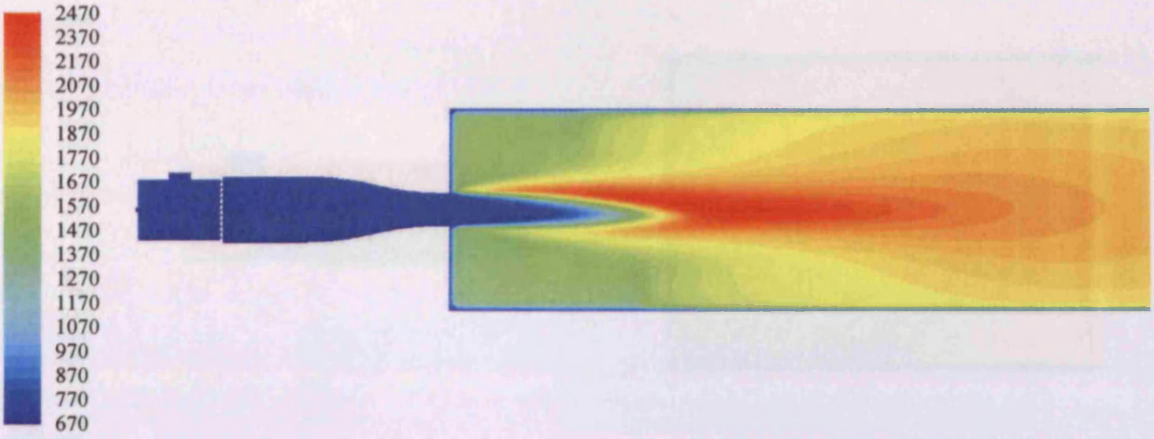

(a): Contours of Static Temperature in [K]

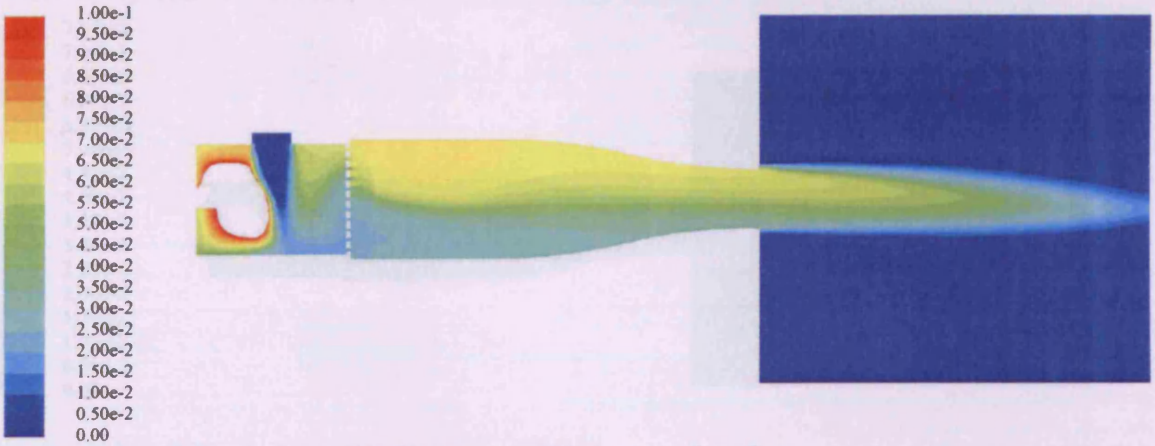

(b): Contours of CH_4 mass fraction

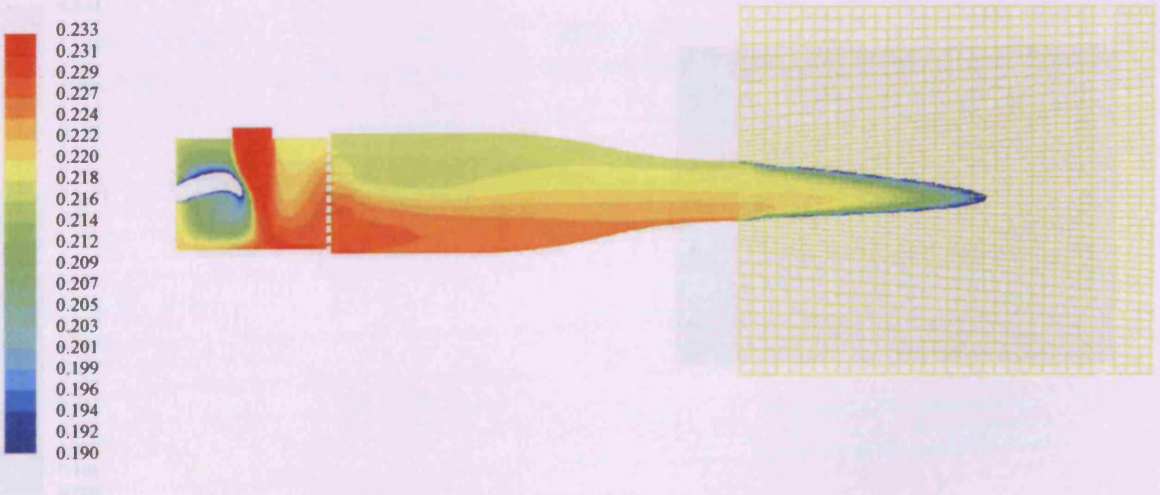

(c): Contours of O_2 mass fraction

Figure 4.16: The simulation of stable flame for CH_4 combustion at 7.11 bar and 674 K

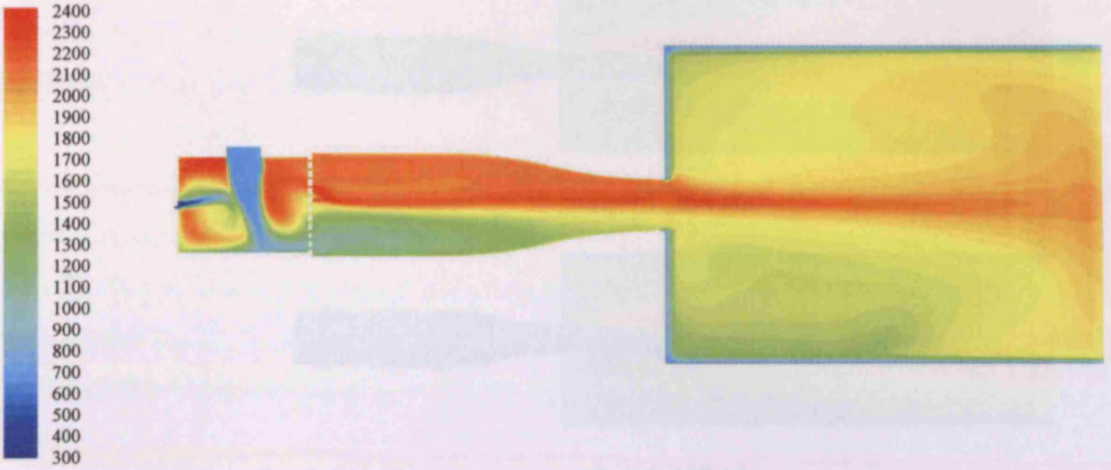

(a): Contours of Static Temperature in [K] – "Flashback"

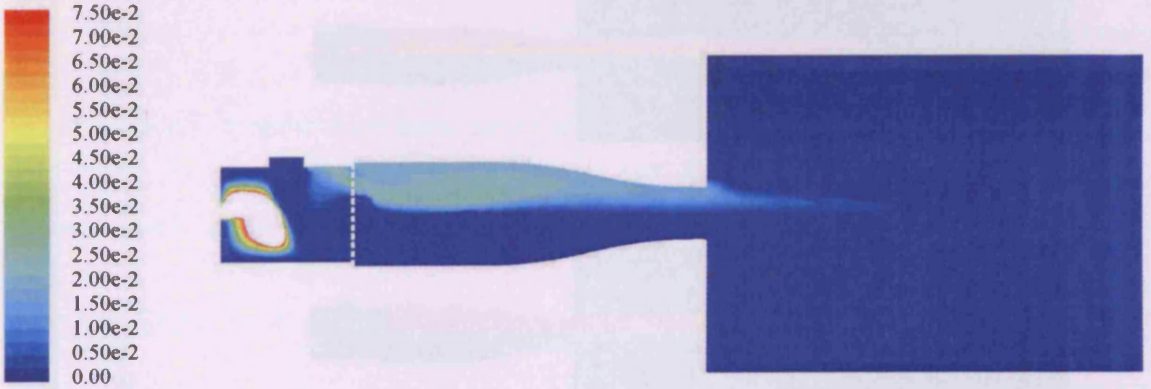

(b): Contours of CH_4 mass fraction

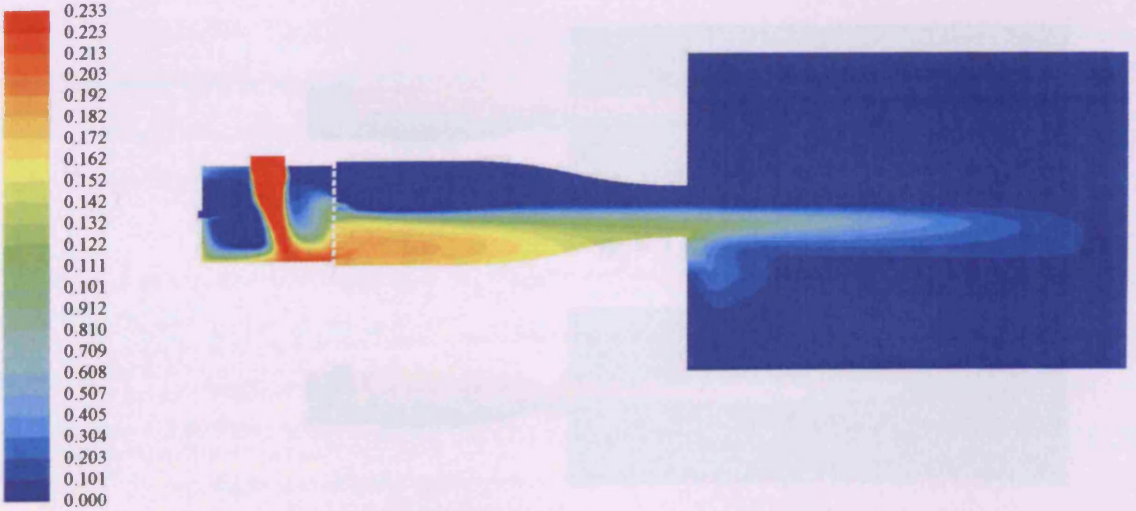

(c): Contours of O_2 mass fraction

Figure 4.17: The simulation of flashback flame for (85%CH_4 +15%CO_2) combustion at 3.01 bar and 674 K

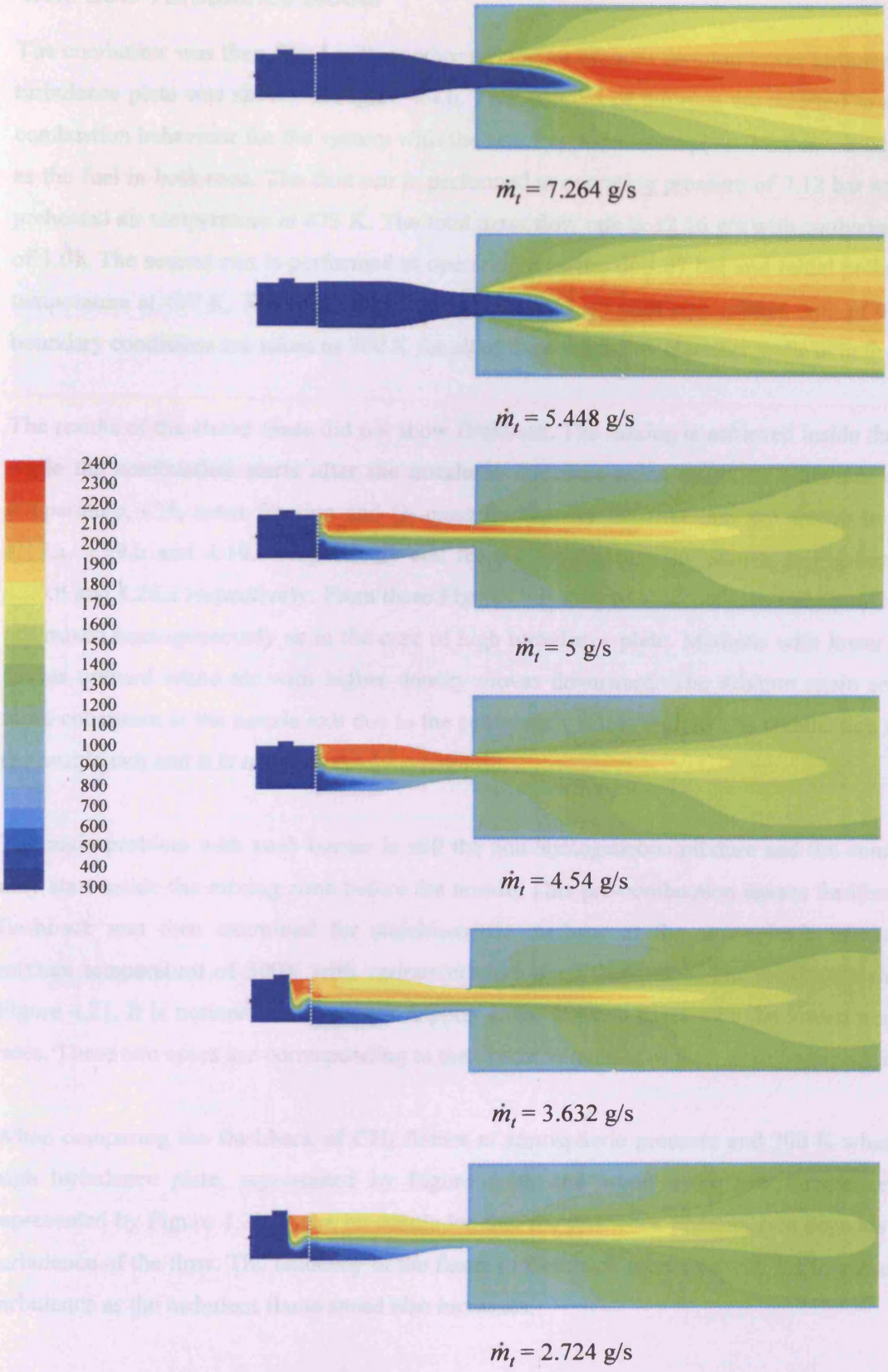

Figure 4.18 : Contours of Static Temperature in [K] for stoichiometric CH_4 combustion at different mass flow rates for the system with high turbulence plate

4.5.2 Low Turbulence Model

The combustor was then fitted with another turbulence plate to develop lower turbulence. This turbulence plate was shown in Figure 4.4.b. Two samples of the runs are selected to show the combustion behaviour for the system with the new low turbulence plate. Methane is considered as the fuel in both runs. The first run is performed at operating pressure of 7.12 bar and initial preheated air temperature at 473 K. The total mass flow rate is 12.16 g/s with equivalence ratio of 1.01. The second run is performed at operating pressure of 3.07 bar and initial preheated air temperature at 477 K. The total mass flow rate is 4.453 g/s with equivalence ratio of 0.96. The boundary conditions are taken as 700 K for all of the combustion chamber walls in both runs.

The results of the above cases did not show flashback. The mixing is achieved inside the burner while the combustion starts after the nozzle in the combustion chamber. Contours of static temperature, CH_4 mass fraction and O_2 mass fraction for the first case are shown in Figures 4.19.a, 4.19.b and 4.19.c respectively and for the second case are shown in Figures 4.20.a, 4.20.b and 4.20.c respectively. From these Figures it is noticed that methane and air mixture are not mixed homogeneously as in the case of high turbulence plate. Methane with lower density moves upward while air with higher density moves downward. The mixture again seems be more consistent at the nozzle exit due to the contraction at this region. The combustion starts at the nozzle exit and it is not completely symmetric.

The main problem with such burner is still the non-homogeneous mixture and the combustion may start inside the mixing zone before the nozzle. This pre-combustion causes flashback. The flashback was then examined for stoichiometric methane at the atmospheric pressure and mixture temperature of 300K with various mixture mass flow rates. The results are shown in Figure 4.21. It is noticed that flashback happen in the last two cases with the lowest mass flow rates. These two cases are corresponding to the lowest velocities of flow as to be expected.

When comparing the flashback of CH_4 flames at atmospheric pressure and 300 K when using high turbulence plate, represented by Figure 4.18, and when using low turbulence plate, represented by Figure 4.21, it can be concluded that the flashback phenomenon depends on the turbulence of the flow. The tendency of the flame to flashback increases with the increase of the turbulence as the turbulent flame speed also increases.

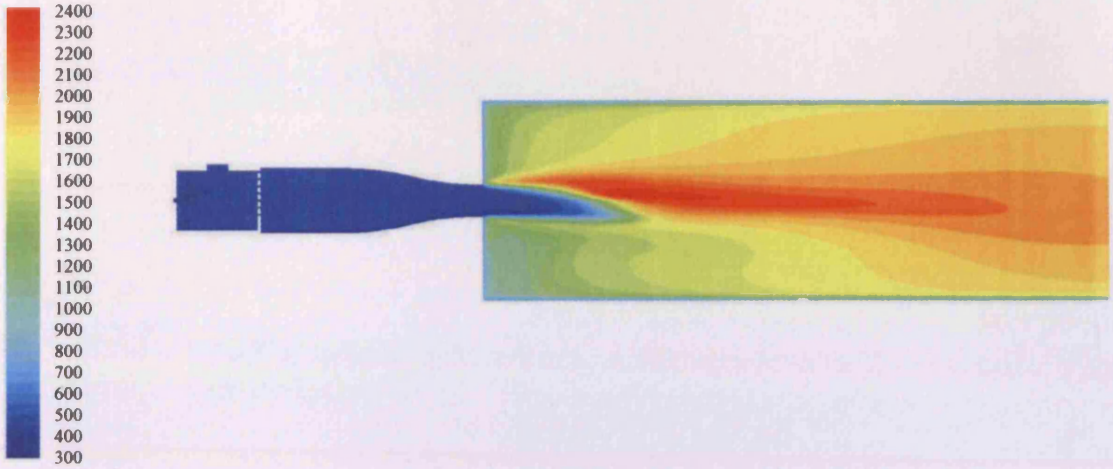

(a): Contours of Static Temperature in [K]

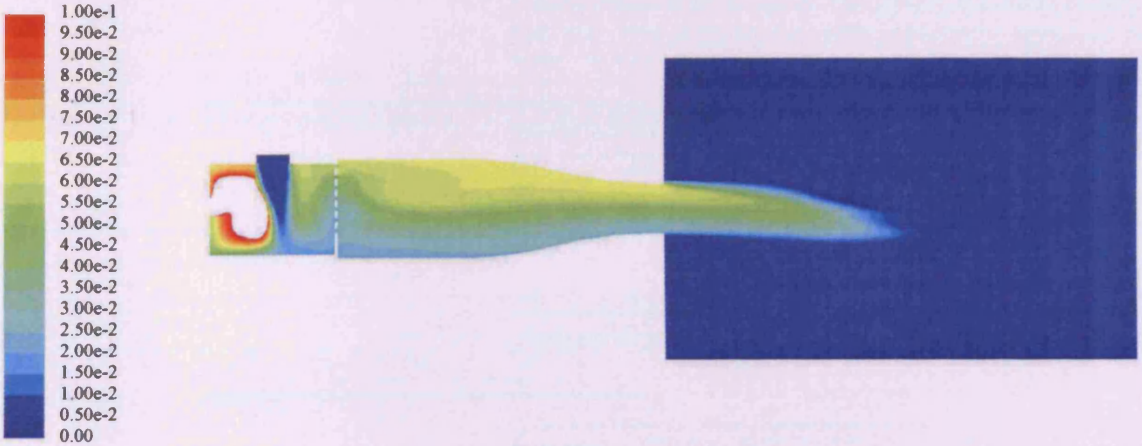

(b): Contours of CH_4 mass fraction

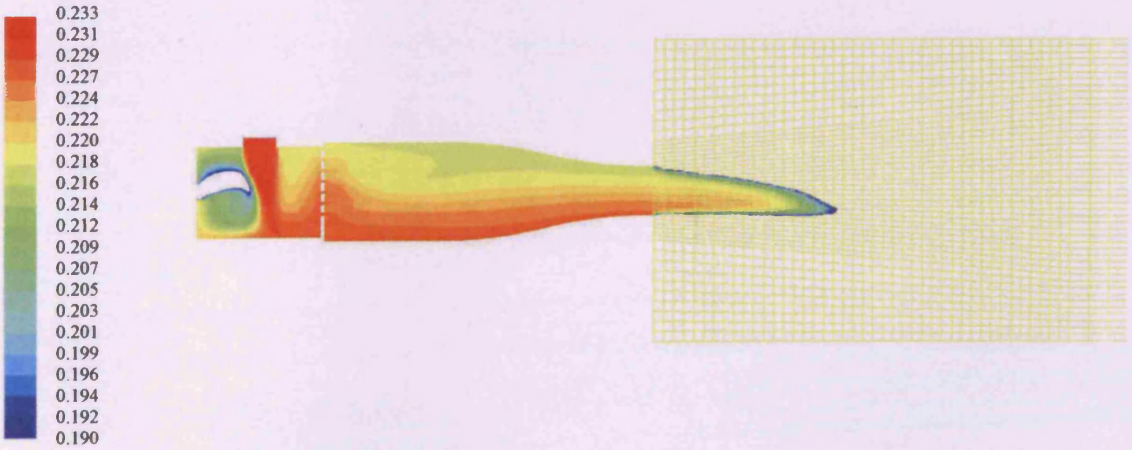

(c): Contours of O_2 mass fraction

Figure 4.19: The simulation of CH_4 combustion at 7.12 bar and 473 K

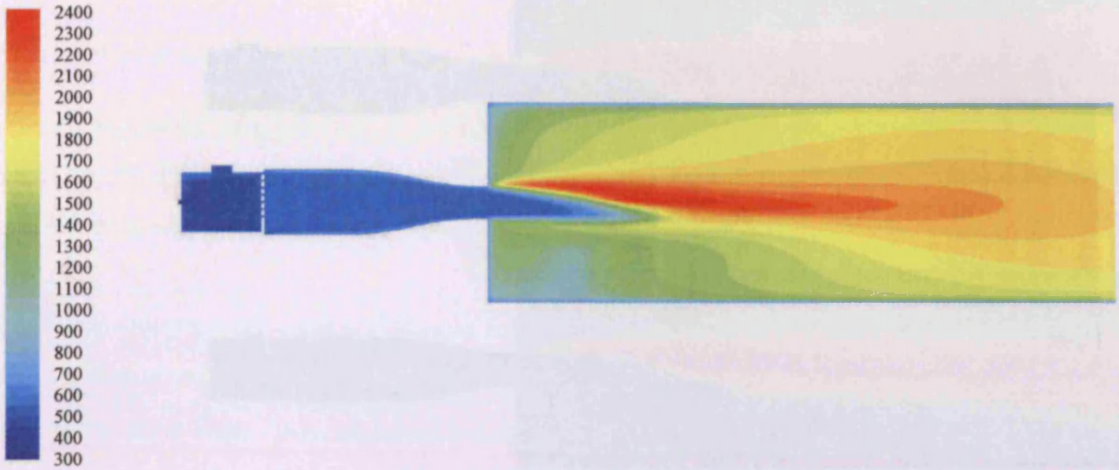

(a): Contours of Static Temperature in [K]

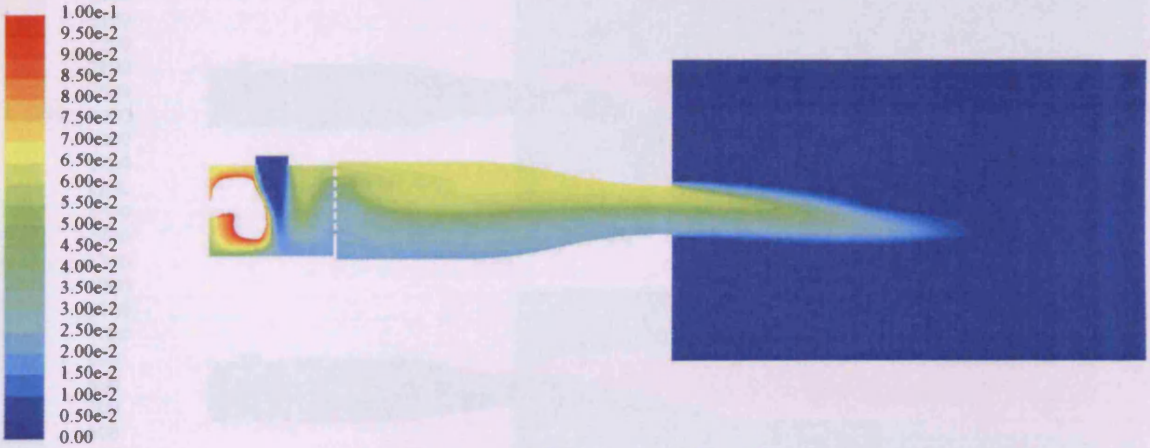

(b): Contours of CH_4 mass fraction

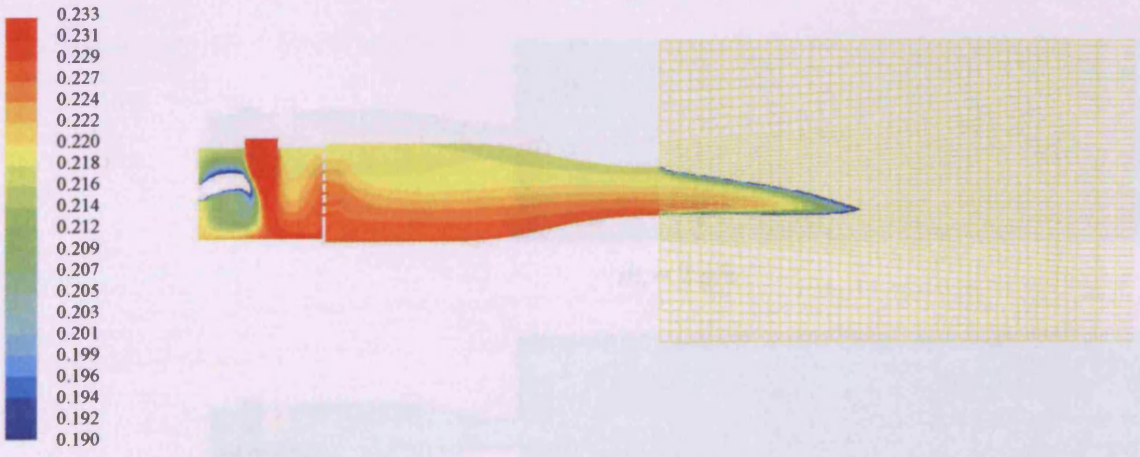

(c): Contours of O_2 mass fraction

Figure 4.20: The simulation of CH_4 combustion at 3.07 bar and 477 K

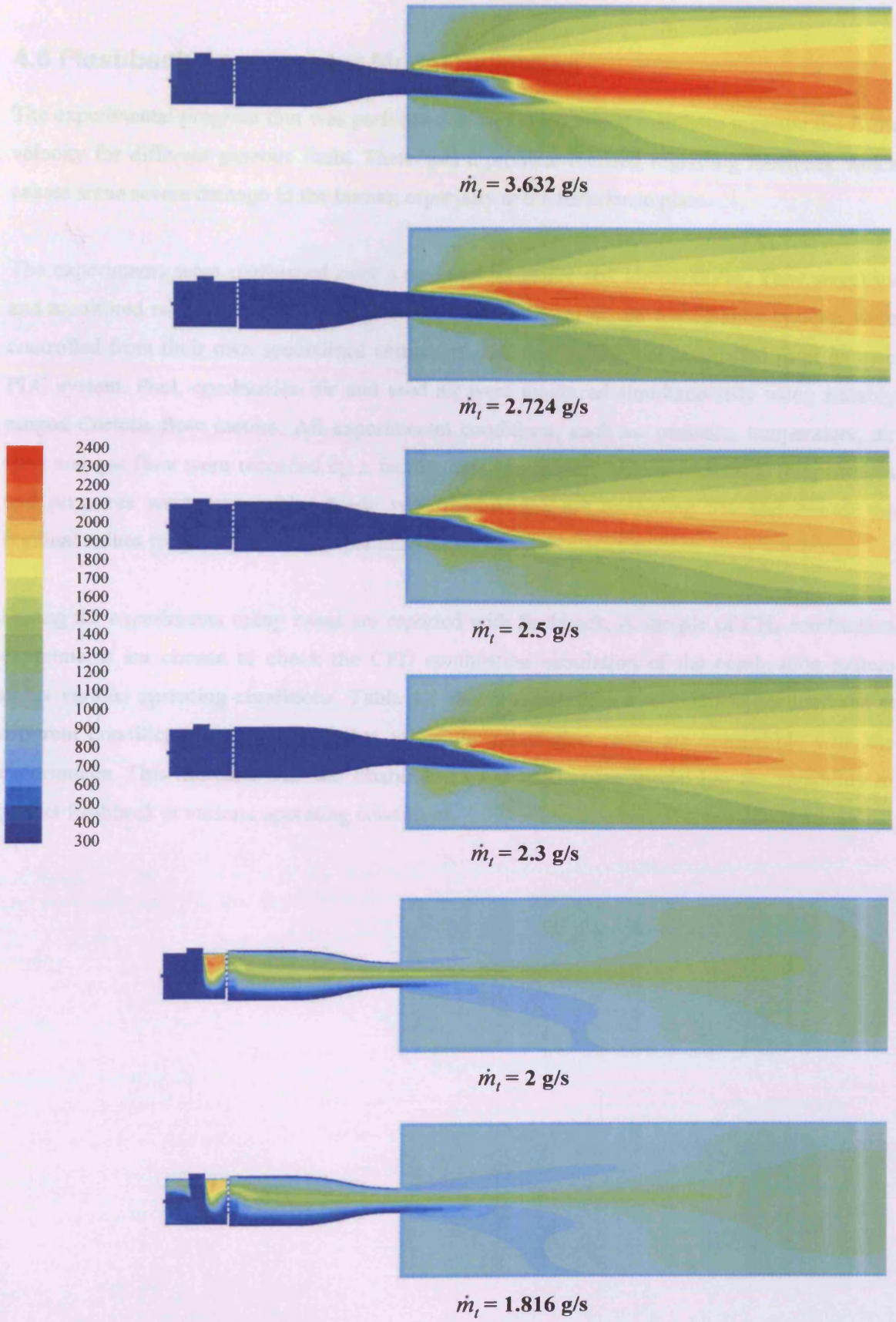

Figure 4.21: Contours of Static Temperature in [K] for stoichiometric CH_4 combustion at different mass flow rates for the system with low turbulence plate

4.6 Flashback Assessment Model Validation

The experimental program that was performed in the GTRC aimed mainly to measure the flame velocity for different gaseous fuels. There was a problem realized regarding flashback which causes some severe damage in the burner, especially in the turbulence plate.

The experiments were performed over a range of pressures and temperatures. They were run and monitored remotely from a control room. LDA and laser planar tomography systems were controlled from their own specialized computers, and the facility was controlled from its own PLC system. Fuel, combustion air and seed air were measured simultaneously using suitably ranged Coriolis flow meters. All experimental conditions, such as: pressure, temperature, air flow and gas flow were recorded by a facility data acquisition system. Measured temperatures and pressures were reasonably steady with fluctuations not exceeding 5% and 3% of the nominal values for pressure and temperature respectively.

During the experiments many cases are reported with flashback. A sample of CH_4 combustion experiments are chosen to check the CFD combustion simulation of the combustion system under various operating conditions. Table 4.1 shows the flashback assessment for methane at different conditions. It is realized that all of the simulation cases are compatible with the experiments. This indicates that the established CFD combustion model has the capability to predict flashback at various operating conditions.

Table 4.1: Flashback assessment validation under various combustion conditions

Case No.	Fuel	P (bar)	T (K)	$\dot{m}_a$ (g/s)	$\dot{m}_f$ (g/s)	ϕ	Flashback		
							Experiment		Modelling
1.		10.19	580	22.30	1.246	0.96	No		No
2.		7.12	473	11.48	0.673	1.01	No		No
3.		7.01	576	13.83	0.814	1.01	No		No
4.		3.07	477	4.5	0.253	0.96	No		No
5.	CH_4	3.0	470	10.90	0.84	1.32	No		No
6.		10	680	5.0	0.18	0.62	Yes		Yes
7.		7.11	678	17.14	0.986	0.99	Yes		Yes
8.		7	476	10.5	0.66	1.08	Yes		Yes
9.		2.96	486	2.17	0.182	1.44	Yes		Yes

4.7 Summary

In this chapter, the physical model in which the research is performed is introduced. Various trials to construct a good mesh which is able to produce good results at a reasonable time are performed. The original combustion system is simulated at different combustion conditions. The following notes can be reported:

- The cell type must be chosen carefully as it affects the solution accuracy and time.
- It is important to make a balance between the number of the mesh cells and the time consumed by the model to reach the convergence.
- The turbulence plays an important role in flame stabilization. The presence of turbulence significantly increases the flame speed due to the increase of mixing rates and, through flame surface wrinkling, the flame surface area.
- The flashback exists at certain combustion conditions depending on some variables. These variables include the fuel mixture, operating pressure, mixture temperature, equivalence ratio, mixture mass flow rate and the turbulence plate used. The effect of these variables on flashback will be studied in the next chapter.
- The original HPOC gas combustion system is suitable for turbulent flame speed calculations although it has some drawbacks. The main problem with it is that it is not able to produce homogeneous mixture for premixed combustion and this issue needs to be addressed. A generic swirl burner will be considered in the next chapters as being indicative of behaviour in realistic gas turbine combustors.

Chapter 5

FLASHBACK LIMITS DETERMINATION IN SWIRL BURNERS

5.1 Introduction

Amongst the most promising technologies used to reduce the impact and production of NOx, lean premixing and swirl stabilized combustion are regarded as very good options. However, premixing is not perfect because usually fuel and air are mixed shortly before entering the combustion chamber leading to a significant degree of unmixedness. This generates a complex process that creates thermoacoustic instabilities which would feedback into the mixing-reaction process of combustion. Swirl flow technologies have shown to give high flame stability taking advantage of coherent structures such as corner and central recirculation zones which anchor the flame, recirculating hot products and active chemical species whilst also increasing their residence time, allowing the use of low equivalence ratios thus giving lower flame temperatures and NOx emissions. However, there are some gaps in the entire understanding of these flames.

A problem of swirl combustion, especially with premixed flames, is the flashback produced by high swirl systems, with a phenomenon observed at the tip of the burner where injectors are positioned for diffusive flames, as for complete flashback into the fuelling system in premixed combustion. The latter is defined as the point where the flame physically propagates upstream of the region where it is supposed to anchor and into premixing passages that are not designed for high temperatures. This occurs when the turbulent flame speed exceeds the flow velocity along some streamline, often occurring in the boundary layers, which usually are the point of lowest flow velocity. However, in swirling flows the process is not only influenced by the turbulent flame speed, but also by combustion instabilities and the axial reversed flow in the central recirculation zone, which can easily extend backwards over the injector under certain conditions and cause the flame to propagate undesirably upstream. It must be remember that flashback is not a continuous upstream propagation but is composed of numerous movements or jumps of the flame from the combustion chamber into the mixing zone. Resistance to these effects have also been linked to preheating temperature, laminar flame speed and fuel composition.

It has been recognised that the shape of the CRZ can influence the final stability of the system. However, vortical structures can be modified by geometrical factors and flow conditions, as

well as by the interaction of unburnt gases and the reaction zone, complicating even more their part in flashback occurrence and avoidance.

Another problem related to partial flashback in recent studies (especially with liquid fuels) is the amount of deposit produced by the high concentration of carbon radicals generated in the CRZ during the combustion process, due to the increased residence time which augments the soot growth nucleation. If the CRZ extends back to the injector, this can leave thick deposits on the injector surfaces, reducing the efficiency and increasing maintenance requirements.

In this chapter, a swirl burner is introduced to perform flashback analysis. Both partial and full flashbacks are considered with nonpremixed and premixed flames. Two modifications for the swirling model with different nozzle geometries are suggested. The modifications are aimed to eliminate the partial flashback. They are used with the possibility of both premixed and diffusive fuel injection. Both modifications are simulated and compared with the original swirl model with different operating conditions. One of these two modifications is selected to continue the simulation and flashback research as it gives better results than the original swirl model.

To determine the stability limits of flames, the effect of combustion operating conditions on flashback is studied. Also, the size and shape of the recirculation zone associated region of high turbulence are studied as they are critical to flame stability, combustion intensity and performance. The operating pressure, temperature, equivalence ratio, and mixture mass flow rate are considered as crucial variables that affects flashback and recirculation zone and hence the stability limits of flames.

5.2 Swirl Burner Model

A swirl burner is used to improve the mixing characteristics and to stabilize the flame. In this burner a swirler is used to achieve the flame stabilization. The new burner is primarily simulated with both non-premixed and premixed combustion.

The swirl burner components are shown in Figure 5.1, and the assembly of these components is shown in Figure 5.2.

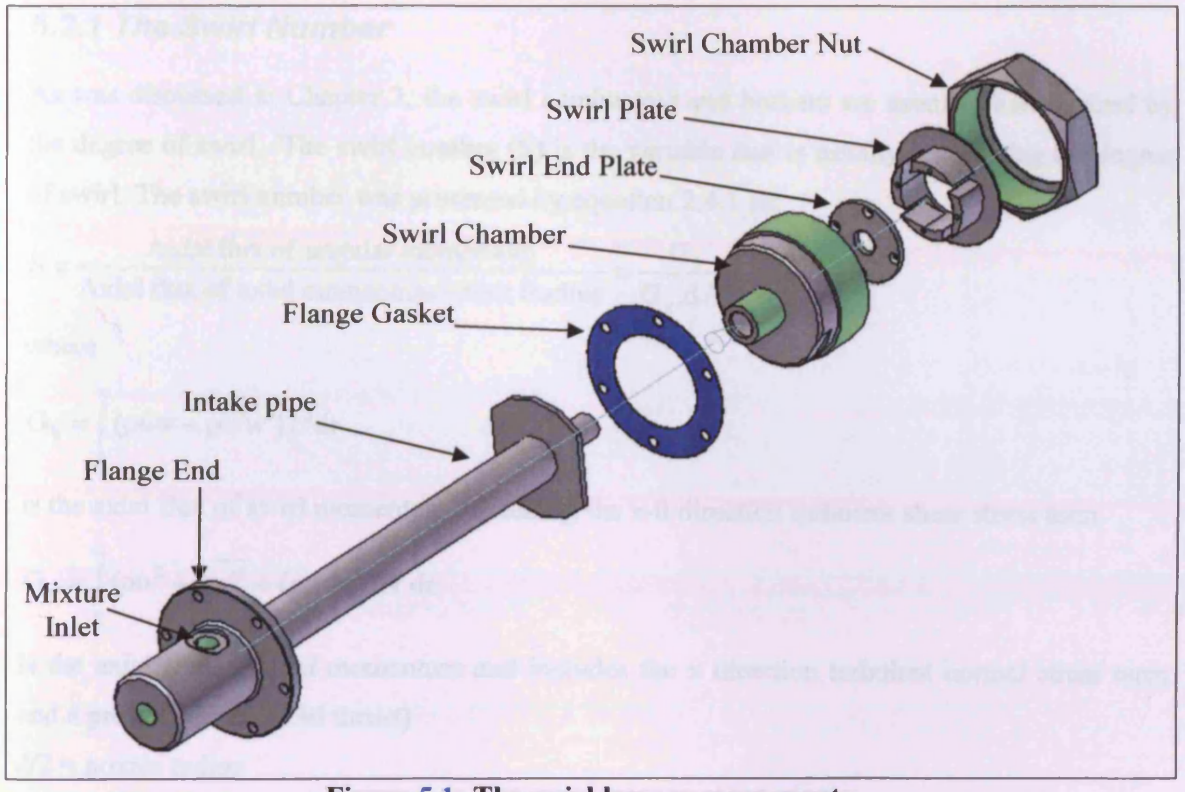

Figure 5.1: The swirl burner components

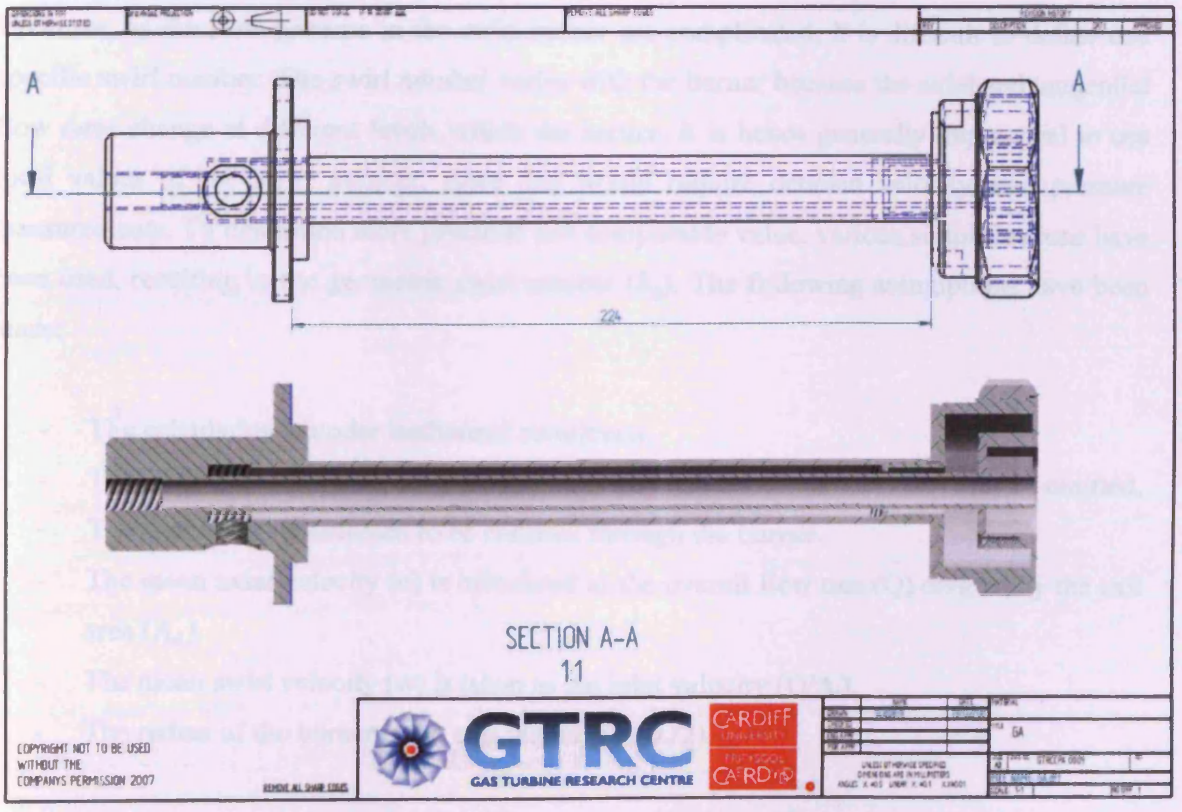

Figure 5.2: The swirl burner assembly

5.2.1 The Swirl Number

As was discussed in Chapter 2, the swirl combustors and burners are usually characterized by the degree of swirl. The swirl number (S) is the variable that is usually introducing the degree of swirl. The swirl number was presented by equation 2.4.1 as:

$$S = \frac{\text{Axial flux of angular momentum}}{\text{Axial flux of axial momentum} \times \text{Exit Radius}} = \frac{G_\theta}{G_x.d/2}$$

where

$$G_\theta = \int_0^\infty (\rho uw + \rho\overline{u'w'})\, r^2 dr$$

is the axial flux of swirl momentum, including the x-θ direction turbulent shear stress term.

$$G_x = \int_0^\infty (\rho u^2 + \rho\overline{u'^2} + (p - p_\infty))\, r\, dr$$

is the axial flux of axial momentum and includes the x direction turbulent normal stress term and a pressure term (axial thrust)

d/2 = nozzle radius

u, v, w = velocity components in (x, r, θ) cylindrical polar coordinate directions.

However, as the flow patterns in the swirl burner are complicated, it is difficult to define one specific swirl number. The swirl number varies with the burner because the axial and tangential flow rates change at different levels within the burner. It is hence generally impractical to use local values of the swirl number, since this would require detailed velocity, and pressure measurements. To determine more practical and comparable value, various simplifications have been used, resulting in the geometric swirl number (S_g). The following assumptions have been made:

- The calculation is under isothermal conditions.
- The static pressure (p) is assumed to be constant across the exit and can thus be omitted.
- The density (ρ) is assumed to be constant through the burner.
- The mean axial velocity (u) is calculated as the overall flow rate (Q) divided by the exit area (A_e).
- The mean swirl velocity (w) is taken as the inlet velocity (Q/A_i).
- The radius of the burner is the exit radius ($r_o = D_o/2$).

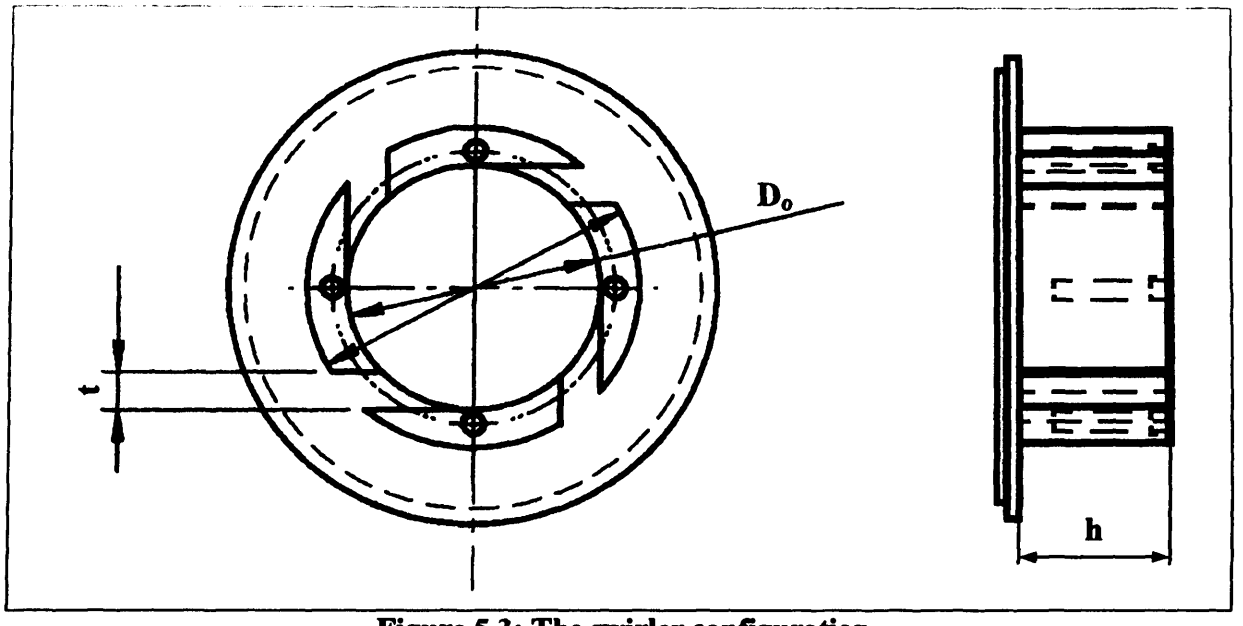

Figure 5.3: The swirler configuration

Hence, the geometric swirl number can be expressed as:

$$S_g = \frac{G_\theta}{G_x.d/2} = \frac{\dot{m}_i w_i r_{eff}}{\dot{m}_o u_o r_o}$$

$$= \frac{w_i r_{eff}}{u_o r_o}$$

$$= \frac{(Q/A_i) r_{eff}}{(Q/A_o) r_o}$$

$$= \frac{A_o r_{eff}}{A_i r_o}$$

$$S_g = \frac{\pi(r_o^2 - r_p^2)(r_i - \frac{t}{2})}{(4 \cdot t \cdot h) r_o} \qquad 5.2.1$$

where

r_o is the radius of the swirl burner at exit, r_p is the radius of the internal pipe (if found), r_i is the radius of the swirl burner at inlet (in this case $r_i = r_o$), t is the flow passage width between the blades, h is the highet of the flow passage.

The geometrical swirl number (S_g) was calculated based on the geometrical configurations given by equation 5.2.1 and it was 1.78.

5.2.2 Mesh Construction

A complete three dimensional model is used for the simulation. The complete system can be easily meshed by a tetrahedral unstructured mesh but it leads to higher number of elements generated which translates to longer computational times, whilst the solution is not stable for some viscous models. A hexahedral mesh was used to give fast and stable solutions. The simulation of the intake pipe starts just prior the swirl passage after a flame arrest protruded edge as shown in Figure 5.4.a. Figure 5.4.b shows a cross section of the swirler grid and the hexahedral elements are shown clearly.

The installation of the swirler in the combustion chamber and the grid is shown in Figures 5.5.

The swirl burner is incorporated with the combustion chamber. It is modelled firstly with both optical and non-optical parts only as shown in Figure 5.6.a. The total number of cells in this model is 91,060 cells. During simulation it is noticed that there exists a reversed flow at the far outlet of the mesh. A suggested solution of eliminating the reversed flow is to extend the simulated volume longitudinally in the direction of flow. This extension can eliminate the reversed flow and helps in the model convergence, this is shown in Figures 5.6.b. The extension was chosen to have the same dimensions as the non-optical part of the combustion chamber (which is similar to the optical part too). This extension increased the total number of the cells by 14,588 cells giving a total number of 101,480. However the reversed flow still existed after adding the first extension so another extension of 10,420 cells was added to the model giving a total of 116,068 cells. The reversed flow at the mesh exit is completely eliminated with the new extension, whilst the results do not show a significant change in the combustion patterns near the burner i.e. there is no change in the combustion characteristics in both the optical and non-optical parts. The only effect of the second extension was the elimination of the reversed flow. So, it is preferred to omit the second extension and continue the simulation with only one extension.

The shape of the cells near the burner exit was also changed as they have high skew. The final model is shown in Figure 5.7. The complete system is shown in Figure 5.7.a. and a cross section in the centre line of the model is shown in Figure 5.7.b. with an enlargement around the burner in Figure 5.7.c. Finally this model has a total number of cells of 123,538 cells.

The selected plane for monitoring the results was the vertical plane crossing the centre line of the model and it is shown in Figure 5.8.

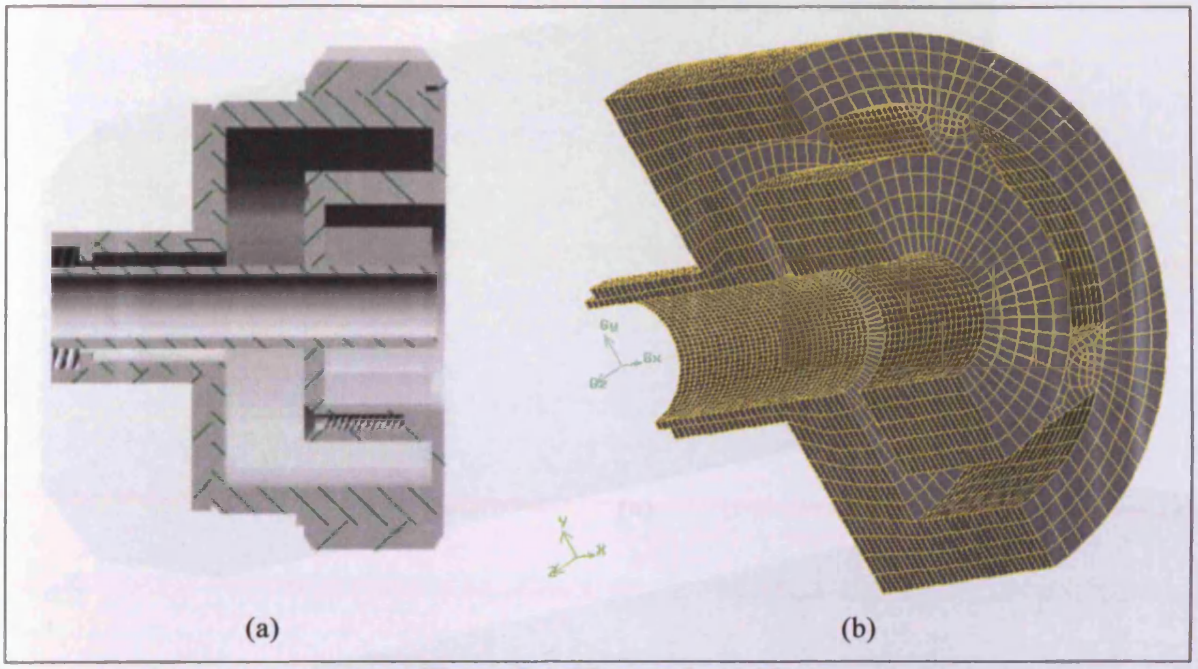

Figure 5.4: The swirler grid

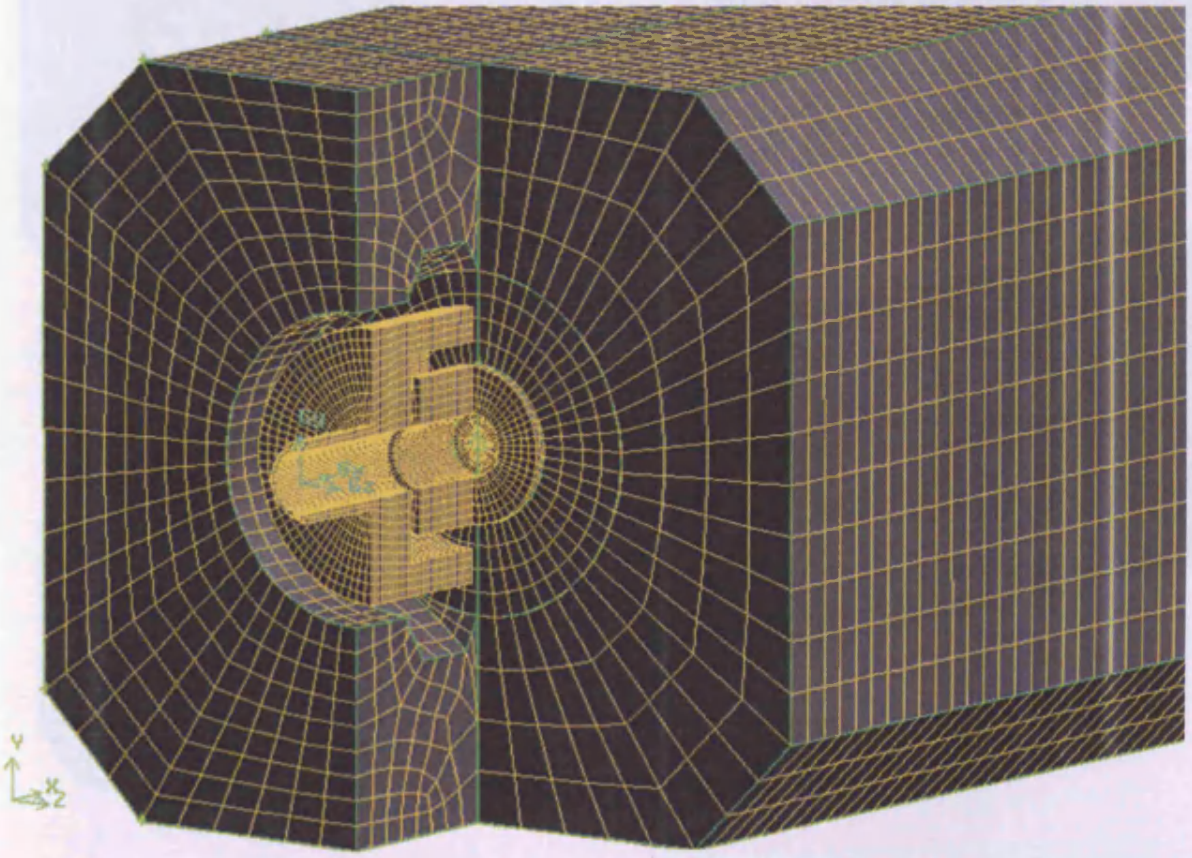

Figure 5.5: A partially cross section showing the swirler installation in the combustion chamber and the model grid

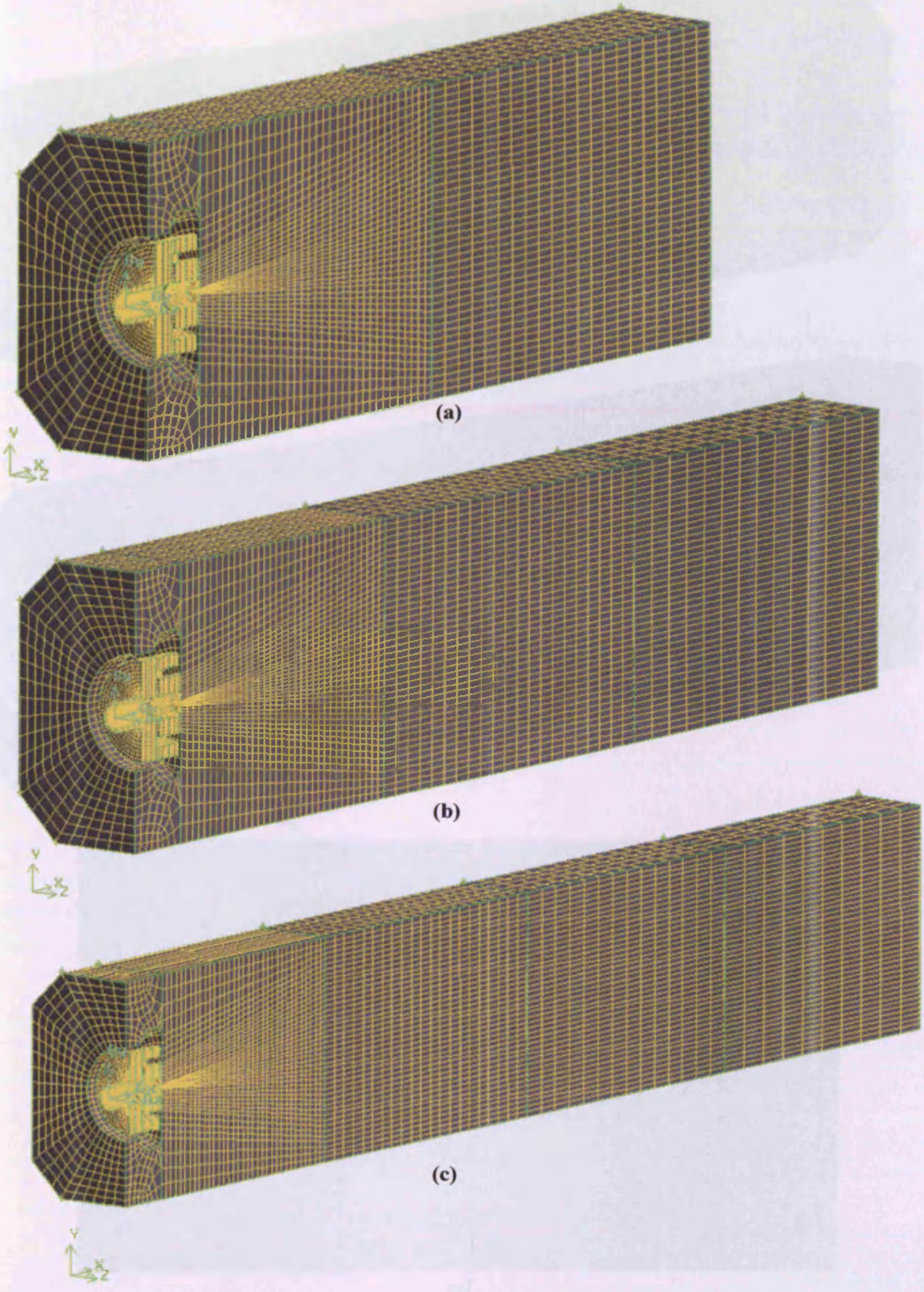

Figure 5.6: Using extensions to eliminate the reversed flow – "model section"

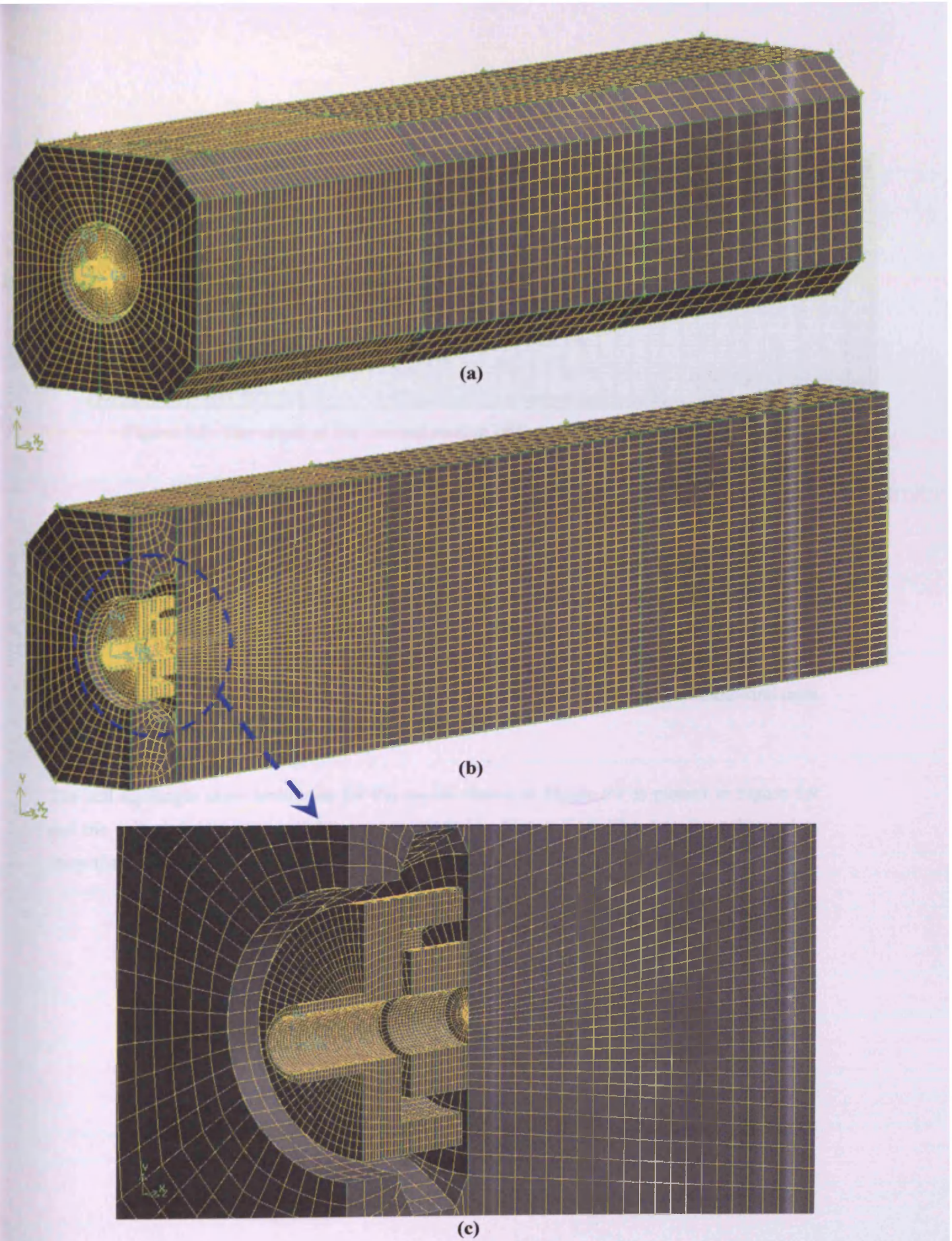

Figure 5.7: The final system with swirl burner mesh

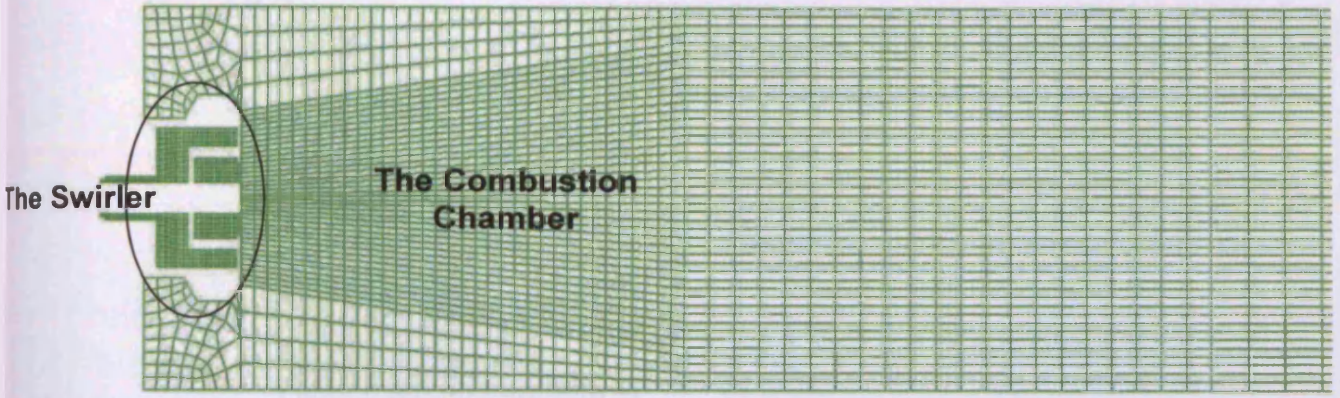

Figure 5.8: The mesh at the central section of the whole system with the swirler

5.2.3 Grid Quality

The grid of Figure 5.7 is checked based on the volume-weighted average method. The cell equiangle skew for the combustion zone is 0.1969 and for the swirler zone is 0.109 and hence the net cell equiangle skew for the whole model is 0.1965. So, refereeing to table 3.1, the mesh quality is considered as excellent. It must be noted that the most of the cells that have high skew in the combustion chamber are those around the nut as it is difficult to adapt the hexahedral cells to fit the curves and cuts smoothly in these positions.

The cell equiangle skew histogram for the model shown in Figure 5.7 is plotted in Figure 5.9 and the cell equivolume skew histogram is plotted in Figure 5.10. The data from these plots show that the grid quality is within the range of good and excellent.

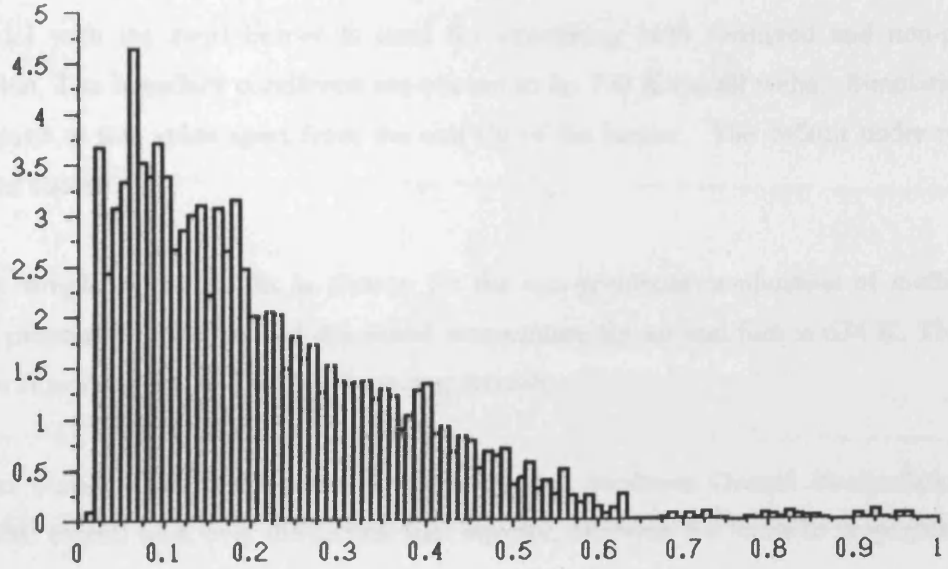

Figure 5.9: The cell equiangle skew histogram for the model shown in Figure 5.7

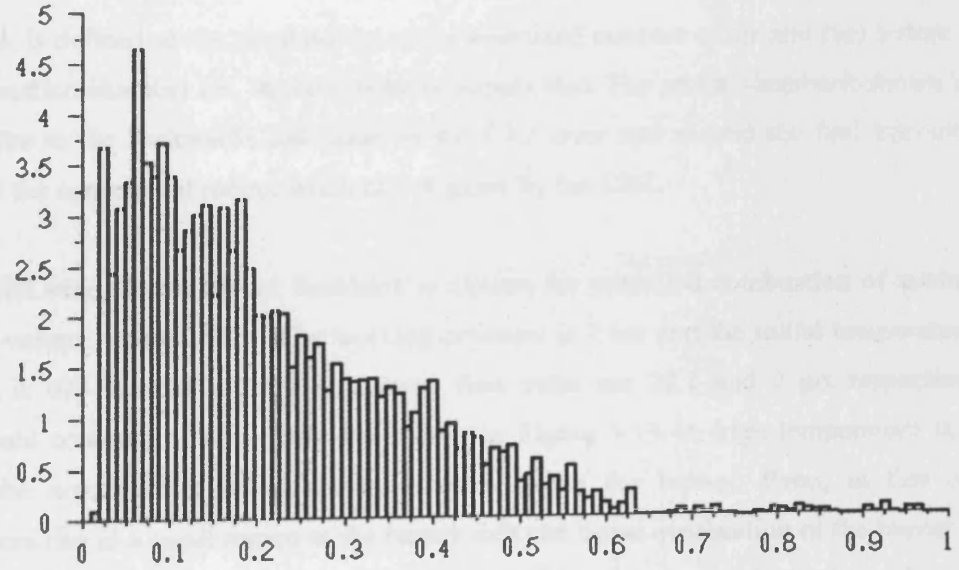

Figure 5.10: The cell equiavolume skew histogram for the model shown in Figure 5.7

5.3 Swirl Burner Simulation

The model with the swirl burner is used for simulating both premixed and non-premixed combustion. The boundary conditions are chosen to be 700 K for all walls. Simulations were not sensitive to this value apart from the exit tip of the burner. The default under relaxation factor was chosen.

The first sample of the results is chosen for the non-premixed combustion of methane. The working pressure is 7.11 bar and the initial temperature for air and fuel is 674 K. The air and fuel mass flow rates are 25.5 and 1.45 g/s respectively.

The swirl burner gives good flame stabilization, but produces Central Recirculation Zones (CRZs) that extend back over the central fuel injector, allowing the flame to propagate into this region as shown in the simulation Figures 5.11 and 5.12. The temperature contours are shown in Figure 5.11. It is noticed that flashback starts to exist inside the swirler. The region at which the flashback exists is corresponding to the region of negative axial velocity generated in the recirculation zone due to the swirling effect as shown in axial velocity contours Figures 5.12. The same results are found for the premixed combustion as well.

Flashback is defined as the combusting of the premixed mixture of air and fuel before entering the combustion chamber i.e., in the swirler or supply line. The partial flashback shown in Figure 5.11 is due to the backwards extension of the CRZ over and around the fuel injector, Figure 5.12, and the consequent recirculation of hot gases by the CRZ.

The second example for partial flashback is chosen for premixed combustion of methane with 15%, by volume, diluted CO_2. The working pressure is 7 bar and the initial temperature for air and fuel is 673 K. The air and fuel mass flow rates are 23.1 and 2 g/s respectively. The temperature contours of such case are shown in Figure 5.13. A high temperature is realized around the nozzle exit and upstream mixture inside the burner. Even, in this case, the temperature rise in a small region at the burner exit can cause overheating of the burner material and may leads to full flashback after a short period of the operation under such conditions.

The full flashback is shown in Figure 5.14 where the combustion of the premixed mixture starts upstream of the CRZ and inside of the burner before the tangential inlets. This case runs under the same conditions of the previous case but the mass flow rates of air and fuel are reduced to the half of its nominated values. The fuel/air mixture is completely combusted inside the upstream burner passages.

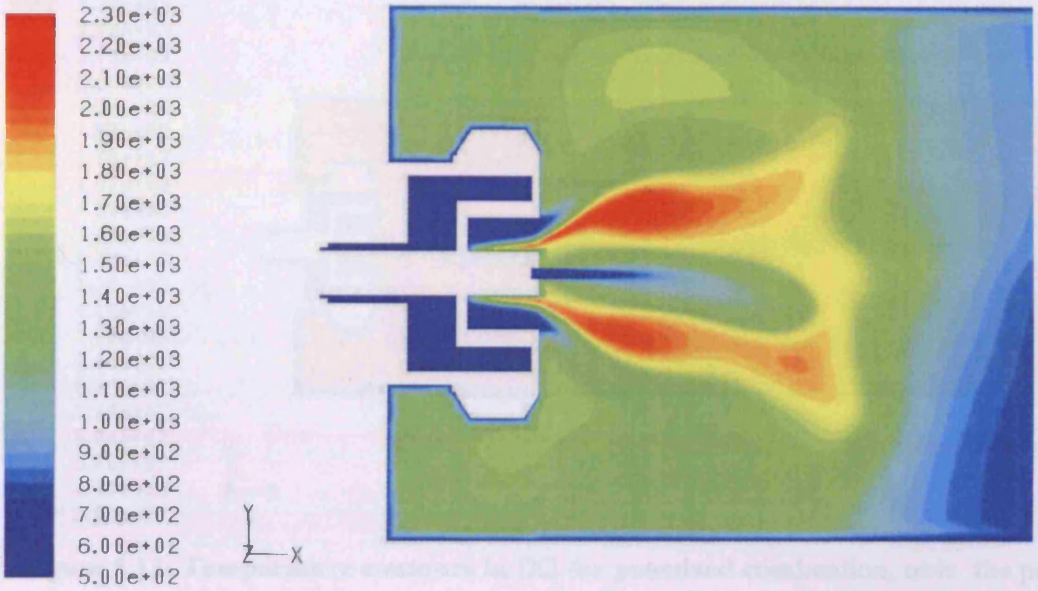

Figure 5.11: Temperature contours in [K] for CH_4 nonpremixed combustion, the flame propagates back to the swirler – partial flashback

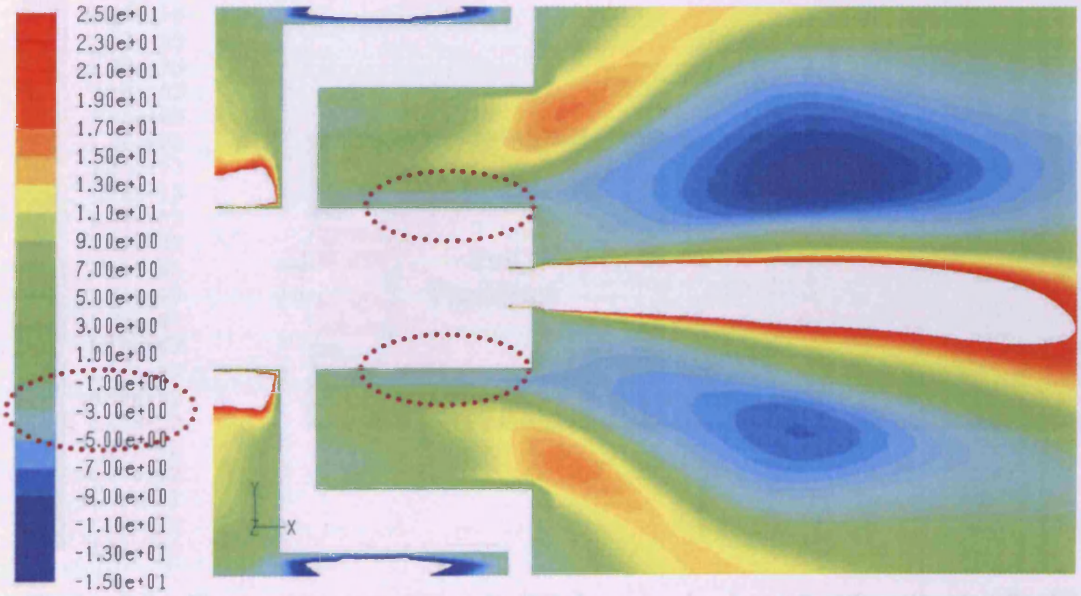

Figure 5.12: Contours of axial velocity in [m/s]

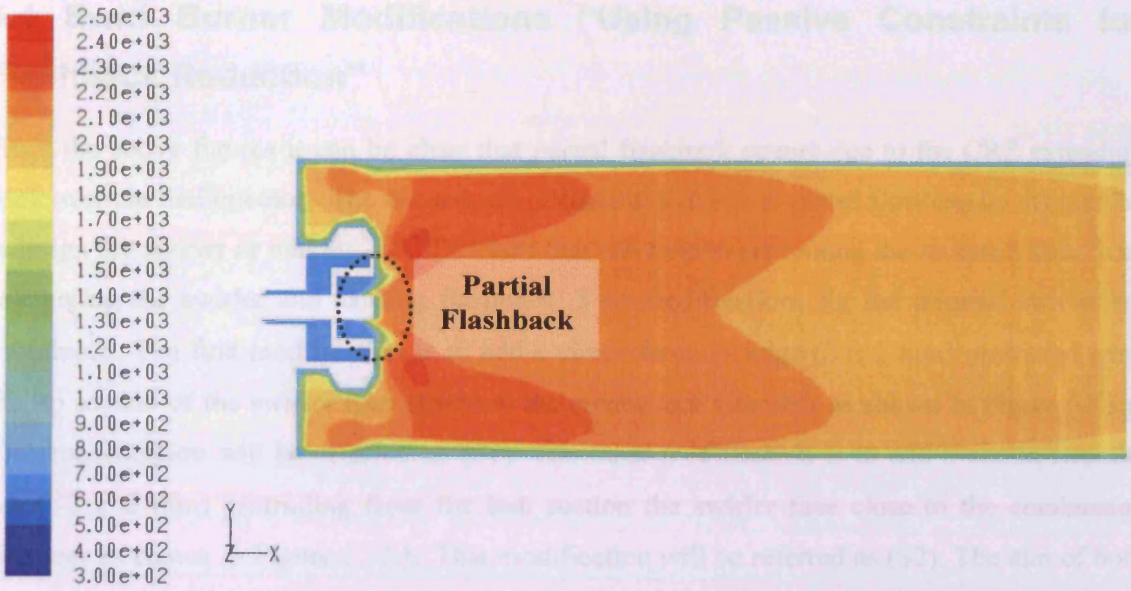

Figure 5.13: Temperature contours in [K] for premixed combustion, note the partial flashback around the fuel injector

Figure 5.14: Temperature contours in [K] for premixed combustion, the full flashback

5.4 Swirl Burner Modifications "Using Passive Constraints for Flashback Reduction"

From the above figures it can be clear that partial flashback occurs due to the CRZ extending back over the fuel injector. The occurrence of flashback due to reversed flow can be avoided by redesign the swirler or making modifications that can help in preventing the reversed flow from re-entering the swirler and causing flashback. Two modifications for the original swirler are introduced. The first modification is to add a circumferential edge (2 × 2 mm) protruded from the tip section of the swirler face closed at the combustion chamber as shown in Figure 5.15.a. This modification will be referred as (S1). The other modification is to add a circumferential edge (2 × 2 mm) protruding from the hub section the swirler face close to the combustion chamber as shown in Figure 5.15.b. This modification will be referred as (S2). The aim of both suggested modifications is to rebuild the recirculation zone in order to prevent the back flow (the fluid with negative velocity) from entering the swirler around the central fuel gun and causing partial flashback.

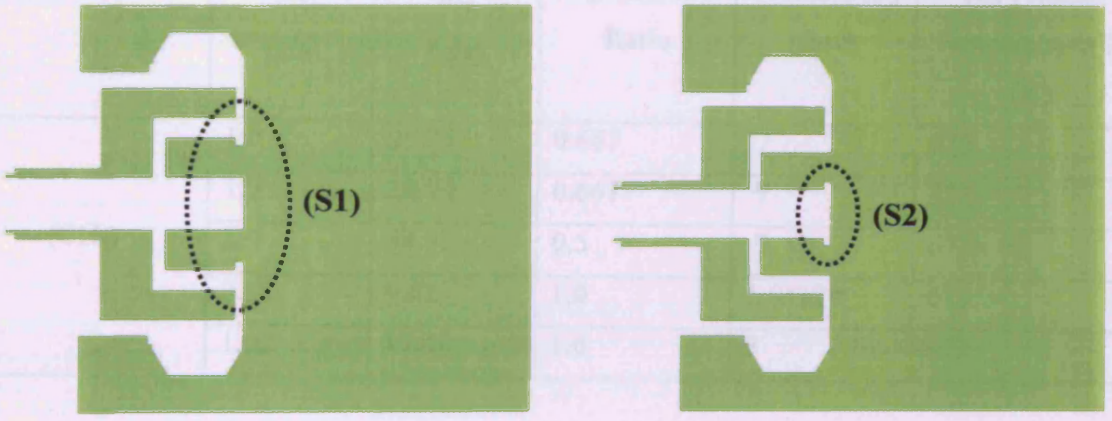

(a) (b)

Figure 5.15: Swirler Modifications

(a): Passive constraint at the tip (S1) & (b): Passive constraint at the hub (S2)

The geometrical swirl number (S_g) was calculated based on the geometrical configurations given by equation 5.2.1 and it was 1.47 for S1 and 1.54 for S2.

Both modifications are checked and compared with the original swirler that is referred as (S0). The comparison is performed for both nonpremixed and premixed combustion with more concentration on premixed combustion as it has more tendency toward flashback.

For nonpremixed combustion, the simulation is performed by using methane with 15%, by volume, CO_2 as a fuel dilutent. The working pressure is 7 bar and air preheat temperature at 673 K. The air and fuel mass flow rates are 23.1 and 2 g/s respectively.

The simulation results shown in Figure 5.16 indicate that a partial flashback exists for the S0 case. This partial flashback is eliminated by using the passive constraint at the nozzle exit as described by S1 and S2 cases.

For premixed combustion, CH_4 is used as the fuel in such comparisons. The combustion is achieved at various conditions of pressure and air preheat temperature. The conditions of simulation that are used for the comparison are tabulated in table 5.1 and correspond to conditions used in the Cardiff GTRC system.

Table 5.1: Simulation conditions used for (S0, S1 and S2) comparison in premixed combustion

Fuel	$\dot{m}_f$ (g/s)	$\dot{m}_a$ (g/s)	Equivalence Ratio	Pressure (P) (bar)	Air Preheat Temperature (T_i) (K)
(CH_4)	1.0	25.74	0.667	7	673
	1.0	25.74	0.667	7	473
	1.0	34.32	0.5	7	673
	0.58	9.42	1.0	1.01325	673
	1.02	17.48	1.0	3	473

The simulation results are shown in Figure 5.17. The first column is for the swirl burner without exhaust constrictions, whilst the other two are for the constricted cases. The temperature contours show that the existence of flashback in (S0) case is beside the fuel gun where the negative axial velocity exists. The results indicate that the back extension of CRZ into the swirl burner body can be largely eliminated by using such S1 and S2 modifications thus reducing this type of flashback. Moreover, the elongated shape of the CRZ, Figure 5.12, that passes back into the burner can be modified to occur solely downstream of the burner exhaust, reducing flashback and also improving the life of components by reducing flame impingement

The modified swirler operates without this type of flashback under many operating conditions as there is no reversed flow inside the swirler. The last case in Figure 5.17 shows full flashback

in S0 but normal combustion in both S1 and S2. Both modifications operate well when modelled. Configuration (S1) case is the most realistic as the modification is easier to carry out and gives better results at low velocities.

From the above results it can be concluded that:

- Flashback resulted due to the reversed flow effect appears in the model with the original swirl burner.
- The modified swirl burner works without flashback due to the reverse flow zone as there is no reversed flow returns inside the swirl burner itself.
- Both modifications operate perfectly under simulation conditions. However, case (S1) is more realistic in practice as it is easier to make a small modification in the swirl burner nut more than attaching a flange to the internal fuel gun of the swirl burner, whilst commercially there is a larger heat sink available at the outside of the burner and the fuel gun is more vulnerable to overheating.
- Beside the burner configuration, flashback depends on the operating pressure, temperature, equivalence ratio, and the combusting mixture mass flow rate.

It is noted that the results are compatible with the experimental findings in [173].

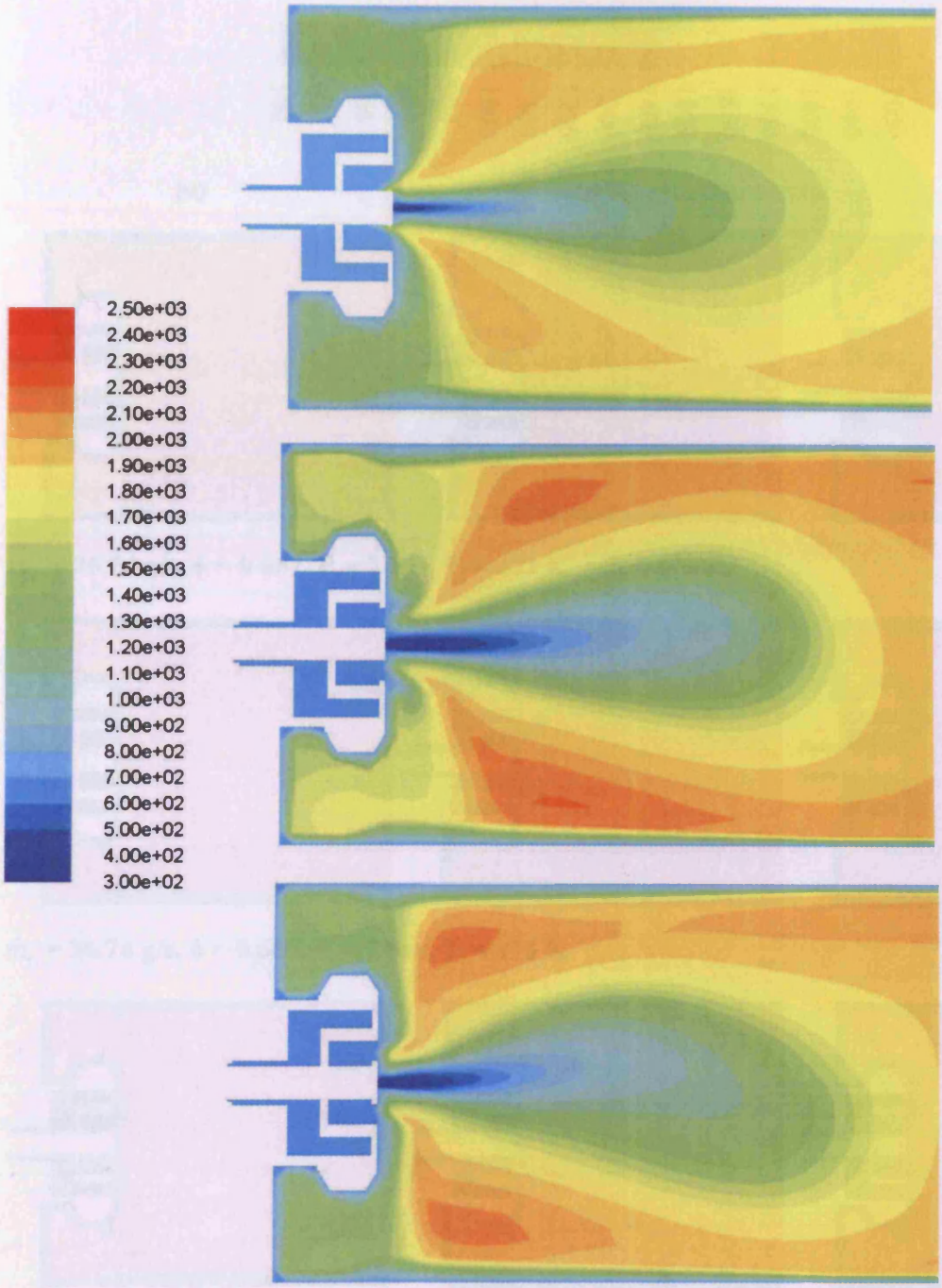

Figure 5.16: Comparison between temperature contours in [K] for normal swirl burner and burners with passive constrictions in the case of nonpremixed combustion

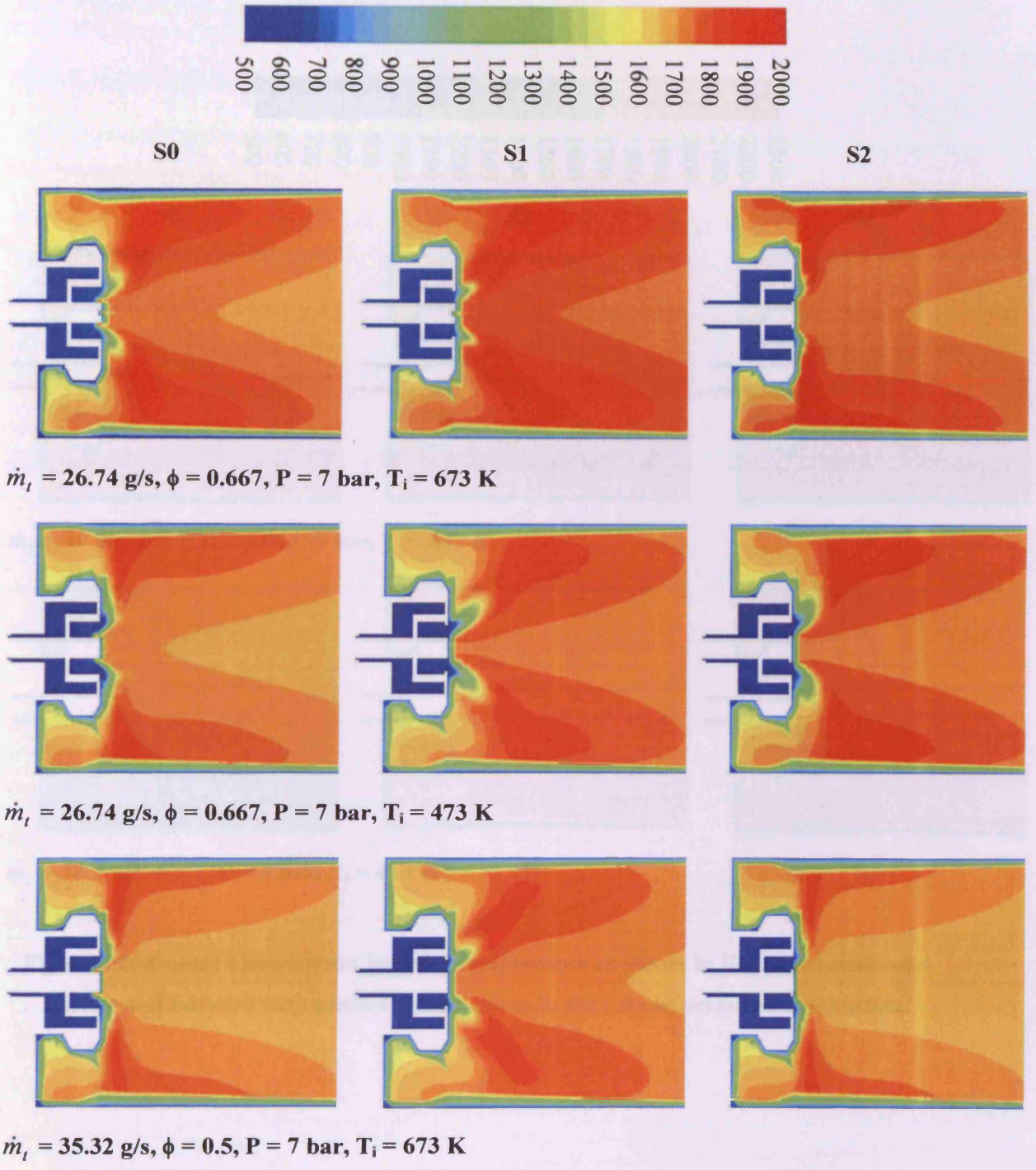

Figure 5.17: Comparison between temperature contours in [K] for normal swirl burner and burners with passive constrictions in the case of premixed combustion.

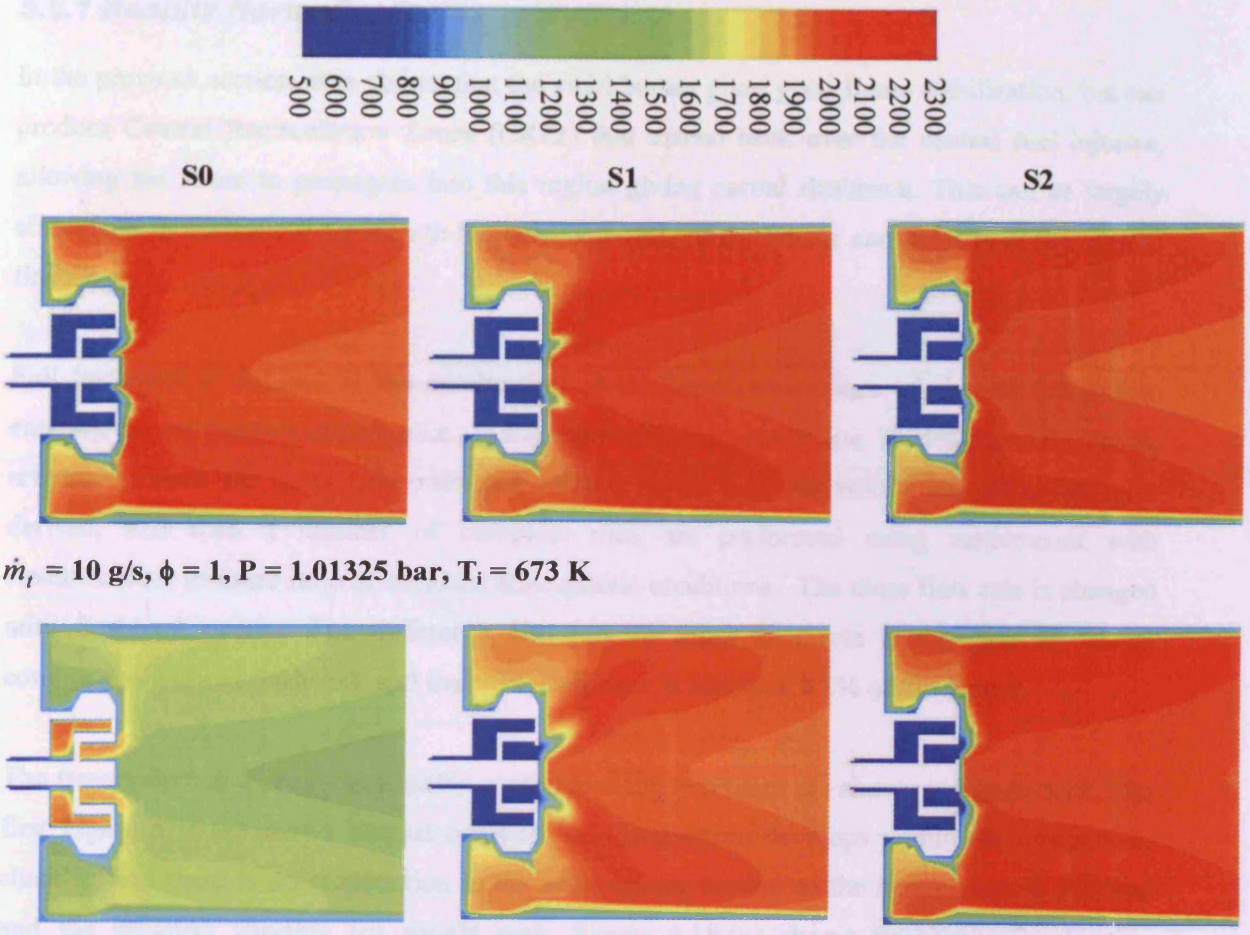

Figure 5.17 Cont. : Comparison between temperature contours in [K] for normal swirl burner and burners with passive constrictions in the case of premixed combustion.

5.5 Flashback determination

5.5.1 Results Normalization

In the previous section, it is shown that the swirl burner gives good flame stabilization, but can produce Central Recirculation Zones (CRZs) that extend back over the central fuel injector, allowing the flame to propagate into this region giving partial flashback. This can be largely eliminated by fitting a sharp step to the exhaust nozzle of the burner and helps to reduce partial flashback.

Full flashback is defined as the combusting of the premixed mixture of air and fuel before entering the combustion chamber i.e., in the swirl burner or supply line. To determine flashback, reference values for mass flow rate and velocity to be used for results normalization were derived, and then a number of complete runs are performed using methane/air with stoichiometric mixture ratio at standard atmospheric conditions. The mass flow rate is changed until flashback occurs. The difference between the mass flow rate in the case of normal combustion without flashback and that with flashback is less than 0.1% of the former.

The temperature and progress variable contours of the two cases are shown in Figure 5.18. The first Figure 5.18.(a) shows normal combustion. Combustion develops within the combustion chamber and there is no combustion in the swirl burner section as the temperature is still low and the progress variable (c) equals zero. Figure 5.18.(b) shows flashback. Combustion extended upstream and the temperature is raised inside the swirl burner passages due to combustion. The progress variable increased to 1 inside the swirl burner showing complete combustion.

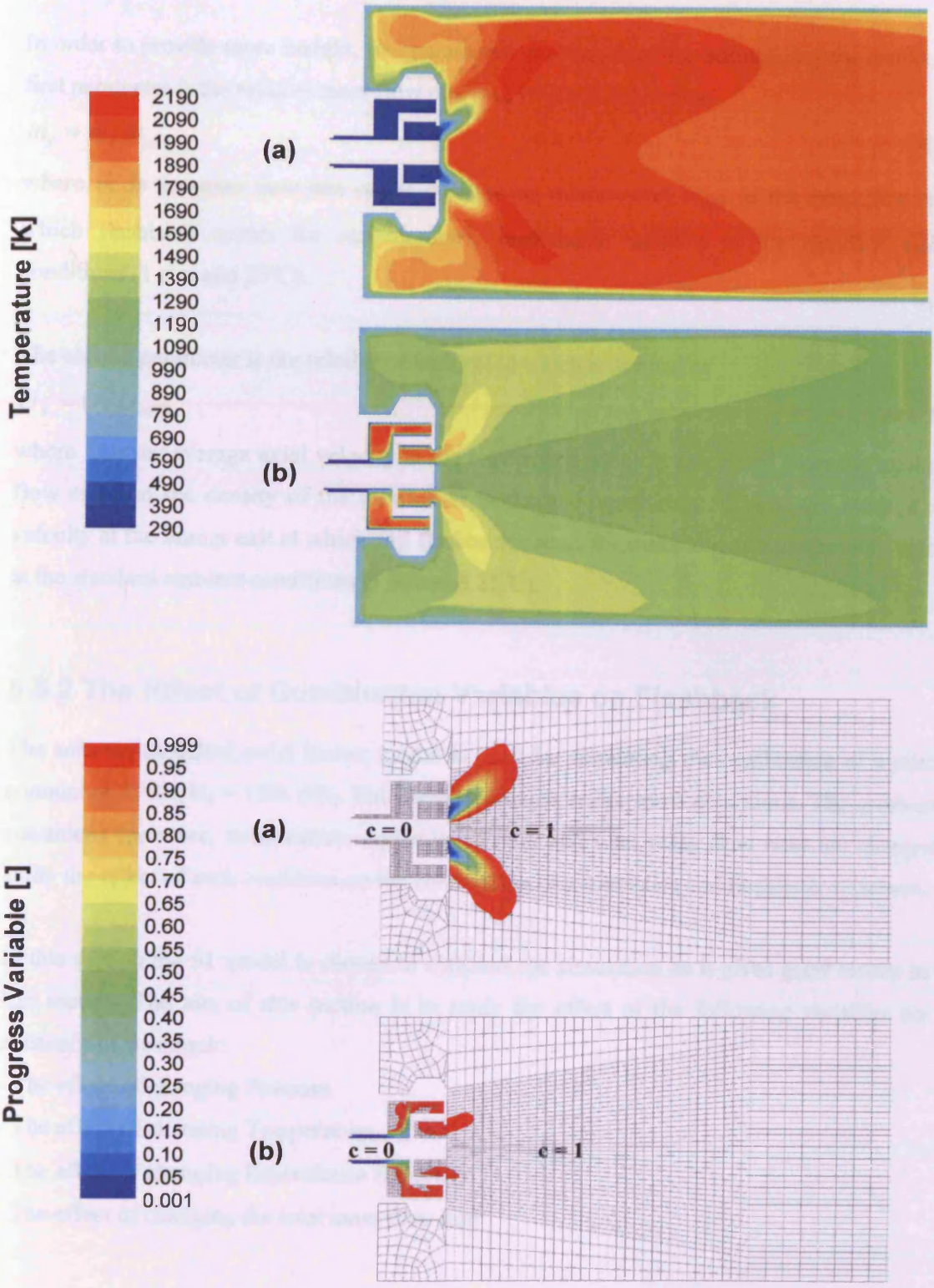

Figure 5.18: Flashback determination for stoichiometric CH_4 mixture at the standard ambient conditions (1 atm and 298K).

(a) Normal Combustion at relative mass flow of 1.005

(b) Full flashback at relative mass flow of 0.997

In order to provide more insight, two parameters are suggested for normalizing the results. The first parameter is the relative mass flow rate (m_r) which is defined as:

$$m_r = \dot{m} / \dot{m}_{oFB} \qquad 5.5.1$$

where $\dot{m}$ is the mass flow rate of the combusting mixture and $\dot{m}_{oFB}$ is the mass flow rate at which flashback occurs for stoichiometric methane/air mixture at the standard ambient conditions (1 atm and 25°C).

The second parameter is the relative velocity (U_r) which is defined as

$$U_r = U / U_{oFB} \qquad 5.5.2$$

where U is the average axial velocity at the burner exit which is calculated from the total mass flow rate and the density of the mixture at isothermal conditions. U_{oFB} is the average axial velocity at the burner exit at which full flashback occurs for stoichiometric methane/air mixture at the standard ambient conditions (1 atm and 25°C).

5.5.2 The Effect of Combustion Variables on Flashback

The selected modified swirl burner model is used for simulating the combustion of a mixture containing 85% CH_4 + 15% CO_2. Full flashback exists under some conditions. The combustion conditions (pressure, temperature, equivalence ratio and total mass flow rate) are changed to study the effect of each condition on the combustion characteristics and flashback existence.

In this section the S1 model is chosen to continue the simulation as it gives good results in the last section. The aim of this section is to study the effect of the following variables on the existence of flashback:

- The effect of changing Pressure
- The effect of changing Temperature
- The effect of changing Equivalence Ratio (ϕ)
- The effect of changing the total mass flow rate

5.5.2.1 The Effect of Changing Pressure

Two pressures are chosen, 7 bar and 3 bar, to study the effect on flashback and other parameters. The following table show the variables at which the runs were made:

Table 5.2: Simulation conditions used for studying the effect of changing Pressure

Run	P (bar)	Temperature (K)	$\dot{m}_f$ (kg/s)	$\dot{m}_a$ (kg/s)	Equivalence Ratio (ϕ)
A	7	673	0.002	Depends on E.R.	1.25, 1.0, 0.8, 0.67, 0.5
B	3	673	0.002	Depends on E.R.	1.25, 1.0, 0.8, 0.67, 0.5

The results are shown in Figure 5.19 where the temperature contours are plotted. It can be noticed that at case A, the flashback exists at equivalence ratio of 1.25, 1.0 and 0.8. These equivalence ratios correspond to lower total mass flow rates as the fuel mass flow rate is kept constant. When the pressure is changed (reduced to 3 bar in case B), the flashback exists only with equivalence ratio of 1.25. This means that the characteristics of flow that cause flashback depend on the pressure and also velocity (via density). It is noticed that as the pressure increases the ability of the mixture to flashback increases at the same equivalence ratio.

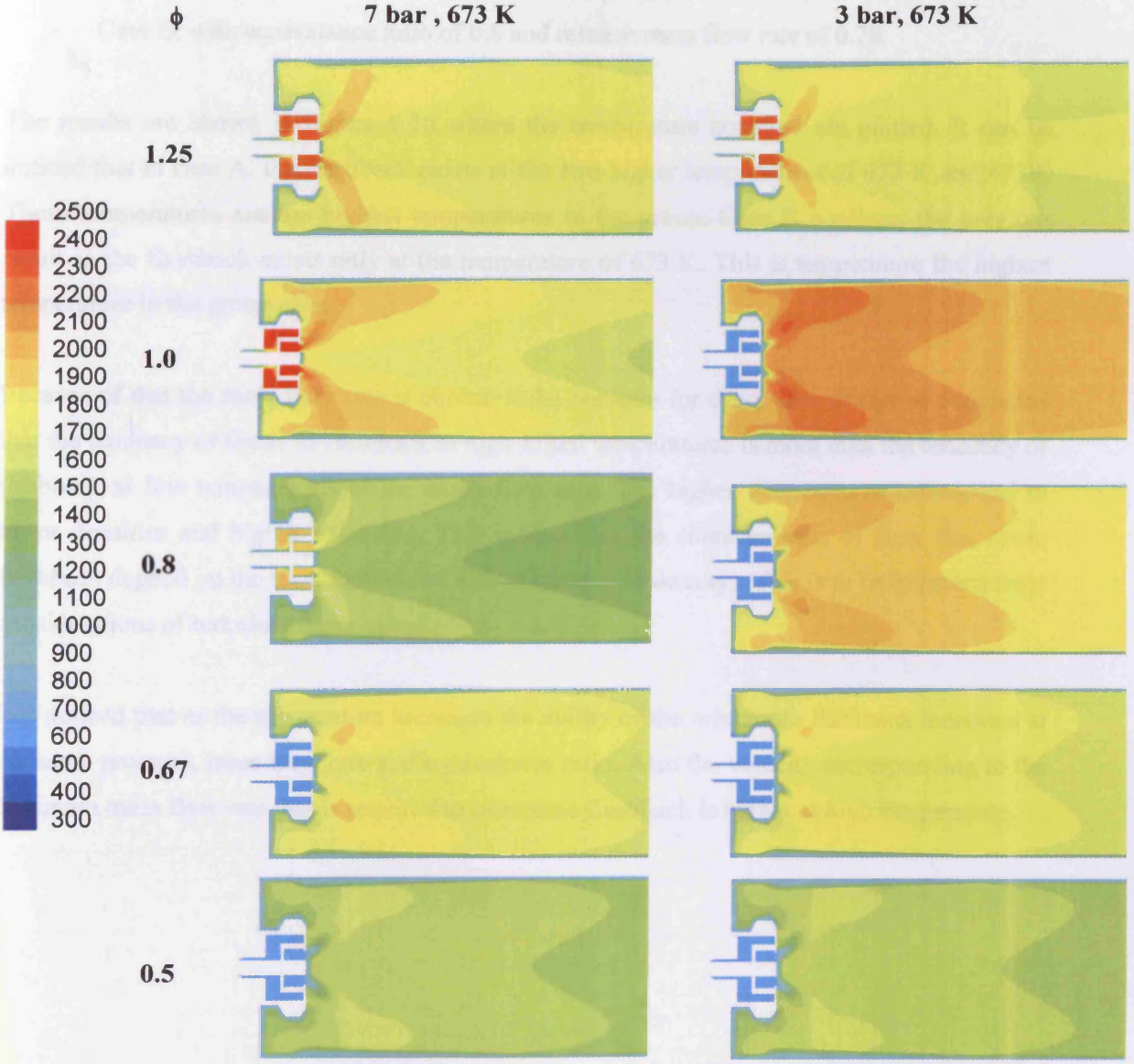

Figure 5.19: The contours of static temperature at various pressures and fixed air preheat temperature at 673 K (fuel : 85% CH_4 + 15% CO_2)

5.5.2.2 The Effect of Changing Initial Temperature

To study the effect initial air (or mixture) temperature on flashback, three air preheat temperature are chosen to perform the runs. The chosen air preheat temperatures are 300 K, 473 K, and 673 K. The operating pressure is fixed at 1.01325 bar. Two cases are checked:

- Case A: with equivalence ratio of 1 and relative mass flow rate of 1.04, and
- Case B: with equivalence ratio of 0.8 and relative mass flow rate of 0.78.

The results are shown in Figure 5.20 where the temperature contours are plotted. It can be noticed that at case A, the flashback exists at the two higher temperatures of 673 K and 473K. These temperatures are the highest temperatures in the group. Case B confirms the previous result as the flashback exists only at the temperature of 673 K. This is temperature the highest temperature in the group also.

Because of that the mass flow rate is chosen to be constant for every case, it can be concluded that the tendency of flame to flashback at high initial temperatures is more than the tendency of flashback at low temperatures at the same flow rate. The higher temperatures correspond to lower densities and higher velocities. This means that the characteristics of flow that cause flashback depend on the temperature and also velocity (via density). This is to be expected from considerations of turbulent flame speed.

It is noticed that as the temperature increases the ability of the mixture to flashback increases at the same pressure, mass flow rate and equivalence ratio. Also the velocity corresponding to the minimum mass flow rate that is required to overcome flashback is higher at high temperature.

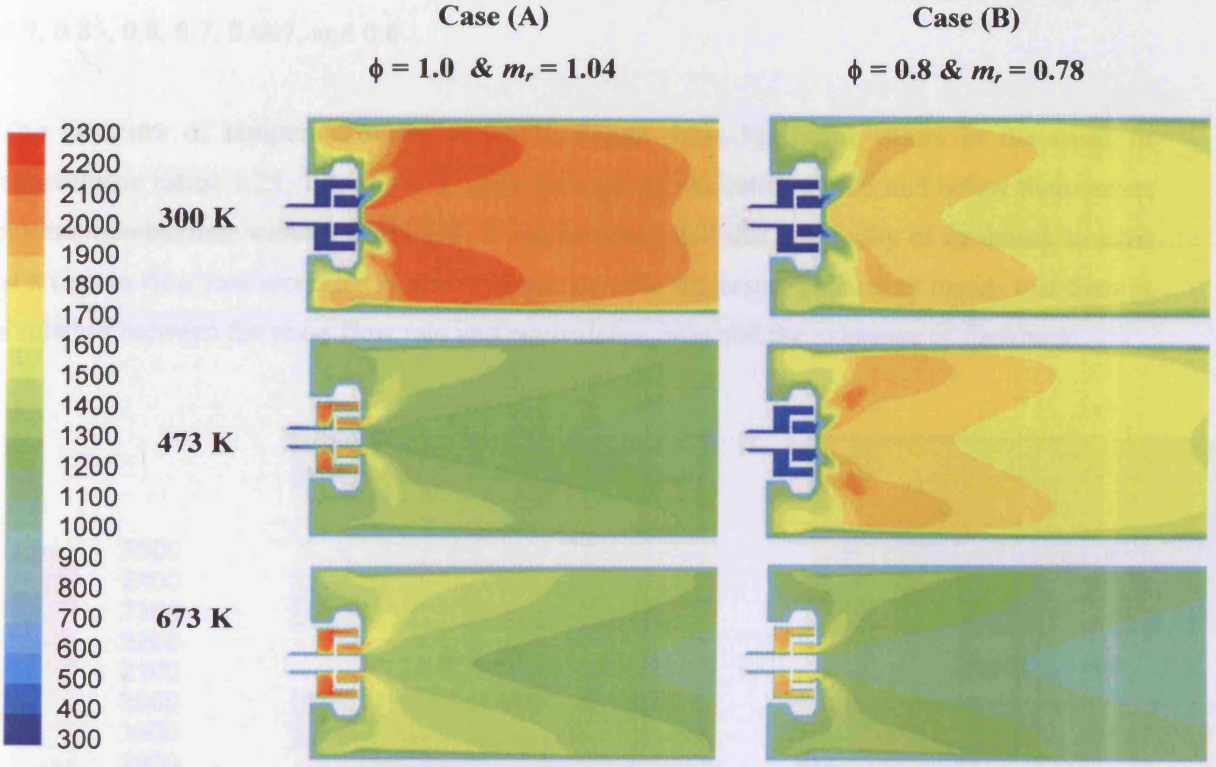

Figure 5.20: The contours of static temperature at various air preheat temperature and fixed pressures of 1.01325 bar (fuel : 85% CH_4 + 15% CO_2)

5.5.2.3 The Effect of Changing Equivalence Ratio (ϕ)

To study the effect of changing the equivalence ratio on the combustion characteristics and flashback on premixed combustion a fixed quantity of air and fuel with relative mass flow rate of 6.35 is taken as a base of the simulation. The pressure and temperature remain constants at 7 bar and 673 K respectively. The equivalence ratio is changed and takes the values of 1.25, 1.0, 0.9, 0.85, 0.8, 0.7, 0.667, and 0.6.

The contours of temperature are shown in Figure 5.21. Flashback exists in the cases of equivalence ratios 1.25, 1.0, and 0.9 while for equivalence ratio of 0.85 and below there exists normal combustion without flashback. It can be concluded that the ability of flashback to exist at a certain flow rate increases as the equivalence ratio increases. This result means that there is a relation between the mass flow rate and equivalence ratio and the existence of flashback.

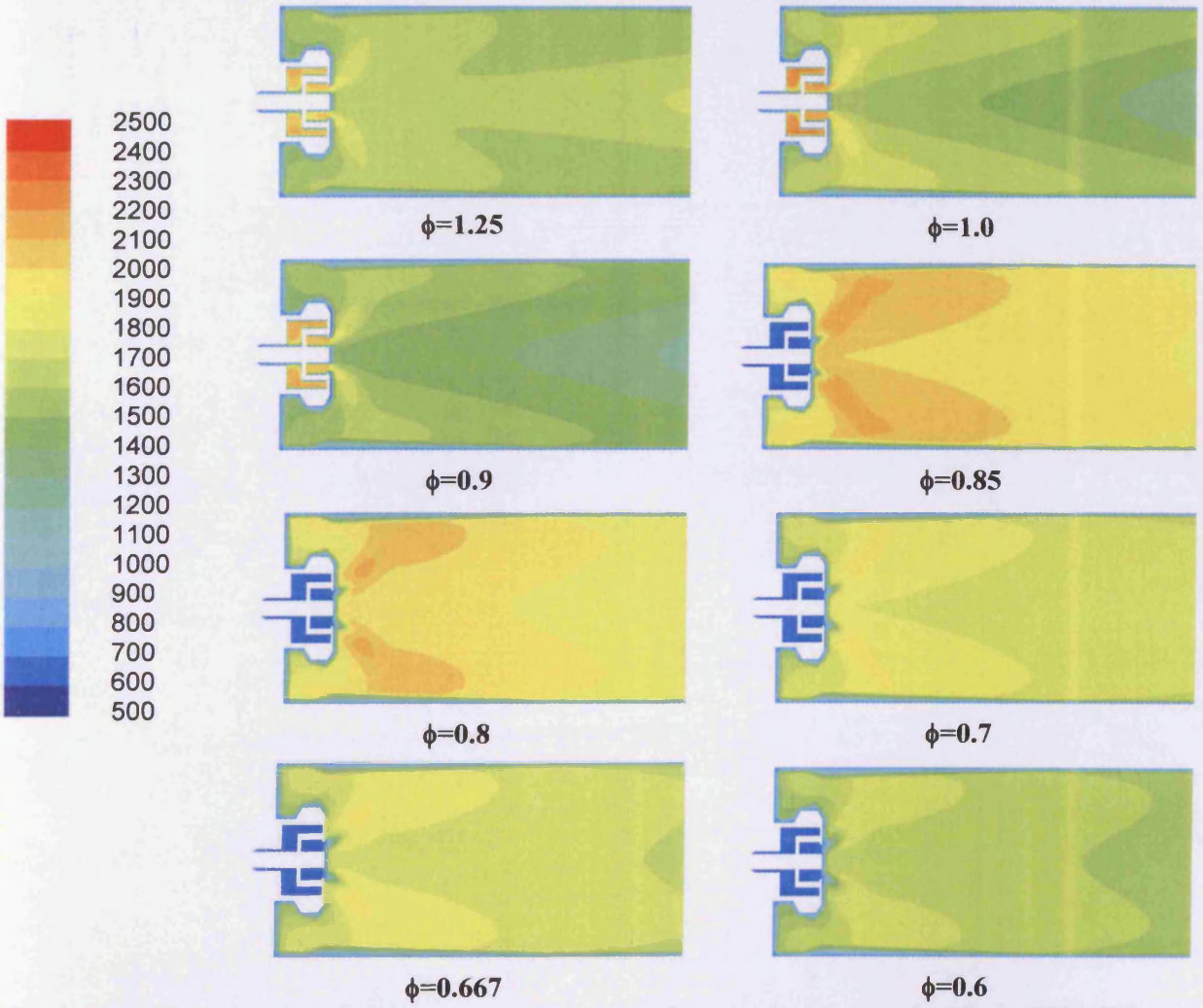

Figure 5.21: The contours of static temperature at various equivalence ratios (fuel : 85% CH_4 + 15% CO_2)

5.5.2.4 The Effect of Changing the Total Mass Flow Rate

To study the effect of changing the total mass flow rate on the combustion characteristics and flashback on premixed combustion an equivalence ratio of 0.6 is taken as a base for the simulation. The pressure and temperature are fixed at 7 bar and 673 K respectively. The relative mass flow is changed and takes the values of 6.35, 4.35, 3.5, 3.16, 2.8, 2.6, 2.34, 2.18, 2.08, 2, 1.9, and 1.7 respectively.

The contours of temperature are shown in Figure 5.22. The flashback exists in the cases of total relative mass flow less than 2 while for relative mass flow equals or more than 2 there exists normal combustion without flashback. It can be concluded that the ability of flashback to exist at a certain equivalence ratio increases as the total mass flow decreases. These results confirm that there is a relation between the mass flow rate, hence velocity and equivalence ratio and the existence of flashback.

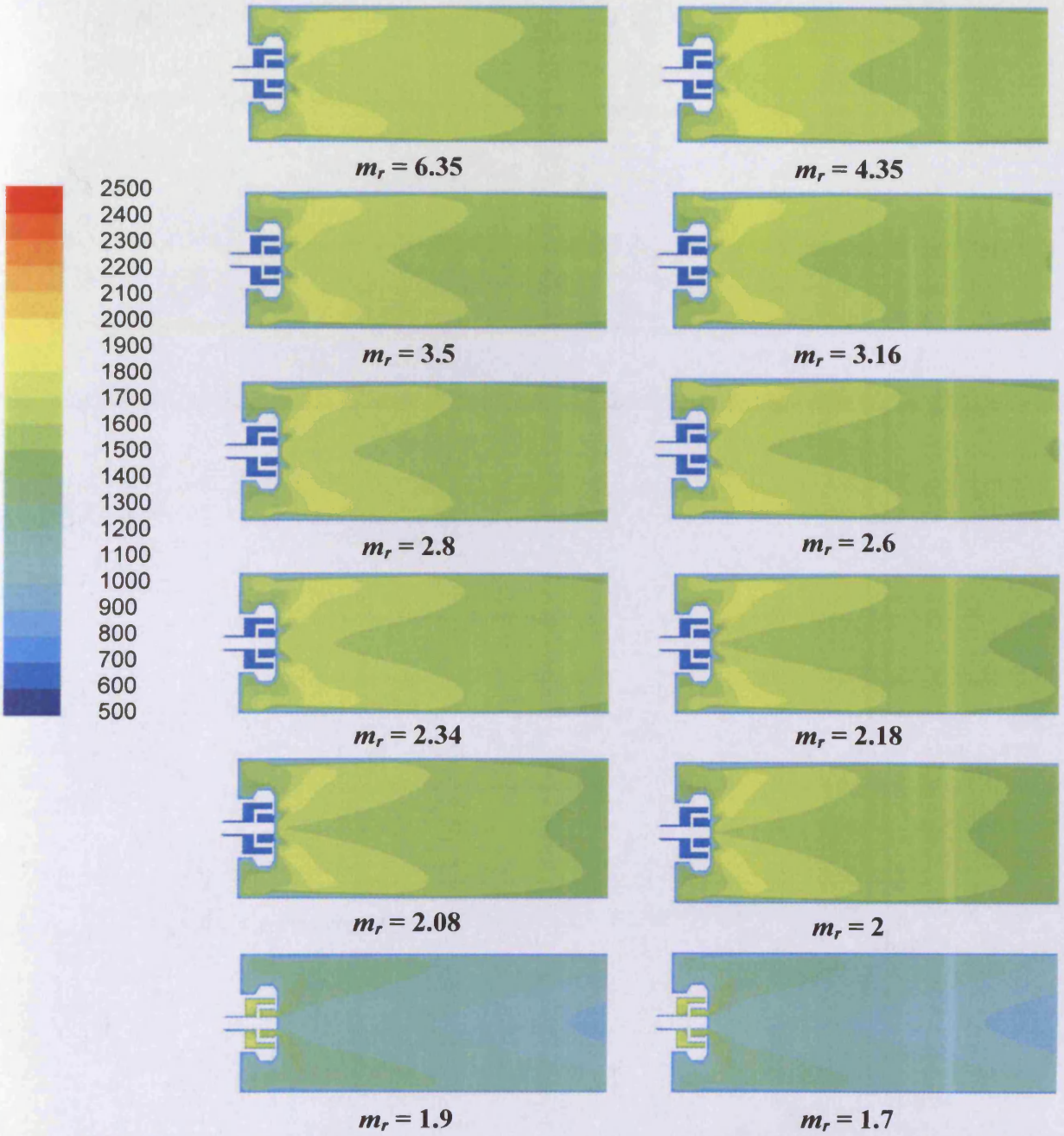

Figure 5.22: The contours of static temperature at various relative mass flow rates (fuel : 85% CH_4 + 15% CO_2)

5.5.3 The Stability Limits

From the observations of the previous section, it was clear that flame stability depends on the operating pressure, initial temperature, equivalence ratio and total mass flow rate of the premixed mixture. To relate all of these variables, several runs were carried out at various operating conditions. The aim of these runs is to determine the conditions at which the flame flashes back. The main target of the flashback determination is to define the limits at which the flame is stable and avoiding the necessity to work under unstable conditions where flashback can exist.

The stability limits for various fuels under various operating conditions are determined and extensively discussed in the next chapters together with some suggestions to improve the stability limits.

A sample of the stability map is shown in Figure 5.23 for (85% CH_4 & 15% CO_2) flames. The operating conditions are 7 bar and air preheat of 673 K. In this Figure the correlation between the relative mass flow rate and the equivalence ratio is shown at a certain pressure and temperature. The correlation can be generalized for other operating pressures and temperatures.

To define the flashback limits at each equivalence ratio, many runs were performed. As shown in Figure 5.23, two different regions of operation are recognizable. The first region above the curve is the region where combustion is stable without flashback. The second region is the region below the curve in which flames are unstable with flashback. Flashback peaks at an equivalence ratio of unity, whilst operation under lean mixture conditions is clearly favourable.

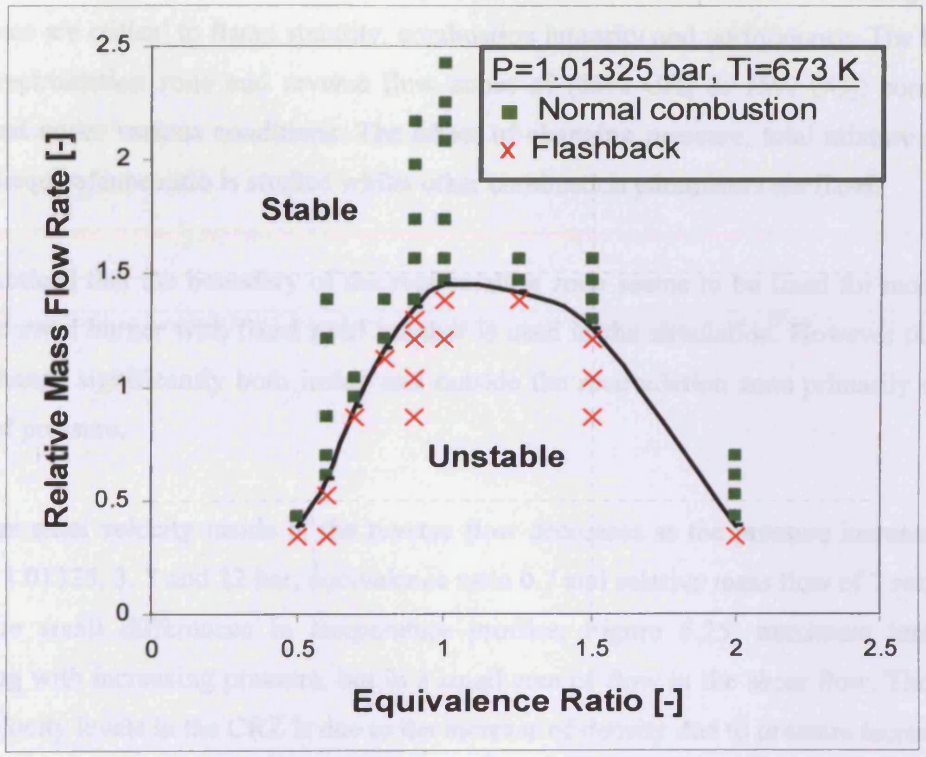

Figure 5.23: The stability limits for (85% CH_4 + 15% CO_2) combustion at atmospheric pressure.

5.5.4 Recirculation Zone

One of the most significant and useful areas in swirling combustion is the recirculation zone. The recirculation zone plays an important role in flame stabilization by providing a hot flow of recirculated combustion products and a reduced velocity region where flame speed and flow velocity can be matched. The size and shape of the recirculation zone associated region of high turbulence are critical to flame stability, combustion intensity and performance. The boundaries of the recirculation zone and reverse flow zones of (85% CH_4 & 15% CO_2) combustion is illustrated under various conditions. The effect of changing pressure, total mixture mass flow rate and equivalence ratio is studied whilst other combustion parameters are fixed.

It was noticed that the boundary of the recirculation zone seems to be fixed for most cases as only one swirl burner with fixed swirl number is used in the simulation. However the velocity levels change significantly both inside and outside the recirculation zone primarily due to the effects of pressure.

The mean axial velocity inside of the reverse flow decreases as the pressure increases, Figure 5.24 for 1.01325, 3, 7 and 12 bar, equivalence ratio 0.7 and relative mass flow of 7 respectively. There are small differences in temperature profiles, Figure 5.25, maximum temperatures increasing with increasing pressure, but in a small area of flow in the shear flow. The decrease in the velocity levels in the CRZ is due to the increase of density due to pressure increase for the specified conditions.

To study the effect of mass flow rate on the recirculation zone, a pressure of 3 bar and equivalence ratio of 0.7 was chosen. The relative mass flow rate (m_r) of the mixture is changed and is taken as 7, 3.8, 2.6, 2.4, 2.1 and 1.9 respectively. The results are shown in Figure 5.26 and as to be expected indicates a reduction in the velocities inside the recirculation zone as the mass flow rate decreases, except for the last case (m_r = 1.9), where flashback occurs. Flashback clearly affects the axial velocity distribution of reverse flow and drives it to higher levels. The same results are noticed when studying the effect of changing the equivalence ratio at fixed pressure and mass flow rates.

In the case of fixed pressure and mass flow rates with variable equivalence ratios, the shape and velocity distribution inside the recirculation zone does not change in normal combustion without flashback as shown in Figure 5.27, in the left column of equivalence ratios of 0.6, 0.7, 0.8 and 1.5 at 7 bar and relative mass flow rate of 7. On the other hand for the flashback cases

with equivalence ratios 0.9, 1.0 and 1.25 the boundary of the recirculation zone is wider and the velocity increases.

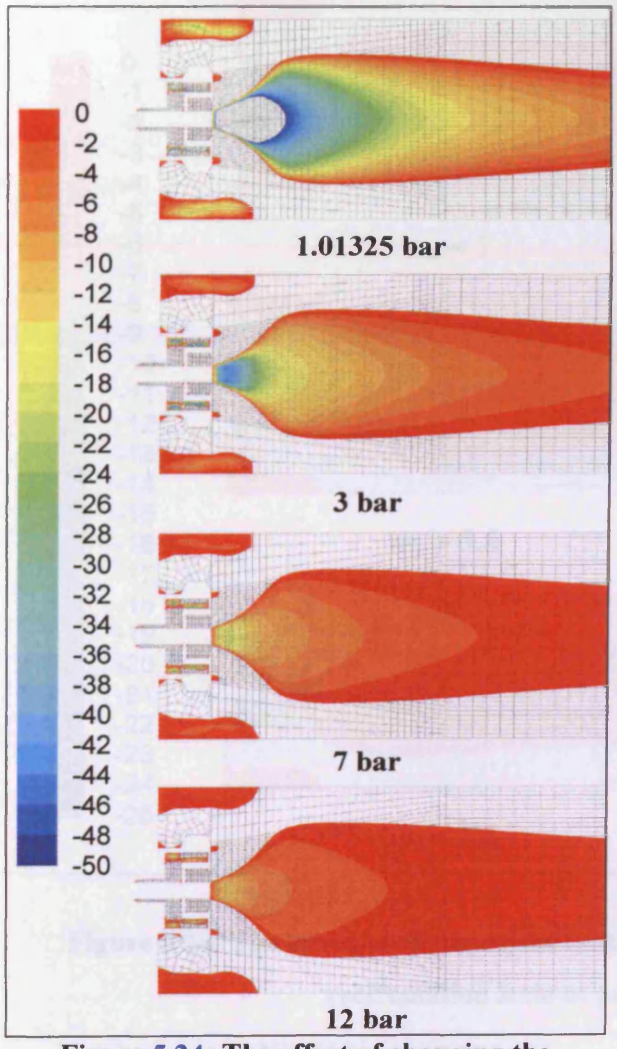

Figure 5.24: The effect of changing the pressure on the axial velocity contours in the recirculation zone at ($\phi = 0.7$ & $m_r = 7$)

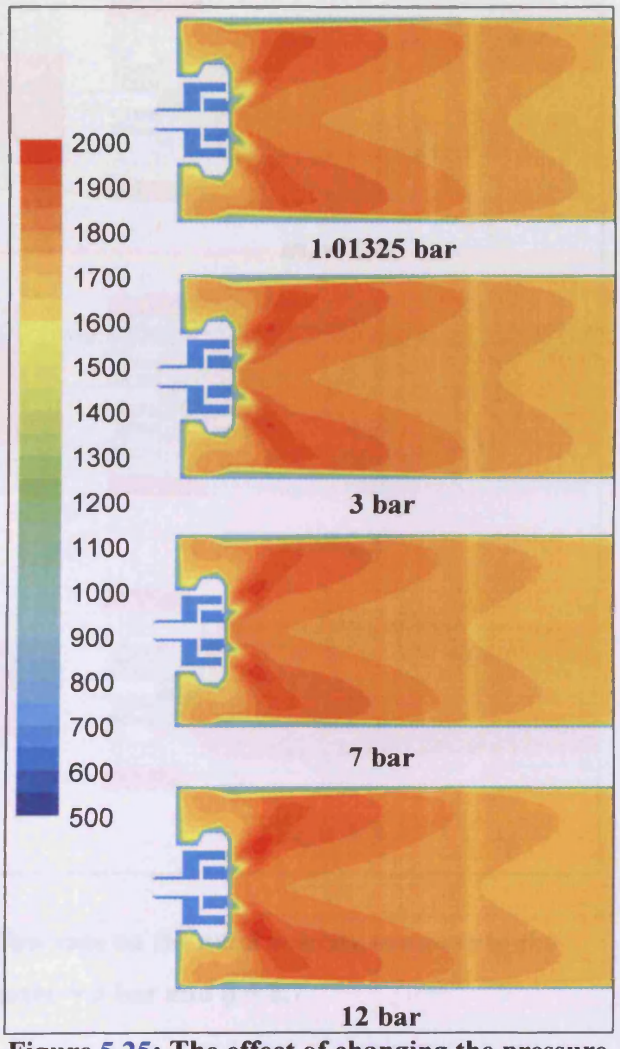

Figure 5.25: The effect of changing the pressure on the temperature contours at ($\phi = 0.7$ & $m_r = 7$)

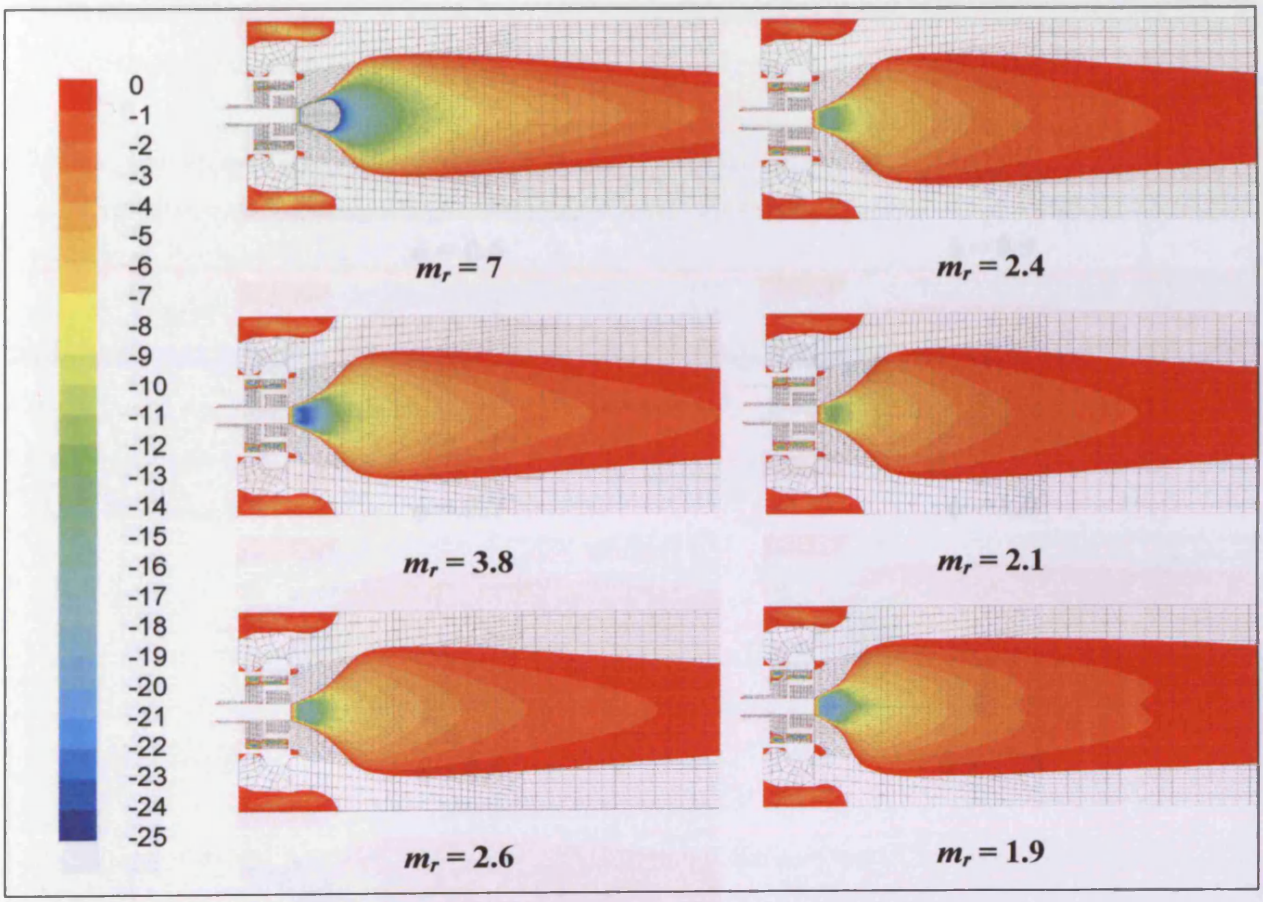

Figure 5.26: The effect of changing the mass flow rate on the axial velocity contours in the recirculation zone at pressure = 3 bar and $\phi = 0.7$

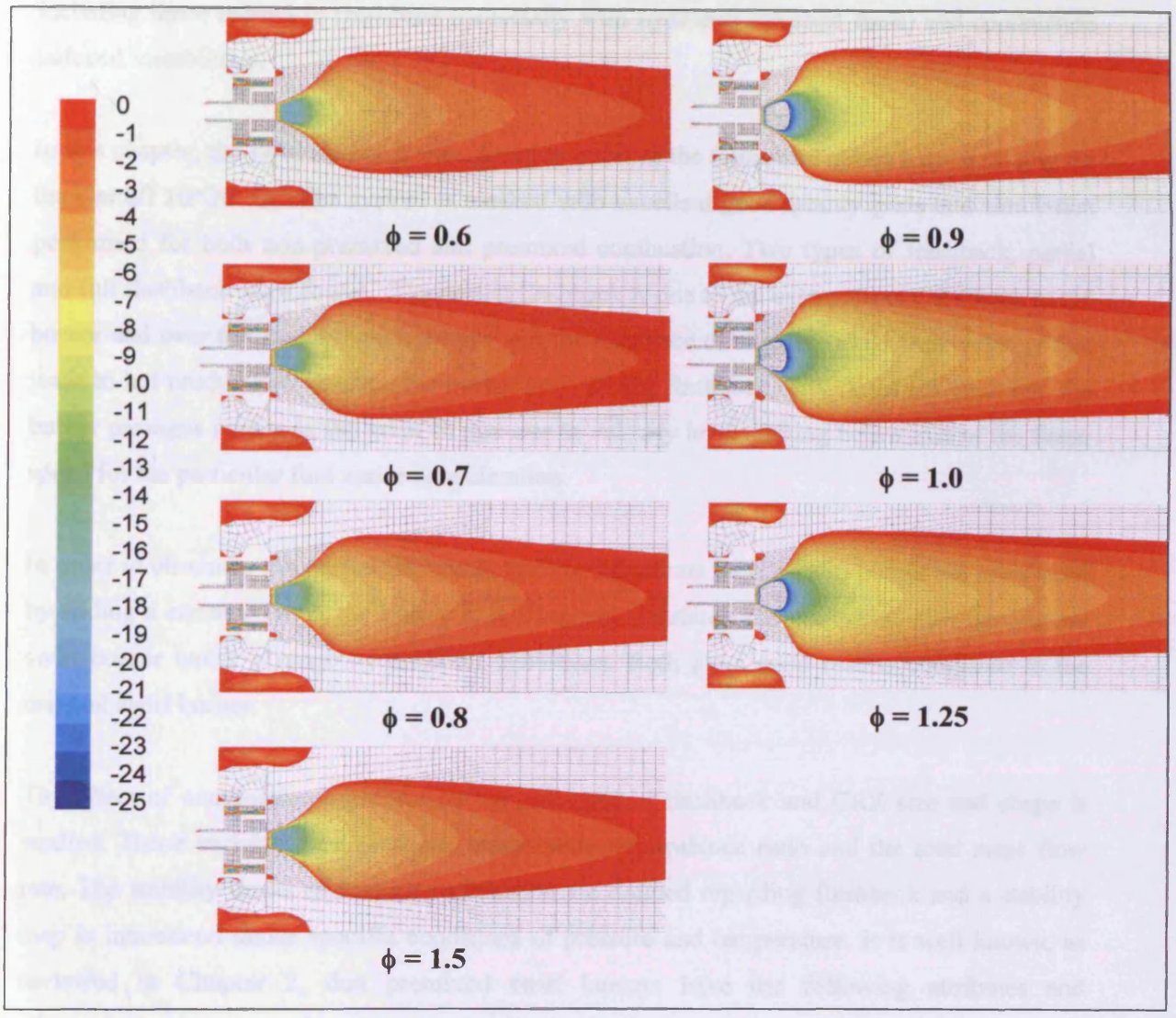

Figure 5.27: The effect of changing the equivalence ratio on the axial velocity contours in the recirculation zone at (Pressure = 7 bar & m_r = 7)

5.6 Summary

Swirl flame stabilisation of lean premixed fuels has been studied and applied to gas turbines for many reasons. It gives considerable benefits in terms of reduced pollutant emission, especially of NOx. However, there are still problems that can occur during the combustion process including those related to flashback (especially with hydrogen enriched fuels) and combustion induced instabilities.

In this chapter, the swirl burner is introduced to stabilize the flame and obtain a good mixing for the Cardiff HPOC rig. The system is meshed with excellent good quality grids and simulation performed for both non-premixed and premixed combustion. Two types of flashback, partial and full flashback were found. The partial flashback is due to the extension of CRZ back to the burner and over the fuel injection nozzle and the existence of negative axial flow velocity that leads to hot products re-entering the burner and causing flashback. Full flashback back into the burner passages occurs in the main stream due to velocity levels falling below that of the flame speed for the particular fuel under consideration.

In order to eliminate the partial flashback, two modifications for the swirl burner are introduced by adding a constriction at the burner exit. They are simulated and compared with the original swirl burner under a range of different conditions. Both gave good results compared to the original swirl burner.

The effect of combustion variables on the existence of flashback and CRZ size and shape is studied. Those variables are pressure, temperature, equivalence ratio and the total mass flow rate. The stability limits of fuel/air combustion are defined regarding flashback and a stability map is introduced under specific conditions of pressure and temperature. It is well known, as reviewed in Chapter 2, that premixed swirl burners have the following attributes and advantages:

- Premixed combustion gives many advantages regarding reducing emissions, although there can be problems due to oscillations and stability.
- The swirl burner produces better stability of the flame due to the aerodynamic gas recirculation.

In this study the following has been found:

- The flashback problem is still a barrier for combustion under certain operating conditions.

- Both partial flashback and full flashback are realized during simulation, matching other work found in the literature.
- It is possible to eliminate the partial flashback using passive constraints at the swirl burner exit.
- As the pressure increases the ability of the mixture to flashback increases at the same equivalence ratio.
- As the air preheat temperature increases the ability of the mixture to flashback increases at the same equivalence ratio.
- The ability of flashback to exist at a certain flow rate increases as the equivalence ratio increases over the range investigated.
- The ability of flashback to exist at a certain equivalence ratio increases as the total mass flow decreases.
- The boundary of the reverse flow zone seems to be fixed under various combustion conditions investigated. The mean axial velocity in the reverse flows decreases as the pressure increases and if the mass flow rate decreases.
- There is no effect of the equivalence ratio on the shape or velocity distribution in the recirculation zone.
- In the case of flashback, the boundary of the recirculation zone is wider and the velocity increases more than the normal combustion.
- It is possible to eliminate the partial flashback by changing the burner geometry, it is impossible to eliminate the full flashback due to the reduction of mixture velocity below the local burning velocity. It is, however, possible to improve the stability limits. This will be discussed in the next chapters.

Chapter 6

EFFECT OF CO_2 ADDITION TO CH_4 FLAME WITH EXPERIMENTAL VALIDATION

6.1 Introduction

The use of different fuels and/or diluents may cause potential changes in properties and flame velocities. The effect of many different diluents, such as N_2, CO_2, H_2O, on the flame characteristics have been studied by many researchers [174-177]. Even when large N_2 dilution levels are used to reduce NOx, they tend to promote flashback, contrary to the intuitive assumption that higher levels are safer. CO_2 can lower flame temperature and laminar flame speed, whilst fuels with similar laminar flame speed may have different turbulent flame speed. Air temperature is also a concern, since it has been found that the onset of flashback shifts to higher air temperatures with higher velocities and small injector diameters [178]. Clearly flashback depends on factors such as pilot fuelling rate and geometry.

In the previous chapters, it was found that flashback depends on many factors such as the burner geometry, the operating pressure, temperature, equivalence ratio, and mass flow rates. It has been shown, as mentioned in Section 2.5, that the addition of significant amounts of CO_2 into the fresh gases of premixed combustion in stationary gas turbines has many advantages in addition to lowering the laminar flame speed of the fuel.

In this chapter, the stability limits of CH_4 flames are determined at various operating conditions. The modified swirl burner model (S1) is used to determine the stability limits for methane flames. The feasibility of improving the stability limits of methane flames by adding CO_2 to the fuel is studied for premixed flames. The flashback limits are modelled for pure CH_4 and with addition of CO_2 up to 30%.

An experimental work programme is performed to determine the stability limits of methane flames. This work is continued to check the effect CO_2 additions to CH_4 flame stability.

6.2 CH_4 Flames Stability Limits

From the observations of the previous chapter, it was clear that flame stability depends on the operating pressure, initial temperature, equivalence ratio and total mass flow rate of the premixed mixture. All of these variables are brought together and a stability map drawn as shown in Figure 5.23. In this section, the stability limits for methane combustion is determined at different conditions. Several runs were carried out at various pressures of 1.01325, 3, and 7 bar and various temperatures of 300, 473, and 673 K. The aim of these runs is to determine the conditions at which the flame flashes back and plot the stability limits of CH_4 flames.

A sample of results is illustrated in Figure 6.1. In this Figure the correlation between the relative mass flow rate, defined by equation 5.5.1, and the equivalence ratio is shown at atmospheric pressure and 300 K. The curve divides the operating conditions into two regions. The first is the region of stable flames which is placed above the curve and the second is the region of unstable, flashback, flame which is placed under the curve. Again this Figure confirms the results obtained in Chapter 5, Section 5.5.3.

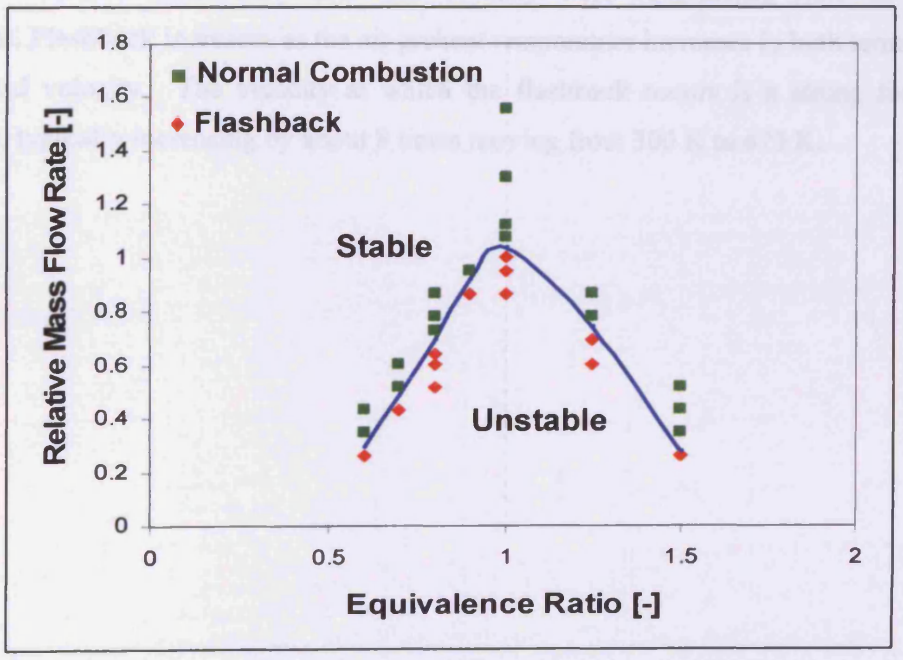

Figure 6.1: Flash determination for methane/air combustion at atmospheric pressure and mixture temperature of 300 K at various equivalence ratios.

Many runs are performed at every specific operating conditions (pressure & temperature and equivalence ratio) and varying the mass flow rate until 'catching' the flashback condition. The final results are shown in Figure 6.2 and 6.3.

The effect of pressure is shown in Figure 6.2. Complete sets of runs were performed at pressures of 1.01325, 3, and 7 bar respectively, the initial mixture temperatures were 300, 473, and 673 K, and results are shown in Figures 6.2.a and 6.2.b. In Figure 6.2.a the correlation between the relative mass flow rate and the equivalence ratio is shown at different pressures. The operating total mass flow rate required to avoid flashback increases with pressure. However, Figure 6.2.b shows that the relative velocity, defined by equation 5.5.2, at which the flashback exists is a weak function of pressure, typically reduced by about 20 % moving from 1.0 bar to 7.0 bar.

In the same way, the effect of inlet raw gases temperature on the stability limits was studied. Complete sets of runs were performed at three different temperatures of 300, 473 and 673 K for operating pressures of 1.01325, 3, and 7 bar. Figure 6.3.a and 6.3.b show the correlation between the relative mass flow rate and velocity with equivalence ratio at different temperatures. Flashback increases as the air preheat temperature increases in both terms of mass flow rate and velocity. The velocity at which the flashback occurs is a strong function of temperature, typically increasing by about 8 times moving from 300 K to 673 K.

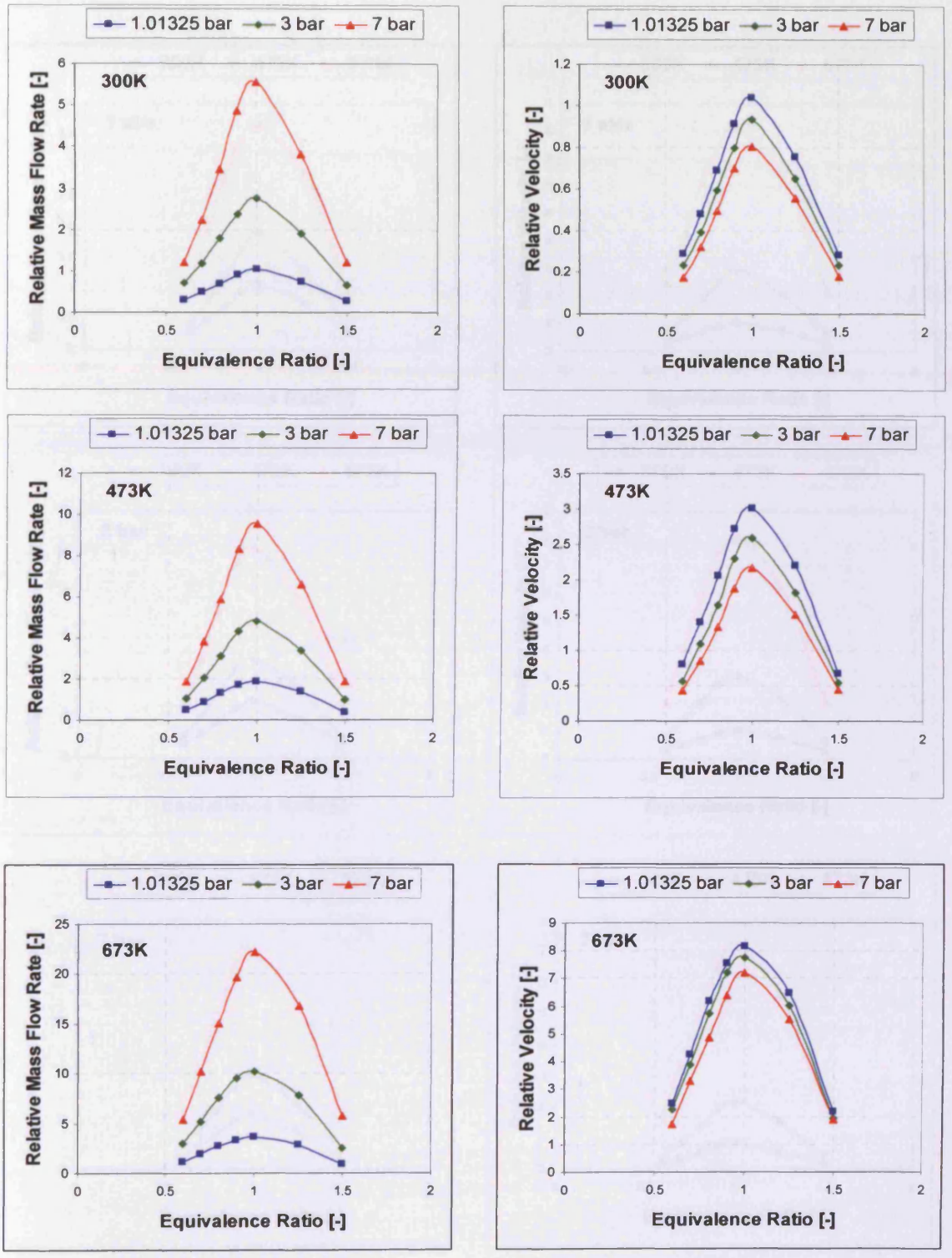

Figure 6.2: The effect of pressure variation on the stability limits for CH_4 combustion at various equivalence ratios and,

(a) The corresponding relative mass flow rates;

(b) The corresponding relative velocity at which flashback occurs.

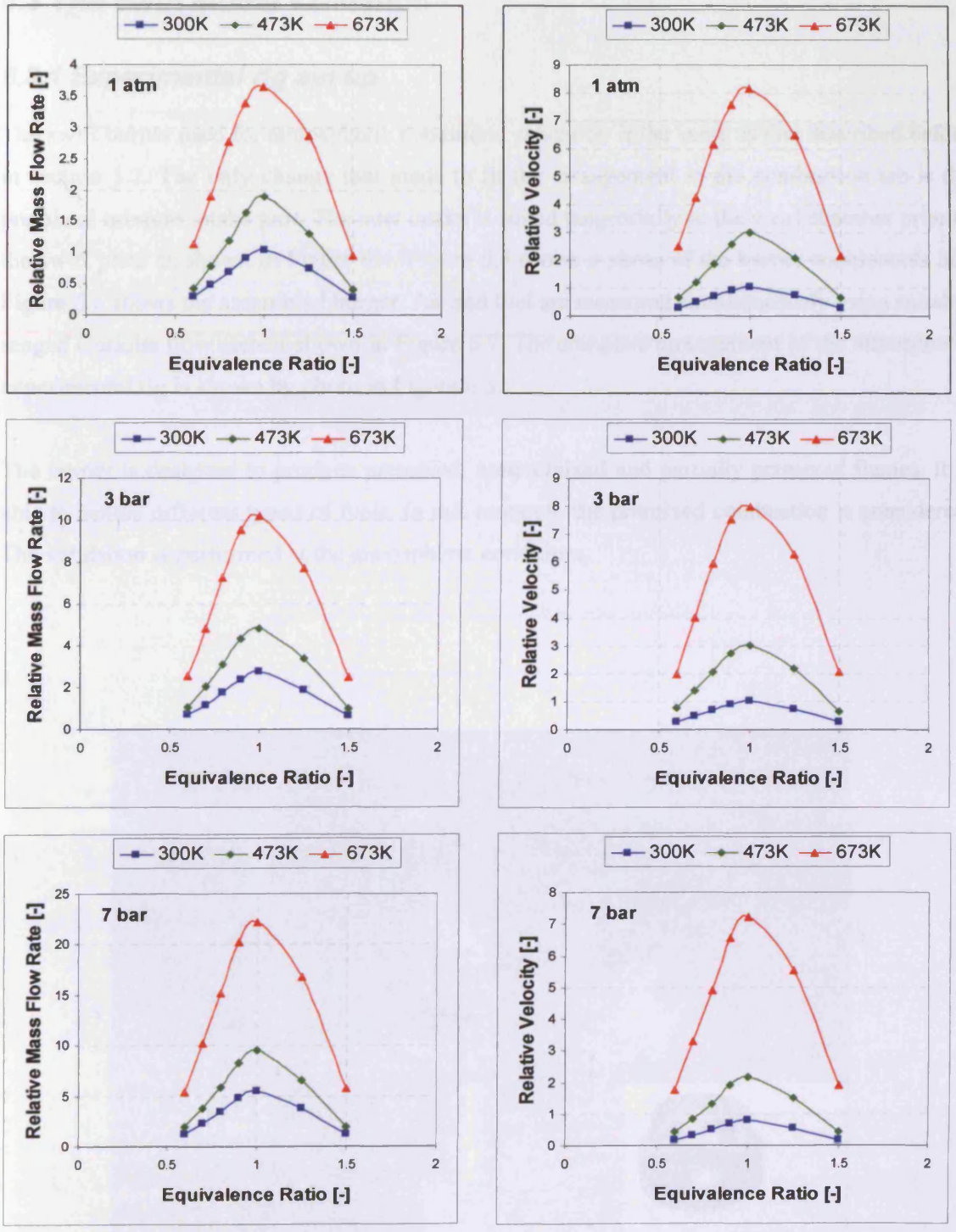

Figure 6.3: The effect of temperature variation on the stability limits for CH_4 combustion at various equivalence ratios and,

(a) The corresponding relative mass flow rates;

(b) The corresponding relative velocity at which flashback occurs.

6.3 The Swirl Model Validation

6.3.1 Experimental rig set up

The swirl burner used for atmospheric conditions validation is the same as that described before in section 5.2. The only change that made to fit the arrangement in the combustion lab is the premixed mixture intake port. The new intake is suited tangentially to the swirl chamber prior to the swirl plate as shown in Figure 6.4. Figure 6.5 shows a photo of the burner components and Figure 6.6 shows the assembled burner. Air and fuel are measured simultaneously using suitably ranged Coriolis flow meters shown in Figure 6.7. The complete arrangement of the atmospheric experimental rig is shown by photo in Figure 6.8.

The burner is designed to produce premixed, nonpremixed and partially premixed flames. It is able to handle different typed of fuels. In this research, the premixed combustion is considered. The validation is performed at the atmospheric conditions.

Figure 6.4: The new swirl chamber with premixed mixture inlet

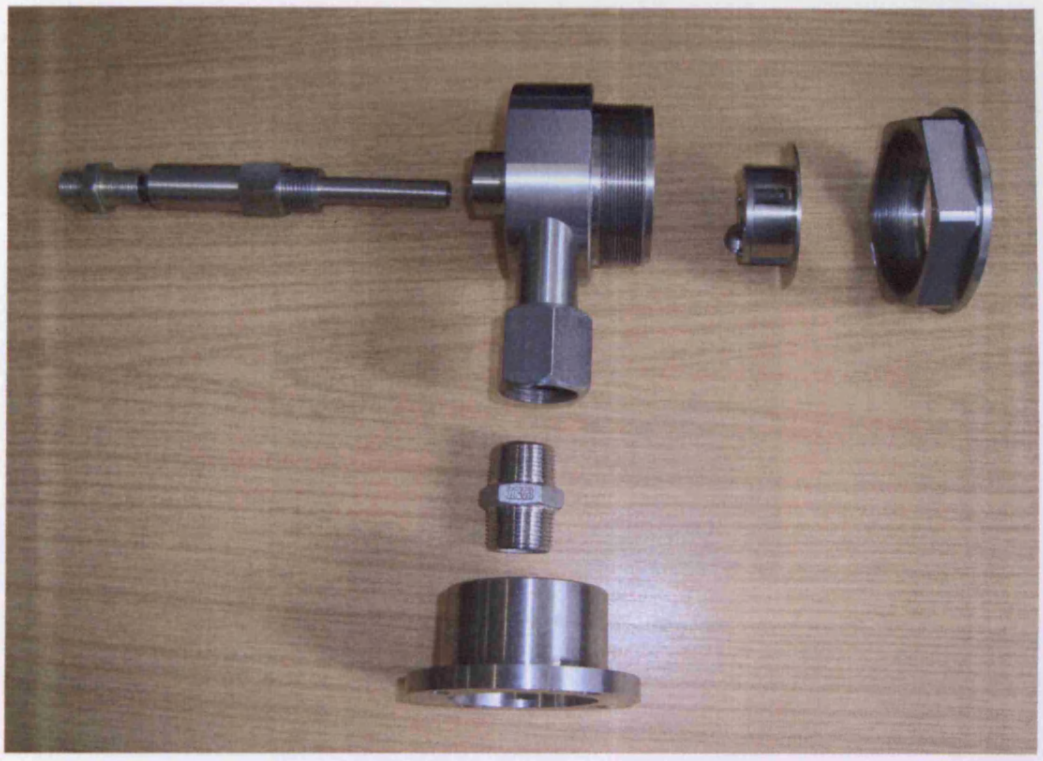

Figure 6.5: The swirl burner components

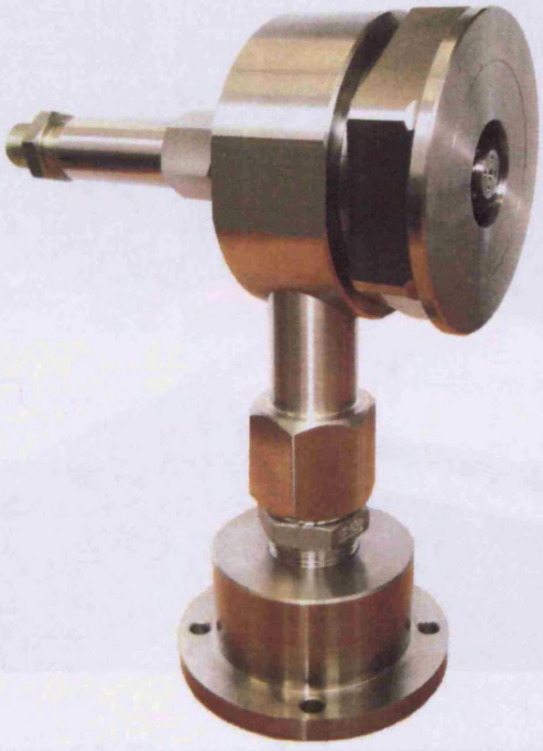

Figure 6.6: The assembled swirl burner

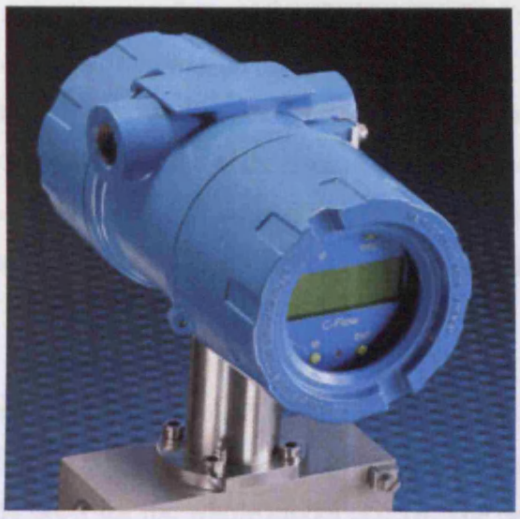

Figure 6.7: Coriolis flow meter

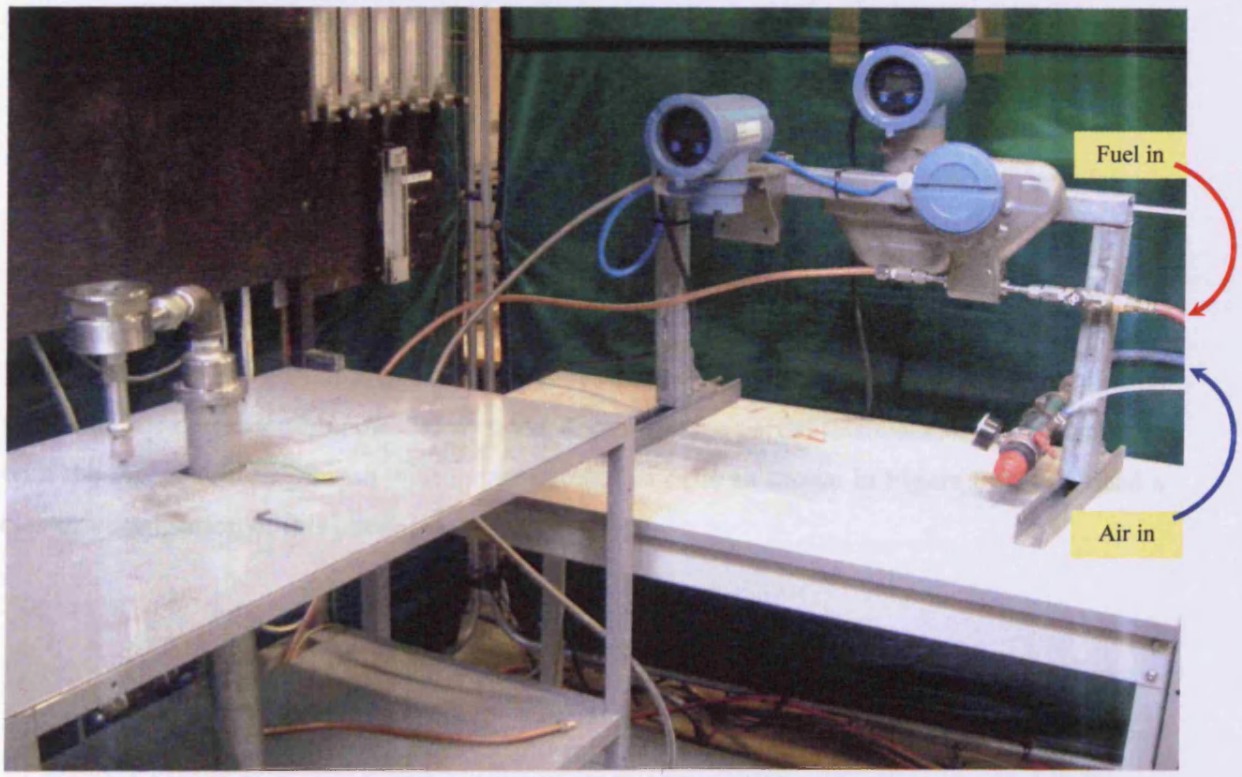

Figure 6.8: The atmospheric experiments rig

It is realized during the experiments that partial flashback exists at some conditions, so the system model is reconstructed with more fine mesh especially at the swirl element of the burner and the burner nozzle. Figure 6.9 shows the new fine mesh for the burner and Figure 6.10 shows the new mesh for the whole system which comprises of the burner and the combustion domain. The new system is meshed using 439,609 cells. The convergence of the solution takes longer, but the simulation results appear to be much better as the partial flashback is realized in the model as well.

The grid quality of the new design is checked based on the volume-weighted average method. The cell equiangle skew for the combustion zone is 0.138 and for the swirler zone is 0.161 and hence the net cell equiangle skew for the whole model is 0.16. The cell equivolume skew for the combustion zone is 0.132 and for the swirler zone is 0.161 and hence the net cell equivolume skew for the whole model is 0.16. So, refereeing to table 3.1, the mesh quality is considered as excellent.

The cell equiangle skew histogram for the new model is plotted in Figure 6.11 and the cell equivolume skew histogram is plotted in Figure 6.12. The data from these plots show that the grid quality is within the range of good and excellent.

The model is adjusted to be compatible with the new design. The burner with the new inlet is simulated under the same previous conditions to check the effect of the new design. The new change in mixture inlet affects has some effect on the turbulence produced at the burner exit and hence affects the flashback limits of the flame. The results are matched to the results obtained before regarding the full flashback and produce limits about 10% higher than the nominated values for the corresponding mass flow rates. Regarding the partial flashback, it emerged clearer with the higher accuracy mesh with larger number of cells as shown in Figure 6.13 produced a clearer visualisation of this phenomena.

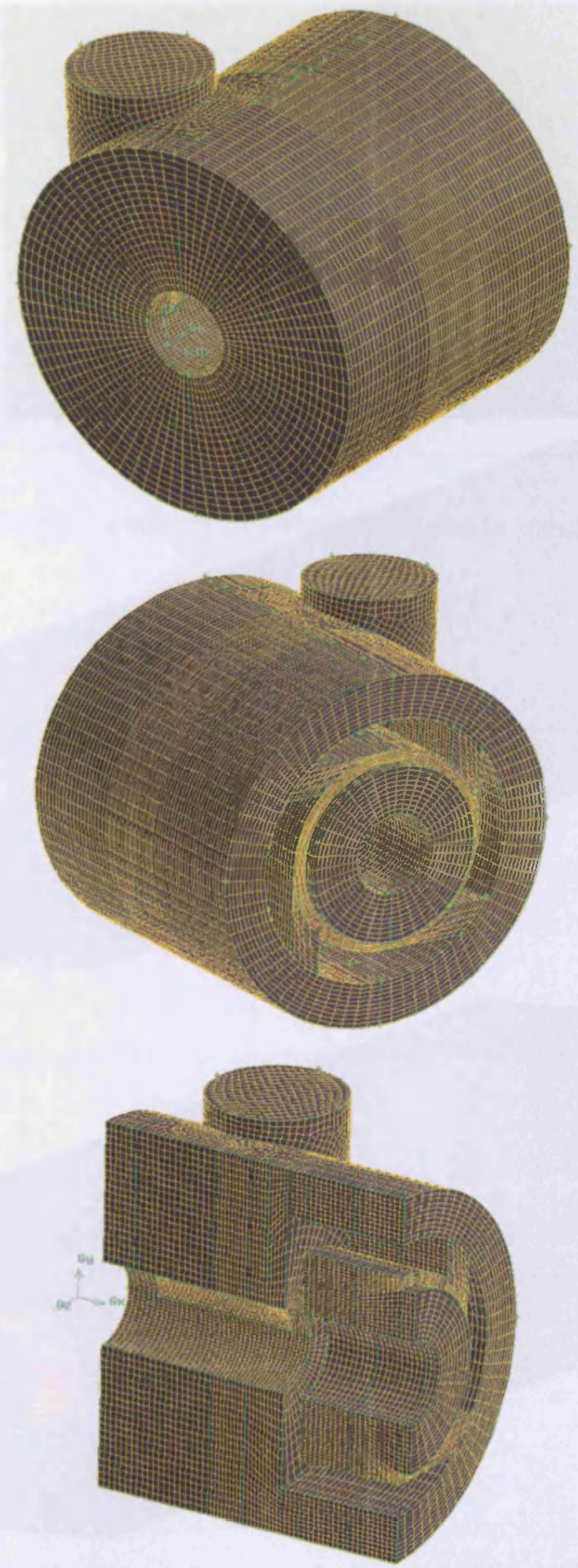

Figure 6.9: Different views for the swirler mesh

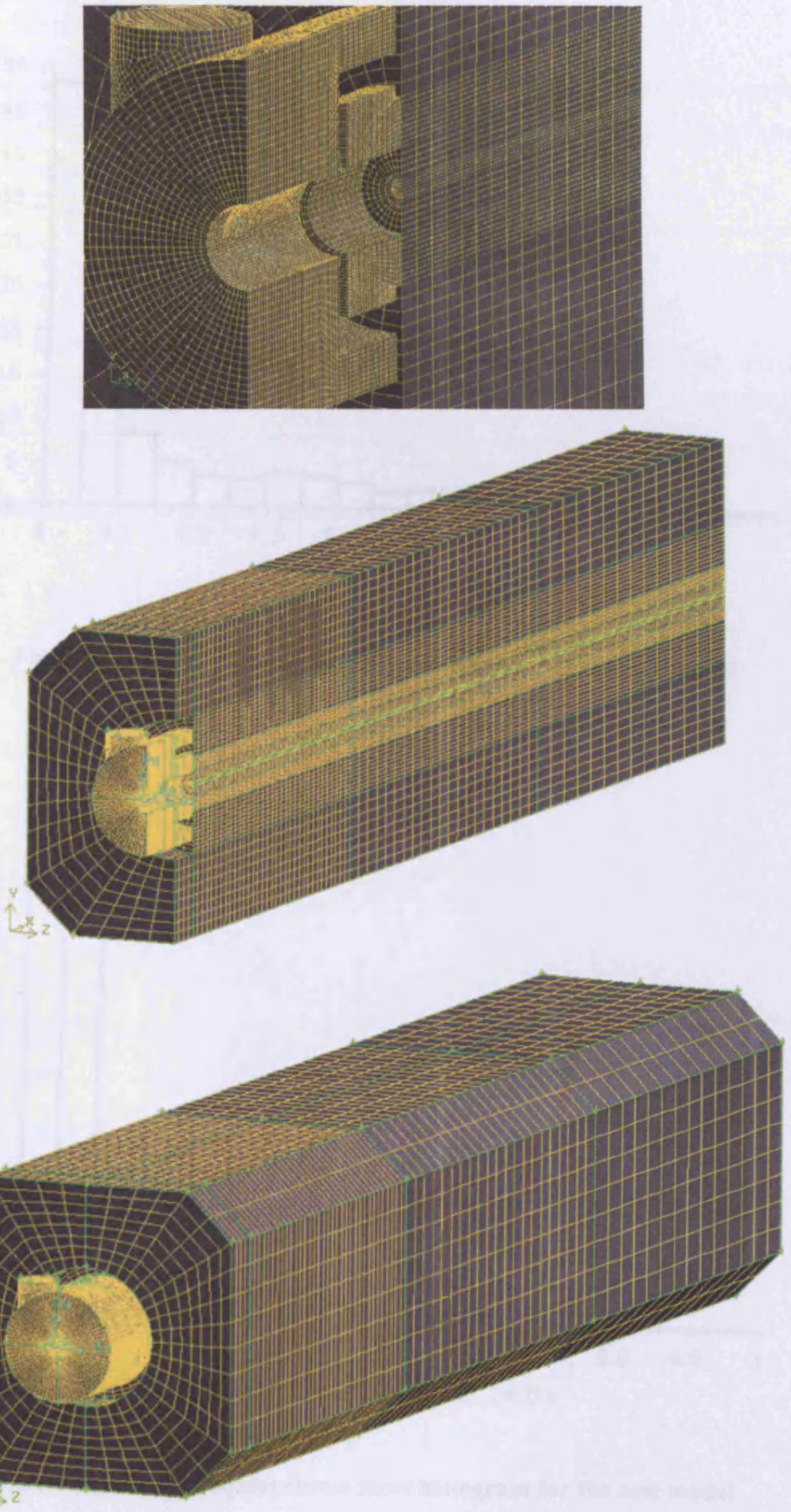

Figure 6.10: The mesh of the whole system, the burner and the combustion chamber.

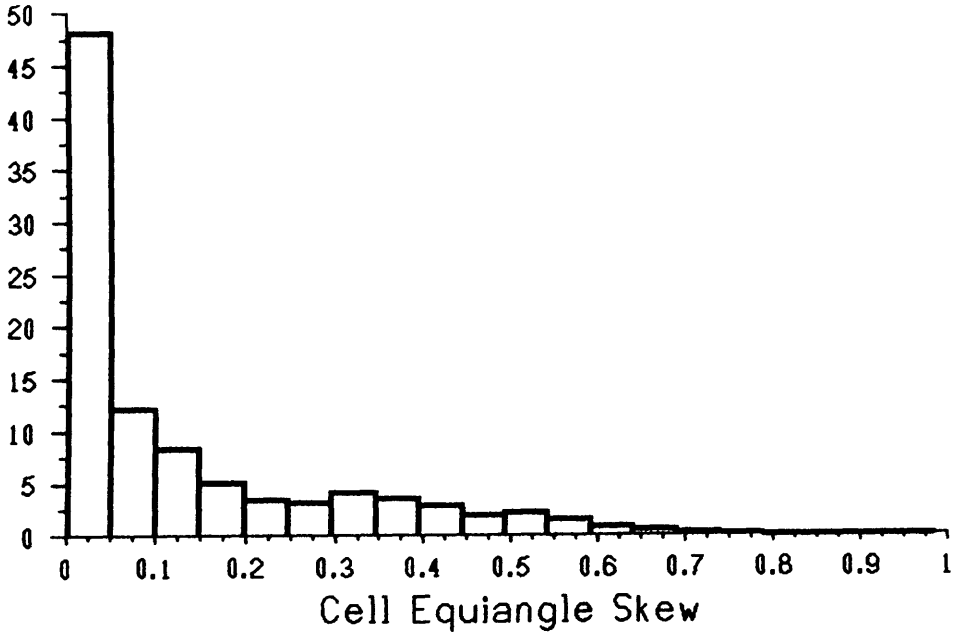

Figure 6.11: The cell equiangle skew histogram for the new model

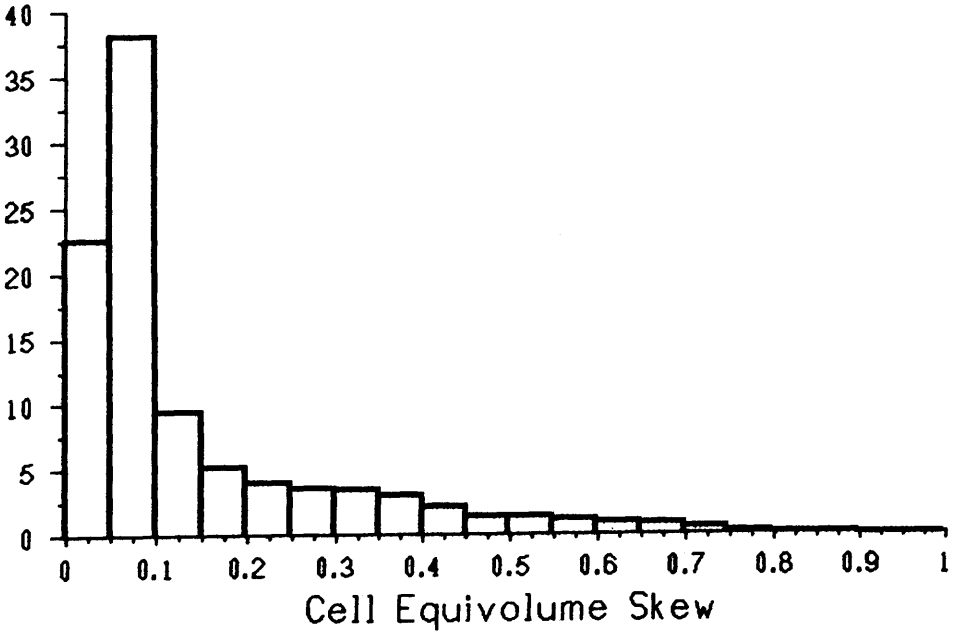

Figure 6.12: The cell equiavolume skew histogram for the new model

6.3.2 CH_4 Combustion and Stability Limits

The experiments are performed for premixed methane combustion at atmospheric conditions (1 atm and 290 K). The runs are performed to measure the stability limits of the flame. The partial flashback is realized due to the flow recirculation in the CRZ as shown in Figure 6.13. The partial flashback is realized more for lean combustion than rich combustion and for lower flow velocities more than higher flow velocities. The partial flashback is clearly visualised during the experiments with a stable flame. The partial flashback turns into full flashback as the flow velocity is reduced.

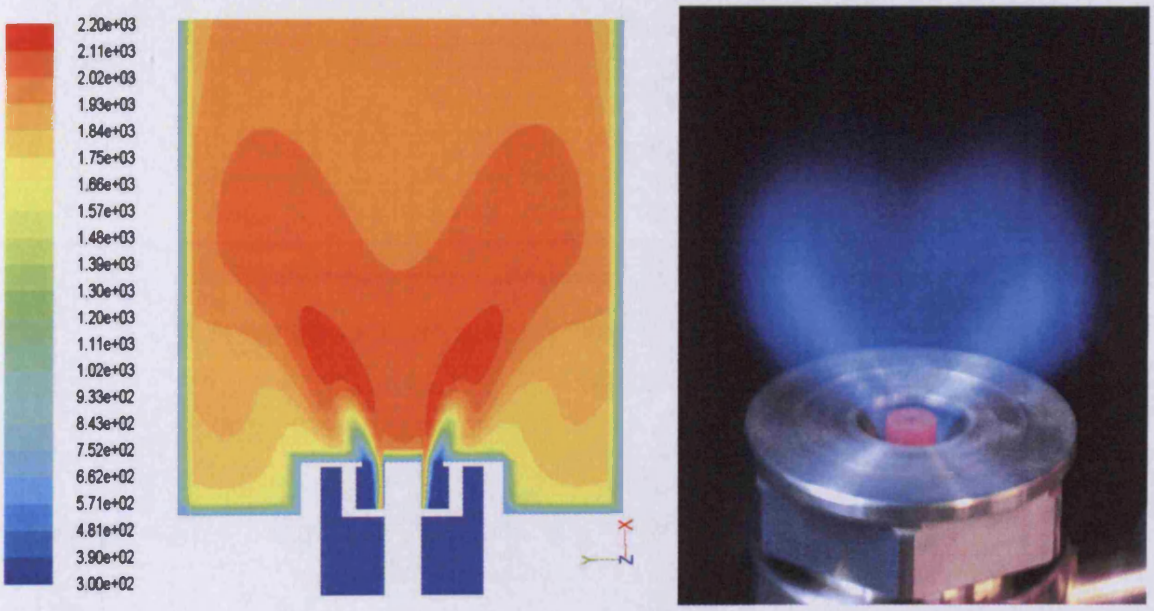

(a) (b)

Figure 6.13: Partial flashback is realized in both model and experiments

(a) Temperature contours in the model

(b) Flame photo in the experiment

Different configurations for the stable flame are photographed and shown in Figure [illegible]. In the stable flames, the flame starts being located out of the burner as shown in the upper photos in Figure 6.14 or with partial flashback due to the gas recirculation as shown in the lower photos in the same figure. The partial flashback is not desirable as it causes overheating of the fuel injector, in the case of diffusive and partially premixed flames.

The full flashback flames are shown in Figure 6.15 where the combustion starts clearly inside the burner tangential inlets. The full flashback results in high temperature in the swirl element inside the burner and the diffusive fuel injector.

The stable and flashback flames are reported under various air and fuels mass flow rates. A stability map is plotted in Figure 6.16 to differentiate the stable and flashback conditions. An interpolation is performed to define the flame stability limits. It is realized that the flame is more stable, regarding flashback, for lean mixtures. The flame flashback tendency increases as the equivalence ratio increases up to (ϕ=0.9) where the flashback tendency reaches its maximum and then reduced for rich mixtures.

Another problem that is realized during the experiments is the flame blow off. It is difficult to keep the flame alight with higher mass flow rates, and is commonly dealt with by using small quantities of diffusive fuel fired directly into the central recirculation zone, this stabilizing the system.. Another technique that can be used to improve the CH_4 flame blow off, is to add H2 to the mixture, however this does then affect the flame flashback. This will be discussed in the next chapter.

The comparison of the stability limits measured experimentally and determined by using the CFD simulation is shown in Figure 6.17. The following conclusions are derived:

- The model and the experiments approximately are matched for lean mixtures up to (ϕ=0.8).
- The peak of the stability limits is at (ϕ=0.9) experimentally where it is at (ϕ=1) in the model.
- The model gives higher values for the minimum flow rate required to overcome flashback over (ϕ=0.8) but with the same trend as the experiments.

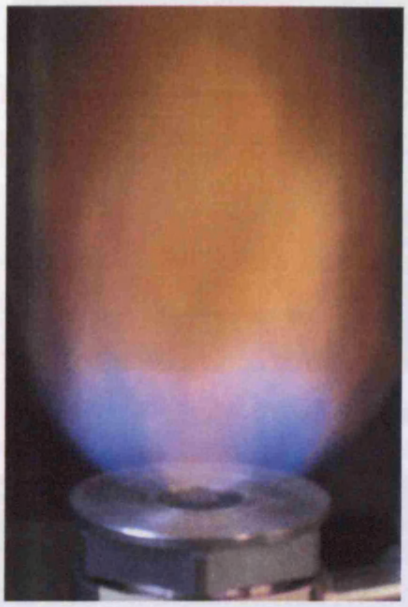

$\dot{m}_t = 3.4, \phi = 2.3$

$\dot{m}_t = 1.08, \phi = 1.37$

$\dot{m}_t = 5.57, \phi = 1.2$

$\dot{m}_t = 2.74, \phi = 0.9$

Figure 6.14: The stable premixed CH_4 flames

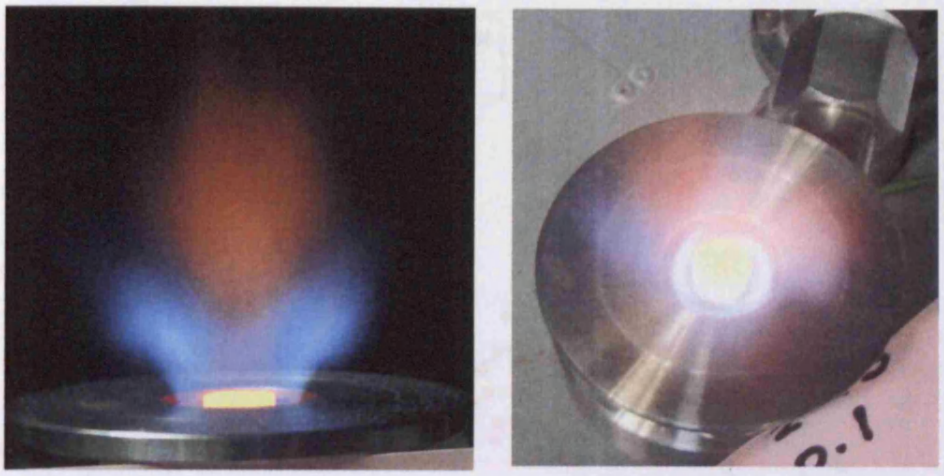

$\dot{m}_t = 2.28, \phi = 0.79$

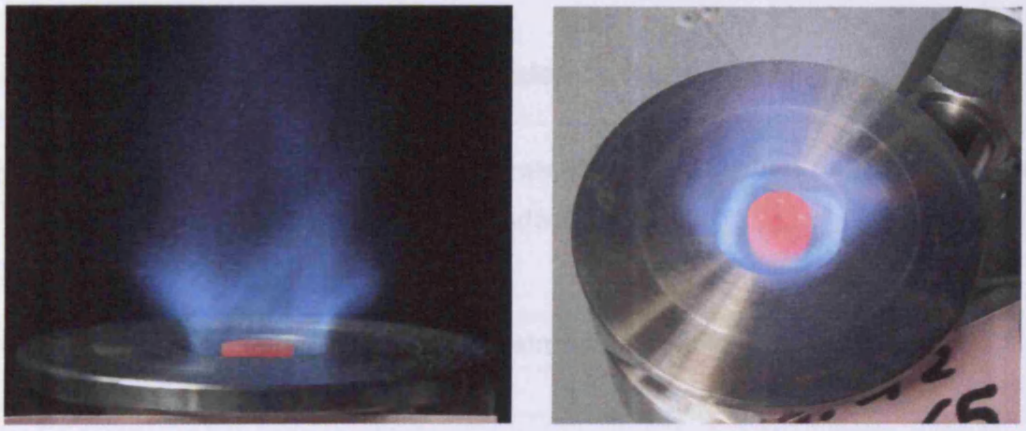

$\dot{m}_t = 1.485, \phi = 0.79$

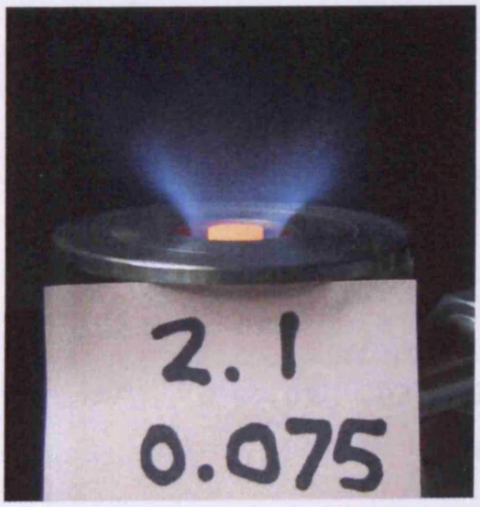

$\dot{m}_t = 2.175, \phi = 0.61$

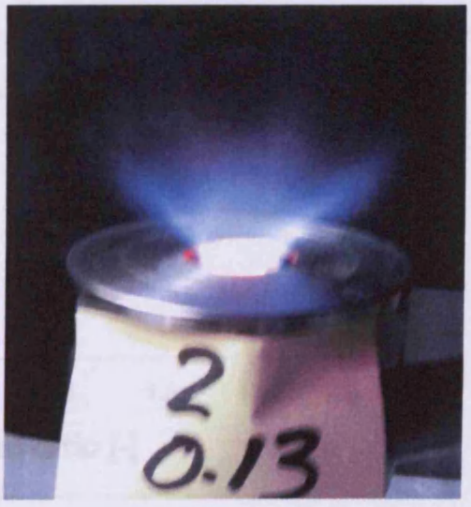

$\dot{m}_t = 2.13, \phi = 0.75$

Figure 6.15: The flame flashback for CH_4 combustion

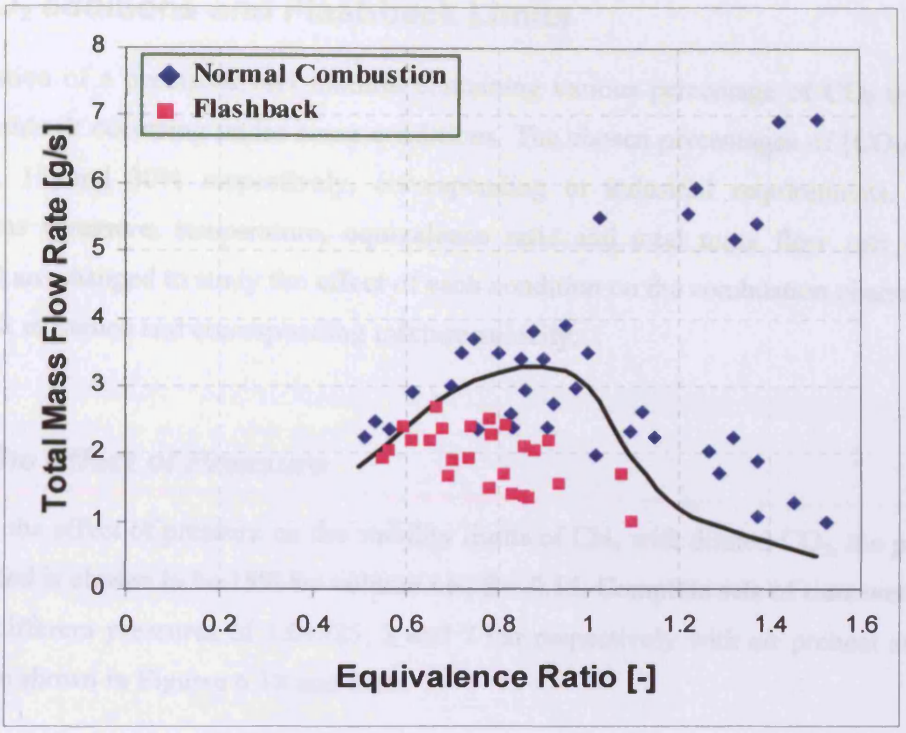

Figure 6.16: The Experimental measurements of the stability limits of CH_4 at atmospheric conditions.

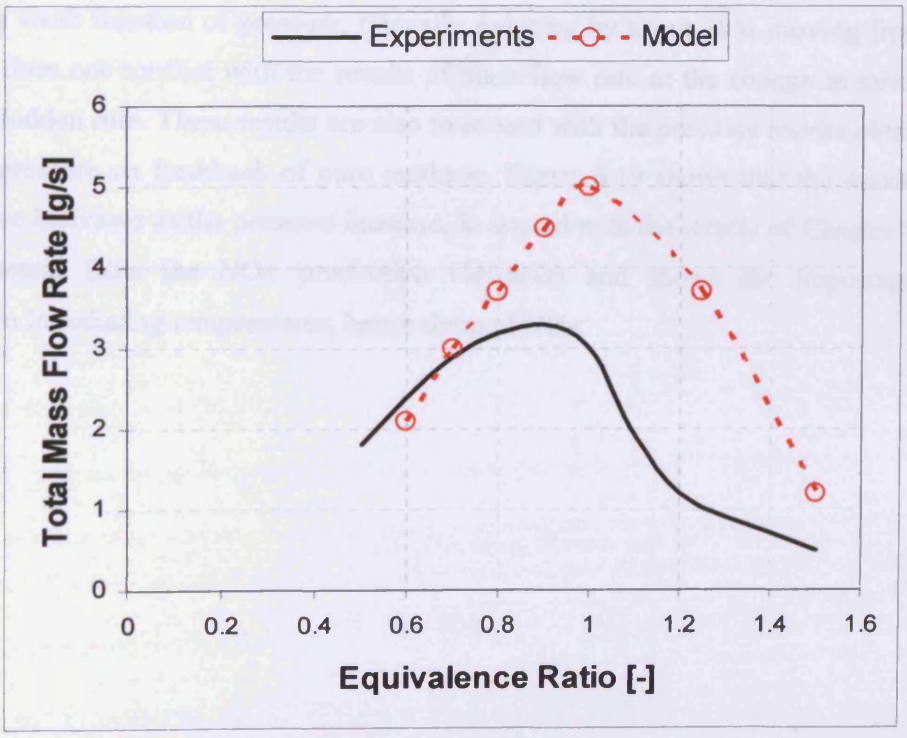

Figure 6.17: Comparison between the CH_4 flame stability limits measured experimentally and determined by CFD simulation.

6.4 CO_2 additions and Flashback Limits

Combustion of a premixed fuel mixture containing various percentage of CO_2 was simulated with flashback occurring under some conditions. The chosen percentages of $[CO_2/(CH_4+CO_2)]$ were 0, 15 and 30% respectively, corresponding to industrial requirements. Combustion conditions (pressure, temperature, equivalence ratio and total mass flow rate of premixed mixture) are changed to study the effect of each condition on the combustion characteristics and flashback existence and corresponding mixture velocity.

6.4.1 The Effect of Pressure

To study the effect of pressure on the stability limits of CH_4 with diluted CO_2, the percentage of CO_2 diluted is chosen to be 15% by volume i.e., $\beta = 0.15$. Complete sets of runs were performed at three different pressures of 1.01325, 3 and 7 bar respectively with air preheat at 673K. The results are shown in Figures 6.18 and 6.19.

In Figure 6.18 the correlation between the relative mass flow rate and the equivalence ratio is shown at different pressures. It was confirmed that the mass flow rate required to overcome flashback increases with pressure increase. Also the relative velocity at which the flashback exists is a weak function of pressure, typically reducing by about 10% moving from 1bar to 7 bar. This does not conflict with the results of mass flow rate as the change in mixture density plays the hidden role. These results are also in accord with the previous results obtained for the effect of pressure on flashback of pure methane. Figure 6.19 shows that the maximum flame temperature increases as the pressure increase, in accord with the results of Chapter 5. This will be detrimental from the NOx production viewpoint and shows the importance of lean combustion in reducing temperatures, hence thermal NOx.

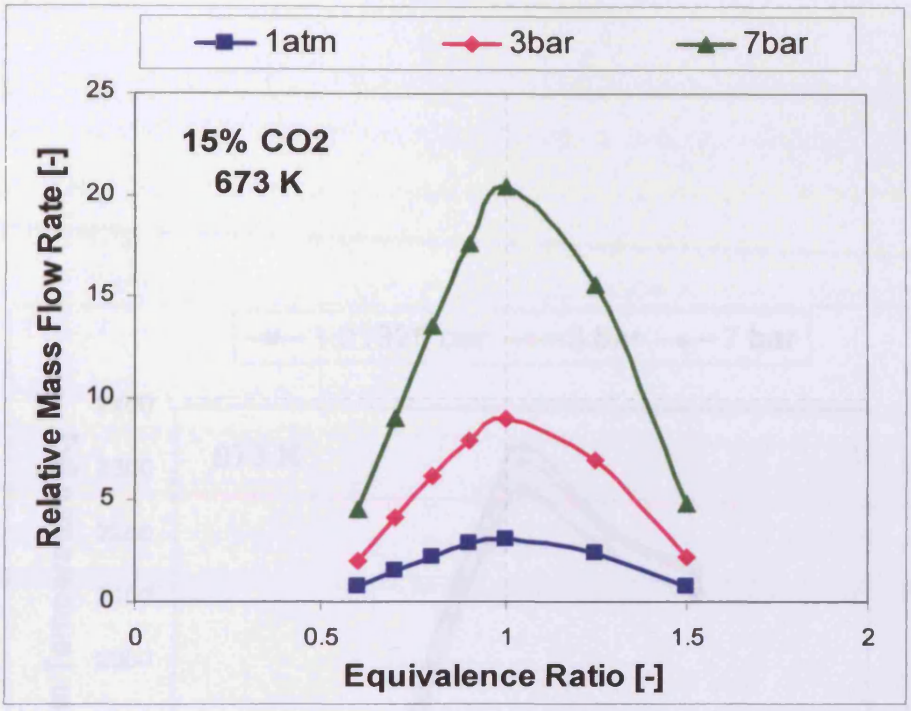

(a)

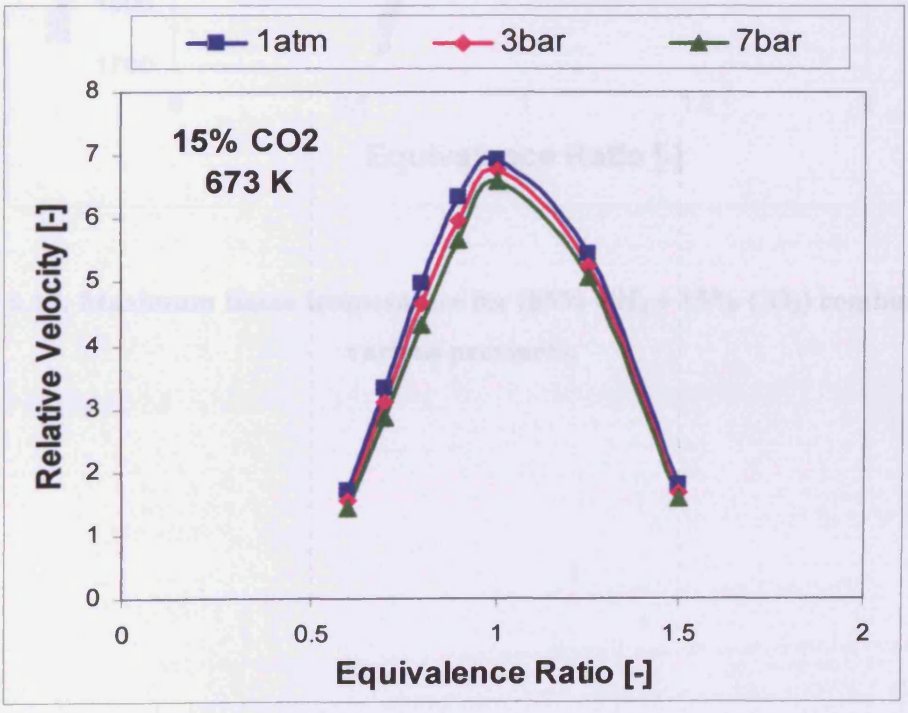

(b)

Figure 6.18: The stability limits for (85% CH_4 + 15% CO_2) at various pressures with air preheat to 673K.

(a) the corresponding relative mass flow rates

(b): the corresponding relative velocity.

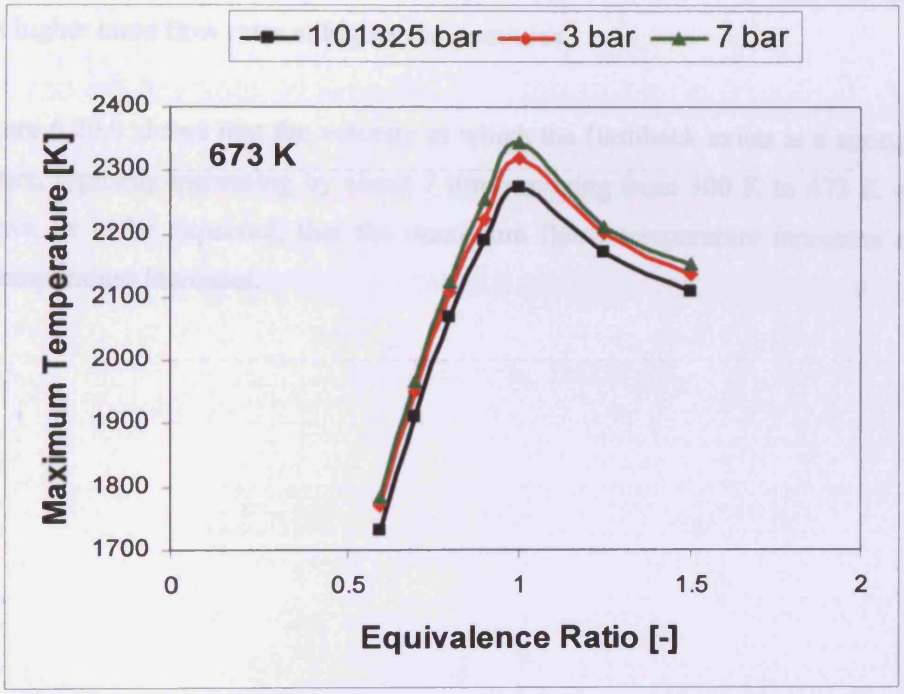

Figure 6.19: Maximum flame temperature for (85% CH_4 + 15% CO_2) combustion at various pressures.

6.4.2 The Effect of Temperature

To study the effect of air preheat temperature on the stability limits and laminar flame speed, the fuel is chosen as (85% CH_4 + 15% CO_2). Complete sets of runs are performed at three different temperatures of 300, 473 and 673 K respectively. Figure 6.20.a shows the correlation between the total mass flow rate and the equivalence ratio at different temperatures. It was found that the occurrence of flashback increases as the temperature increases. This confirms that flashback occurs at higher mass flow rates at higher temperatures.

Also Figure 6.20.b shows that the velocity at which the flashback exists is a strong function of temperature, typically increasing by about 7 times moving from 300 K to 673 K whilst Figure 6.21 shows, as to be expected, that the maximum flame temperature increases as the initial mixture temperature increases.

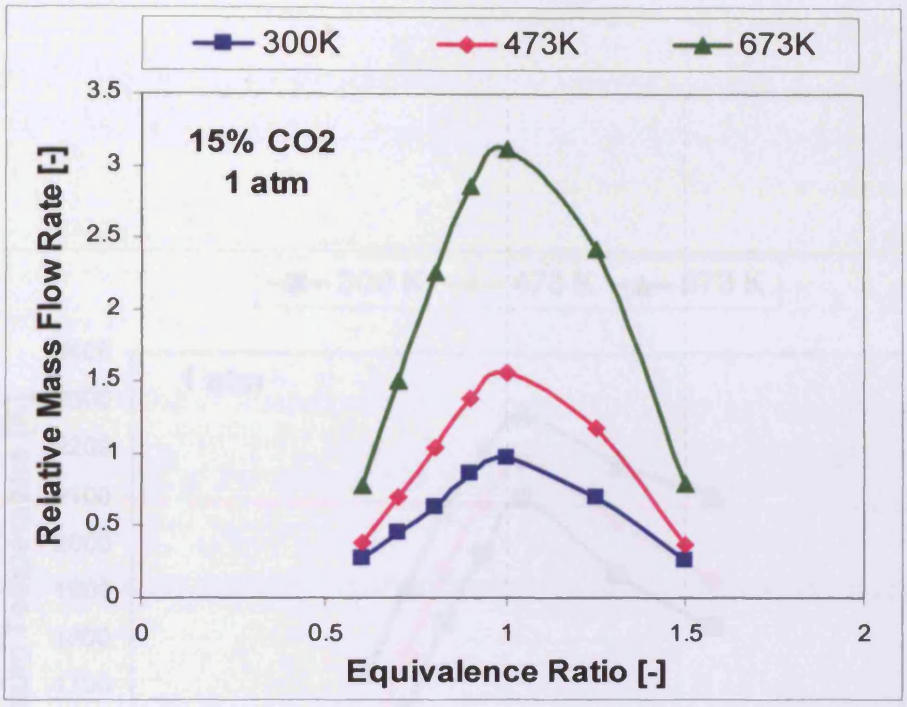

(a)

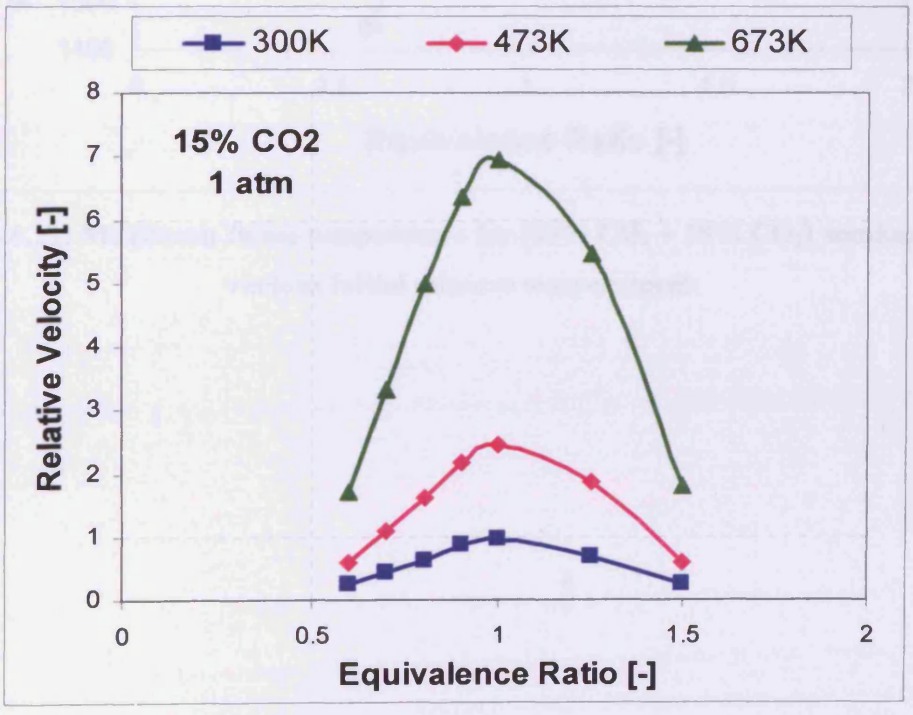

(b)

Figure 6.20: The stability limits for (85% CH_4 + 15% CO_2) at atmospheric pressure with various initial mixture temperatures.

(a) the corresponding relative mass flow rates

(b) the corresponding relative velocity.

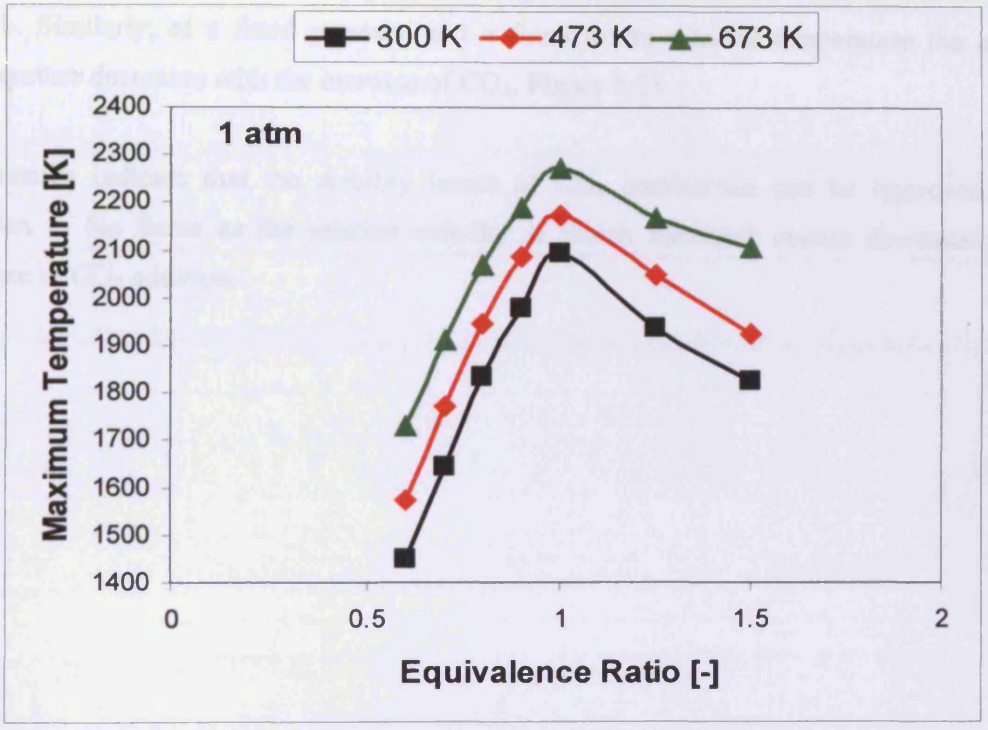

Figure 6.21: Maximum flame temperature for (85% CH_4 + 15% CO_2) combustion at various initial mixture temperatures.

6.4.3 The Effect of Higher Levels of CO_2 Addition

As before, the flashback limits are modelled for CH_4 with CO_2 dilution up to 30%. The results are shown in Figures 6.22 and 6.23. Figure 6.22 shows that flashback limits are improved with the addition of CO_2 as the mass flow rate corresponding to flashback decreases as the CO_2 addition increases, as shown in Figure 6.22.a, hence the velocity decreases as shown in Figure 6.22.b. Similarly, at a fixed pressure and a fixed mixture initial temperature the maximum temperature decreases with the increase of CO_2, Figure 6.23.

The results indicate that the stability limits of CH_4 combustion can be improved by CO_2 addition to the flame as the relative velocity at which flashback occurs decreases with the increase of CO_2 addition.

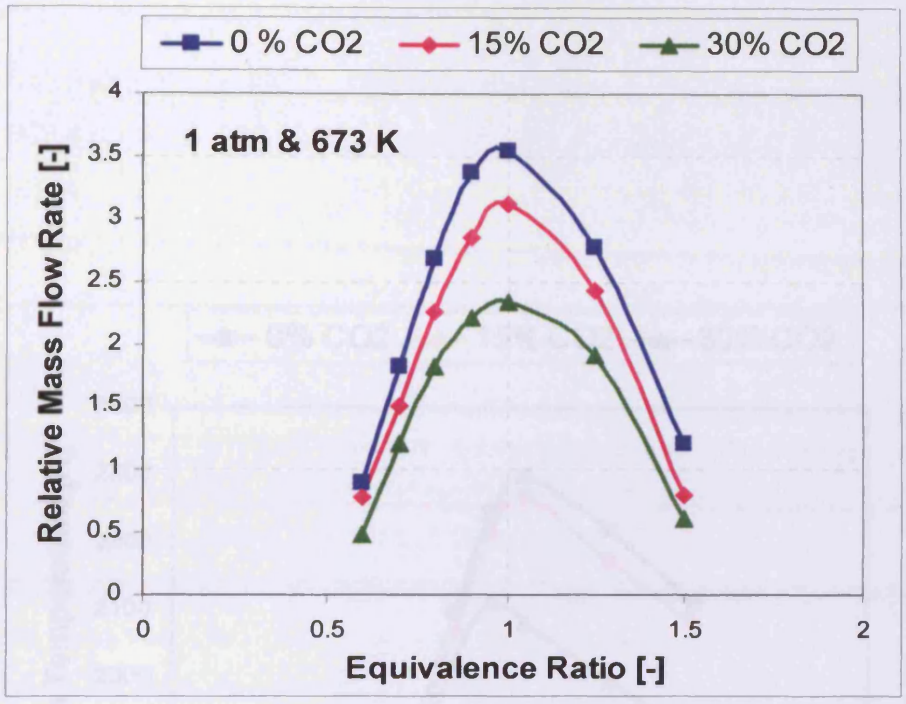

(a)

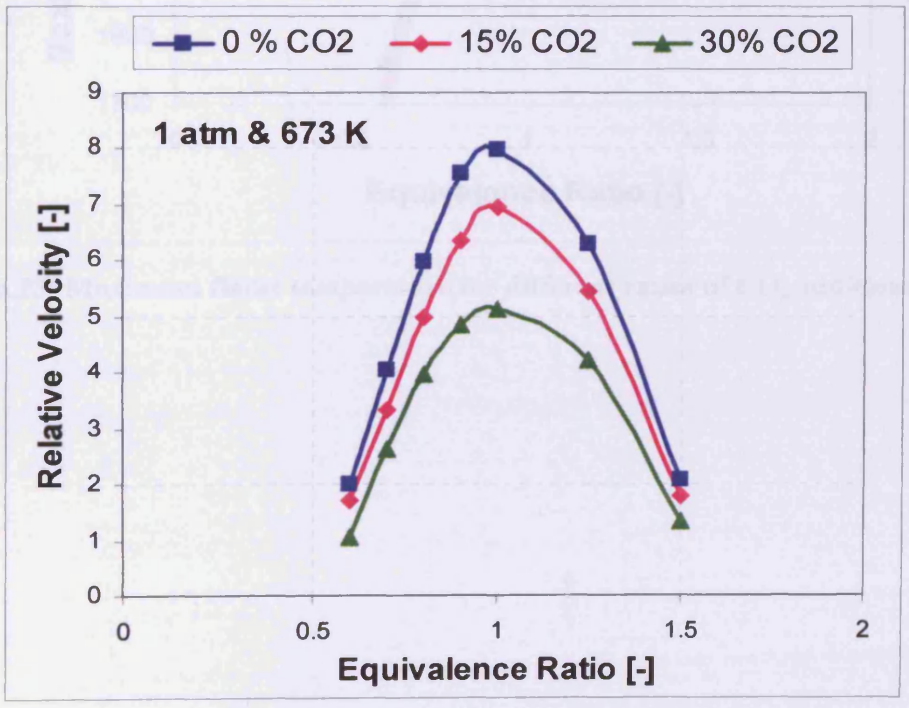

(b)

Figure 6.22: The stability limits for (CH_4 + β% CO_2) at atmospheric pressure with and initial mixture temperatures of 673 K.

(a) the corresponding relative mass flow rates

(b) the corresponding relative velocity.

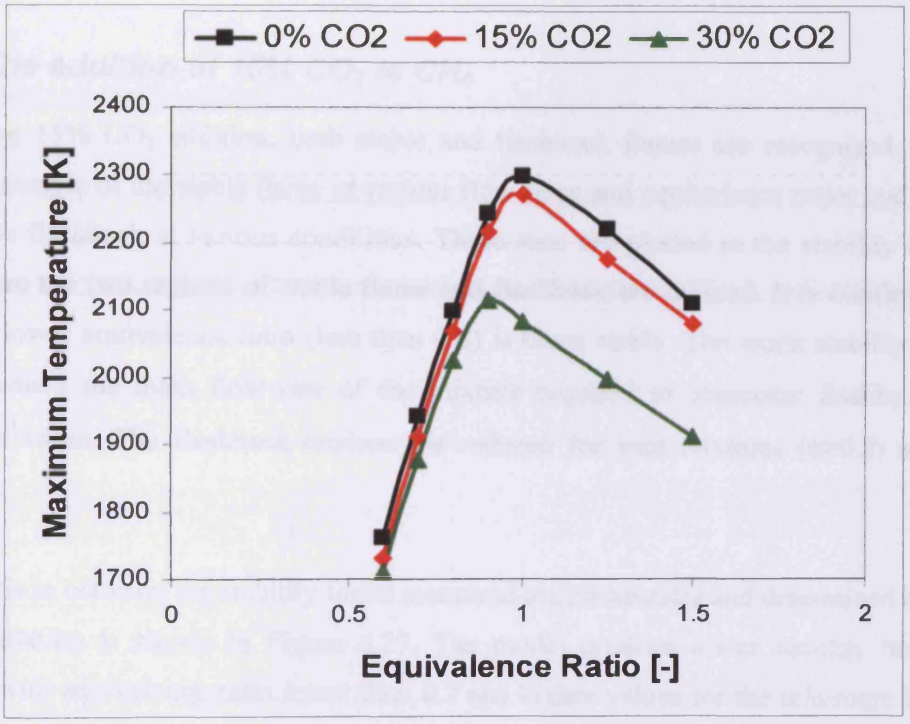

Figure 6.23: Maximum flame temperature for different ratios of CO_2 additions to CH_4.

6.5 The Experimental Validation for CO_2 Addition to CH_4 Model

Experiments were performed to check the effect of CO_2 addition to CH_4 flames at the atmospheric conditions. The chosen percentages of $[CO_2/(CH_4+CO_2)]$ were 15 and 30% by volume respectively. A complete set of runs are performed to determine the stability limits for each mixture.

6.5.1 The addition of 15% CO_2 to CH_4

Regarding 15% CO_2 addition, both stable and flashback flames are recognized. Figure 6.24 shows a sample of the stable flame at various flow rates and equivalence ratios and Figure 6.25 shows the flashback at various conditions. These runs are plotted in the stability map, Figure 6.26 where the two regions of stable flame and flashback are defined. It is confirmed that the flame at lower equivalence ratio (less than 0.8) is more stable. The worst stability emerges at (ϕ=0.8) where the mass flow rate of the mixture required to overcome flashback is at the maximum value. The flashback tendency is reduced for lean mixtures (ϕ>0.8) and for rich mixtures.

A comparison between the stability limits measured experimentally and determined by using the CFD simulation is shown in Figure 6.27. The model produce lower stability limits for the mixtures with equivalence ratio lower than 0.7 and higher values for the minimum flow rate of stable flame for the mixtures with equivalence ratio over 0.7 . The peak of the model is at the stoichiometric mixture while experimentally it is at (ϕ=0.8). The experiments/model match is worse than the pure methane model.

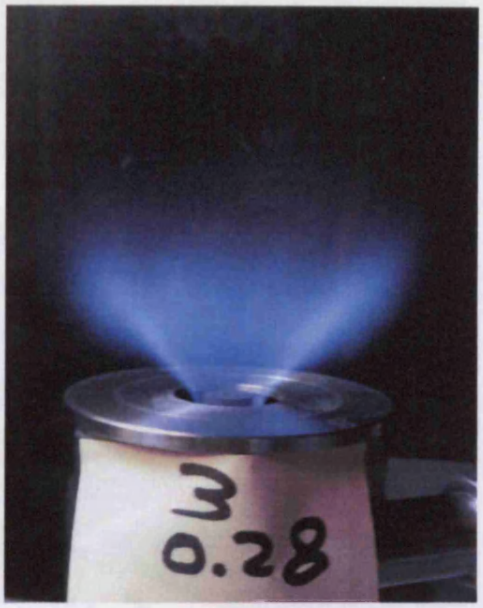

$\dot{m}_t = 3.28, \phi = 1.1$

$\dot{m}_t = 2.15, \phi = 0.87$

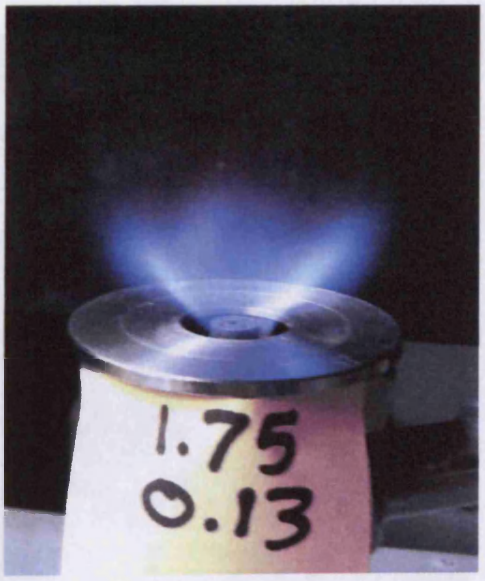

$\dot{m}_t = 1.88, \phi = 0.858$

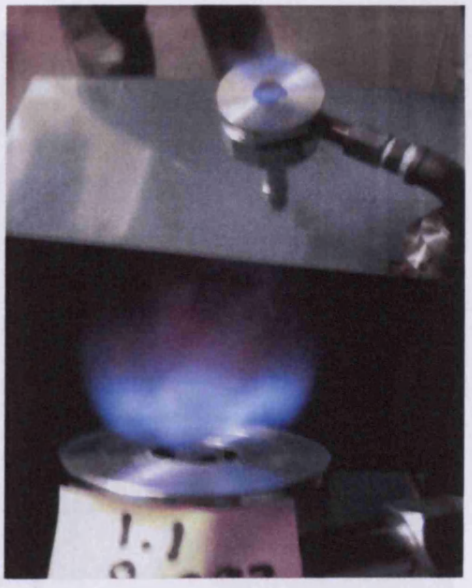

$\dot{m}_t = 1.193, \phi = 0.97$

Figure 6.24: The stable premixed (85% CH_4 + 15% CO_2) flames

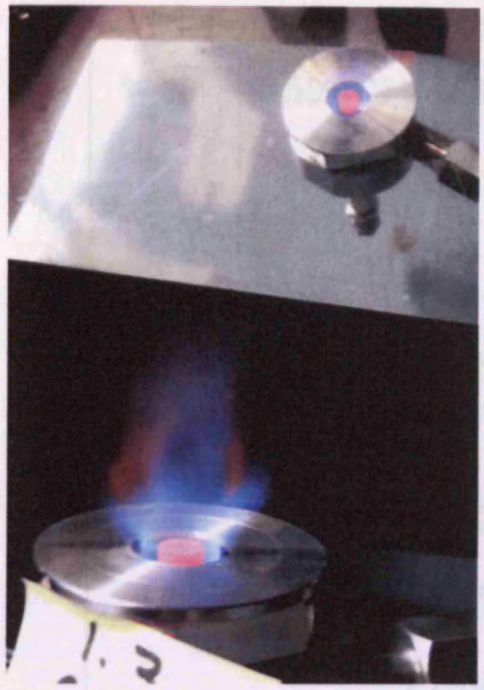

$\dot{m}_t = 1.393, \phi = 0.83$

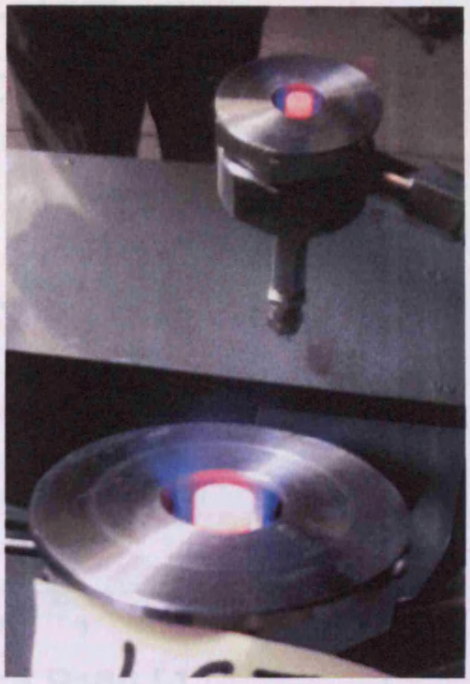

$\dot{m}_t = 1.763, \phi = 0.8364$

$\dot{m}_t = 1.92, \phi = 0.83$

$\dot{m}_t = 2.01, \phi = 0.8$

Figure 6.25: The flame flashback for (85% CH_4 + 15% CO_2) flames

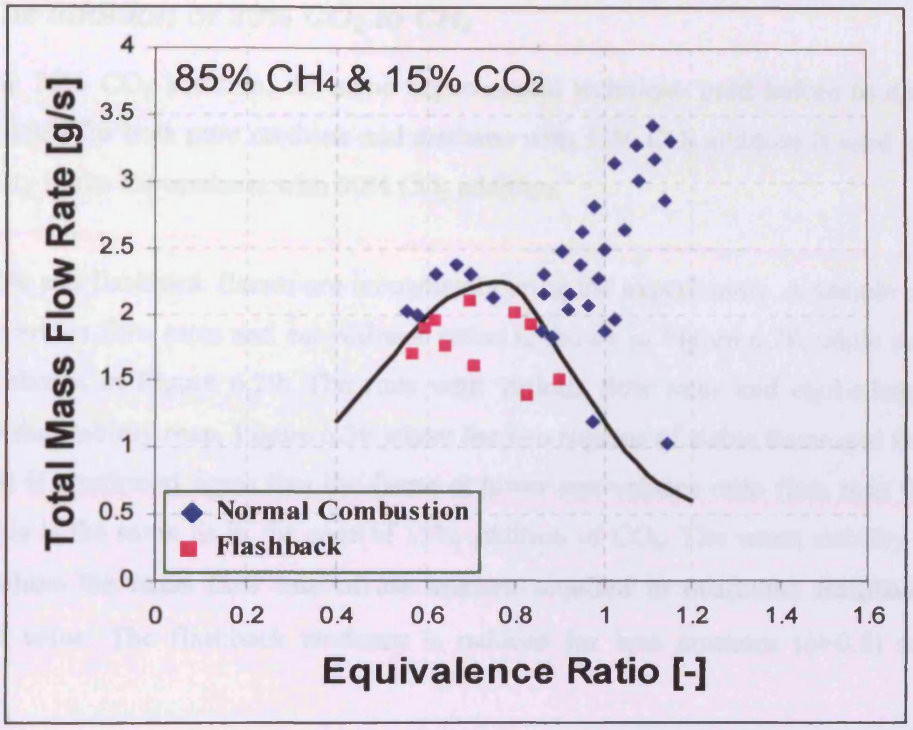

Figure 6.26: The Experimental measurements of the stability limits of (85% CH_4 + 15% CO_2) at atmospheric conditions.

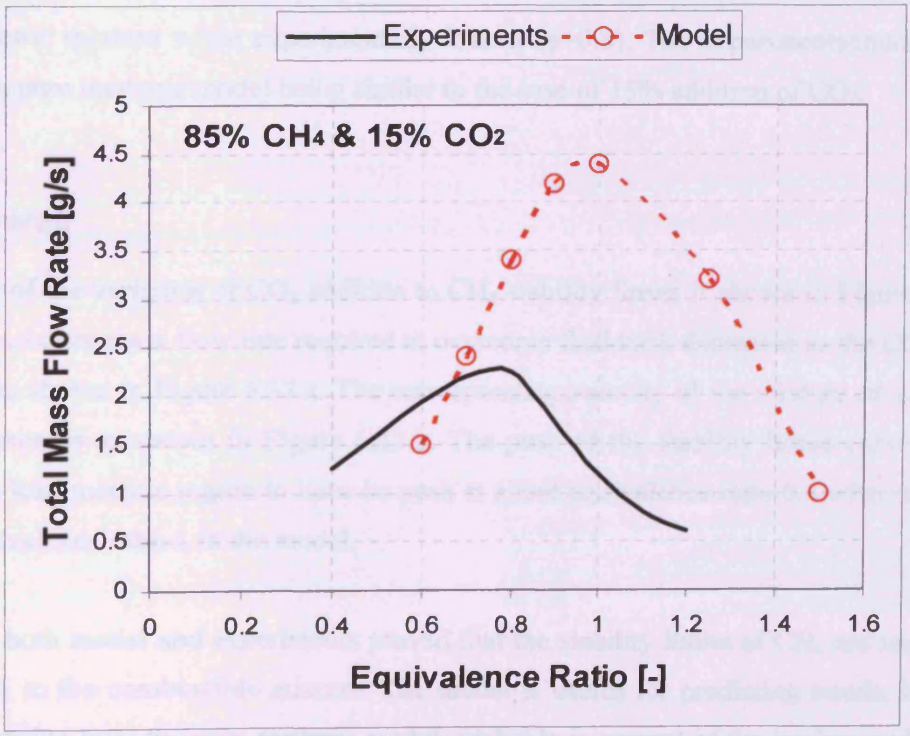

Figure 6.27: Comparison between the flame stability limits measured experimentally and determined by CFD simulation for (85% CH_4 + 15% CO_2).

6.5.2 The addition of 30% CO_2 to CH_4

Regarding 30% CO_2 addition, the same experimental technique used before to determine the stability limits for both pure methane and methane with 15% CO_2 addition is used to determine the stability limits for methane with 30% CO_2 addition.

Both stable and flashback flames are recognized during the experiments. A sample of the stable flame at various flow rates and equivalence ratios is shown in Figure 6.28, while the flashback flame is shown in Figure 6.29. The runs with various flow rates and equivalence ratio are plotted in the stability map, Figure 6.30 where the two regions of stable flame and flashback are defined. It is confirmed again that the flame at lower equivalence ratio (less than 0.8) is more stable. This is the same as in the case of 15% addition of CO_2. The worst stability emerges at (ϕ=0.8) where the mass flow rate of the mixture required to overcome flashback is at the maximum value. The flashback tendency is reduced for lean mixtures (ϕ>0.8) and for rich mixtures.

A comparison between the stability limits measured experimentally and determined by using the CFD simulation is shown in Figure 6.31. The model produce lower stability limits for the mixtures with equivalence ratio lower than 0.7 and higher values for the minimum flow rate of stable flame for the mixtures with equivalence ratio over 0.7 . The peak of the model is at the stoichiometric mixture while experimentally it is at (ϕ=0.8). The experiments/model match is worse than pure methane model being similar to the case of 15% addition of CO_2.

6.5.3 Overall

The effect of the variation of CO_2 addition to CH_4 stability limits is shown in Figure 6.32. The minimum mixture mass flow rate required to overcome flashback decreases as the CO_2 addition increases as shown in Figure 6.32.a. The corresponding velocity of the mixture of stable flame is also decreases as shown in Figure 6.32.b. The peak of the stability limits curve is shifted toward the lean mixture region to have its peak at about equivalence ratio 0.8 whereas the peak was at equivalence ratio 1 in the model.

Generally, both model and experiments proved that the stability limits of CH_4 are improved by adding CO_2 to the combustible mixture. The model is useful for predicting trends, but clearly needs improving over the pure methane model, probably in respect of the laminar and turbulent flame speed as discussed in the section on hydrogen addition.

$\dot{m}_t$ =5.03, ϕ =2.5

$\dot{m}_t$ =2.72, ϕ = 1.86

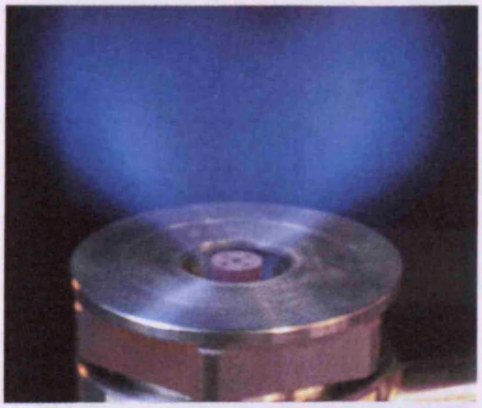

$\dot{m}_t$ =7.69, ϕ =1.8

$\dot{m}_t$ =6.72, ϕ =1.7

$\dot{m}_t$ =1.46, ϕ =0.9

$\dot{m}_t$ =1.589 , ϕ =0.88

Figure 6.28: The stable premixed (70% CH_4 + 30% CO_2) flames

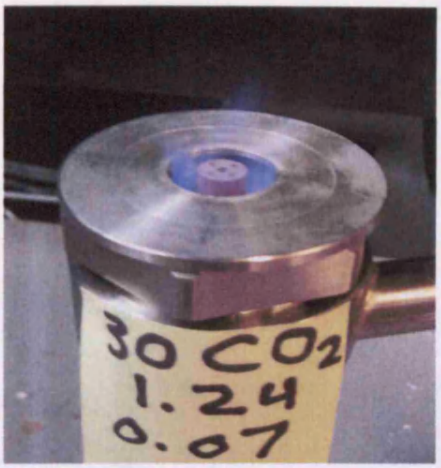

$\dot{m}_t$ =1.31 , ϕ =0.44

$\dot{m}_t$ =1.21 , ϕ =0.63

$\dot{m}_t$ =1.518 , ϕ = 0.66

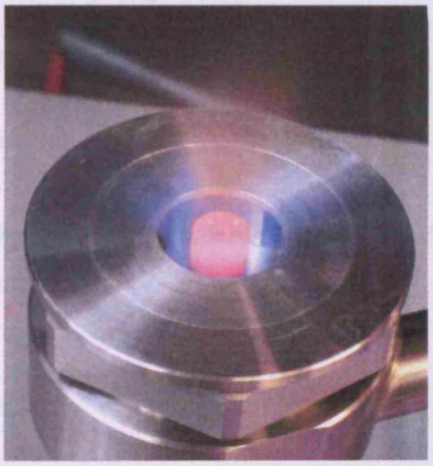

$\dot{m}_t$ =1.7 , ϕ =0.76

$\dot{m}_t$ =1.43 , ϕ =0.79

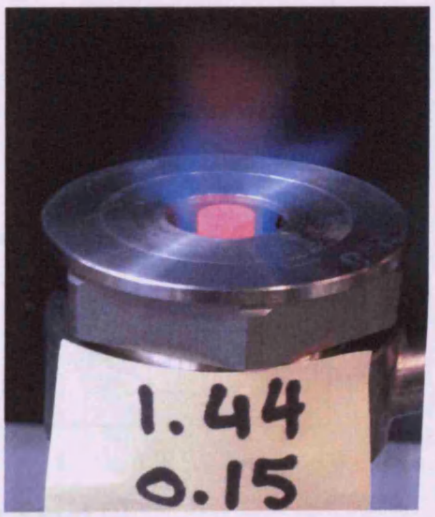

$\dot{m}_t$ =1.59 , ϕ = 0.82

Figure 6.29: The flame flashback for (70% CH_4 + 30% CO_2) flames

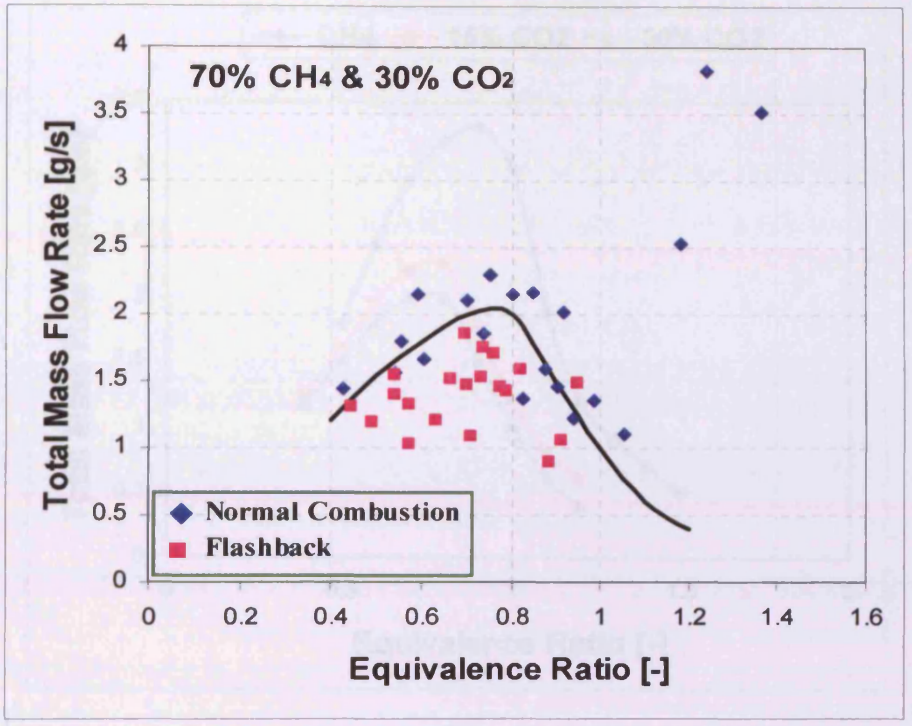

Figure 6.30: The Experimental measurements of the stability limits of (70% CH_4 + 30% CO_2) at atmospheric conditions.

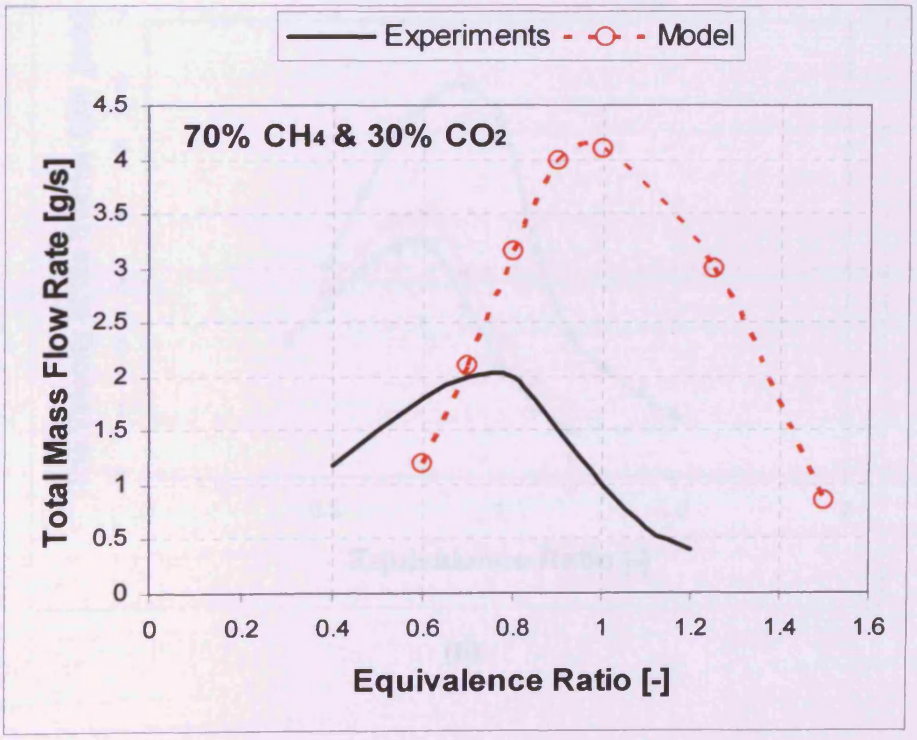

Figure 6.31: Comparison between the flame stability limits measured experimentally and determined by CFD simulation for (70% CH_4 + 30% CO_2).

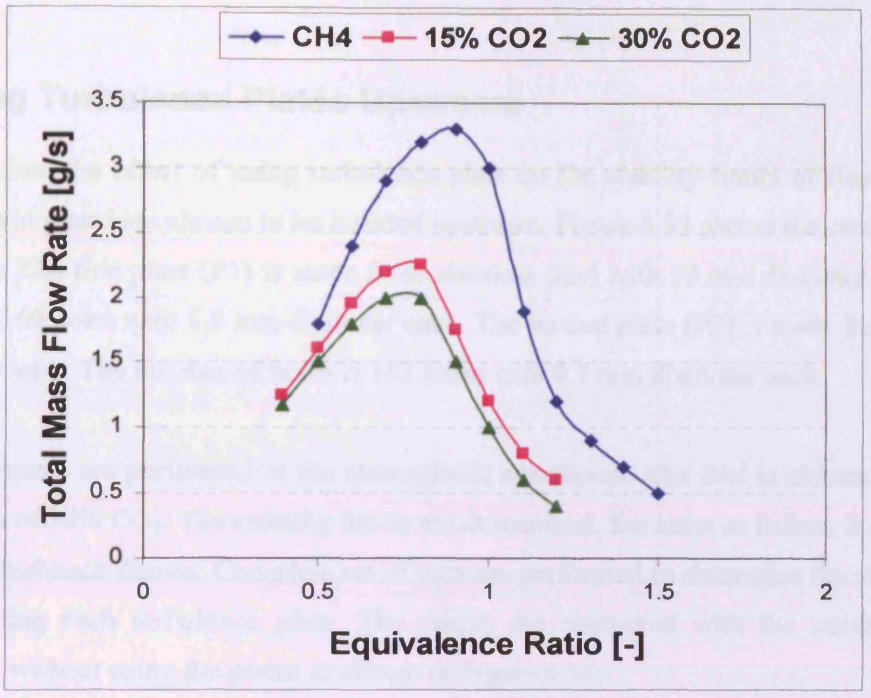

(a)

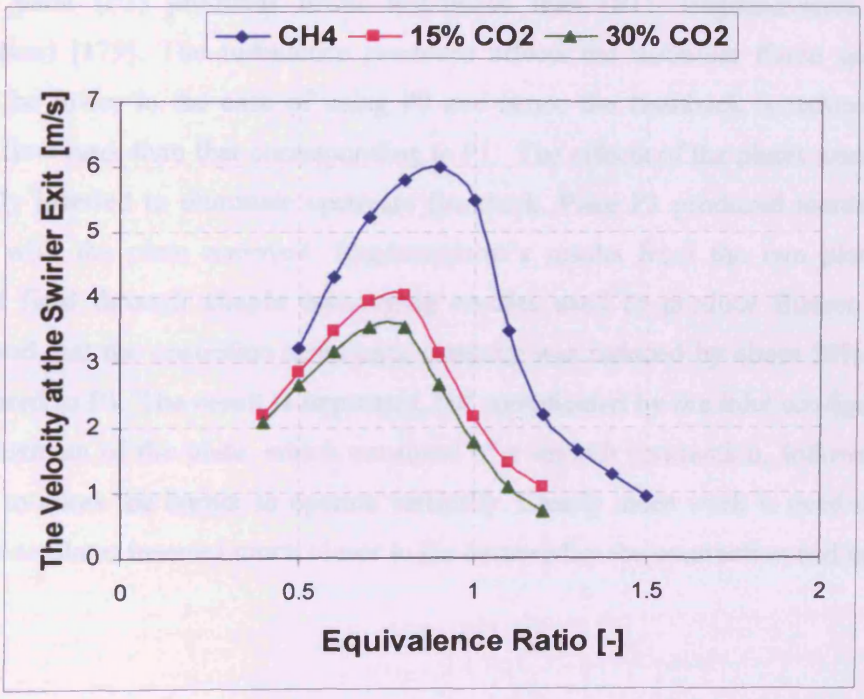

(b)

Figure 6.32: The effect of CO_2 addition to CH_4 stability limits based on the experimental results. (a) The corresponding mass flow rates. (b) The corresponding velocity at the burner exit.

6.6 Using Turbulence Plates Upstream

In this section, the effect of using turbulence plate on the stability limits of flame is studied. Two different plates are chosen to be inserted upstream. Figure 6.33 shows the configuration for both plates. The first plate (P1) is made from stainless steel with 50 mm diameter. The number of holes is 169 holes with 1.5 mm diameter each. The second plate (P2) is made from brass with 50 mm diameter. The number of holes is 163 holes with 0.7 mm diameter each.

The experiments are performed at the atmospheric conditions. The fuel is chosen as CH_4 with the addition of 30% CO_2. The stability limits are determined, the same as before, by defining the stable and flashback flames. Complete set of runs are performed to determine the stability limits when inserting each turbulence plate. The results are compared with the stability limits of combustion without using the plates as shown in Figure 6.34.

It is noticed that the stability limits can be improved by inserting the turbulence plate upstream. Turbulence plate (P2) produces lower turbulence than (P1), Bagdanavicius, A. (private communication) [179]. The turbulence produced affects the turbulent flame speed which is expected to be lower in the case of using P2 and hence the flashback is reduced, starting at lower mass flow rates than that corresponding to P1. The effects of the plates were unexpected, and primarily inserted to eliminate upstream flashback. Plate P1 produced identical results to the system with the plate removed. Bagdanavicius's results from the two plates when the resulting jet fired through simple converging nozzles used to produce Bunsen burner type flames showed that the centreline turbulence intensity was reduced by about 50% for plate P2 when compared to P1. The result is important, but complicated by the inlet configuration to the burner downstream of the plate, which consisted of a smooth contraction, followed by a wide radius bend to allow the burner to operate vertically. Clearly more work is needed in this area with turbulence plates inserted much closer to the burner after the contraction and bend.

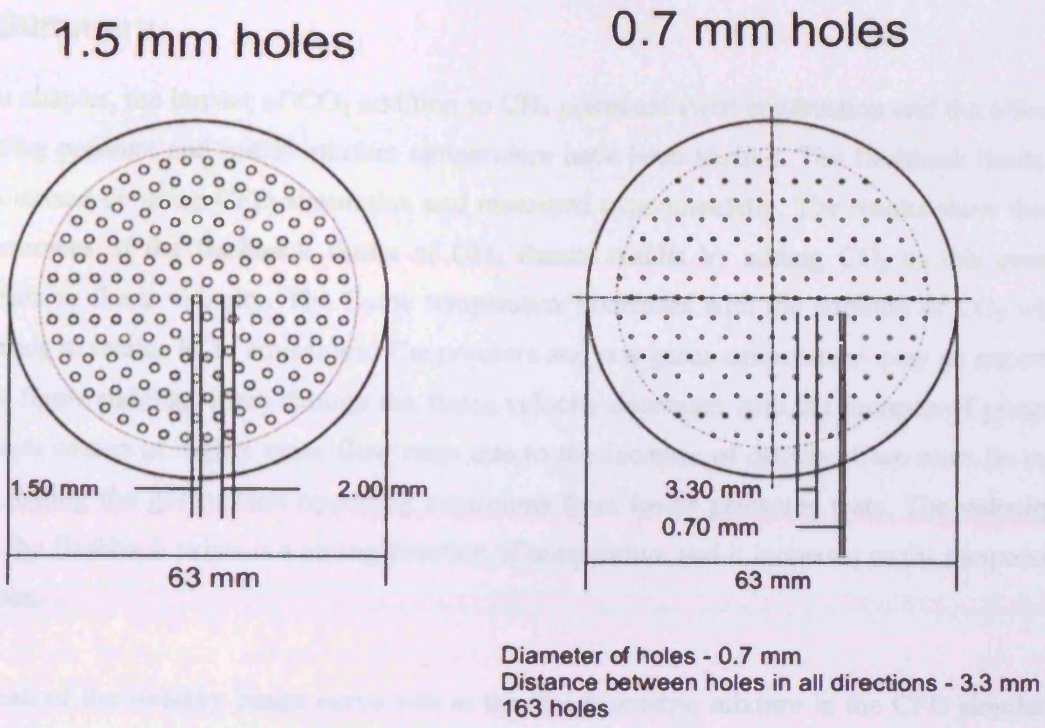

Figure 6.33: Turbulence plates configuration

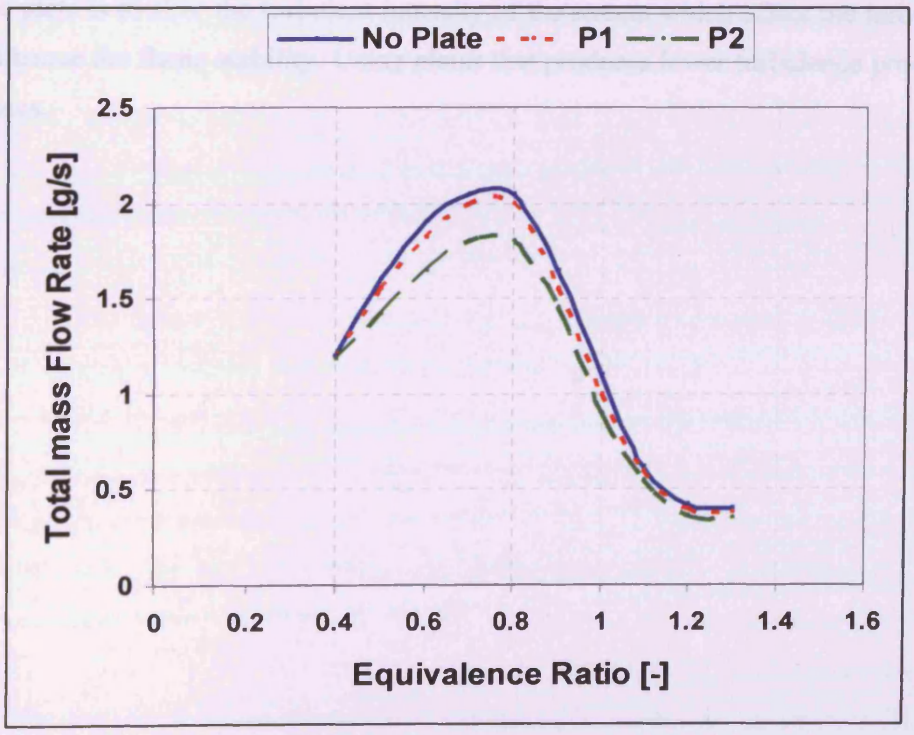

Figure 6.34: The effect of turbulence plates on the stability limits

6.6 Summary

In this chapter, the impact of CO_2 addition to CH_4 premixed swirl combustion and the effect of operating pressure and initial mixture temperature have been studied. The flashback limits are characterised by using CFD simulation and measured experimentally. The results show that an improvement of the flashback limits of CH_4 flames results by adding CO_2 as this cause a reduction in flame velocity. The flame temperature decreases with the addition of CO_2 which also tends to reduce NOx emissions. The pressure and raw gases temperature play an important role in flame stability. Even though the flame velocity decreases with the increase of pressure, flashback occurs at higher mass flow rates due to the increase of density. Care must be taken when scaling the gas turbine operating conditions from lower pressures tests. The velocity at which the flashback exists is a strong function of temperature and it increases as the temperature increases.

The peak of the stability limits curve was at the stoichiometric mixture in the CFD simulation while it was found at equivalence ratio of 0.8 experimentally. Although the CFD model shows similar trends to the experimental result clearly improvements in the turbulent combustion model are needed especially with operation removed from the lean combustion regime.

Inserting a turbulence plate upstream affects the stability limits of flames. The effect of the turbulence plate is to alter the turbulent intensity of the stream which affect the turbulent flame speed and hence the flame stability. Using plates that produces lower turbulence produces more stable flames.

Chapter 7

EFFECT OF CH_4 ADDITION TO H_2 FLAME

7.1 Introduction

Combustor reliability to hold the flame in a quiet, safe mode has always concerned the manufacturers. Industrial companies and research groups are focusing their efforts in the analysis of new fuels including biofuel blends or those with high hydrogen contents in order to reduce the emission of CO_2. Whilst the aviation sector is focusing its efforts on biofuels whose heat value content are similar to kerosene, stationary turbines are being investigated with high hydrogen fuel mixes in efforts to develop technologies for syngas fuels. Unfortunately, the study of the latter has proved to be difficult, with forced flashback tests under industrial conditions causing burner damage at high air velocities in tests.

Flashback is an important issue in lean premixed combustion systems that use hydrogen as an additive fuel due to the widely varying flame speeds of the mixtures considered. The importance of using hydrogen as part of the energetic variety of sources has increased due to expectations that oil supplies will become constrained and increase dramatically in price, with the inevitable increment of population and the higher concern about CO_2 footprint around the globe.

In this chapter, two main topics are considered; the first is the determination of laminar flame speed for H_2/CH_4 blends and the second is the determination of stability limits of such blends using CFD simulation and validating the simulation at atmospheric conditions.

The laminar flame speed was calculated for H_2/CH_4 blends from pure methane up to pure hydrogen at various pressures, temperatures and equivalence ratios. This was done by using CHEMKIN-PRO software package with PREMIX code and an algebraic expression derived by asymptotic methods incorporated with Le Chatelier's Rule-like correlation. The feasibility of using a new approximation for laminar flame speed of H_2/CH_4 blends based on the gravimetric mixture ratio was checked and compared with the previous calculations. The new approximation gave a good prediction at various conditions. The numerical values for laminar flame speed calculated by CHEMKIN are then fed to a FLUENT CFD model to create a PDF table for turbulent premixed combustion calculations and flashback studies. Flashback limits were defined and determined for H_2/CH_4 blends ranging from 0% (pure methane) up to 100% (pure hydrogen) based on the volumetric composition at atmospheric pressure and 300K for

various equivalence ratios. The results show that the use of up to 50% blends – by volume – of methane and hydrogen causes fewer problems with flame stability and flashback compared with the use of pure hydrogen. Also, the flashback limits depend on the values for both laminar and turbulent flame speed. What emerges is the need for more theoretical and experimental research work to obtain more accurate values for flame speeds.

The stability limits of methane-dominated combustion (up to 50% blends of methane and hydrogen) has been extensively studied at different pressures and temperatures to show the effect of the combustion conditions on H_2/CH_4 blends flame stability [180, 181].

Experimental measurements of the stability limits for H_2/CH_4 blends up to γ=0.30 are performed. The measurements are carried out at the atmospheric conditions. Both stable flames and flashback are reported to determine the stability limits. The experimental measurements are compared with the simulation results.

7.2 Laminar Flame Speed

The laminar burning velocities of hydrogen, methane and H_2-CH_4 /air mixtures at different pressures and temperatures were calculated by varying the equivalence ratio from lean to rich conditions and the fuel composition from pure methane (γ=0) to pure hydrogen (γ=1).

7.2.1 Laminar Flame Speed of H_2 and CH_4

The laminar flame speed of H_2 is calculated at elevated temperatures and pressures using the O'Conaire, GRI-Mech and San Diego kinetic mechanisms. The results of the calculations are presented in Figure 7.1. Three mechanisms: O'Conaire et al. mechanism, San Diego mechanism and GRI-Mech, have been compared at 7 bara 473 K and 673 K. The O'Conaire et al. mechanism has been developed to simulate the combustion of hydrogen and oxygen in a variety of combustion environments and over a wide range of temperatures, pressures and equivalence ratios.

The GRI-Mech mechanism under predicts hydrogen flame speed in the region of equivalence ratio up to 1 and above 1.5 in comparison with O'Conaire mechanism. The San Diego mechanism predictions are more accurate in comparison with GRI-Mech. The O'Conaire mechanism predicts the highest flame speed.

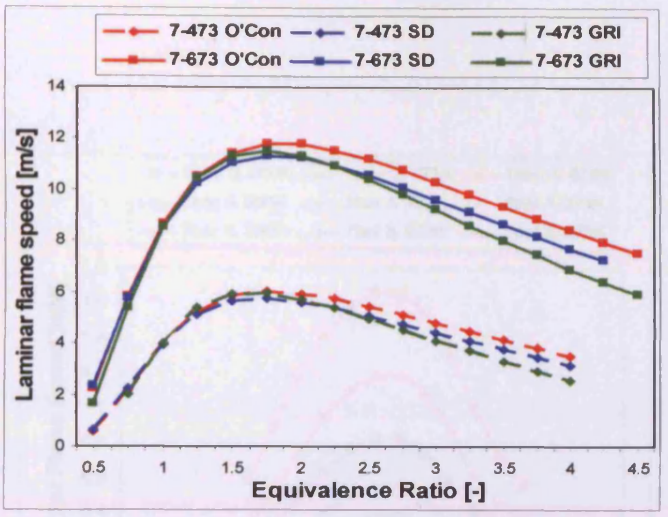

Figure 7.1: CHEMKIN calculated laminar flame speed of hydrogen at 7 bar; 473 K and 673 K; O'Con – O'Conaire mechanism, SD – San Diego mechanism, GRI – GRI-Mech mechanism.

For pure methane and pure hydrogen, the laminar flame speed was calculated by CHEMKIN at 1.01325, 3 and 7 bar each at 300, 473 and 673 K. The GRI-Mech mechanism was used for CH_4 laminar flame speed calculations while O'Conaire et al. mechanism is used for H_2. The results are shown in Figure 7.2.a for methane and Figure 7.2.b. for hydrogen. It is recognized that the laminar flame speed increases as the temperature increases but decreases with pressure. This is applicable for both CH_4 and H_2 up to the stoichiometric mixture ratio (ϕ=1) but for H_2 rich mixture, the pressure proportionality is not applicable.

A comparison between the laminar flame speed values arising from Chemkin and Fluent analysis is performed at the same pressure and temperature range stated above for both CH_4 and H_2. The results are shown in Figure 7.3 and 7.4. It was found that the values appear to be within about ± 10 % deviation for lean mixtures up to the stoichiometric mixture ratio. For rich mixtures Fluent produces higher predicted values compared to Chemkin. Chemkin results are taken to be more accurate so it is used for establishing a PDF table for turbulent combustion and flashback analysis in the next section.

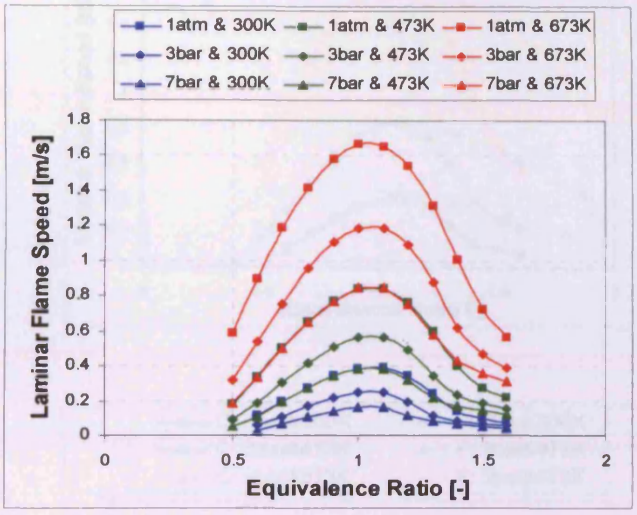

(a)

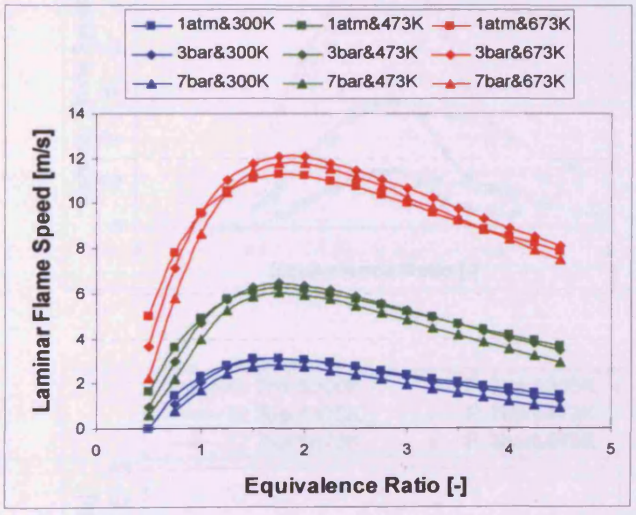

(b)

Figure 7.2: Laminar flame speed calculated by CHEMKIN for (a) CH_4, (b) H_2 at different pressures and temperatures.

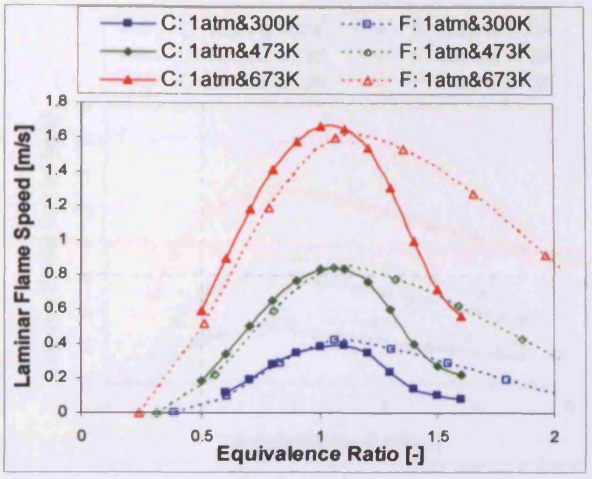

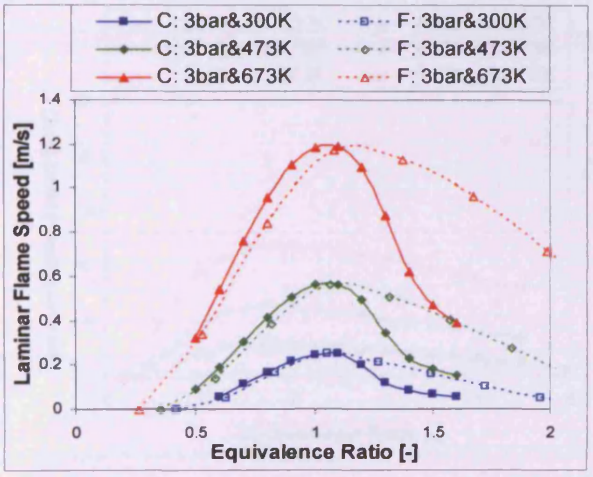

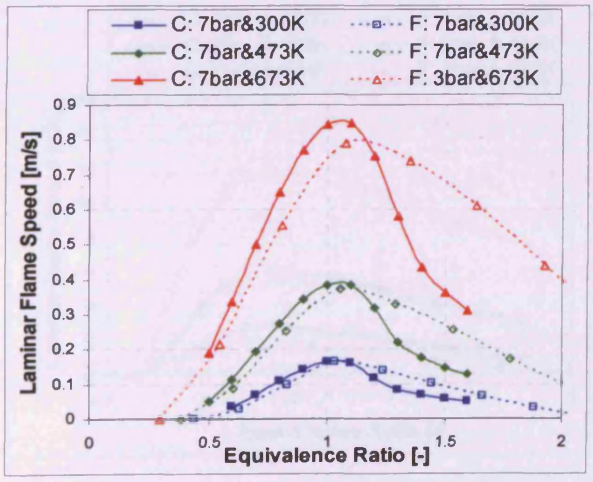

Figure 7.3: Comparison between laminar flame speed values calculated by CHEMKIN and FLUENT at various pressures and temperatures for CH_4.

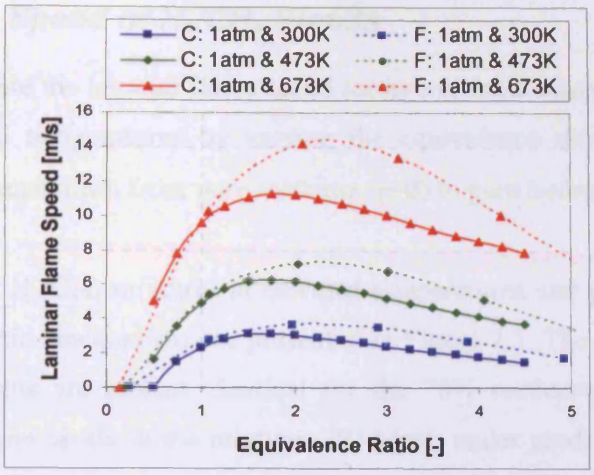

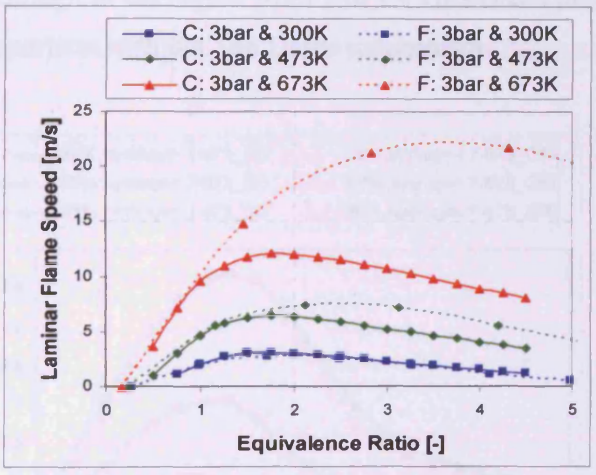

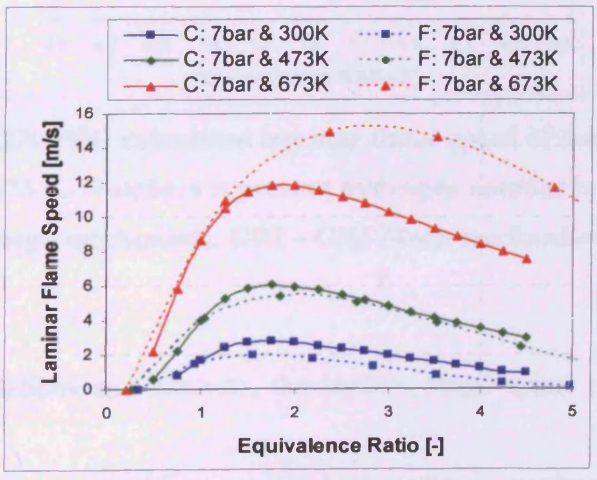

Figure 7.4: Comparison between laminar flame speed values calculated by CHEMKIN and FLUENT at various pressures and temperatures for H_2.

7.2.2 Laminar Flame Speed of H_2/CH_4 Blends

Chemkin is used to calculate the laminar flame speed for hybrid fuels containing H_2/CH_4 blends at different pressures and temperatures by varying the equivalence ratio from lean to rich conditions and the fuel composition from pure methane (γ=0) to pure hydrogen (γ=1).

The calculation results of H_2/CH_4 mixtures at elevated temperatures and pressures using GRI-Mech and San Diego kinetic mechanisms are presented in Figure 7.5. The results of GRI-Mech and San Diego mechanisms are almost identical for the 70% methane and 30% hydrogen mixture. At higher hydrogen levels in the mixture GRI-Mech under predicts flame speed. The discrepancies between these two models can be observed in the region of equivalence ratio below 1 and above 1.4, although in the region from 1 to 1.4 GRI-Mech produces slightly higher flame speed results in comparison with the San Diego mechanism.

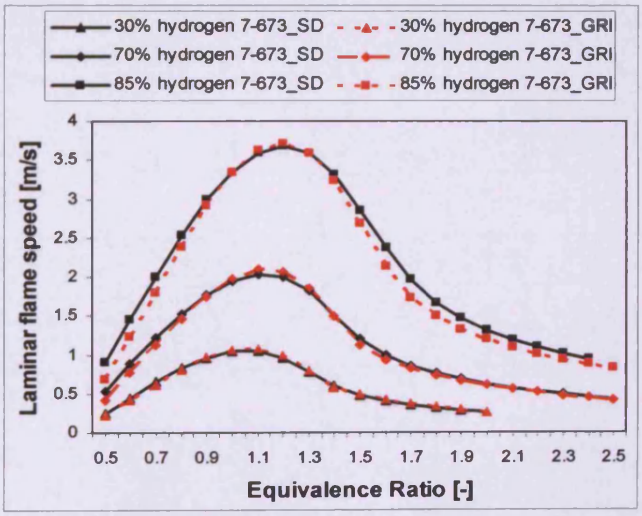

Figure 7.5: CHEMKIN-PRO calculated laminar flame speed of methane hydrogen mixtures at 7 bar and 673 K. Numbers represent hydrogen amount in the mixture; SD – San Diego mechanism, GRI – GRI-Mech mechanism.

From the previous calculations and analysis, the laminar flame speed of H_2/CH_4 Blends is calculated as follows:

- GRI-Mech mechanism is used for pure CH_4 laminar flame speed calculations.
- GRI-Mech mechanism is used for H_2/CH_4 Blends ($\gamma \leq 0.5$)
- The San Diego mechanism is used for H_2/CH_4 Blends ($0.5 < \gamma < 1$)
- The O'Conaire et al. mechanism is used for pure H_2.

The calculations are performed at different pressures and temperatures. The chosen pressures are 1.01325, 3 and 7 bar and the chosen temperatures are 300, 473 and 673 K. The final results are shown in Figure 7.6. From this figure, the following can be noted:

- The laminar flame speed (S_L) is highly dependent on equivalence ratio.
- The peak of S_L is around the stoichiometric ratio (between $1<\phi<1.1$) for H_2/CH_4 blends ($0 < \gamma < 0.5$). This peak is significantly shifted for blends with ($0.5 < \gamma$) to between $1.7<\phi<1.8$ for pure H_2.
- S_L increases as the temperature increases.
- S_L decreases as the pressure increases.
- S_L for H_2 is significantly larger than for conventional hydrocarbon fuels (CH_4 in this figure).
- S_L for H_2/CH_4 blends ($0 < \gamma < 0.5$) is only slightly changed while for ($0.5 < \gamma < 1$) the change is relatively larger. For example: S_L for stoichiometric CH_4 at 1 atm and 300 K is about 0.4 m/s and for a bend with $\gamma = 0.5$, S_L equals 0.6 m/s (the change is about 50%). For pure H_2 ($\gamma = 1$), S_L equals 2.3 m/s, about 6 times that of CH_4.

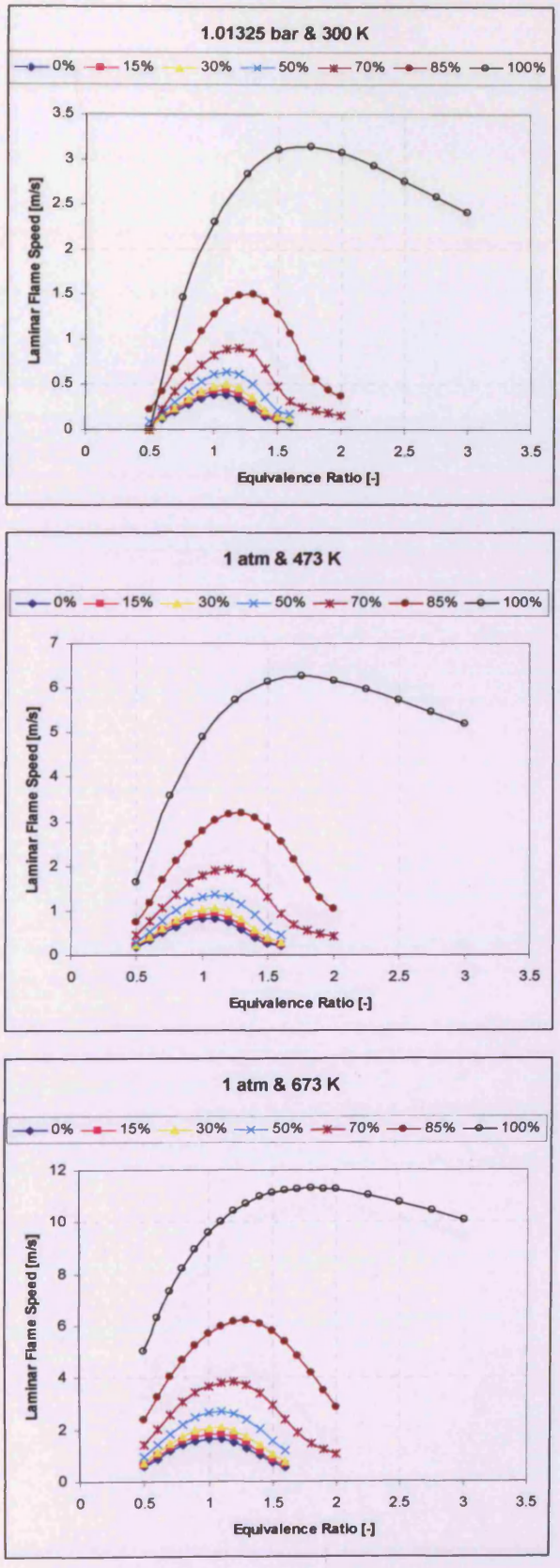

Figure 7.6: The laminar flame speed of H_2/CH_4 mixtures at different pressures and temperatures.

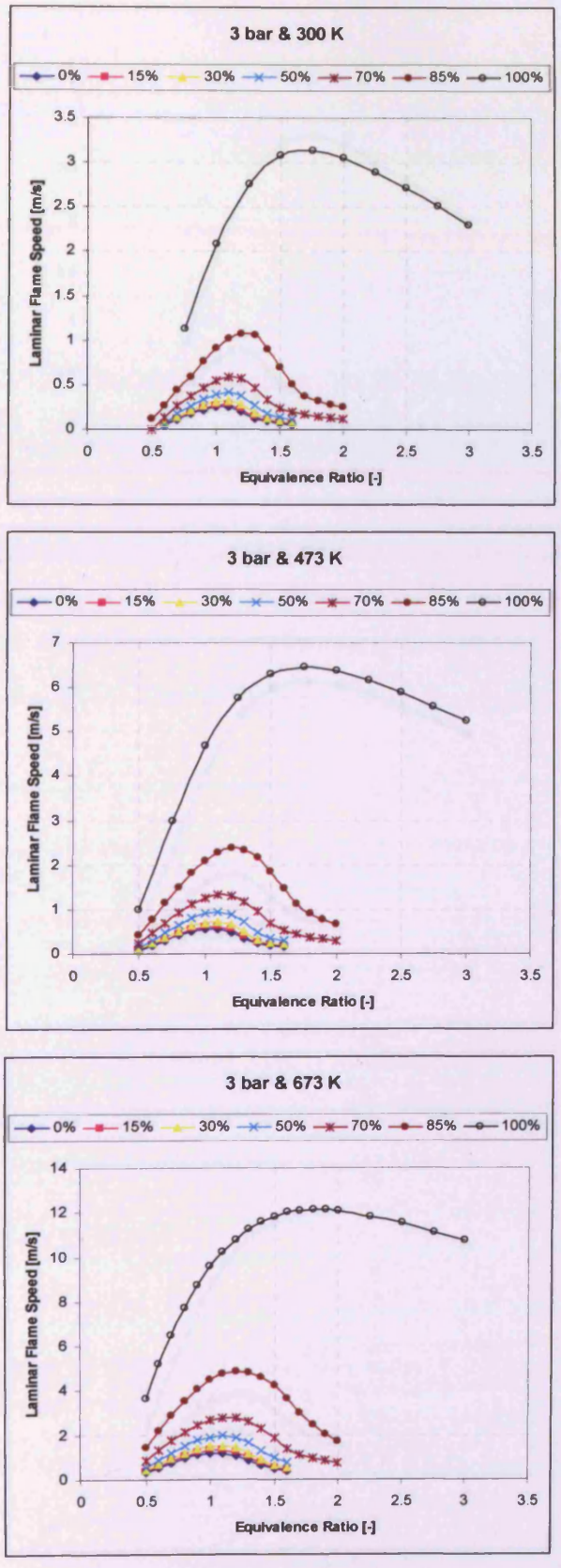

Figure 7.6: Cont.

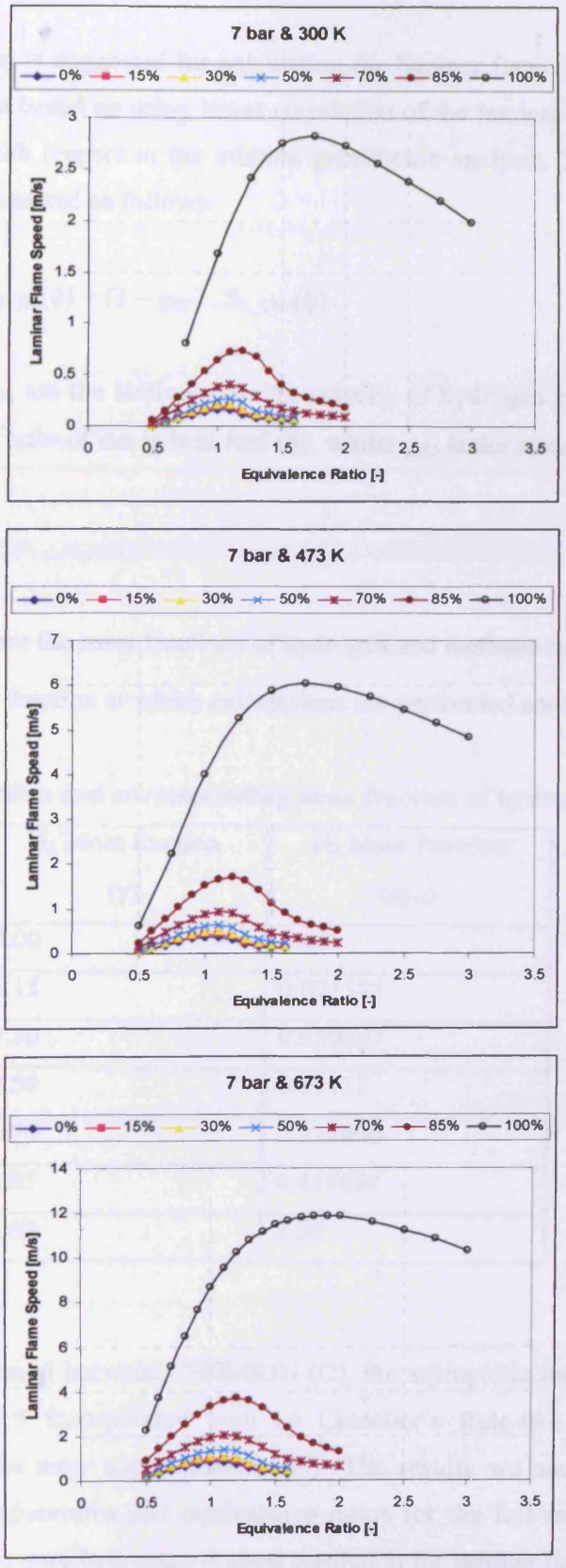

Figure 7.6: Cont.

A new approximation is suggested for calculating the laminar flame speed of H_2/CH_4 blends. This approximation is based on using linear correlation of the laminar burning velocities of the pure compositions with respect to the mixture gravimetric analysis. The blend laminar flame speed then can be calculated as follows:

$$S_{L\_linear}(\phi, g) = g_{H2} \cdot S_{L\_H2}(\phi) + (1 - g_{H2}) \cdot S_{L\_CH4}(\phi) \qquad 7.2.1$$

where S_{L_H2} and S_{L_CH4} are the laminar burning velocity of hydrogen and methane evaluated at the same equivalence ratio of the hybrid fuel (ϕ), whilst g_{H2} is the mass fraction of hydrogen in H_2/CH_4 mixture.

$$g_{H2} = \frac{m_{H_2}}{m_{H_2} + m_{CH_4}} \qquad 7.2.2$$

where m_{H_2} and m_{CH_4} are the mass fractions of hydrogen and methane respectively.

The values of H_2 mass fraction at which calculations are performed are tabulated in Table 7.1.

Table 7.1: Mole fraction and corresponding mass fraction of hydrogen in H_2/CH_4 blends

H_2 Mole fraction (γ)	H_2 Mass Fraction (g_{H2})
0.00	0.00
0.15	0.021583
0.30	0.050847
0.50	0.11111
0.70	0.225806
0.85	0.414634
1.00	1.00

A comparison is performed between CHEMKIN (C), the asymptotic method (A) described by equations 3.9.1 to 3.9.5 incorporated with Le Chatelier's Rule-like correlation stated by equation 3.9.12, and the new approximation (N). The results are shown in Figure 7.7 for different pressures, temperatures and equivalence ratios for the full range of H_2/CH_4 blends from pure methane up to pure hydrogen. A good prediction for laminar flame speed by using the new approximation is demonstrated especially at 1 atm and for methane-dominated combustion region i.e. up to γ equals 0.5. The results of the new approximation are still acceptable at high pressure as the deviation is limited to about 15% of the Chemkin values.

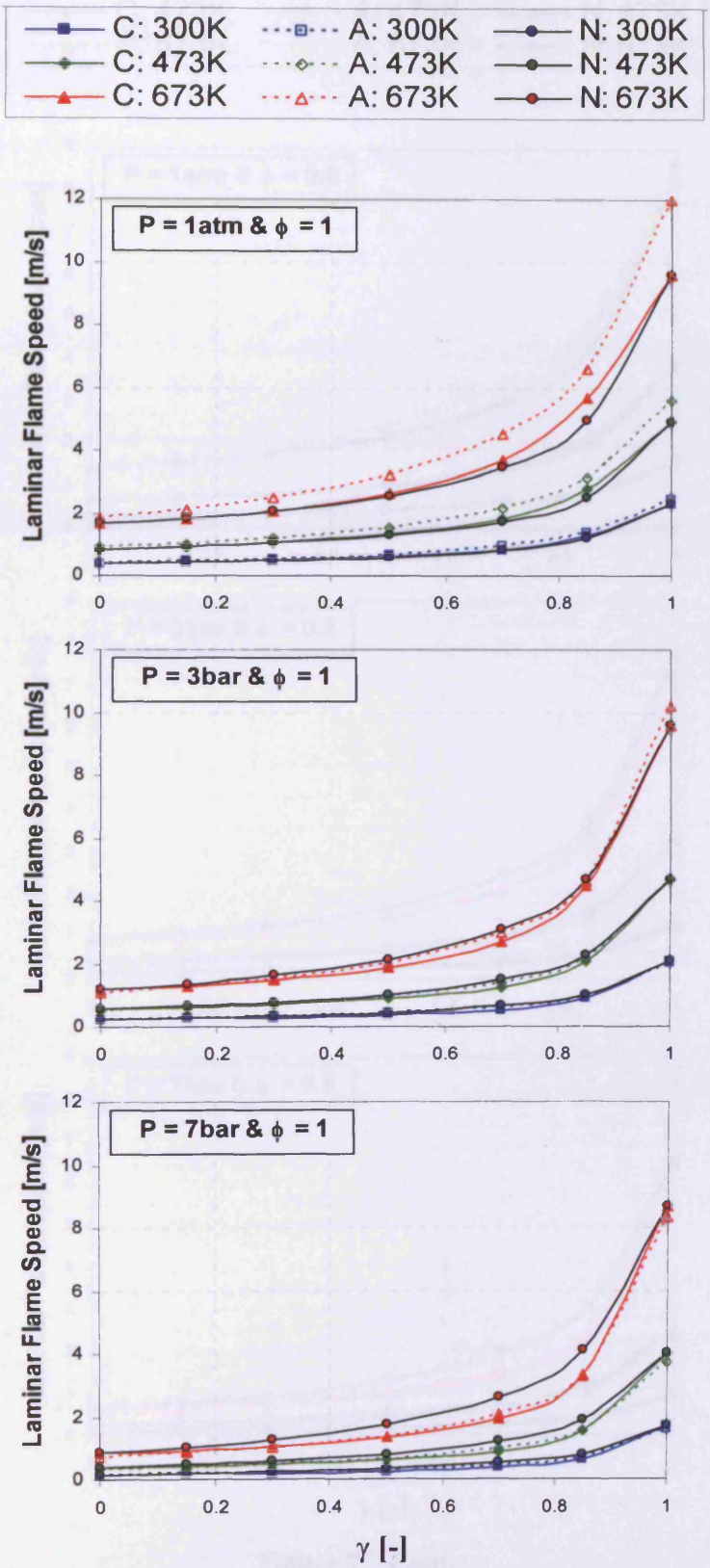

Figure 7.7: Comparison between three methods for calculating the laminar flame speed for H_2/CH_4 hybrid fuel at different pressures, Equivalence ratios, and temperature.

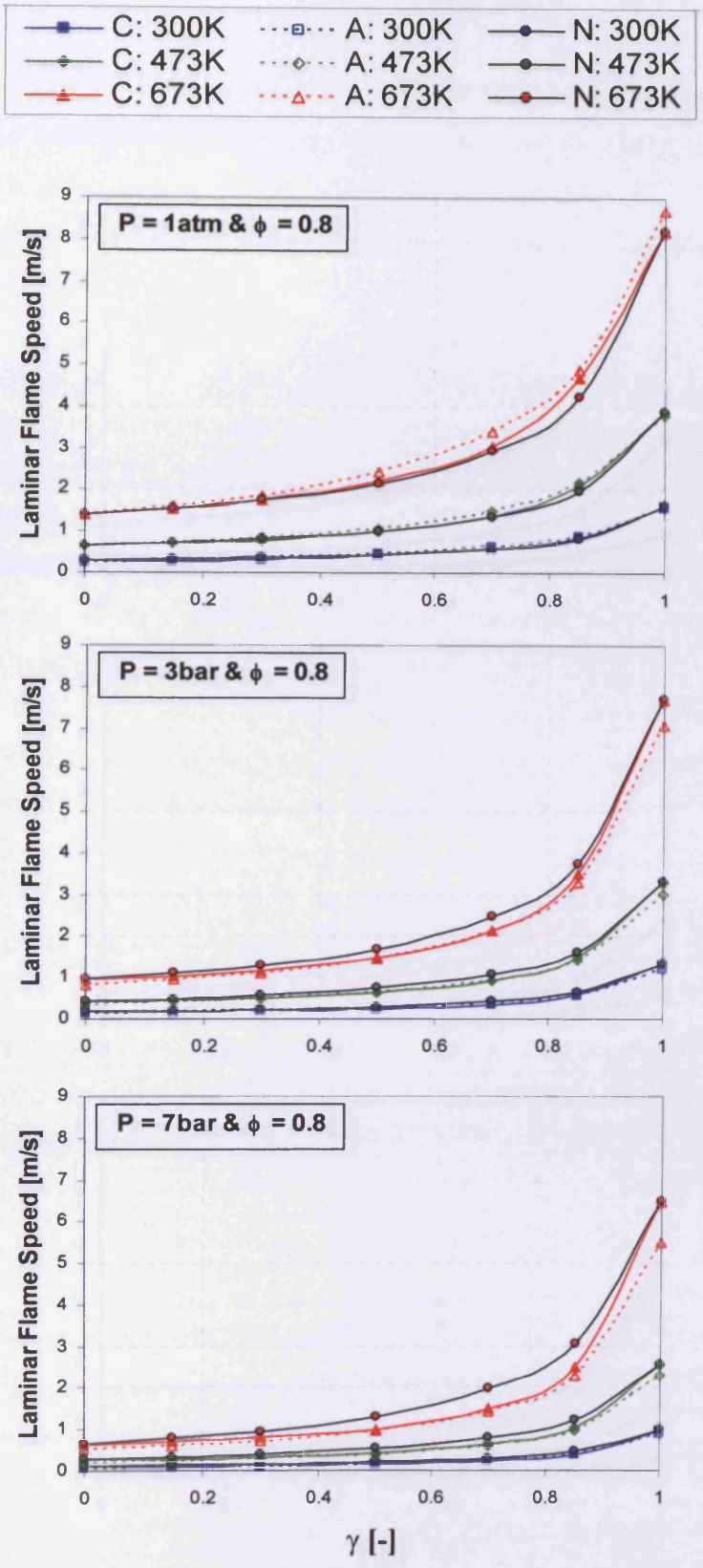

Figure 7.7 Cont.

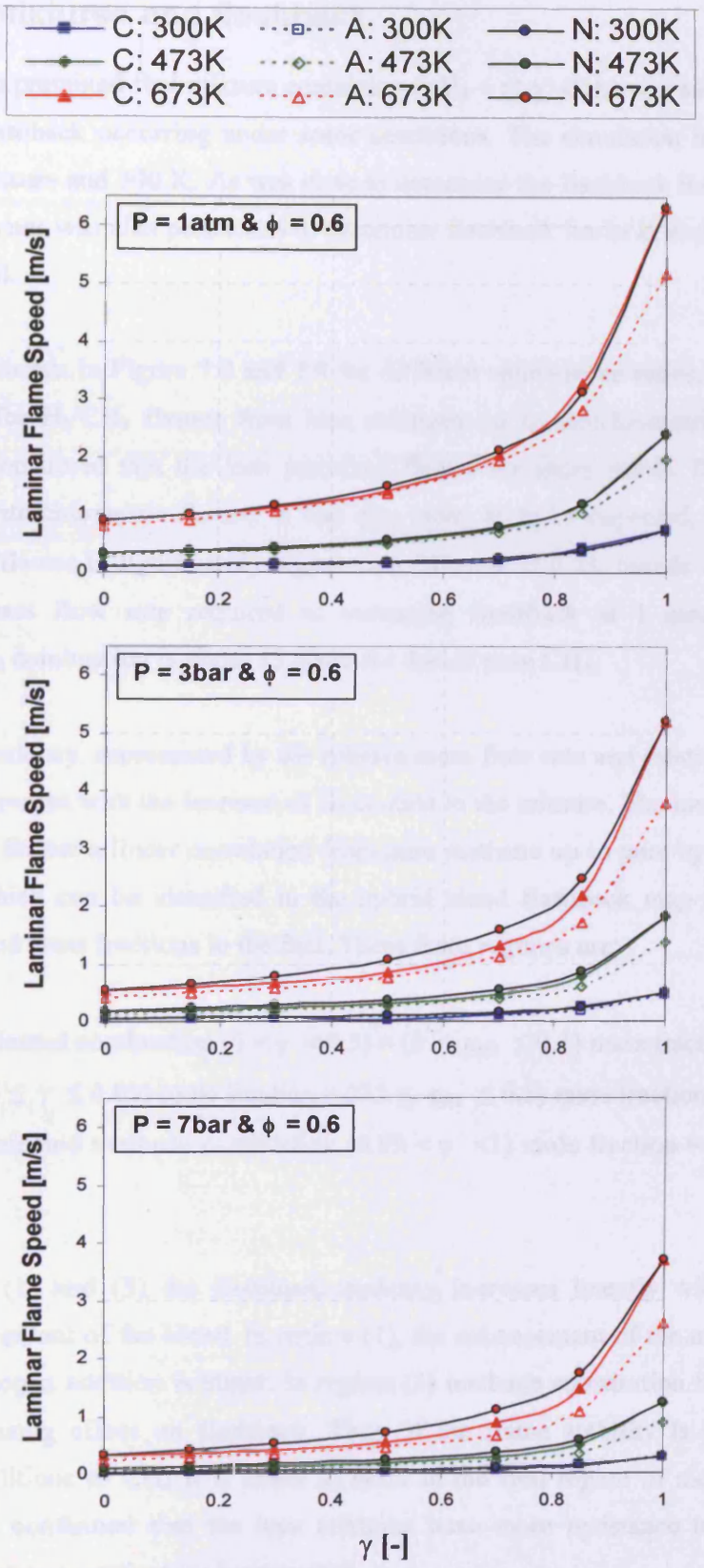

Figure 7.7 Cont.

7.3 H_2/CH_4 mixtures and flashback

Combustion of a premixed fuel mixture containing (γ H_2 + (1-γ) CH_4) was simulated from $\gamma = 0$ up to 1 with flashback occurring under some conditions. The simulation is performed under atmospheric pressure and 300 K. As was done to determine the flashback limits for methane, a complete set of runs was also performed to determine flashback limits at each H_2 mole fraction in the hybrid fuel.

The results are shown in Figure 7.8 and 7.9 for different equivalence ratios. In Figure 7.8, the stability limits for H_2/CH_4 flames from lean mixtures up to stoichiometric combustion are shown. It was confirmed that the lean premixed flames are more stable, from the flashback viewpoint, than stoichiometric flames. It was also clear, as to be expected, that the flashback tendency for H_2 flames is significantly higher than CH_4 and H_2/CH_4 blends up to $\gamma = 0.5$. For example, the mass flow rate required to overcome flashback at 1 atm and 300 K for stoichiometric H_2 combustion is about 15 times for that of pure CH_4.

The flashback tendency, represented by the relative mass flow rate and relative velocity shown in Figure 7.9, increases with the increase of H_2 content in the mixture. The increase in flashback tendency doesn't follow a linear correlation from pure methane up to pure hydrogen. There are three regimes which can be identified in the hybrid blend flashback map depending on the hydrogen mole and mass fractions in the fuel. These three regimes are:

(1) methane-dominated combustion ($0 < \gamma < 0.5$) $\equiv$ ($0 < g_{H2} \leq 0.1$) mass fraction;
(2) transition ($0.5 \leq \gamma \leq 0.89$) mole fraction $\equiv$ ($0.1 \leq g_{H2} \leq 0.5$) mass fraction; and
(3) hydrogen dominated methane combustion ($0.89 < \gamma < 1$) mole fraction $\equiv$ ($0.5 \leq g_{H2} < 1$) mass fraction.

In both regimes (1) and (3) the flashback tendency increases linearly with increasing the hydrogen molar content of the blend. In regime (1), the enhancement of the methane flashback tendency by hydrogen addition is slight. In regime (3) methane substitution to hydrogen has a significant decreasing effect on flashback. Thus, if the flame stability is considered when discussing H_2 additions to CH_4 it is better to work in the first region of methane-dominated combustion. It is confirmed that the lean mixtures have more resistance to flashback than stoichiometric mixtures, again as to be expected.

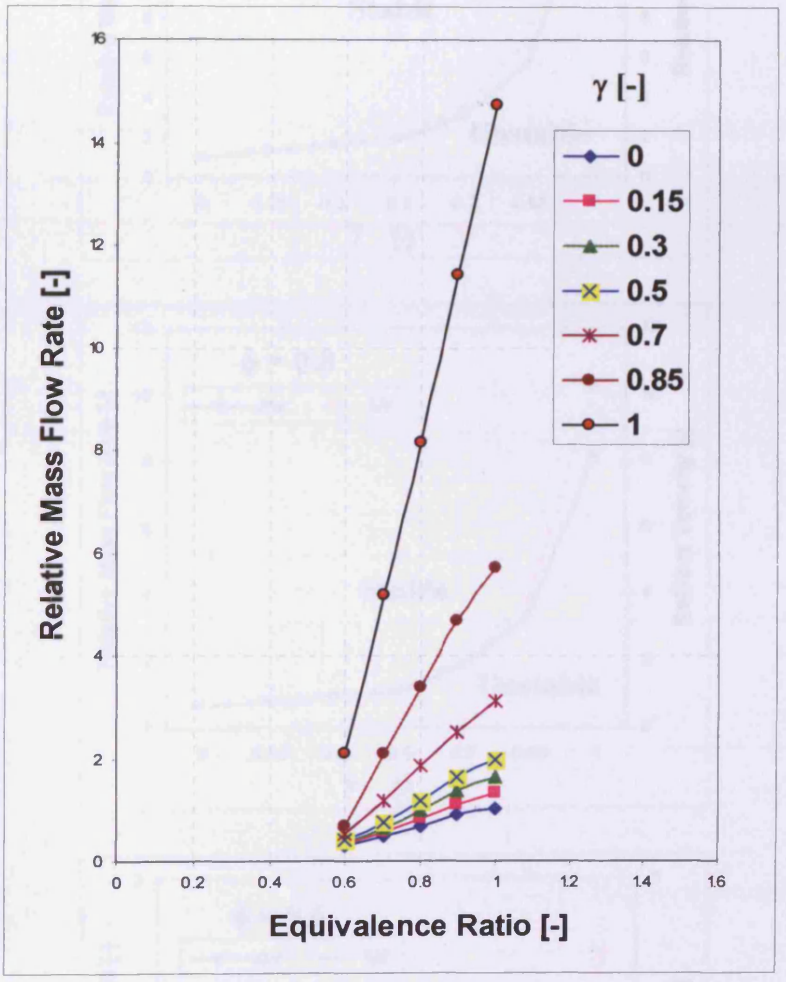

Figure 7.8: The stability limits for H_2/CH_4 flames from lean mixtures up to stoichiometric combustion.

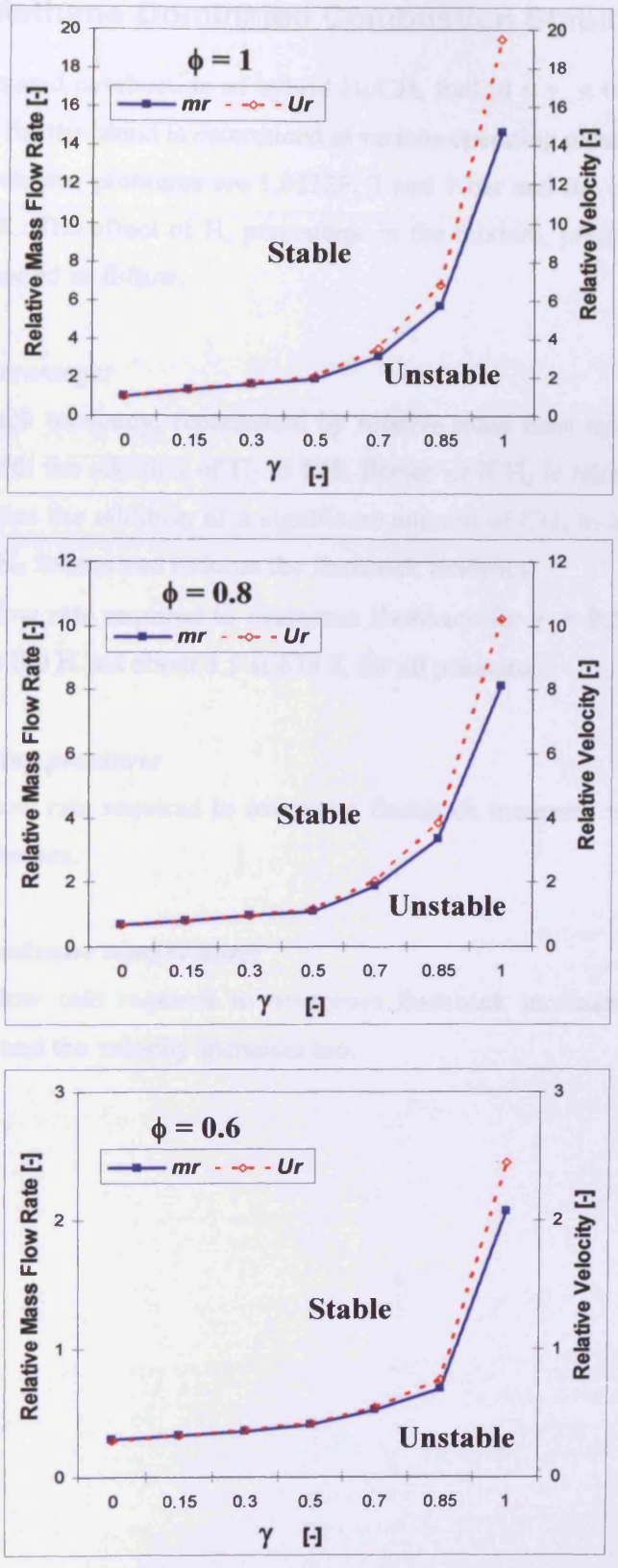

Figure 7.9: Flashback tendency map for H_2/CH_4 combustion represented by relative mass flow rate and relative velocity for full range of hybrid fuel.

7.4 H_2/CH_4 – Methane Dominated Combustion Stability Limits

The methane-dominated combustion of hybrid H_2/CH_4 fuel ($0 < \gamma < 0.5$) is thus studied here. The stability limits for the blend is determined at various operating pressures and initial mixture temperatures. The chosen pressures are 1.01325, 3 and 7 bar and the chosen temperatures are 300, 473 and 673 K. The effect of H_2 percentage in the mixture, pressure, and initial mixture temperature is discussed as follow:

The effect of H_2 percentage:

- The flashback tendency, represented by relative mass flow rate and relative velocity, increases with the addition of H_2 to CH_4 flames or if H_2 is taken as the base, it can be concluded that the addition of a significant amount of CH_4 to H_2 flames improves the stability of H_2 flames and reduces the flashback tendency.
- The mass flow rate required to overcome flashback for $\gamma = 0.5$ is about twice that of pure CH_4 at 300 K but about 1.5 at 673 K for all pressures.

The effect of operating pressure:

- The mass flow rate required to overcome flashback increases with pressure while the velocity decreases.

The effect of initial mixture temperature:

- The mass flow rate required to overcome flashback increases with initial mixture temperature and the velocity increases too.

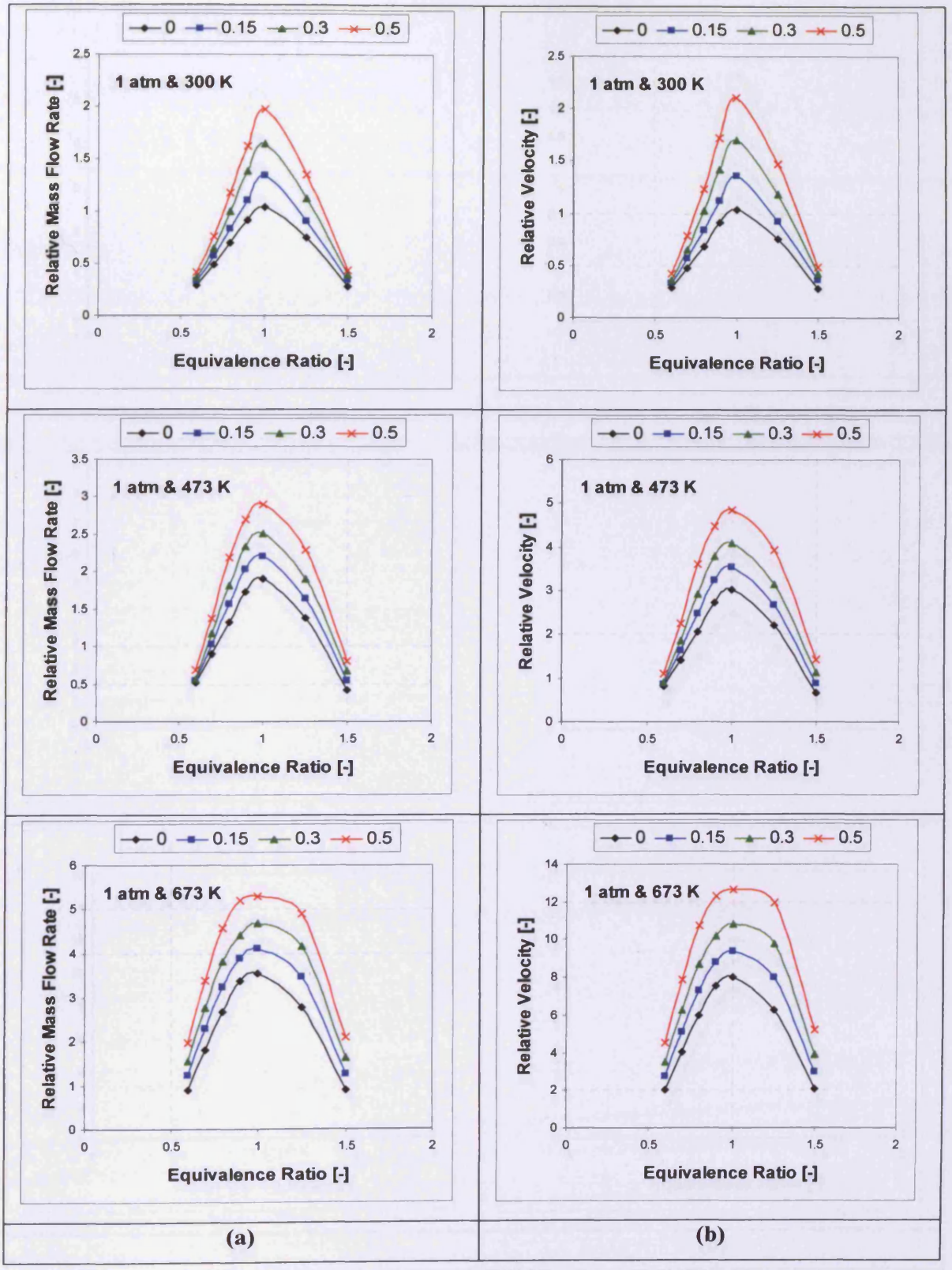

Figure 7.10: The stability limits of H_2/CH_4 combustion (up to $\gamma = 0.5$) at atmospheric pressure at different initial temperatures.

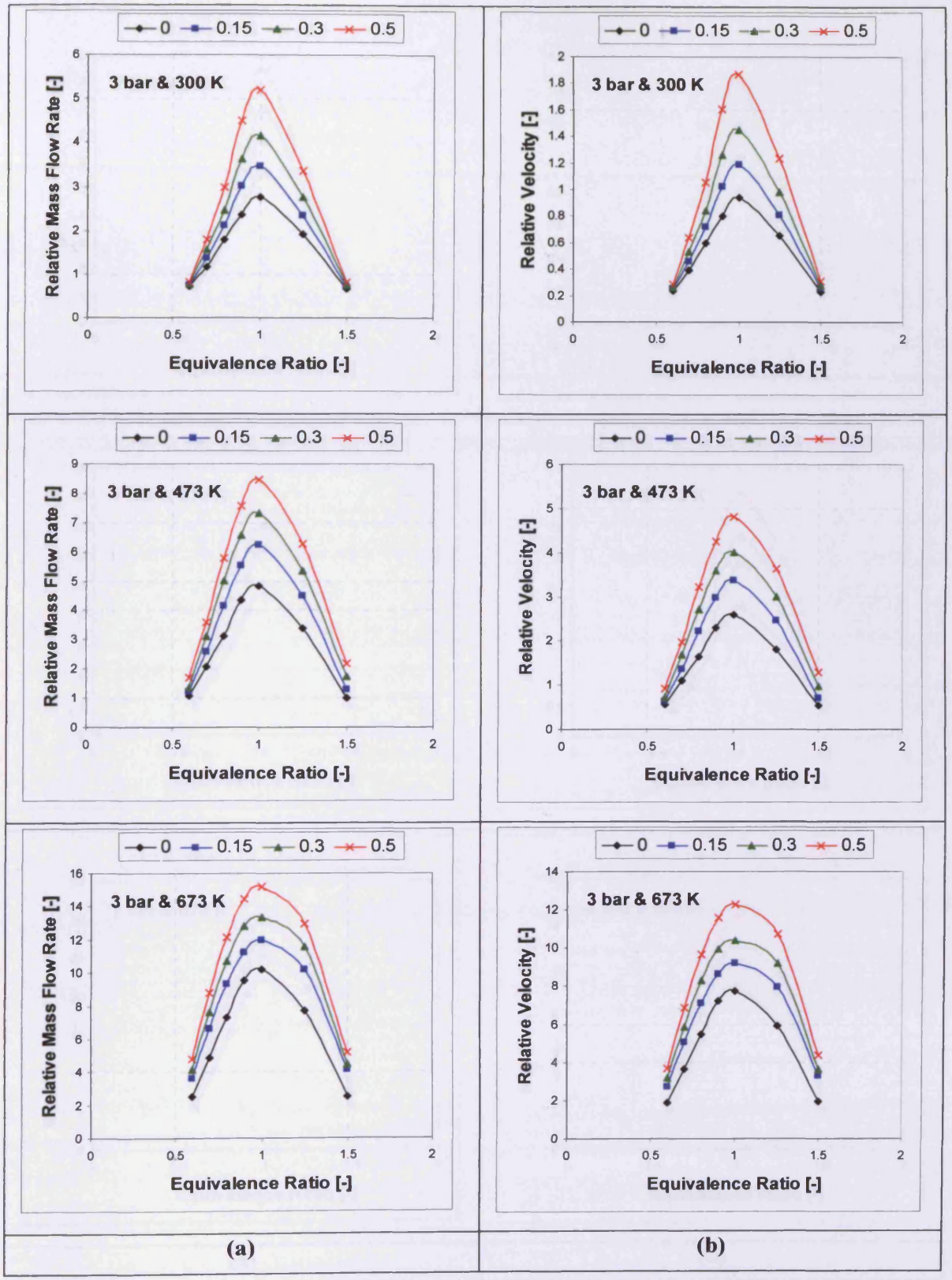

Figure 7.10: Cont.

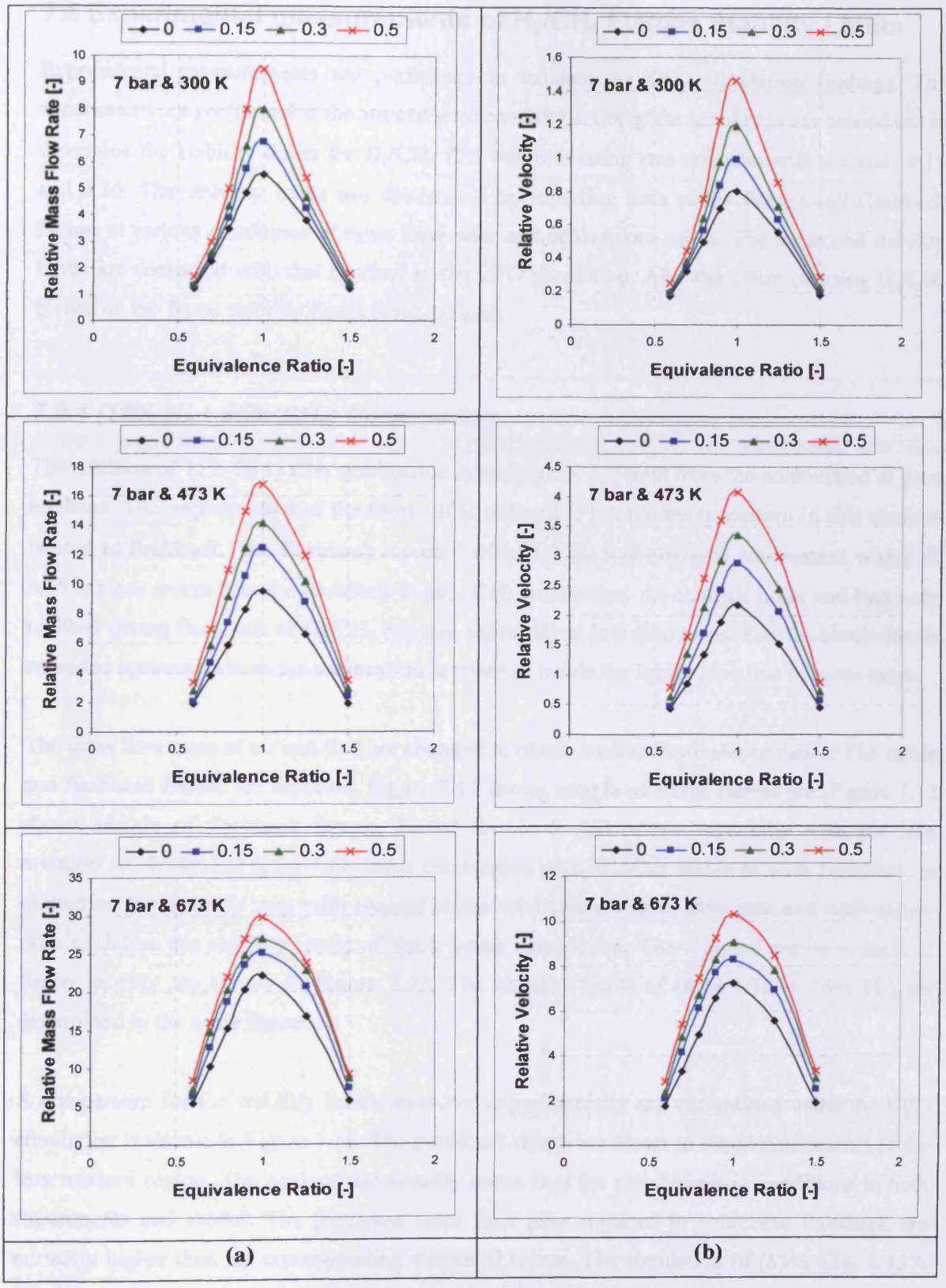

Figure 7.10: Cont.

7.5 Experimental measurements of H_2/CH_4 Flames Stability Limits

Experimental measurements are performed to validate the CFD simulation findings. The experiments are performed at the atmospheric conditions. Complete set of runs are carried out to determine the stability limits for H_2/CH_4 fuel mixtures using two mixtures with γ equals 0.15 and 0.30. The stability limits are determined by reporting both stable flames and flashback flames at various conditions of mass flow rates and equivalence ratios. The measured stability limits are compared with that resulted in the CFD simulation. Also the effect of using H_2/CH_4 blends on the flame stability limits is recognized.

7.5.1 (15% H_2 + 85% CH_4) Combustion

The addition of 15% H_2 to CH_4 combustion is completely different from the combustion of pure methane. The improvement of the blow off is noticeable but the main concern in this study is related to flashback. The flashback reported with H_2/CH_4 fuel mixtures combustion with γ of 0.15 is more severe than the flashback in pure CH_4 combustion. An acoustic noise and bangs are realised during flashback of H_2/CH_4 mixture especially at low flow rates. The flashback also is extended upstream where the combustion is reported inside the intake pipe line in some cases.

The mass flow rates of air and fuel are changed to obtain various equivalence ratios. The stable and flashback flames are reported. Figure 7.11 shows sample of stable flames and Figure 7.12 shows sample of flashback flames. Partial flashback still occurs especially with the lean mixtures as shown in Figure 7.11. Each combustion case, whether stable or with flashback, is plotted on the stability map with respect to the total mixture mass flow rate and equivalence ratio to define the stability limits of the mixture combustion. The reported measurements of flame stability are shown in Figure 7.13. The stability limits of (85% CH_4 + 15% H_2) are determined in the same figure.

A comparison for the stability limits measured experimentally and determined using the CFD simulation is shown in Figure 7.14. The predicted values are closer to the measurements at the lean mixture region. The peak of the stability curve is at the stoichiometric conditions in both experiments and model. The predicted mass flow rates required to overcome flashback are normally higher than the corresponding measured values. The simulation of (85% CH_4 + 15% H_2) gives better results regarding the prediction of flashback than the case of CO_2 addition to methane combustion discussed in the previous chapter.

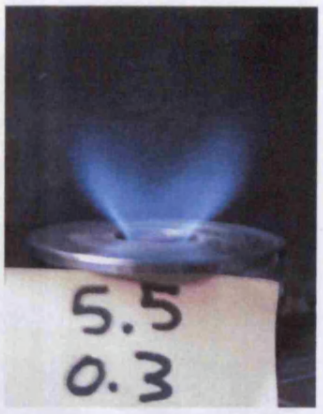

$\dot{m}_t$ = 5.8, ϕ = 0.96

$\dot{m}_t$ = 5.3, ϕ = 1.1

$\dot{m}_t$ = 4.97, ϕ = 1

$\dot{m}_t$ = 4.8, ϕ = 1.17

$\dot{m}_t$ = 4.2, ϕ = 0.88

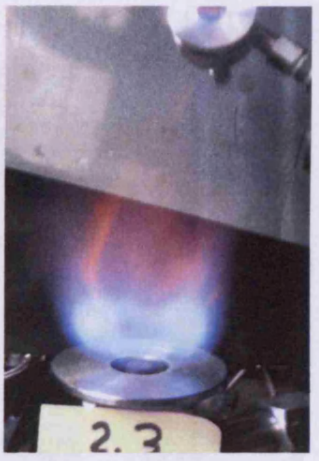

$\dot{m}_t$ = 3.42, ϕ = 1.2

$\dot{m}_t$ = 3.28, ϕ = 0.72

$\dot{m}_t$ = 3.15, ϕ = 1.5

$\dot{m}_t$ = 2.144, ϕ = 1.2

Figure 7.11: Stable flames for (85% CH_4 + 15% H_2) at various conditions.

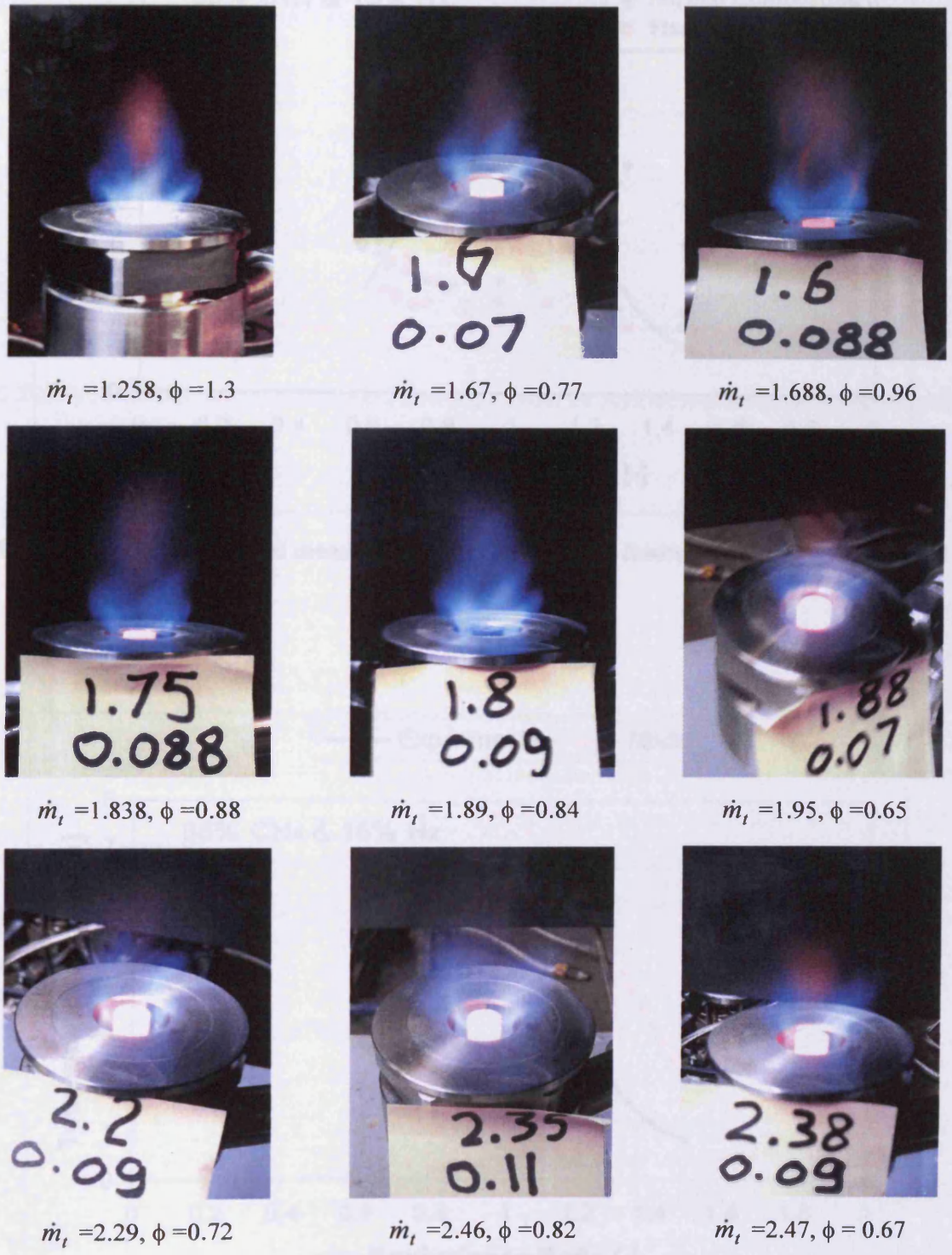

$\dot{m}_t$ =1.258, ϕ =1.3 | $\dot{m}_t$ =1.67, ϕ =0.77 | $\dot{m}_t$ =1.688, ϕ =0.96

$\dot{m}_t$ =1.838, ϕ =0.88 | $\dot{m}_t$ =1.89, ϕ =0.84 | $\dot{m}_t$ =1.95, ϕ =0.65

$\dot{m}_t$ =2.29, ϕ =0.72 | $\dot{m}_t$ =2.46, ϕ =0.82 | $\dot{m}_t$ =2.47, ϕ = 0.67

Figure 7.12: Flames flashback for (85% CH_4 + 15% H_2) at various conditions.

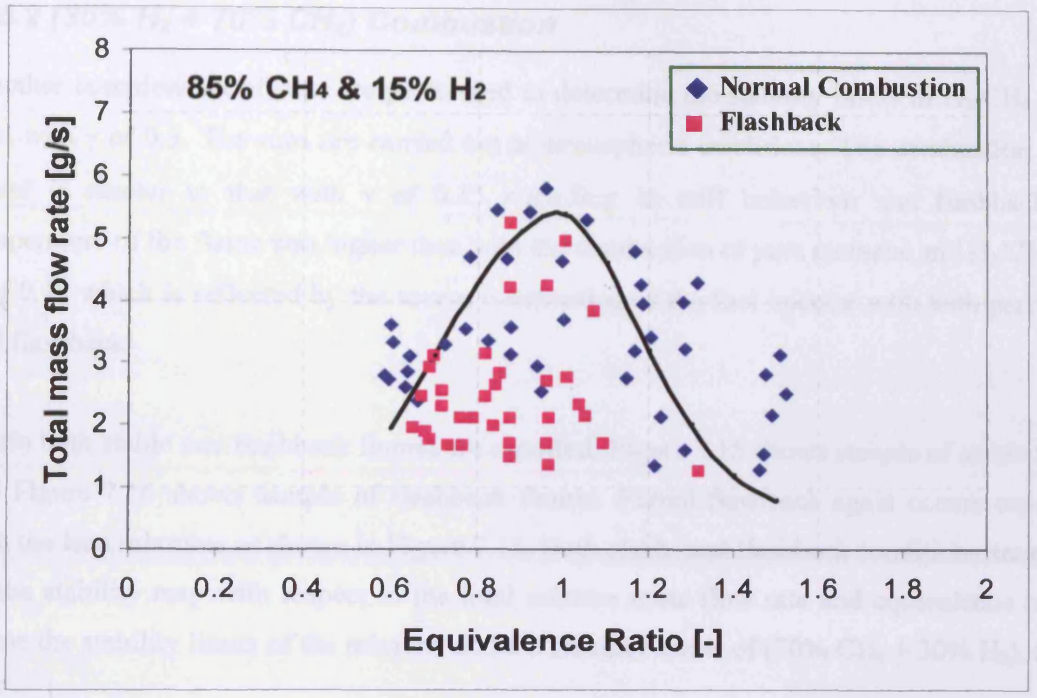

Figure 7.13: Experimental measurements of the stability limits of (85% CH_4 + 15% H_2) flames.

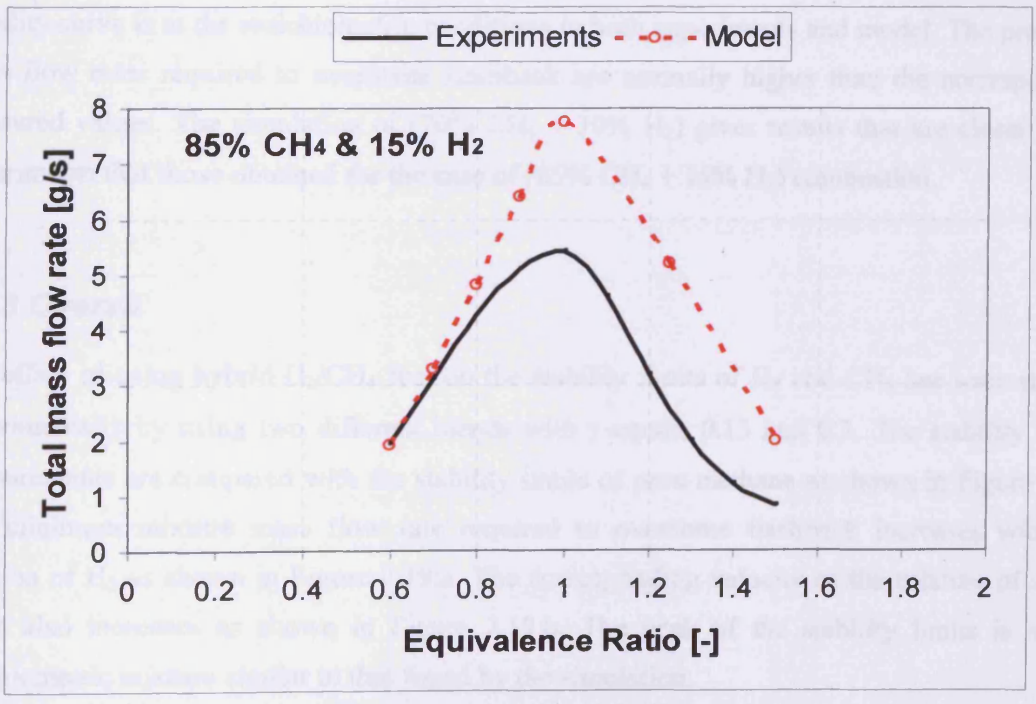

Figure 7.14: Comparison between the stability limits flames measured experimentally and determined by CFD simulation for (85% CH_4 + 15% H_2).

7.5.2 (30% H_2 + 70% CH_4) Combustion

Another complete set of runs are performed to determine the stability limits of H_2/CH_4 hybrid fuel with γ of 0.3. The runs are carried out at atmospheric conditions. The combustion of this blend is similar to that with γ of 0.15 regarding its stiff behaviour and flashback. The temperature of the flame was higher than with the combustion of pure methane and H_2/CH_4 with γ of 0.15 which is reflected by the severe overheating of the fuel injector with both partial and full flashback.

Again both stable and flashback flames are reported. Figure 7.15 shows sample of stable flames and Figure 7.16 shows sample of flashback flames. Partial flashback again occurs especially with the lean mixtures as shown in Figure 7.15. Both stable and flashback conditions are plotted on the stability map with respect to the total mixture mass flow rate and equivalence ratio to define the stability limits of the mixture and the stability limits of (70% CH_4 + 30% H_2), Figure 7.17.

A comparison of the stability limits measured experimentally and determined using the CFD simulation is shown in Figure 7.18. The predicted values are again closer to the measurements at the lean mixture region and much better than those with CH_4/CO_2 mixtures. The peak of the stability curve is at the stoichiometric conditions in both experiments and model. The predicted mass flow rates required to overcome flashback are normally higher than the corresponding measured values. The simulation of (70% CH_4 + 30% H_2) gives results that are closer to the experiments that those obtained for the case of (85% CH_4 + 15% H_2) combustion.

7.5.3 Overall

The effect of using hybrid H_2/CH_4 fuel on the stability limits of H_2 and CH_4 has been studied experimentally by using two different blends with γ equals 0.15 and 0.3. The stability limits measurements are compared with the stability limits of pure methane as shown in Figure 7.19. The minimum mixture mass flow rate required to overcome flashback increases with the addition of H_2 as shown in Figure 7.19.a. The corresponding velocity of the mixture of stable flame also increases as shown in Figure 7.19.b. The peak of the stability limits is at the stoichiometric mixture similar to that found by the simulation.

Generally, both model and experiments proved that the stability limits of H_2 are improved by adding CH_4 to the combustible mixture, whilst the CH_4 combustion is improved regarding its

blow off limits. The simulations produce a good prediction of the stability limits of H_2/CH_4 mixture especially in the lean combustion region.

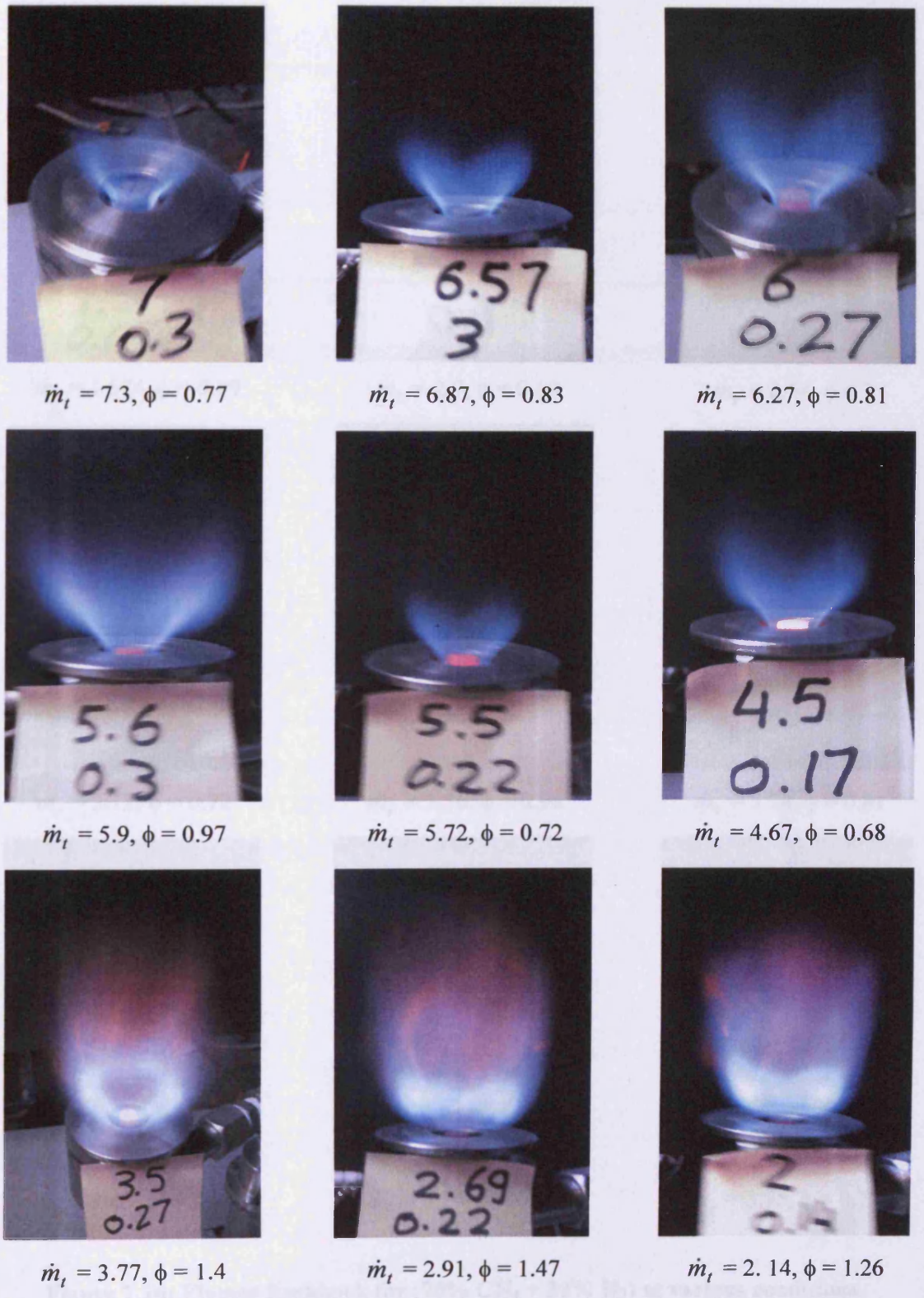

$\dot{m}_t = 7.3, \phi = 0.77$ $\dot{m}_t = 6.87, \phi = 0.83$ $\dot{m}_t = 6.27, \phi = 0.81$

$\dot{m}_t = 5.9, \phi = 0.97$ $\dot{m}_t = 5.72, \phi = 0.72$ $\dot{m}_t = 4.67, \phi = 0.68$

$\dot{m}_t = 3.77, \phi = 1.4$ $\dot{m}_t = 2.91, \phi = 1.47$ $\dot{m}_t = 2.14, \phi = 1.26$

Figure 7.15: Stable flames for (70% CH_4 + 30% H_2) at various conditions.

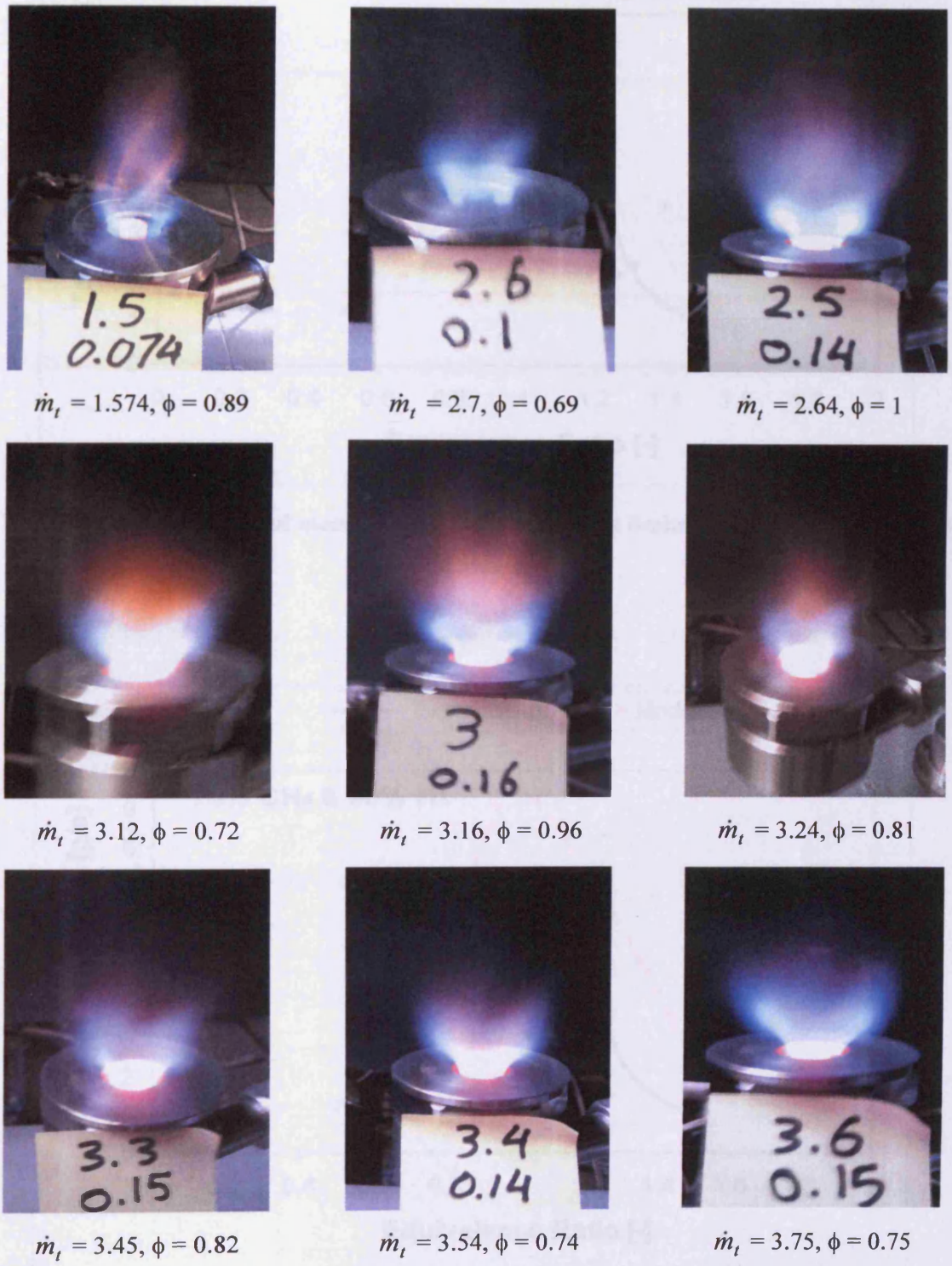

$\dot{m}_t = 1.574, \phi = 0.89$ $\dot{m}_t = 2.7, \phi = 0.69$ $\dot{m}_t = 2.64, \phi = 1$

$\dot{m}_t = 3.12, \phi = 0.72$ $\dot{m}_t = 3.16, \phi = 0.96$ $\dot{m}_t = 3.24, \phi = 0.81$

$\dot{m}_t = 3.45, \phi = 0.82$ $\dot{m}_t = 3.54, \phi = 0.74$ $\dot{m}_t = 3.75, \phi = 0.75$

Figure 7.16: Flames flashback for (70% CH_4 + 30% H_2) at various conditions.

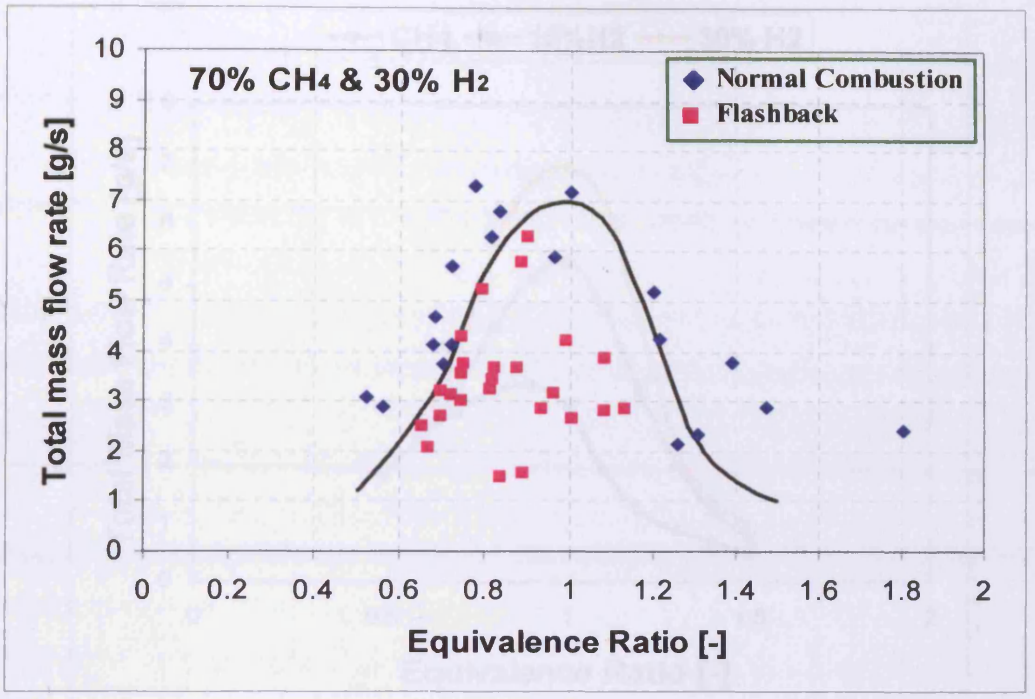

Figure 7.17: Experimental measurements of the stability limits of (70% CH_4 + 30% H_2) flames.

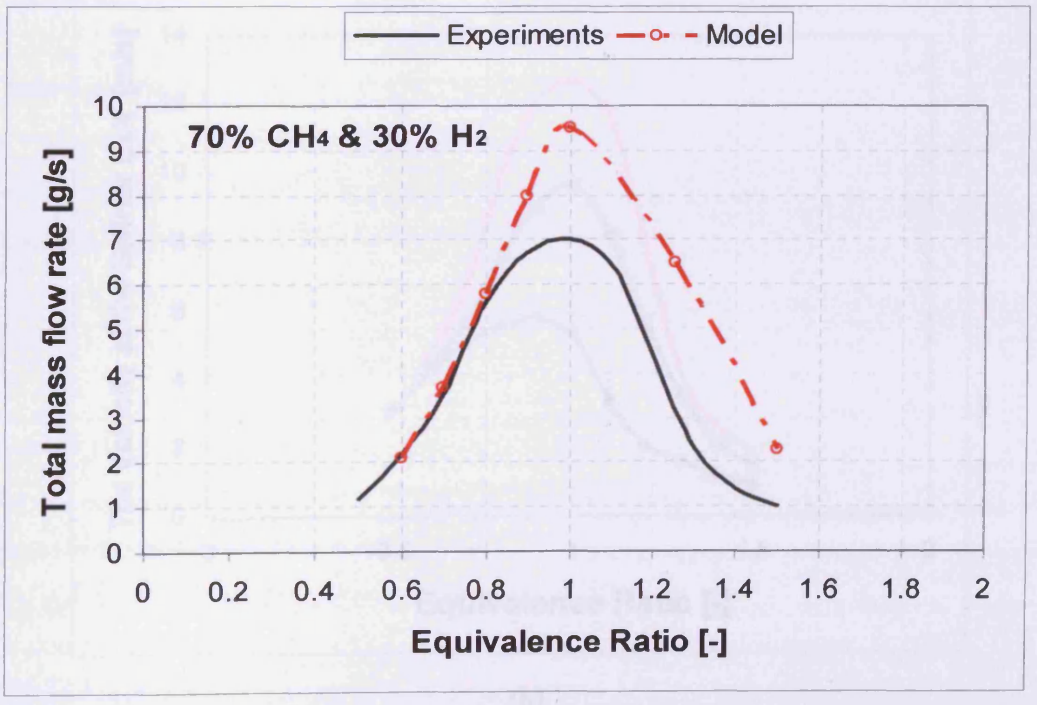

Figure 7.18: Comparison between the stability limits measured experimentally and determined by CFD simulation for (70% CH_4 + 30% H_2) flames.

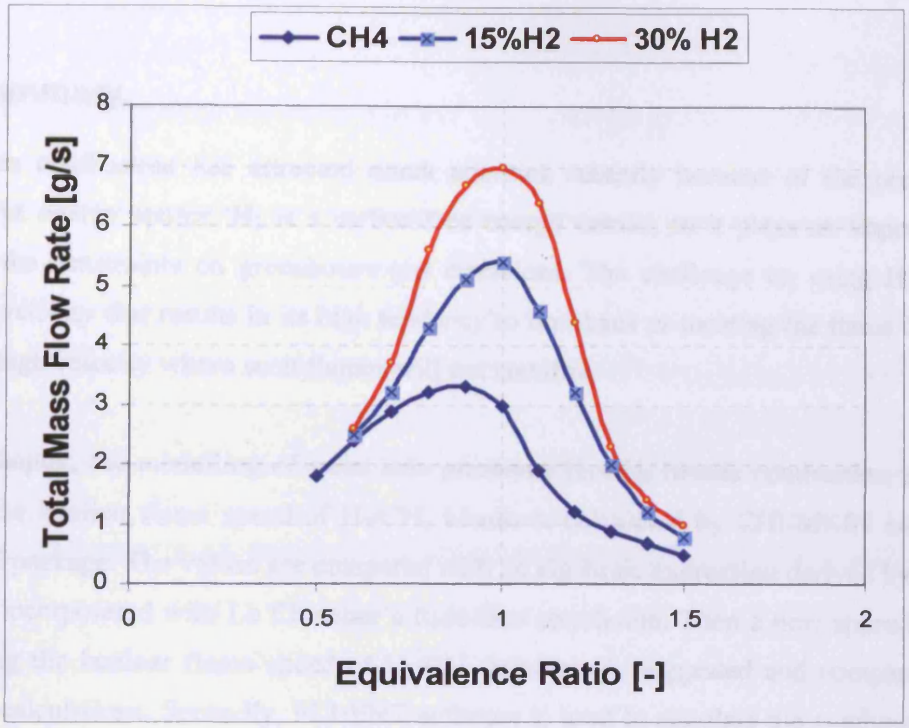

(a)

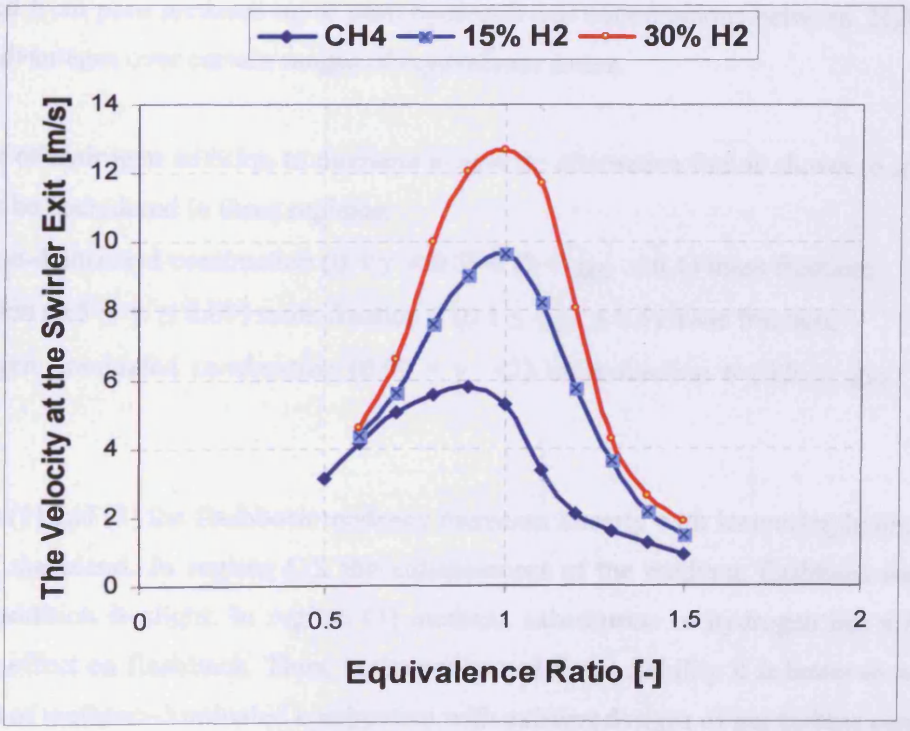

(b)

Figure 7.19: The stability limits of hybrid H_2/CH_4 fuel up to γ = 0.30 based on the experimental results. (a) The corresponding mass flow rates. (b) The corresponding velocity at the burner exit.

7.6 Summary

Hydrogen combustion has attracted much attention recently because of the need for clean alternative energy source. H_2 is a carbon-free energy carrier, so it plays an important role in serving the constraints on greenhouse gas emissions. The challenge on using H_2 is its high burning velocity that results in its high tendency to flashback or locating the flame in regions of relative high velocity where such flames will not stabilize.

In this chapter, the modelling of swirl lean premixed H_2/CH_4 blends combustion is discussed. Firstly, the laminar flame speed of H_2/CH_4 blends is calculated by CHEMKIN software with PREMIX package. The values are compared with an algebraic expression derived by asymptotic methods incorporated with Le Chatelier's Rule-like correlation. Then a new approximation for calculating the laminar flame speed of H_2/CH_4 mixtures is suggested and compared with the previous calculations. Secondly, FLUENT software is used to simulate the combustion of pure methane and H_2/CH_4 blends in a high pressure gas turbine combustor. The effect of the blend ratio on the flame stability is studied. Also the flashback limits of H_2/CH_4 combustion are determined from pure methane up to pure hydrogen and combinations between. H_2/CH_4 hybrid fuel has advantages over certain ranges of equivalence ratios.

The effect of hydrogen addition to methane to give an alternative fuel is shown to gives effects which can be considered in three regimes:

(1) methane-dominated combustion ($0 < \gamma < 0.5$) $\equiv$ ($0 < g_{H2} \leq 0.1$) mass fraction;

(2) transition ($0.5 \leq \gamma \leq 0.89$) mole fraction $\equiv$ ($0.1 \leq g_{H2} \leq 0.5$) mass fraction;

(3) hydrogen dominated combustion ($0.89 < \gamma < 1$) mole fraction $\equiv$ ($0.5 \leq g_{H2} < 1$) mass fraction.

In regimes (1) and (3) the flashback tendency increases linearly with increasing hydrogen molar content of the blend. In regime (1), the enhancement of the methane flashback tendency by hydrogen addition is slight. In regime (3) methane substitution to hydrogen has a significant decreasing effect on flashback. Thus, in the context of flame stability it is better to work in the first region of methane-dominated combustion with existing designs of gas turbine combustor. It is confirmed that the lean mixtures have more resistance to flashback more than those near an equivalence ratio of 1.

The experimental measurements performed at the atmospheric conditions are used to determine the stability limits for H_2/CH_4 flames and to validate the CFD simulation findings. Also, the effect of mixing H_2 and CH_4 on the stability limits is recognized. Two blends are used with γ equals 0.15 and 0.30. The measurements results are compatible with the predicted findings resulted by the CFD simulation. The measurements confirmed that the minimum mass flow rate required to overcome flashback increases with the addition of H_2 to CH_4. Or in another words, CH_4 additions can improve the stability limits of H_2 combustion. Also, it is noted that methane combustion is improved regarding the blow off with the addition of H_2. Of especial note is the point that for all the fuel blends, pure CH_4 and H_2/CH_4 blends and equivalence ratios <0.65 flashback limits are similar, indicating methodologies by which combustors can be designed to avoid flashback, whilst blow off limits are improved when H_2 is added to the fuel mix. Over this range the simulations are in agreement with these experimental results giving some confidence in extrapolation to conditions of higher temperature and pressure. As shown in Figure 7.10, the stability limits of H_2/CH_4 blends up to γ of 0.5 are approximately the same at equivalence ratio of 0.6 at 300 and 473 K for 1.01325, 3 and, 7 bar. The stability limits have a little divergence at the corresponding equivalence ratio and 673 K for the same pressure range. This divergence results upon the fact of the exponential proportionality of the laminar flame speed with the temperature. So, the gas turbines designers must have to take this note into their consideration to create a save scheme for the working conditions and for the load control as well.

The CFD simulation prediction for CH_4 and H_2/CH_4 combustion produces better results more than the prediction of CH_4/CO_2 combustion, discussed in the previous chapter. This is probably due to the use of the available extensive literature to predict laminar flame speeds for H_2/CH_4 mixes, such literature does not seem to exist for CH_4/CO_2 mixtures. More theoretical and experimental work is obviously required to derive more accurate results for laminar flame speed and stability limits for different alternative fuels.

Chapter 8

CONCLUSIONS AND FUTURE RESEARCH WORK

8.1 Conclusions

Lean premixed combustion is promoted as one of the new technologies that when applied to gas turbine combustors enables significant reduction of pollutant emissions, especially NOx. The swirl lean premixed combustion provides the initial stability and flexibility for the system. However, the gains made by this combustion route can be accompanied by stability problems. There are still problems that can occur during the combustion process including those related to flashback especially for high burning velocity fuels such as hydrogen enriched fuels. The flashback problem may causes failure of the combustion system which makes it one of the gas turbine industry priority issues that needs attention.

CFD modelling can be considered as an advanced tool for design due to its advantages regarding cost, time and hazard conditions managements. CFD code, Fluent, is used to simulate the combustion in a generic premixed swirl burner that uses different types of fuels. A three dimensional – finite volume model is used to study the occurrence of the flashback phenomenon. Experimental measurements are used to validate the CFD simulation findings.

It was realized that two different types of flashback can take place, partial flashback and full flashback. The partial flashback exists due to the extension of a Central Recirculation Zone (CRZ) back into the burner exit and that allows the hot gases to return to the burner and cause flashback. The other type of flashback is caused by the low velocity of the raw gases that may drop below the local burning velocity and thus allow full flashback. The results show the possibility of reducing the effect of partial flashback by using passive constrictions at the burner exit which can manipulate the CRZ and hence avoid partial flashback. The passive constrictions are not able to prevent full flashback but there are other methods that can be used to improve the stability limits of the flame. Full flashback can be avoided or reduced by operating at overall equivalence ratios < 0.65, lowering the turbulent intensity, adding carbon dioxide to the fuel and/or using hybrid fuel blends in hydrogen combustion.

The various factors affecting the stability limits of flame are studied. The effect of total mixture mass flow rate, equivalence ratio, operating pressure and, mixture temperature on the flame stability is investigated. The stability limits of flames regarding flashback are defined and

represented by both total mixture mass flow rate (or mixture velocity) and equivalence ratio at a specific pressure and mixture temperature.

The stability limits of CH_4 are determined by using CFD simulations and validated experimentally at atmospheric conditions. Also the effect of adding CO_2 to methane flames is studied by simulation and experimentally. An improvement of the methane flames stability limits was noticed with the addition of CO_2 in both simulations and experiments.

The feasibility of using H_2/CH_4 blends is studied from the view point of flame stability. An extensive work programme is carried out to determine the laminar flame speed of H_2/CH_4 blends to feed their values to fluent and built reliable inputs for the simulation program. A new approximation for calculating the laminar flame speed of H_2/CH_4 blends based on the gravimetric mixture ratio is suggested. The new approximation gave a good prediction at various conditions when compared with the values obtained by CHEMKIN-PRO software package with PREMIX code and an algebraic expression derived by asymptotic methods incorporated with Le Chatelier's Rule-like correlation. Flashback limits were determined for H_2/CH_4 blends ranging from 0% (pure methane) up to 100% (pure hydrogen) based on the volumetric composition at atmospheric pressure and 300K for various equivalence ratios. The results show that the use of up to 50% blends of methane and hydrogen causes fewer problems with flame stability and flashback compared with the use of pure hydrogen. Experimental measurements are performed at the atmospheric conditions to validate the CFD simulation findings. Also, the effect of mixing H_2 and CH_4 on the stability limits is recognized. The stability limits for H_2/CH_4 flames are measured for two blends with γ of 0.15 and 0.30 and compared with the CFD simulation results. The results produced by the CFD modelling simulation and by experimental measurements are found to be broadly compatible with each other, especially for equivalence ratios less than around 0.65. Both model and experiments confirm that the addition of CH_4 to H_2 improves its stability regarding the flashback while the addition of H_2 to CH_4 improves its stability regarding the blow off, operation at equivalence ratios at or below 0.65 is especially beneficial as the H_2/CH_4 flashback curves coalesce here at atmospheric pressure conditions and air inlet temperatures ~300K. Subsequent simulations at 3 bar and 7 bar and air inlet temperatures of 300K and 473K show the same trend. However for all operating pressures, air inlet temperatures of 673K started to produce significant separation between the pure CH_4 results and the H_2/CH_4 blends for equivalence ratios less than 0.65

The conclusions can be made:

Premixed Combustion:

- Lean premixed combustion is considered as one of the most promising concepts for substantial reduction of gas turbine emissions, especially NOx, while maintaining high efficiency.
- Premixed combustion gives many advantages regarding reducing emissions, although there can be problems due to oscillations and stability.
- The main problem for all premixed combustion systems is the instability problem and the tendency of the combustible mixture toward flashback.

Swirl Combustion:

- Most of gas turbines use swirl burners.
- The swirl burner produces better stability of the flame due to the aerodynamic gas recirculation.
- Under a certain conditions, partial and full flashback may occur in the swirl burner.

CFD Modelling:

- Computational Fluid Dynamics (CFD) is an important tool for analysing systems involving fluid flow, heat transfer and combustion.
- It is preferable to use CFD methods as they are cheap (in cost and maintenance), fast (in time) and safe (in hazard design processes) and often give satisfactory results, when suitably calibrated against available experimental data.
- The commercial CFD packages contain three main elements: a pre-processor, a solver and, a post-processor.
- CFD codes are structured around the numerical algorithms that can tackle fluid flow problems. The solution is based on solving the main flow governing equations.
- There is no general turbulent model that is able to perfect for all turbulent flow problems.
- Many Turbulent models are available in Fluent software. The designer must choose the turbulent model that can perform the modelling requirements with acceptable accuracy and time.
- Fluent provides several models for chemical species transport and chemical reactions. The choice of the suitable combustion model must consider the system physics and the model restrictions.
- The model preparation (mesh construction) plays an important role in the simulation accuracy and the solution convergence.
- The cell type must be chosen carefully as it affects the solution accuracy and time.
- It is important to make a balance between the number of the mesh cells and the time consumed by the model to reach the convergence.

- Fluent uses segregated solver to solve the combustion models problems.
- Laminar flame velocity is an important parameter in both laminar and turbulent combustion modelling.

Flashback:

- The flashback problem is still a barrier for combustion under certain operating conditions.
- The flashback exists at certain combustion conditions depending on some variables. These variables include the fuel mixture, operating pressure, mixture temperature, equivalence ratio, mixture mass flow rate and the turbulence plate used. The effect of these variables on flashback is studied this thesis.
- The original HPOC gas combustion system is suitable for turbulent flame speed calculations although it has some drawbacks. The main problem with it is that it is not able to produce homogeneous mixture for premixed combustion and this issue needs to be addressed.
- The turbulence plays an important role in flame stabilization. As the turbulence increases the tendency of the flame to flashback increases.
- Both partial flashback and full flashback are realized during simulation, matching other work found in the literature.
- It is possible to reduce and sometimes eliminate the partial flashback using passive constraints at the swirl burner exit.
- As the pressure increases the ability of the mixture to flashback increases at the same equivalence ratio.
- As the air preheat temperature increases the ability of the mixture to flashback increases at the same equivalence ratio.
- The ability of flashback to exist at a certain flow rate increases as the equivalence ratio increases over the range investigated.
- The ability of flashback to exist at a certain equivalence ratio increases as the total mass flow decreases.
- The boundary of the reverse flow zone seems to be fixed under various combustion conditions investigated, this needs to be validated experimentally in future work. The mean axial velocity in the reverse flows decreases as the pressure increases and if the mass flow rate decreases.
- There is no effect of the equivalence ratio on the shape or velocity distribution in the recirculation zone.
- In the case of flashback, the boundary of the recirculation zone is wider and the velocity increases more than the normal combustion.

- It is possible to eliminate the partial flashback by changing the burner geometry, it is impossible to eliminate the full flashback due to the reduction of mixture velocity below the local burning velocity. It is, however, possible to improve the stability limits.

CO_2 Additions:

- CO_2 dilution in methane combustion is a new research topic. It can be used for NOx emission reduction as a result of reducing the flame temperature.
- The impact of CO_2 addition to CH_4 premixed swirl combustion and the effect of operating pressure and initial mixture temperature have been studied.
- The results show that an improvement of the flashback limits of CH_4 flames results by adding CO_2 as this cause a reduction in flame velocity.
- The flame temperature decreases with the addition of CO_2 which also tends to reduce NOx emissions.
- The pressure and raw gases temperature play an important role in flame stability. Even though the flame velocity decreases with the increase of pressure, flashback occurs at higher mass flow rates due to the increase of density. Care must be taken when scaling the gas turbine operating conditions from lower pressures tests. The velocity at which the flashback exists is a strong function of temperature and it increases as the temperature increases.
- The CFD simulation of the addition of CO_2 to CH_4 was significantly worse than for H_2/CH_4 blends, despite using the best available data for laminar and turbulent flame speed. This appears to be a neglected area and both fundamental experimental and theoretical analysis is needed to gain a better understanding of the processes occurring with CO_2/CH_4 fuel blends. Indeed this could well be important with natural gas combustion in gas turbines as natural gas properties are normally measured commercially by Wobbe Number, a measure of heating value; this work indicates that variable quantities of CO_2, commonly present in natural gas, can well affect flame stability and flashback. This is clearly an area for further work.

H_2 Combustion:

- Hydrogen combustion has attracted much attention recently because of the need for clean alternative energy source. H_2 is a carbon-free energy carrier, so it plays an important role in serving the constraints on greenhouse gas emissions.
- The challenge on using H_2 is its high burning velocity that results in its high tendency to flashback or locating the flame in regions of relative high velocity where methane flames will not stabilize.

- There are many studies concerned about the measurement and analysis of flame velocities, both laminar and turbulent.
- Fluent provides data for laminar flame velocity that can be used for pure CH_4 and pure H_2 combustion simulation from lean mixtures up to stoichiometric mixtures.
- For fuel blends, such as H_2/CH_4, laminar flame speed must be calculated by other mean (chemical kinetics software, analytically or experimentally) and then fed to Fluent as an input data to establish a PDF table for turbulent combustion calculations.
- A new approximation of calculation H_2/CH_4, laminar flame speed is suggested and the results are matched with the other numerical methods.
- H_2/CH_4 hybrid fuel may have advantages over certain ranges of equivalence ratios.
- The experimental measurements were found to be close to the CFD simulation in the lean premixed region for equivalence ratios less than about 0.65. This result was then used to estimate flashback behaviour for pressurised combustion at different air inlet temperatures, little effect being found from increased pressure or air inlet temperatures up to 473K.

8.2 Future Research

Due to the great importance of thermal energy and its wide applications, it is required to design generic combustors that are able to burn different types of fuels. The flashback problem emerged especially with the use of premixed combustion (which is used for emissions reduction) and the use of hydrogen rich fuels (which is considered as a clean future fuel).

This research work focused on the flame stability and the measurements of the stability limits of various fuel mixes and how these limits can be improved; it also touches other important fields of research such as:

- Using alternative fuels in gas turbines:
    - Using H_2 and H_2/CH_4 blends.
    - Using biomass and low calorific value producer gases.
- Pollution reduction:
    - by using lean premixed combustion.
    - by using CO_2 recirculation.
    - by using clean alternative fuels such as H_2.
- Laminar flame speed measurements and calculations.
- Combustion modelling and model validation.

So, in order to enhance the future fuels combustion technologies, this research should be extended. Some recommendations for the future research are as follows:

Modelling:

- Studying the effect of using different cell shape and size.
- Performing a comprehensive comparison using different turbulent models.
- Comparing the effects of different combustion models.
- More numerical and experimental studies are needed to derive the values of laminar flame speed of various alternative fuels.
- Studying the sources of uncertainty in the combustion modelling especially that related to the laminar flame speed and flame speed/turbulence correlations to produce more reliable results that would be compatible with the experiments.

Combustion:

- Studying the effect of the nozzle exit shape on the flame stability.
- Performing a comprehensive study on the optimum CO_2 percentage that can be added to CH_4 in terms of stability, flame characteristics and emissions reduction.
- Studying the stability of alternative fuels that are in perspective as a new gas turbine feed fuels.
- Determining the emissions for every fuel blend that was used to improve the combustion stability.
- Introducing a correlations for flashback and the burner geometry (represented by turbulent intensity), fuel (represented by laminar flame speed), and operating conditions (represented by pressure and temperature) that can be generalized for any/most burners.

REFERENCES

[1] BP, 2009, "BP Statistical Review of World Energy," http://www.bp.com/liveassets/bp_internet/globalbp/globalbp_uk_english/reports_and_publications/statistical_energy_review_2008/STAGING/local_assets/2009_downloads/statistical_review_of_world_energy_full_report_2009.pdf.

[2] IEA, 2008, "Key World Energy Statistics," http://www.iea.org/textbase/nppdf/free/2008/key_stats_2008.pdf.

[3] OECD, 2008, "OECD Key Environmental Indicators," http://www.oecd.org/dataoecd/20/40/37551205.pdf.

[4] Shelil, N., 2007, "The Potential Impact of Using Biomass Energy – An Egyptian Perspective," Cardiff University, Cardiff.

[5] IPCC, "The IPCC Assessment Reports ", http://www.ipcc.ch/.

[6] Wall, T. F., 2007, "Combustion processes for carbon capture," Proceedings of the Combustion Institute, 31(1), pp. 31-47.

[7] IEA, 2009, "CO_2 Emissions from Fuel Combustion."

[8] Cho, H. M., and He, B. Q., 2007, "Spark ignition natural gas engines-A review," Energy Conversion and Management, 48(2), pp. 608-618.

[9] Shelil, N., 2007, "Boiler Types and Burner Systems," Cardiff University, Cardiff.

[10] Encyclopedia Britannica, I., "Open-cycle constant-pressure gas turbine engine," http://www.britannica.com/EBchecked/topic-art/187279/19424/Open-cycle-constant-pressure-gas-turbine-engine.

[11] Siemens, "CAD image of an SGT6-6000G gas turbine.," http://www.powergeneration.siemens.com/press/press-pictures/gas-turbines/gas-turbine-9.htm.

[12] Wikipedia, "Gas Turbine," http://en.wikipedia.org/wiki/Gas_turbine.

[13] HowStuffWorks, "How Gas Turbine Engines Work ", http://science.howstuffworks.com/turbine2.htm.

[14] Bahr, D. W., 1996, "Aircraft turbine engine NOx emission abatement," Unsteady combustion, F. E. C. Culick, M. V. Heitor, and J. H. Whitelaw, eds., Kluwer Academic Publisher, Netherlands.

[15] Correa, S. M., 1992, "A review of NOx formation under gas-turbine combustion conditions," Combustion Science and Technology, 87, pp. 329-362.

[16] Correa, S. M., 1998, "Power generation and aeropropulsion gas turbines: From combustion science to combustion technology," Symposium (International) on Combustion, 27(2), pp. 1793-1807.

[17] Lefebvre, A. H., 1995, "The Role of Fuel Preparation in Low-Emission Combustion," Journal of Engineering for Gas Turbines and Power, 117(4), pp. 617-654.

[18] Huang, Y., and Yang, V., 2009, "Dynamics and stability of lean-premixed swirl-stabilized combustion," Progress in Energy and Combustion Science, 35(4), pp. 293-364.

[19] Lefebvre, A. H., 1999, Gas Turbine Combustion, Taylor & Francis Group, LLC, Oxon, UK

[20] Gupta, A. K., Lilley, D. J., and Syred, N., 1984, Swirl Flows, Abacus Press, Tunbridge Wells, United Kingdom.

[21] Goy, C. J., James, S. R., and Rea, S., 2005, "Monitoring combustion instabilities: E.ON UK's experience," Combustion instabilities in gas turbine engines: operational experience, fundamental mechanisms, and modeling, T. Lieuwen, and V. Yang, eds., Progress in Astronautics and Aeronautics, pp. 163-175.

[22] Schefer, R. W., White, C., and Keller, J., 2008, "Lean Hydrogen Combustion," Lean Combustion, Technology and Control, D. Dunn-Rankin, ed., Elsevierr Inc., USA.

[23] Lefebvre, A. H., 1983, Gas Turbine Combustion, Taylor & Francis Group, LLC, USA

[24] Gökalp, I., and Lebas, E., 2004, "Alternative fuels for industrial gas turbines (AFTUR)," Applied Thermal Engineering, 24(11-12), pp. 1655-1663.

[25] Date, A. W., 2005, Introduction to Computational Fluid Dynamics, Cambridge University Press.
[26] Baukal, C. E., Jr., V. Y. G., and Li, X., 2001, Computational Fluid Dynamics in Industerial Combustion, CRC Press.
[27] Gaydon, A. G., and Wolfhard, H. G., 1970, Flames, Their structure, radiation and temperature, Chapman and Hall LTD, London.
[28] Bender, W. R., "Lean Premixed Combustion," http://www.netl.doe.gov/technologies/coalpower/turbines/refshelf/handbook/3.2.1.2.pdf.
[29] Sankaran, R., Hawkes, E. R., Chen, J. H., Lu, T., and Law, C. K., 2006, "Direct Numerical Simulations of Turbulent Lean Premixed Combustion," Journal of Physics, 46, pp. 38-42.
[30] Huang, Y., and Yang, V., 2005, "Effect of swirl on combustion dynamics in a lean-premixed swirl-stabilized combustor," Proceedings of the Combustion Institute, 30(2), pp. 1775-1782.
[31] Coghe, A., Solero, G., and Scribano, G., 2004, "Recirculation phenomena in a natural gas swirl combustor," Experiments in Thermal Fluid Science, 28, pp. 709–714.
[32] Valera-Medina, A., Syred, N., and Griffiths, A., 2008, "Characterization of Large Coherent Structures in a Swirl Burner," AIAA International Meeting 2008, ref. AIAA 2008-1019.
[33] Vanoverberghe, K., 2004, "Flow, Turbulence and Combustion of Premixed Swirling Jet Flame," PhD, Faculty of Engineering, Katholieke Universiteit Leuven, Belgium.
[34] Barmina, I., Desnickis, A., Meijere, A., and Zake, M., 2007, "Active Electric Control of Emissions from Swirling Combustion," Advanced Combustion and Aerothermal Technologies, NATO Science for Peace and Security Series, Springer, pp. 405-412.
[35] Law, C. K., 2006, Combustion Physics.
[36] Putnam, A. A., 1948, "Application of Dimensionless Numbers to Flash-Back and Other Combustion Phenomena.," Third Symposium on Combustion, Flame, and Explosion Phenomena pp. 89-98.
[37] Wohl, K., 1952, "Quenching, Flash-Back, Blow-Off Theory and experiment," 4th International Symposium on Combustion, pp. 69-89.
[38] Kieswetter, F. K., 2003, "Two-Dimensional Flashback Simulation in Strongly Swirling Flows," Proceedings of the ASME Turbo Expo.
[39] Kroner, M. F., 2002, "Flashback Limits for Combustion Induced Vortex Breakdown in a Swirl Burner," ASME Paper GT-2002-30075. Amsterdam: ASME Turbo Expo.
[40] Brown, G. L., 1990, "Axisymmetric Vortex Breakdown Part 2: Physical MEchanisms," J. Fluid Mech., 221, pp. 553- 576.
[41] Lieuwen, T. M., 2006, "Fuel Flexibility Influences on Premixed Combustor Blowout, Flashback, Autoignition and Stability," Proceedings of the ASME Turbo Expo 2006: Power for Land, Sea and Air. Paper no. GT2006-90770, Barcelona, Spain.
[42] Noble, D. R., May 2006, "Syngas Mixture Composition Effects Upon Flashback and Blowout," ASME Turbo Expo: Power for Land, Sea, and Air GT2006-90470Barcelona, Spain.
[43] Lamnaouer, M., "Flashback Analysis for ULN Hydrogen Enriched Natural Gas Mixtures," Department of Mechanical Engineering, University of Central Florida, Orlando, FL 32826.
[44] Fritz, J., Kroner, M., and Sattelmayer, T., 2004, "Flashback in a Swirl Burner with Cylindrical Premixing Zone," Journal of Engineering for Gas Turbines and Power, 126(2), pp. 276-283.
[45] Kroner, M., Fritz, J., and Sattelmayer, T., 2003, "Flashback Limits for Combustion Induced Vortex Breakdown in a Swirl Burner," Journal of Engineering for Gas Turbines and Power, 125(3), pp. 693-700.
[46] Subramanya, M., and Choudhuri, A., 2007, "Investigation of Combustion Instability Effects on the Flame Characteristics of Fuel Blends," 5th International Energy Conversion Engineering Conference and Exhibit (IECEC) AIAA, St. Louis, Missouri.

[47] Lewis, B., and Elebel, G., 1987, Combustion, Flames and Explosions of Gases, Academic Press, New York.
[48] Plee, S. L., and Mellor, A. M., 1978, "Review of Flashback Reported in Prevaporizing/Premixing Combustors," Combustion and Flame, 32, pp. 193-203.
[49] Dobbeling, K., Erglu, A., Winkler, D., Sattelmayer, T., and Keppel, W., 1997, "Low Nox Premixed Combustion of MBTu Fuels in a research Burner," ASME J. Eng. Gas Turbine Power, 119, pp. 553-558.
[50] Syred, N., and Beer, J. M., 1973, "Effect of Combustion upon Precessing Vortex Cores Created by Swirl Combustors," 14 th Symposium (int.) on Combustion, T. C. Institute, ed.Pittsburgh, PA, pp. 537-549.
[51] Shimokuri, D., and Ishizuka, S., 2005, "Flame stabilization with a tubular flame," Proceedings of the Combustion Institute, 30(1), pp. 399-406.
[52] Stöhr, M., Sadanandan, R., and Meier, W., 2009, "Experimental study of unsteady flame structures of an oscillating swirl flame in a gas turbine model combustor," Proceedings of the Combustion Institute, In Press, Corrected Proof.
[53] Syred, N., 2007 Springer, " Generation and Alleviation of Combustion Instabilities in Swirling Flow," Advanced Combustion and Aerothermal Technologies, N. Syred, and A. Khalatov, eds., Springer, pp. 3–20.
[54] Syred, N., and Beer, J., 1974, "Combustion in Swirling Flows: a Review," Combustion and Flame, 23, pp. 143-201.
[55] Beer, J. M., and Chigier, N. A., 1972, Combustion Aerodynamics, Applied Science Publishers, London.
[56] Wall, T. F., 1987, Principles of Combustion Engineering for Boilers, Academic Press, London.
[57] Alexander, R., 1949, "Fundamentals of Cyclone Design and Operation," Proceedings of the Australian Institution of Mining and Metalurgy, pp. 203-228.
[58] Iinoya, K., 1953, "Study of the Cyclone," Memoirs of the Faculty of Engineering, Nagoya University 5(131).
[59] Vonnegut, B., 1956, "A Vortix Whistle," Journal of Accoustic Socity, 26, pp. 18-23.
[60] Chanaud, R. C., 1965, "Observations of Oscillatory Motion in Certain Swirling Flows," Journal of Fluid Mechanics, 21(1), pp. 111-127.
[61] Escudier, M. P., and Keller, J. J., 1985, "Recirculation in Swirling Flow: a Manifestation of Vortex Breakdown," AIAA journal, 23(1), pp. 111-116.
[62] Lucca-Negro, O., and O'Doherty, T., 2001, "Vortex breakdown: a review," Progress in Energy and Combustion Science, 27(4), pp. 431-481.
[63] Syred, N., and Beer, J. M., 1971, "Attenuating the precession of Vortix Cores During Combustion in a Swirler," Gas Waerme International, Bd. 20, Nr. 12.
[64] Syred, N., Fick, W., O'Doherty, T., and Griffiths, A. J., 1997, "The effect of the precessing vortex core on combustion in a swirl burner," Combustion Science and Technology, 125(1-6), pp. 139-157.
[65] Fick, W., 1998, "Characterisation and Effects of the Precessing Vortex Core in Swirl Burners," University of Wales, Cardiff.
[66] Syred, N., 2006, "A Review of Oscillation Mechanisms and the role of the Precessing Vortex Core (PVC) in Swirl Combustion Systems," Progress in Energy and Combustion Systems, 32(2), pp. 93-161.
[67] Schildmacher, K. U., and Koch, R., 2005, "Experimental investigation of the interaction of unsteady flow with combustion," Journal of Engineering for Gas Turbines and Power, 127(2), pp. 295-300.
[68] Li, G., Yi, T., and Gutmark, E., 2004, "Experimental Study of Large Coherent Structure in Multiple Swirler Combustor " 42nd AIAA Aerospace Sciences Meeting and ExhibitReno, Nevada.
[69] Syred, N., and Dahman, K. R., 1978, "Effect of High Levels of Confinement upon the Aerodynamics of Swirl Burners," Journal of Energy, 2, pp. 8-15.

[70] Syred, N., Dahmen, K. R., Styles, A. C., and Najim, S. A., 1977, "A Review of Combustion Problems associated with Low Calorific Value Gasess," International Institute of Fuel, 50, pp. 195-207.

[71] Gupta, A. K., Beer, J. M., and Swithenbank, J., 1976, "Concentric Multi-Annular Swirl Burner: Stability Limits and Emission Characteristics," Symp (Int) on Combustion, 16th, MITCambridge, pp. 79-91.

[72] Grinstein, F. F., Young, T. R., Gutmark, E. J., Li, G., Hsiao, G., and Mongia, H. C., 2002, "Flow dynamics in a swirling jet combustor," Journal of Turbulence, 3.

[73] Tangirala, V., Chen, R. H., and Driscoll, J. F., 1987, "Effect of Heat Release and Swirl on the Recirculation within Swirl-Stabilized Flames," Combustion Science and Technology, 51(1), pp. 75 - 95.

[74] Broda, J. C., Seo, S., Santoro, R. J., Shirhattikar, G., and Yang, V., 1998, "Experimental study of combustion dynamics of a premixed swirl injector," Symposium (International) on Combustion, 2, pp. 1849-1856.

[75] Seo, S., 1999, "Parametric Study of Lean Premixed Combustion Instability in a Pressured Model Gas Turbine Combostor," Department of Mechanical Engineering, The Pennsylvania State University, University Park, PA.

[76] Stone, C., and Menon, S., 2002, "Swirl Control of Combustion Instabilities in a Gas Turbine Combustor," Proceedings of the Combustion Institute, 29, pp. 155–160.

[77] Stone, C., and Menon, S., 2003, "Open-loop control of combustion instabilities in a model gas turbine combustor," Journal of Turbulence, 4, p. N20.

[78] Huang, Y., H.G. Sung, S. Y. H., and Yang, V., 2003, "Large-Eddy Simulation of Combustion Dynamics of Lean-Premixed Swirl-Stabilized Combustor," J. Propul. Power, 19, pp. 782–794.

[79] Huang, Y., and Yang, V., 2004, "Bifurcation of flame structure in a lean- premixed swirl-stabilized combustor: transition from stable to unstable flame," Combust. Flame 136, pp. 383–389.

[80] Huang, Y., and Yang, V., 2005, "Modeling and Control of Combustion Dynamics in Lean Premixed Swirl-Stabilized Combustor," Proceeding of Sixth Symposium on Smart Control of Turbulence. Tokyo, Japan.

[81] Huang, Y., and Yang, V., 2009, "Dynamics and stability of lean-premixed swirl-stabilized combustion," Progress in Energy and Combustion Science, In Press, Corrected Proof.

[82] Park, J., Hwang, D. J., Kim, K.-T., Lee, S.-B., and Keel, S.-I., 2004, "Evaluation of chemical effects of added CO_2 according to flame location," Int. J. Energy Res., 28(6), pp. 551–565.

[83] Kobayashi, H., Hagiwara, H., Kaneko, H., and Ogami, Y., 2007, "Effects of CO_2 dilution on turbulent premixed flames at high pressure and high temperature," Proceedings of the Combustion Institute, 31(1), pp. 1451-1458.

[84] Cohé, C., Chauveau, C., Gökalp, I., and Kurtulus, D. F., 2009, "CO_2 addition and pressure effects on laminar and turbulent lean premixed CH_4 air flames," Proceedings of the Combustion Institute, 32(2), pp. 1803-1810.

[85] Gelfand, B. E., Kapov, V. P., and Popov, E., 1999, "Turbulent flames in lean H_2-air-CO_2 mixtures," Mediterranean combustion symposium. Antalya , Turquie

[86] Kobayashi, H., Tamura, T., maruta, K., and Niioka, T., 1996, "Burning Velocity of Turbulent Premixed Flames in a High Pressure Environment," Twenty-Sixth Symposium (International) on Combustion, The Combustion Institute, pp. 389–396.

[87] Park, J., Kim, S.-G., Lee, K.-M., and Kim, T. K., 2002, "Chemical effect of diluents on flame structure and NO emission characteristic in methane–air counterflow diffusion flame," Int. J. Energy Res., 26, pp. 1141–1160.

[88] Zhu, D. L., Egolfopoulos, F. N., and Law, C. K., 1989, "Experimental and Numerical Determination of Laminar Flame Speeds of Methane/(Ar, N_2, CO_2)-Air Mixtures as Function of Stoichiometry, Pressure, and Flame Temperature," Twenty-Second Symposium (International) on Combustion, The Combustion Institute, Pittsburgh, PA, pp. 1539-1545.

[89] Park, J., Kwon, O. B., Yun, J. H., Keel, S. I., Chang Cho, H., and Kim, S., 2008, "Preferential diffusion effects on flame characteristics in H_2/CO syngas diffusion flames diluted with CO_2," International Journal of Hydrogen Energy, 33(23), pp. 7286-7294.

[90] Cohe', C., Halter, F., Chauveau, C., Gokalp, I., and Gulder, O. L., 2007, "Fractal characterisation of high-pressure and hydrogen-enriched CH_4–air turbulent premixed flames," Proceedings of the Combustion Institute, 31, pp. 1345–1352.

[91] Chiesa, P., Lozza, G., and Mazzocchi, L., 2005, "Using Hydrogen as Gas Turbine Fuel," Journal of Engineering for Gas Turbines and Power, 127, pp. 73-80.

[92] Shy, S. S., Chen, Y. C., Yang, C. H., Liu, C. C., and Huang, C. M., 2008 "Effects of H_2 or CO_2 addition, equivalence ratio, and turbulent straining on turbulent burning velocities for lean premixed methane combustion," Combustion and Flame 153, pp. 510–524.

[93] Di Sarli, V., and Benedetto, A. D., 2007, "Laminar burning velocity of hydrogen-methane/air premixed flames," International Journal of Hydrogen Energy, 32(5), pp. 637-646.

[94] Badin, J. S., and Tagore, S., 1997, "Energy pathway analysis - A hydrogen fuel cycle framework for system studies," International Journal of Hydrogen Energy, 22(4), pp. 389-395.

[95] Ogden, J. M., 1999, "Developing an infrastructure for hydrogen vehicles: A Southern California case study," International Journal of Hydrogen Energy, 24(8), pp. 709-730.

[96] Thomas, C. E., James, B. D., and Lomax Jr, F. D., 1998, "Market penetration scenarios for fuel cell vehicles," International Journal of Hydrogen Energy, 23(10), pp. 949-966.

[97] Verhelst, S., and Sierens, R., 2001, "Aspects concerning the optimisation of a hydrogen fueled engine," International Journal of Hydrogen Energy, 26(9), pp. 981-985.

[98] Law, C. K., and Kwon, O. C., 2004, "Effects of hydrocarbon substitution on atmospheric hydrogen-air flame propagation," International Journal of Hydrogen Energy, 29(8), pp. 867-879.

[99] Karim, G., Wierzba, I., and Al-Alosi, Y., 1996, "Methane-Hydrogen mixtures as Fuels," Int. J. Hydrogen Energy, 21(7), pp. 625-631.

[100] Nagalingam, B., Duebel, F., and Schmillen, K., 1983, "Performance Study Using Natural Gas, Hydrogen-Supplemented Natural Gas and Hydrogen in AVL Presearch Engine," Int. J. Hydrogen Energy, 8(9), pp. 715-720.

[101] Scholte, T. G., and Vaags, P. B., 1959, "Burning velocities of mixtures of hydrogen, carbon monoxide and methane with air," Combustion and Flame, 3(C), pp. 511-524.

[102] Liu, Y., Lenze, B., and Leuckel, W., 1989, "Investigation on the laminar and turbulent burning velocities of premixed lean and rich flames of CH_4-H_2-Air mixtures," Progress in Astronautics and Aeronautics, 131, pp. 259-259.

[103] Halter, F., Chauveau, C., Djebaïli-Chaumeix, N., and Gökalp, I., 2005, "Characterization of the effects of pressure and hydrogen concentration on laminar burning velocities of methane-hydrogen-air mixtures," Proceedings of the Combustion Institute, 30(1), pp. 201-208.

[104] Milton, B. E., and Keck, J. C., 1984, "Laminar burning velocities in stoichiometric hydrogen and hydrogen-hydrocarbon gas mixtures," Combustion and Flame, 58(1), pp. 13-22.

[105] Ren, J. Y., Qin, W., Egolfopoulos, F. N., and Tsotsis, T. T., 2001, "Strain-rate effects on hydrogen-enhanced lean premixed combustion," Combustion and Flame, 124(4), pp. 717-720.

[106] Yu, G., Law, C. K., and Wu, C. K., 1986, "Laminar flame speeds of hydrocarbon + air mixtures with hydrogen addition," Combustion and Flame, 63(3), pp. 339-347.

[107] Miller, D. R., Evers, R. L., and Skinner, G. B., 1963, "Effects of various inhibitors on hydrogen-air flame speeds," Combustion and Flame, 7(1), pp. 137-142.

[108] Schefer, R., and Oefelein, J., 2003, "Reduced Turbine Emissions Using Hydrogen-Enriched Fuels," Sandia National Laboratories, Livermore CA.

[109] Schefer, R. W., Wicksall, D. M., and Agrawal, A. K., 2002, "Combustion of hydrogen-enriched methane in a lean premixed swirl-stabilized burner," Proc. Combust. Inst.(29), pp. 843-851.

[110] Schefer, R. W., 2001, "Combustion of Hydrogen-Enriched Methane in a Lean Premixed Swirl Burner," Proceedings of the 2001 DOE Hydrogen Program Review.
[111] Wicksall, D. M., Schefer, R. W., Agrawal, A. K., and Keller, J. O., 2003, "Fuel Composition Effects on the Velocity Field in a Lean Premixed Swirl-Stabilized Burner " 48th ASME International Gas Turbine and Aero Engine Technical Congress and Exposition, Proceedings of ASME Turbo Expo 2003, Atlanta, GA
[112] Jackson, G. S., Sai, R., Plaia, J. M., Boggs, C. M., and Kiger, K. T., 2003, "Erratum: Influence of H_2 on the response of lean premixed CH_4 flames to high strained flows (Combustion and Flame (2003) 132:3 (503-511) PII: S0010218002004960)," Combustion and Flame, 135(3), p. 363.
[113] Kido, H., Huang, S., Tanoue, H., and Nitta, T., 1994, "A study of the premixed turbulent combustion mechanism taking the preferential diffusion effect into consideration," JSME Rev. , 15, pp. 165-167.
[114] Bradley, D., 1992, "How fast can we burn?," Symposium (International) on Combustion, 24(1), pp. 247-262.
[115] Zhao, K., Cui, D., Xu, T., Zhou, Q., Hui, S., and Hu, H., 2008, "Effects of hydrogen addition on methane combustion," Fuel Processing Technology, 89(11), pp. 1142-1147.
[116] Zhang, Y., Wu, J., and Ishizuka, S., 2009, "Hydrogen addition effect on laminar burning velocity, flame temperature and flame stability of a planar and a curved CH_4-H_2-air premixed flame," International Journal of Hydrogen Energy, 34(1), pp. 519-527.
[117] Wang, J., Huang, Z., Tang, C., Miao, H., and Wang, X., 2009, "Numerical study of the effect of hydrogen addition on methane-air mixtures combustion," International Journal of Hydrogen Energy, 34(2), pp. 1084-1096.
[118] Tabet-Helal, F., Sarh, B., and Gokalp, I., 2008, "A Comprative Study of Turbulence Modelling in Diluted Hydrogen Non-premixed Flames," IFRF Combustion Journal.
[119] Versteeg, H. K., and Malalasekera, W., 1995, An Introduction to Computational Fluid Dynamics – The Finite Volume Method, Longman Group Ltd.
[120] Löhner, R., 2001, Applied Computational Fluid Dynamics Techniques: an Introduction Based on Finite Element Methods, John Wiley & Sons Ltd, Chichester; New York.
[121] Sayma, A., 2009, Computational Fluid Dynamics, Ventus Publishing ApS.
[122] "Finite volume method," http://www.cfd-online.com/Wiki/Finite_volume.
[123] 2005, Fluent 6.2 Users Guides, Lebanon, USA.
[124] Hinze, J. O., 1975, Turbulence, McGraw-Hill Inc.
[125] Fraser, T., 2003, "Numerical Modelling of an Inverted Cyclone Gasifier," Cardiff University, Cardiff.
[126] Batchelor, G. K., 1953, The theory of Homogeneous Turbulence, Cambridge University Press, Cambridge, UK.
[127] Fox, R. O., 2003, Computational Models for Turbulent Reacting Flows, Cambridge University Press, Cambridge, UK.
[128] Lesieur, M., 1990, Turbulence in Fluid, Kluwer, Dordrecht.
[129] McComb, W. D., 1990, The Physics of Fluid Turbulence, Oxford University Press, Oxford.
[130] Monin, A. S., and Yaglom, A. M., 1975, Statistical Fluid Mechanics: Mechanics of Turbulent, MIT Press, Cambridge.
[131] Panchev, S., 1971, Random Functions and Turbulence, Pergamon Press, Oxford.
[132] Pope, S. B., 2008, Turbulent Flows, Cambridge University Press, Cambridge, UK.
[133] Wilcox, D. C., 1993, Turbulence Modeling for CFD, DCW Industeries Inc., La Canada, California, USA.
[134] Chilka, A., and Kulkarni, A., "Modeling Turbulent Flows in Fluent," http://www.fluent.com/software/university/blog/turbulent.pdf.
[135] Menter, F. R., 1994, "Two-Equation Eddy-Viscosity Turbulence Models for Engineering Applications," AIAA Journal, 32(8), pp. 1598-1605.
[136] Magnussen, B. F., and Hjertager, B. H., 1976, "On mathematical models of turbulent combustion with special emphasis on soot formation and combustion," 16th Symp. (Int'l.) on Combustion., The Combustion Institute.

[137] Magnussen, B. F., 1981, "On the Structure of Turbulence and a Generalized Eddy Dissipation Concept for Chemical Reaction in Turbulent Flow," Nineteeth AIAA MeetingSt. Louis.
[138] Zimont, V., 2000, "Gas Premixed Combustion at High Turbulence. Turbulent Flame Closure Model Combustion Model," Experimental Thermal and Fluid Science, 21, pp. 179-186.
[139] Zimont, V., Polifke, W., Bettelini, M., and Weisenstein, W., July 1998, "An Efficient Computational Model for Premixed Turbulent Combustion at High Reynolds Numbers Based on a Turbulent Flame Speed Closure," J. of Gas Turbines Power, 120, pp. 526-532.
[140] Zimont, V. L., Biagioli, F., and Syed, K. J., 2001, "Modelling Turbulent Premixed Combustion in the Intermediate Steady Propagation Regime," Progress in Computational Fluid Dynamics, 1(1), pp. 14-28.
[141] Zimont, V. L., and Lipatnikov., A. N., 1995, "A Numerical Model of Premixed Turbulent Combustion of Gases," Chem. Phys. Report, 14(7), pp. 993-1025.
[142] Douglas, J. F., Gasiorek, J. M., and Swaffield, J. A., 1979, Fluid Mechanics, Pitman International Text, UK.
[143] "Quality Meshes Lead to Accurate Analyses," http://www.pointwise.com/gridgen/quality.shtml.
[144] Hermanns, R. T. E., 2007, "Laminar Burning Velocities of Methane-Hydrogen-Air Mixtures," Technische Universiteit Eindhoven.
[145] Peters, N., 2000, Turbulent Combustion, Cambridge University Press.
[146] Kobayashi, H., Kawabata, Y., and Maruta, K., 1998, "Experimental Study on General Correlations of Turbulent Burning Velocity at High Pressure," Proc. Combust. Inst., 27, pp. 941-948.
[147] Lipatnikov, A. N., and Chomiak, J., 2002, "Turbulent Flame Speed and Thickness: Phenomenology, Evaluation, and Application in Multi-Dimensional Simulations," Prog. Energ. Combust. , 28, pp. 1-74.
[148] Briones, A. M., Aggarwal, S. K., and Katta, V. R., 2008, "Effects of H_2 enrichment on the propagation characteristics of CH_4–air triple flames," Combustion and Flame, 153, pp. 367–383.
[149] El-Sherif, S. A., 2000, "Control of emissions by gaseous additives in methane-air and carbon monoxide-air flames," Fuel, 79(5), pp. 567-575.
[150] Göttgens, J., Mauss, F., and Peters, N., 1992, "Analytic approximations of burning velocities and flame thicknesses of lean hydrogen, methane, ethylene, ethane, acetylene, and propane flames," Symposium (International) on Combustion, 24(1), pp. 129-135.
[151] Ilbas, M., Crayford, A. P., Yilmaz, I., Bowen, P. J., and Syred, N., 2006, "Laminar-burning velocities of hydrogen-air and hydrogen-methane-air mixtures: An experimental study," International Journal of Hydrogen Energy, 31(12), pp. 1768-1779.
[152] Mandilas, C., Ormsby, M. P., Sheppard, C. G. W., and Woolley, R., 2007, "Effects of hydrogen addition on laminar and turbulent premixed methane and iso-octane-air flames," Proceedings of the Combustion Institute, 31(1), pp. 1443-1450.
[153] Müller, U. C., Bollig, M., and Peters, N., 1997, "Approximations for burning velocities and markstein numbers for lean hydrocarbon and methanol flames," Combustion and Flame, 108(3), pp. 349-356.
[154] Alavandi, S. K., and Agrawal, A. K., 2008, "Experimental study of combustion of hydrogen-syngas/methane fuel mixtures in a porous burner," International Journal of Hydrogen Energy, 33(4), pp. 1407-1415.
[155] Bradley, D., Lawes, M., Liu, K., Verhelst, S., and Woolley, R., 2007, "Laminar burning velocities of lean hydrogen-air mixtures at pressures up to 1.0 MPa," Combustion and Flame, 149(1-2), pp. 162-172.
[156] Huang, Z., Zhang, Y., Zeng, K., Liu, B., Wang, Q., and Jiang, D., 2006, "Measurements of laminar burning velocities for natural gas-hydrogen-air mixtures," Combustion and Flame, 146(1-2), pp. 302-311.

[157] Müller, U. C., Bollig, M., and Peters, N., 1998, "Approximation for burning velocities and markstein numbers for lean hydrocarbon and methanol flames, combustion and flame 108:349-356 (1997)," Combustion and Flame, 112(1-2), pp. 284-284.
[158] Peters, N., and Williams, F. A., 1987, "The Asymptotic Structure of Stoichiometric Methane-Air lames," Combustion and Flame, 68(2), pp. 185-207.
[159] Kwon, O. C., Aung, K. T., Tseng, L. K., Ismail, M. A., and Faeth, G. M., 1999, "Comment on "Approximations for burning velocities and Markstein numbers for lean hydrocarbon and methanol flames," by U. C. Müller, M. Bollig, and N. Peters," Combustion and Flame, 116(1-2), pp. 310-312.
[160] 2008, "CHEMKIN-PRO," Reaction Design, San Diego.
[161] Kee, R. J., Grcar, J. F., Smooke, M. D., and Miller, J. A., 1983, "PREMIX: A Fortran Program for Modeling Steady, Laminar, One-Dimensional Premixed Flames," Sandia National Laboratories, Livermore.
[162] Smith, G. P., Golden, D. M., Frenklach, M., Moriarty, N. W., Eiteneer, B., Goldenberg, M., Bowman, C. T., Hanson, R. K., Song, S., Gardiner, W. C., Lissianski, V. V., and Qin, Z., "GRI-Mech 3.0," http://www.me.berkeley.edu/gri_mech/.
[163] Serrano, C., Hernández, J. J., Mandilas, C., Sheppard, C. G. W., and Woolley, R., 2008, "Laminar burning behaviour of biomass gasification-derived producer gas," International Journal of Hydrogen Energy, 33(2), pp. 851-862.
[164] Liu, F., and Gulder, O. L., 2005, "Effects of H_2 and H Preferential Diffusion and Unity Lewis Number on Superadiabatic Flame Temperatures in Rich Premixed Methane Flames," Combustion and Flame, 143, pp. 264-281.
[165] Zhang, Y., Wu, J., and Ishizuka, S., 2009, "Hydrogen Addition Effect on Laminar Burning Velocity, Flame Temperature and Flame Stability of a Planar and a Curved CH_4-H_2-air premixed flame," International Journal of Hydrogen Energy, 34, pp. 519-527.
[166] Ströhle, J., and Myhrvold, T., 2007, "An evaluation of detailed reaction mechanisms for hydrogen combustion under gas turbine conditions," International Journal of Hydrogen Energy, 32(1), pp. 125-135.
[167] Aung, K. T., Hassan, M. I., and Faeth, G. M., 1998, "Effects of Pressure and Nitrogen Dilution on Flame/Stretch Interactions of Laminar Premixed $H_2/O_2/N_2$ Flames," Combustion and Flame, 112, pp. 1-15.
[168] O'Conaire, M., Curran, H. J., Simmie, J. M., Pitz, W. J., and Westbrook, C. K., 2004, "A comprehensive modeling study of hydrogen oxidation," International Journal of Chemical Kinetic, 36(11), pp. 603-622.
[169] Li, J., Zhao, Z., Kazakov, A., and Dryer, F. L., 2004, "An Updated Comprehensive Kinetic Model of Hydrogen Combustion," International Journal of Chemical Kinetic, 36(10), pp. 566-575.
[170] Konnov, A. A., 2004, "Refinement of the Kinetic Mechanism of Hydrogen Combustion.," Khimicheskaya Fizika, 23(8), pp. 5-18.
[171] Konnov, A. A., 2008, "Remaining uncertainties in the kinetic mechanism of hydrogen combustion," Combustion and Flame 152, pp. 507-528.
[172] Lafay, Y., Renou, B., Cabot, G., and Boukhalfa, M., 2008, "Experimental and Numerical Investigation of the Effect of H_2 Enrichment on Laminar Methane-Air Flame Thickness," Combustion and Flame, 153, pp. 540-561.
[173] Valera-Medina, A., Abdulsada, M., Shelil, N., Griffiths, A. J., and Syred, N., 2009, "Flame Stabilization and Flash-back Avoidance Using Passive Nozzle Constrictions," The 16th IFRF Members' Conference in Boston, IFRF, USA.
[174] Dhanuka, S. K., Temme, J. E., Driscoll, J. F., and Mongia, H. C., 2009, "Vortex-shedding and mixing layer effects on periodic flashback in a lean premixed prevaporized gas turbine combustor," Proceedings of the Combustion Institute, 32(2), pp. 2901-2908.
[175] Lenze, M., and Carroni, R., 2007, "Public Summary Report of ENCAP deliverable D.23.3 Report on limits of current burner using H_2-rich fuel mixtures."
[176] Lieuwen, T., McDonell, V., Petersen, E., and Santavicca, D., 2008, "Fuel Flexibility Influences on Premixed Combustor Blowout, Flashback, Autoignition, and Stability," Journal of Engineering for Gas Turbines and Power, 130(1), p. 011506.

[177] OMEGA, 2008, "Aviation in a sustainable World," http://www.omega.mmu.ac.uk/international-conference-on-alternative-fuels.htm

[178] Markides, C. N., and Mastorakos, E., 2008, "Flame Propagation Following the Autoignition of Axisymmetric Hydrogen, Acetylene, and Normal-Heptane Plumes in Turbulent Coflows of Hot Air," Journal of Engineering for Gas Turbines and Power, 130(1), pp. 011502-011509.

[179] Bagdanavicius, A., 2009, "The Effect of Turbulence on Flame Speed,"Cardiff.

[180] Shelil, N., Bagdanavicius, A., Griffiths, A. J., Roberts, P., and Syred, N., 2009, "Flashback Analysis for Hydrogen/Methane Mixtures for Premixed Swirl Combustion," The 16th IFRF Members' Conference in Boston, IFRF, USA.

[181] Shelil, N., Griffiths, A. J., and Syred, N., 2009, "Numerical Study on the Effect of CH_4 Addition to H_2 Flames Flashback," 2009 Fall Technical Meeting Organized by the Eastern States Section of the Combustion Institute and Hosted by the University of Maryland College Park, The Combustion Institute, Maryland, USA.